

A Field Guide to Foldamers

David J. Hill,[†] Matthew J. Mio,[‡] Ryan B. Prince,[§] Thomas S. Hughes,[†] and Jeffrey S. Moore^{*,†}

Roger Adams Laboratory, Departments of Chemistry and Materials Science & Engineering, The Beckman Institute for Advanced Science and Technology, University of Illinois at Urbana–Champaign, Urbana, Illinois 61801; Department of Chemistry, Macalester College, 1600 Grand Avenue, St. Paul, Minnesota 55105; and 3M Adhesive Technology Center, 3M Center, 201-3N-04, St. Paul, Minnesota 55144

Received September 5, 2001

Contents

I. Introduction—Definition, Scope, and Relevance	3894	2. Pyridine–Pyrimidines with Hydrazal Linkers	3945
II. Generating Foldamers—Design, Synthesis, Purification, and Characterization	3897	3. Pyridine–Pyridazines	3946
A. Foldamer Design	3897	C. Backbones Utilizing Solvophobic Interactions	3947
1. The General Folding Problem	3897	1. Qualification	3947
2. Foldamers: Secondary Structure	3902	2. Guanidines	3947
3. Tyligomers: Secondary and Tertiary Structure	3904	3. Aedamers	3947
4. Designing Folding Molecules: Toward Tyligomers	3907	4. Cyclophanes	3949
B. Foldamer Synthesis and Purification—The Chemistry of Oligomers	3909	5. Side Chain–Backbone Interactions	3949
C. Foldamer Characterization—Experimental and Instrumental Methods	3910	D. Backbones Utilizing Hydrogen-Bonding Interactions	3961
III. Foldamer Research	3910	1. Aromatic Amide Backbones	3961
A. Overview	3910	2. Receptor Motif Backbones	3962
B. Motivation	3910	E. Backbones Utilizing Metal Coordination	3963
C. Methods	3910	1. Overview	3963
D. General Scope	3912	2. Metal-Binding Backbones	3964
IV. Peptidomimetic Foldamers	3912	3. Anionic-Binding Backbones—Hexapyrrins	3966
A. The α -Peptide Family	3913	VI. Nucleotidomimetic Foldamers	3967
1. Peptoids	3913	A. Overview	3967
2. <i>N,N</i> -Linked Oligoureas	3914	B. Isomeric Oligonucleotides	3968
3. Oligopyrrolinones	3915	1. Iso-RNA and Iso-DNA	3968
4. Oxazolidin-2-ones	3916	2. α -DNA, <i>alt</i> -DNA, and L-DNA	3969
5. Azatides and Azapeptides	3916	C. Carbohydrate Modifications	3969
B. The β -Peptide Family	3917	1. Backbones with C1'-Base Connectivities	3969
1. β -Peptide Foldamers	3917	2. Backbones with C2'-Base Connectivities	3973
2. α -Aminoxy Acids	3937	3. Torsionally Restricted Oligonucleotides	3975
3. Sulfur-Containing β -Peptide Analogues	3937	4. Torsionally Flexible Oligonucleotides	3977
4. Hydrazino Peptides	3938	D. Modifications of the Nucleotide Linkage	3977
C. The γ -Peptide Family	3938	1. PNAs	3978
1. γ -Peptide Foldamers	3938	2. NDPs	3980
2. Other Members of the γ -Peptide Family	3941	3. Fused Sugar–Base Backbones	3980
D. The δ -Peptide Family	3941	4. Cationic Linkages	3980
1. Alkene-Based δ -Amino Acids	3941	E. Alternative Nucleobases	3981
2. Carbopeptoids	3941	VII. Multistranded Abiotic Foldamers	3982
V. Single-Stranded Abiotic Foldamers	3944	A. Hydrogen-Bonding-Stabilized Foldamer Multiplexes	3982
A. Overview	3944	B. Duplexes Stabilized by Hydrogen-Bonding and Aromatic–Aromatic Interactions	3986
B. Backbones Utilizing Bipyridine Segments	3944	1. Zipper Duplexes	3986
1. Pyridine–Pyrimidines	3944	2. Pyridylamide Oligomers	3986
		C. Helicates: Metal-Coordinating Foldamer Duplexes	3988
		1. Oligopyridines	3988
		2. Linked Oligopyridines	3990
		3. Pyridine Analogues	3994
		4. Catecholates	3995

[†] University of Illinois at Urbana–Champaign.

[‡] Macalester College.

[§] 3M and Company.

D. Multistranded Receptors	3995
E. Foldamer–Oligomer Interactions	3997
1. Minor Groove Binding Oligomers	3998
2. Peptide–Oligomer Complexes	3999
VIII. Conclusion	4000
IX. Acknowledgments	4000
X. References	4000



David J. Hill (second from left) was born in Monterey, CA, in 1973. He attended Point Loma Nazarene University in San Diego, CA, where he worked with Professor Victor L. Heasley on the halogenation of unsaturated carbonyl compounds. After receiving his B.A. degree in Chemistry in 1997, he began his graduate career at the University of Illinois with Professor Jeffrey S. Moore. Currently he is in his fifth year investigating solvent effects on the helix–coil transition in oligo(*m*-phenylene ethynylene) foldamers.

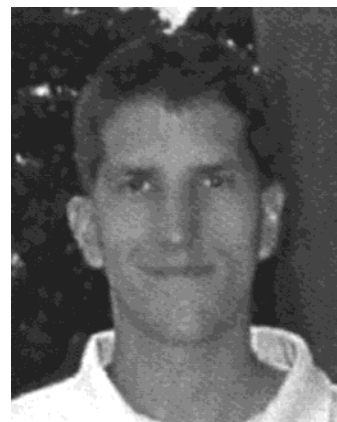
Matthew J. Mio (left) was born in Michigan in 1974. He attended the University of Detroit Mercy, where he worked with Professor Kevin D. Belfield (now at the University of Central Florida) on the synthesis of nonlinear optical chromophores for use in polymeric systems. He graduated with his B.S. degree in Chemistry in 1997. Later that year, he began his graduate career at the University of Illinois at Urbana–Champaign with Professor Jeffrey S. Moore. There, Matt studied the synthesis and solution/solid-state properties of oligo(*m*-phenylene ethynylene) foldamers and graduated with his Ph.D. degree in 2001. He then went to the Chemistry Department at Macalester College (St. Paul, MN) as a Mellon Postdoctoral Fellow to study the synthesis of novel CpCo–cyclobutadienyl-bridged cyclophanes with Professor Ronald G. Brisbois.

Thomas S. Hughes (right) is currently a postdoctoral fellow in the research group of Professor Jeff Moore at the University of Illinois. He was born in 1970 in Philadelphia, PA, and received his B.S. degree from Temple University in 1991. In 1999 he received his Ph.D. degree from Cornell University, where he worked in the laboratories of Professor Barry Carpenter. He is currently studying the association kinetics of the binding of a helical oligomer to a rodlike guest. He is also investigating the thermodynamics of oligo(phenylene ethynylene) folding using molecular mechanics.

Jeffrey S. Moore (second from right) was born in Illinois in 1962. After receiving his B.S. degree in Chemistry from the University of Illinois in 1984, he completed his Ph.D. degree in Materials Science and Engineering, also at the University of Illinois, with Samuel Stupp (1989). He then went to the California Institute of Technology as an NSF postdoctoral fellow to study with Robert Grubbs. In 1990 he joined the chemistry faculty at the University of Michigan in Ann Arbor. He returned to the University of Illinois in 1993, where he is currently a Professor of Chemistry and Materials Science and Engineering. In 1995 he became a part-time faculty member of the Beckman Institute for Advanced Science and Technology, where he now serves as co-chairman of the Molecular and Electronic Nanostructures Main Research Theme.

1. Introduction—Definition, Scope, and Relevance

The breadth of structure and function displayed by the molecules of biology is remarkable. Considering



Ryan B. Prince was born in Robbinsdale, MN, in 1972. He graduated from Southeast Missouri State University in 1995 with his B.S. degree in Chemistry, where he worked for Professor Jin K. Gong on the synthesis and characterization of transition-metal complexes that bind and activate carbon dioxide. He then went to the University of Illinois and worked with Professor Jeffrey S. Moore on the synthesis and study of oligo(*m*-phenylene ethynylene) foldamers. He completed his Ph.D. degree in Organic Chemistry in 2000 and is currently a senior research chemist at 3M Company in St. Paul, MN.

that there are only three major biopolymer backbones (proteins, ribonucleic acids, and polysaccharides), nature vividly teaches that copolymer sequence is a powerful way to meet diverse chemical challenges. It is logical then to ask are biomacromolecule building blocks are *matchless* in their suitability for life? Systematic studies on alternative monomers closely related to those found in nature have provided clues about the fitness of α -amino acids, ribofuranosyl (5'–3') nucleic acids, and phosphodiester linkages. Yet “why nature is such, and not otherwise”¹ is a question that continues to be asked. Looking beyond the biopolymers and their related derivatives however, it is possible to imagine that other chain molecules are capable of similar functions. This prediction has only recently begun to be tested, raising questions of great fundamental interest. On a more practical level, the discovery of new functional polymers clearly has widespread potential for both chemistry and biology.

Most of the interesting functions carried out by biomacromolecules, such as molecular recognition, information storage, and catalysis, involve stable, compact solution structures that approach conformational uniqueness. These high molecular weight macromolecules might be described as glassy-like, nanometer-sized particles² that are suspended in solution and consist of one to, at most, a few chains. The spatial position of most of the backbone atoms is fixed, except for minor fluctuations about their equilibrium coordinates. There is also a congruency between particles having identical or even similar sequences. The surface of these particles includes three-dimensional, molecular-sized crevices lined with information-rich surfaces, and it is from here that affinity, specificity, and catalytic activity spring forth. Reasoning by analogy, the quest for function in synthetic chains should thus be closely tied to the invention of new polymer molecules that acquire ordered solution structures.

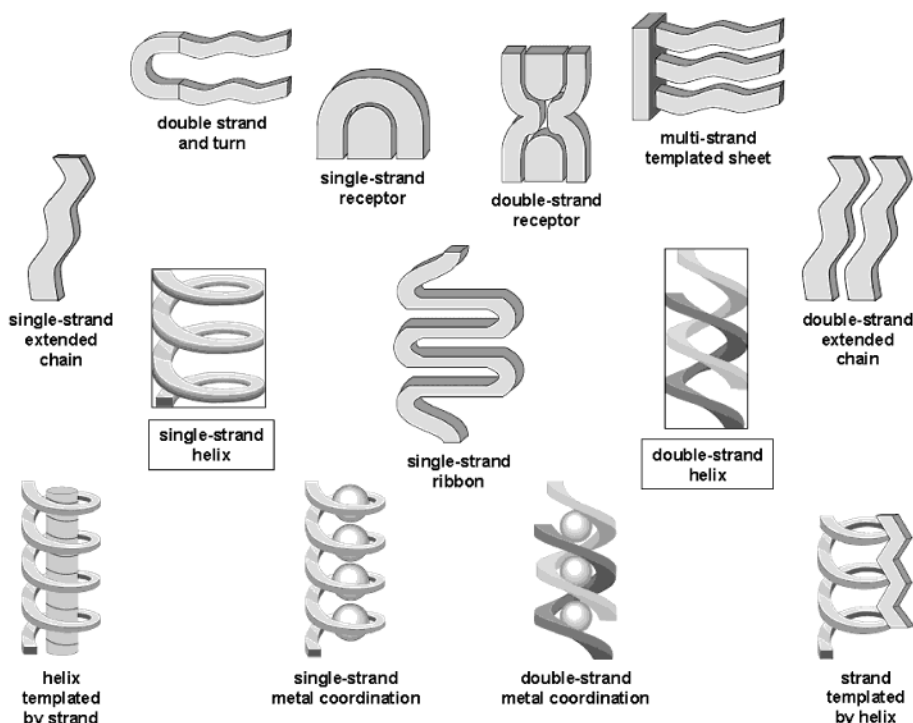


Figure 1. Illustrations depicting the different types of foldamer secondary structures.

Thus, the motivation for developing new chain molecules that adopt ordered solution conformations can be stated as an attempt to gain deeper insight into the fitness of nature's biomacromolecules and to identify new polymers that perform functions that are, at least in part, outside of those seen in nature. Toward these goals, chemists have endeavored to intentionally generate unnatural oligomeric sequences that take on well-defined conformations in solution. This subject has come to be known as the field of foldamers.³ This review covers the literature relevant to foldamers, as specified below, through July 2001. Progress to date has been encouraging, and the field is developing rapidly as demonstrated by the various architectures that have been generated, schematically represented in Figure 1. Yet, today we are still far from producing high molecular weight polymers that mimic the sophistication of biomacromolecules, either in form or function.

A foldamer has previously been defined as "any polymer with a strong tendency to adopt a specific, compact conformation".⁴ Upon inspection of the literature, we thought this definition was in need of clarification. First, the "foldamers" described in the literature are not polymers; they are oligomers. Second, the word "compact" is ambiguous and invokes high molecular weight globular proteins, unlike the smaller segments of secondary structure typical of this area. Third, a crucial aspect of chain conformation is its dynamic character, which in the case of foldamers is manifested in the context of folding and unfolding. Specifically, the "folding reaction" is the process that transforms the conformationally disordered oligomer into a conformationally ordered state, which corresponds to a small set of nearly congruent conformations.

Our definition of a foldamer is any oligomer that folds into a conformationally ordered state

in solution, the structures of which are stabilized by a collection of noncovalent interactions between nonadjacent monomer units. There are two major classes of foldamers: single-stranded foldamers that only fold (peptidomimetics and their abiotic analogues) and multiple-stranded foldamers that both associate and fold (nucleotidomimetics and their abiotic analogues). Before discussing this definition in detail, let us briefly reconsider high molecular weight biomacromolecules. We imagine that a foldamer will not be a very good mimic of a biomacromolecule. In other words, there is something beyond foldamers. This "something" is perhaps a high molecular weight polymer that consists of a collection of foldamers, just as proteins can be viewed as a collection of secondary structures. To clearly distinguish a foldamer, as defined above, from this higher molecular weight "something", we suggest the term *tyliger*. Tyliger is derived from *tyligos*, meaning "to fold", and *meros*, meaning "part" (i.e., a structure consisting of folded parts). Thus, foldamer relates to an element of secondary structure, in the same way that tyliger relates to a tertiary or quaternary conformation.

Let us now examine our definition in detail, since this has been used to limit the scope of this review. First, a foldamer is a chain molecule, meaning that there will almost certainly be a regularly repeating motif within the backbone. Second, foldamers are of oligomeric (not polymeric) size, consistent with the recent literature. Third, the verb in our definition is "to fold", which conveys the dynamic character of conformation, i.e., the folding reaction. Oligomers where no folding reaction can occur, such as helixes,^{5,6} cannot be considered foldamers (Figure 2a). The folding reaction also assumes that the *association* of multiple foldamer strands involves a similar type of entropy loss as folding. Fourth, when folded,

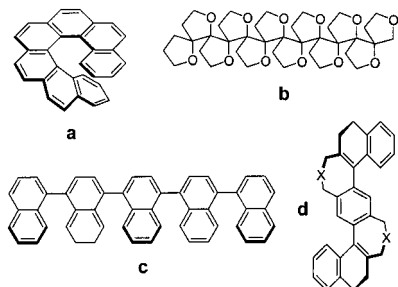


Figure 2. Oligomers not classified as foldamers: (a) helicenes,^{5,6} (b) polyoxapolyspiroalkanones,¹² (c) oligo(naphthalene)s,¹⁴ and (d) “gelander” molecules.¹³

the chain molecules populate a small set of nearly superimposable conformations, meaning that in the folded form all molecules can be described by a unique set of atomic coordinates (or at most a few different sets). Fifth, the folded form is of interest in solution, implying that the solvent is both a fundamental part of the folded state and that the dynamic character of the liquid environment will result in fluctuations about the chain's equilibrium set of atomic coordinates. Sixth, the chain's conformation is defined by noncovalent interactions between non-adjacent monomer units. This point requires special clarification. Many synthetic oligomers adopt stable, extended helical conformations in solution. Examples include poly(isocyanate)s,⁷ poly(proline)s,⁸ poly(aldehyde)s,⁹ poly[(triarylmethyl) methacrylates],¹⁰ and some oligo(saccharide)s.¹¹ However, in these cases, the chain's conformation is determined by the repeat unit's torsional potential energy surface. To distinguish a foldamer from a chain that adopts a regular conformation based on the repeat unit's torsional potential energy surface, we specify that the defining noncovalent interactions must be between atoms that are not contained within adjacent repeat units. By insisting on the role of these interactions in our definition, we are simply being consistent with the notion that foldamers are the synthetic analogues of secondary structure elements, as secondary structure fits this description. Oligomers where conformations are “predetermined” such as polyoxapolyspiroalkanones,¹² “gelander” molecules,¹³ and oligonaphthalenes¹⁴ will not be considered as foldamers (Figure 2b–d).

The accumulation of noncovalent interactions that dictate conformation has no direct counterpart in small molecule chemistry. These interactions arise from the simple reason that the chain segments are either all connected by covalent bonds or form through interstrand complementarity, both of which give rise to a high probability for various monomer pairs to encounter one another. Although the strength of the interaction between monomer pairs is generally weak, the *number of possible interactions* is high and is, presumably, chain-length dependent. A consequence of these collective interactions is that oligomers are apt to undergo cooperative conformational transitions.¹⁵ Thus, although an ordered solution conformation is a necessary criterion of what constitutes a foldamer, it is not sufficient. In addition, noncovalent interactions between nonadjacent monomer units, on some level, play a deciding role in

setting the chain's conformation. In other words, conformational order is stabilized by a collection of interactions acting within or between chains, reminiscent of some supramolecular assemblies.¹⁶

One additional point of distinction between intrinsically preset conformations and those derived primarily from the noncovalent interactions described above centers on environmental responsiveness. Given the weak nature of noncovalent forces, solvent can modulate their strength in a very significant way. It is thus possible to go from a state in which monomers repel one another to one in which the monomer interactions are attractive simply by changing the temperature, pH, or quality of the solvent. In contrast, the torsional potential energy surface is virtually independent of extrinsic variables and therefore is an invariant force to a chain's structure and dynamics. Consequently, the contribution of a monomer's local potential energy surface to an oligomer's conformation can be calculated by statistical mechanical methods such as the rotational isomeric state model.¹¹ Because conformational ordering in foldamers depends on interactions whose strength varies with the environment, these chains can undergo abrupt order-disorder transitions—the folding reaction. Oligomers that have intrinsically stable conformations will be less likely to exhibit this cooperative behavior. This is more than an academic distinction, since there are many potential functions of foldamers that may depend on the reversibility of the folding reaction.

Hopefully, this discussion has helped to shape the reader's view of the term foldamer and accordingly serves to define the scope and relevancy of this review. We note that as chemists have begun to tackle the challenging problem of conformational control in flexible organic molecules, it is becoming fashionable to abuse terms that incorporate the root “fold” (e.g., “folding molecule”, “self-folding”, “folded”). In this review we restrict our coverage to chain molecules (i.e., structures that have a repetitive structure) that have been experimentally demonstrated to exhibit a high degree of conformational order in solution, predominantly derived from noncovalent, intra- and interchain segmental interactions. The emphasis will be on unnatural backbones, although biological oligomers will be discussed as prototypical examples of foldamers.¹⁷ (For example, we have discerned that bilirubins are an excellent model of nature's minimal foldamer. Although the conformation of these molecules has been studied since the late 1980s,^{18,19} investigations into bilirubins' solution conformation continue to the present day.^{20–24}) This review is constrained to the size regime of oligomers, since there are as yet no high polymer tylogomers. We do not cover small molecule fragments that are described in the literature as “folded”,²⁵ although in some cases²⁶ extension of these structures to chain molecules may be obvious. We do not review here polymers that are a mixture of chemical structures or are conformationally incongruent, even if they are referred to in the literature as being “folded.”^{27–29} By analogy to its well-established usage in protein chemistry,³⁰ we

suggest that descriptions involving the verb “fold” should be reserved for conformationally defined chain molecules and not be used for polymeric mixtures. For example, a compact polymeric micelle certainly exists in multiple lowest energy conformations but should not be considered to adopt folded conformations.

Overall, it is the purpose of this article to present a thorough review of foldamer research contained within our definition. A survey of what is involved in the generation of foldamers is in order first, followed by a discussion of specific contributions to the field of foldamers.

II. Generating Foldamers—Design, Synthesis, Purification, and Characterization

The foundation for foldamer research was laid in the early 20th century, during the rise of modern synthetic polymer chemistry,³¹ molecular biology, and more recently through supramolecular chemistry.¹⁶ Upon examination of these disciplines, it becomes clear why and how modern foldamer research has evolved into a stimulating scientific field. It is hoped that the lessons learned in the roots of the foldamer field can be brought to bear upon the problems of designing, creating, and evaluating foldamers and, eventually, biomimetic tyligomers. Before reviewing the current state of the field of foldamers, a summary of various aspects impacting foldamer design will be presented.

A. Foldamer Design

Since the initial use of the term “foldamer” in 1996,³² the field has witnessed several design approaches. We begin by clarifying the context in which we use the word “design”. Our use of this word will be in the same sense as “building a house”—choosing raw materials, mapping out the blueprint for the structure, constructing the necessary subunits into the final framework, and performing interior decoration. Gellman’s daunting steps⁴ to generate useful foldamers echoes this analogy: determining novel backbones that can fold, developing efficient synthetic methods and integrating chemical function. Of course, it is presumptuous for the authors to profess knowledge of how published foldamers were initially conceived. Rather, we intend to detail the logical thought processes that must necessarily be considered in the generation of a successful foldamer.³³

The broad philosophical foundations of foldamer design draw on concepts developed over the past decades in the fields of polymer physics, condensed matter physics, and, in particular, biophysics. It is evident that oligomeric foldamers are not large or complex enough to form anything other than simple, secondary structures such as helices or sheets. A clear logical next step in the field would be to design larger, more complex chain molecules capable of folding into truly tertiary structures or structures having long-range intrachain energetic interactions.⁴ The designs of both simple and complex systems share many features, and much of the discussion below will be general whether tertiary structure is

present in the folded state or not. There are, however, several issues unique to tyligomers which mirror the more complex issues of the long-standing protein folding problem³⁴ and which will be treated below. Since a goal of the field is to endow synthetic foldamers, and eventually tyligomers, with the structural (and functional) specificity reminiscent of folding biopolymers, the theoretical models that describe these phenomena should be considered.

To rationally design a foldamer, it will be necessary to understand the properties of known foldamers, which are those secondary-structure domains of sequence-specific biopolymers that have been metabolically synthesized by living organisms, i.e., proteins, nucleic acids, and oligosaccharides. Each of these biopolymers derives its function from a conformationally well-defined folded state, which for proteins is usually called the “native state”.³⁰ The process of going from a large ensemble of extended conformations to this folded state is called the folding reaction,³⁵ and elucidating the general mechanism of this reaction involves the identification of the critical thermodynamic and kinetic parameters. It will then be instructive to relate these parameters to the properties of unnatural synthetic oligomers that can be adjusted by the synthetic chemist.

Three issues shared with the field of protein folding must be dealt with to make the design of foldamers possible: foldability, structure prediction (reverse engineering), and designability (forward engineering). The first of these refers to an individual chain’s ability to fold to a unique structure or a set of closely related structures; a chain that does so efficiently is said to have a high foldability. The second issue deals with the *ab initio* determination of the folded state structure given the primary sequence structure. The third issue, designability, refers to the number of these chains that will fold to a particular structure of interest; a folded structure that can be formed by many different, highly foldable sequences is said to have a high designability. By the very nature of their length, short oligomeric chains participate in relatively short-range intrachain contacts and as a result usually form structurally simple folded states that are straightforward to design. Longer chains are capable of folding into structures with very long-range interactions, making design more difficult because of the large number of potential contacts. The foldability of tyligomers has been treated analytically and by simulations of simple models. Although some progress has been made, the best methods for *ab initio* determination of a long sequence’s folded structure have been worked out in essentially taxonomic ways for the most well-studied biopolymer, proteins.^{36,37} Designability has been investigated but only for very simple systems. The fundamental idea that emerges from these models is that some structures are much more designable than others.

1. The General Folding Problem

Consider an oligomer or polymer chain consisting of N monomer units, each having ω torsionally accessible conformations. The parameter ω is dependent on the rigidity of the chain backbone and is

equivalent to the number of minima on a Ramachandran-like surface for the backbone repeat unit. This chain has ω^N accessible conformations, neglecting those conformations that are inaccessible as a consequence of the chain folding back upon itself in a sterically prohibitive manner (the so-called excluded-volume conformers). This simple calculation gives an overestimation of the total number of conformations but does accurately reflect the magnitude of the number of states. For polypeptides, ω has been determined to be between 2 and 3.³⁸ The exponential ω^N rapidly becomes very large with increasing chain length, to the point of being unimaginably large for a chain that would be capable of performing any sort of chemically or biologically significant function. As mentioned previously (Figure 2), oligomers may appear to be folded but in fact lack a folding reaction because ω is roughly equal to 1. Such oligomers have very few minima on their overall potential energy surface, since ω^N is very small for all values of N .

For an oligomer to populate a small subset of the ω^N conformations, this folded state, **F**, must have an energy that is much lower than the unfolded state, **U**. This must be the case if the lowest energy conformations are able to dominate the equilibrium mixture of conformers. The thermodynamics of the folding reaction are controlled by two main factors. The unfolded state must lose the *conformational entropy* present in its much larger conformational ensemble in order to realize the *enthalpic gain* present in the folded state. Multistranded systems are more complex since they must also lose some translational and rotational entropy upon association as well as chain conformational entropy. Yet, their thermodynamics are similar. The thermodynamic properties observed in biological folding reactions can be reproduced by a simple model having a single folded structure separated from **U** by an energy gap, illustrated in more detail below. To reach its lowest energy state, an oligomer will have to maximize its favorable energetic interactions and minimize those that are unfavorable, including both intrachain and chain–solvent interactions. The existence of an optimized set of unfavorable and favorable contacts in the folded state has been called the “minimally frustrated” state.³⁹

Noncovalent interactions involve much weaker and reversible interactions than covalent linkages, which allows for the exploration of many chain conformations during the folding reaction. The net strength of the nonadjacent contacts that determine the thermodynamics of folding are essentially the differences between the strengths of the chain–chain and the solvent–chain interactions. Undoubtedly, if solvent–chain contacts are stronger than chain–chain contacts, the molecule will not fold; such is the case in denaturing solvents. A subtle balance then exists in solvent–foldamer interactions; the solvent must solvate the molecule without competing for nonadjacent contacts while providing the chain with an environment in which to undergo the folding reaction.

The formation of unique, folded structures requires the presence of favorable nonadjacent chain–chain

contacts or unfavorable chain–solvent forces. For oligomers containing residues that are poorly solvated, collapse to a set of compact conformations can occur before the folded state is populated. In a protein, the minimization of the solvophobic force between apolar residues and polar solvent, namely, water, lowers the free energy of the protein–solvent system and is the primary driving force for collapse.^{40,41} This collapse minimizes the unfavorable solvation interactions and maximizes whatever favorable intrachain interactions exist, typically involving electrostatic and van der Waals forces. There is usually a gain in entropy for the solvent, since a higher degree of solvent ordering around the chain segment is required to solvate solvophobic segments than would be required to solvate solvophilic segments. The solvophobic collapse is then caused by a free energy gradient—having both entropic and enthalpic origins—toward states whose structures have a minimum of solvophobic segment–solvent contacts.

In the absence of any bias toward an energetically preferred folded state, this collapse will result in a random ensemble of compact conformations. For a chain that is able to fold reliably to a single folded state, the mechanism of folding is essentially a question of how the system loses entropy en route to the folded state. Two mechanisms of efficient overall entropy loss can be imagined. Initial collapse to the ensemble of compact conformations could be followed by a search through that ensemble to find the folded state or the collapse could take place concurrently with the formation of folded structure. Both types of behavior are observed for real biopolymers,⁴² and a general picture of oligomer folding must take both scenarios into account.

Especially for long chains capable of tertiary structure formation, it should also be noted that not every sequence that has a nondegenerate global minimum spontaneously folds to a unique state. A parallel can be drawn between the folding process and the condensation of individual molecules during crystallization or the condensation of atoms to form clusters. Just as there are some solid materials that crystallize quite efficiently, there are those that do not relax to their global thermodynamic minimum but form glasses instead.^{43,44} These glasses are formed when the entropy loss occurs faster than the loss of energy or equivalently when the barriers to interconversion between different conformations begin to dominate the kinetics of relaxation. Likewise, well-designed tylogomers efficiently find their folded state, while most random sequences do not fold to a unique structure but rather merely collapse to a ‘molten globule’ state or a unimolecular glass.

What then is required of a chain to fold reliably? Does the chain have a minimum energy state that is much lower in energy than the rest of the unfolded conformations **U**? If so, is this folded state thermodynamically accessible from **U** at temperatures and other conditions that allow characterization and perhaps function? For longer chains capable of many more contacts and potentially tertiary structure, is this transition kinetically accessible? Beyond predicting the existence of a folding reaction, what do the

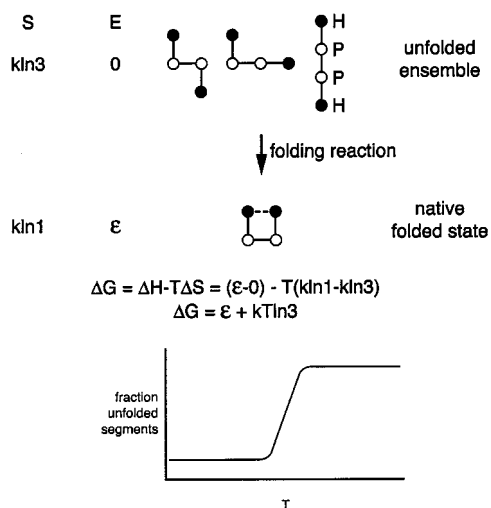


Figure 3. 2-D lattice tetramer toy model. Black circles represent solvophobic repeat units (H) and open circles polar repeat units (P). The sigmoidal plot shows the fraction of folded molecules as a function of temperature.

folded structures look like? Prediction of structure from sequence and prediction of sequence from structure are currently difficult for much studied polypeptides, let alone for any arbitrary monomer type that may be of interest to the foldamer chemist. Insight into these questions has been provided by simplified folding models.

a. Lattice Models of Folding. Minimalist models of biopolymers have been used for many years to analyze the general mechanism of folding and have proved fruitful toward understanding the folding mechanisms of proteins. These models provide computational accessibility, facile visualization, and easy conceptualization of the folding reactions known for proteins. Since the models do not rely on any properties specific to polypeptides, they are useful to chemists designing nonbiological folding systems. Go and co-workers⁴⁵ developed a widely used model that consists of a chain of different residue types that are constrained to the points of a lattice. Nonadjacent interactions are accounted for by assigning energies to neighboring lattice points occupied by residues that are not adjacent in the sequence.

Varying degrees of heterogeneity can be modeled by including any number of residue types and assigning energy values to the different pairs of neighboring nonbonded residues. In the simplest version of the model (the so-called HP model) a two-letter alphabet is employed, where H represents a solvophobic monomer and P represents a polar, or solvophilic, residue. The choice of a two-letter code reflects and models the importance of the solvophobic collapse of proteins as a key step in the folding process. Lattices with 2-D square, 3-D cubic, and even 2-D hexagonal geometries have been employed by different groups; some of this work will be described in later sections. An excellent review of these models by Chan and Dill⁴⁶ describes the picture they have provided of biopolymer folding.

Consider the tetramer toy model (TTM),⁴⁶ which is a 2-D square lattice chain consisting of two types of monomers, H and P (Figure 3). This is perhaps the simplest model that still captures many of the

key features of the folding reaction. A favorable interaction of magnitude ϵ exists between neighboring nonbonded H monomers. The exact nature of this interaction need not be defined to demonstrate the concepts involved. There are four possible conformations, one of which has energy ϵ lower than the other three (Figure 3). The three unfolded conformations make up the unfolded ensemble, and the single collapsed structure is the folded state. Note that there are fewer than ω^N (3^4) conformations for this system. This number is not reduced by excluded volume effects but by symmetry and the fact that only nonterminal monomer units have ω available conformations. Much of the thermodynamics of simple foldamers can be predicted by this model.

b. Thermodynamics of Folding. The size of the unfolded ensemble and the large number of potential folding pathways connecting this ensemble to the folded state suggest a statistical approach to the problem of folding. The thermodynamics of the folding reaction can be examined using statistical mechanics. This requires evaluating the partition function Z , which is given by eq 1 where $n(E)$ is the number of states that have an energy of E , and kT refers to the product of Boltzmann's constant and the temperature. The partition function is the Boltzmann-weighted sum of all the states, which for the TTM is given by the last term of eq 1.

$$Z = \sum_i e^{-E_i/kT} = \sum n(E) e^{-E/kT} = 3 + e^{-\epsilon/kT} \quad (1)$$

The fractions of the population in the unfolded and folded states at equilibrium for the TTM are given by eq 2, and the free energy of folding is given by eq 3 (the last term is specific to the TTM).

$$P(F) = \frac{e^{-\epsilon/kT}}{3 + e^{-\epsilon/kT}} \quad P(U) = \frac{3}{3 + e^{-\epsilon/kT}} \quad (2)$$

$$\Delta G_{\text{folding}} = -kT \ln K_{\text{eq}} = -kT \ln \left(\frac{P(F)}{P(U)} \right) = \epsilon + kT \ln 3 \quad (3)$$

Alternatively, the free energy of folding can be derived by considering the ΔH and ΔS of the reaction. The enthalpy change is clearly ϵ . The loss of entropy can be calculated by taking the sum of the loss of entropy of each chain segment. As each segment has ω conformations available, the sum of the entropy lost over the whole N -long chain is approximately $-k \ln(\omega^N)$ or $-kN \ln \omega$. At constant pressure and volume, it then follows that the free energy change is given by eq 4.

$$\Delta G = \Delta H - T\Delta S$$

$$\Delta G = \epsilon + kTN \ln \omega \quad (4)$$

It should be noted that this formulation has been used to experimentally estimate the entropy lost per chain segment and thus the average number of conformations available to each residue. Eq 4 suggests that there exists a folding temperature at which the population is evenly divided between

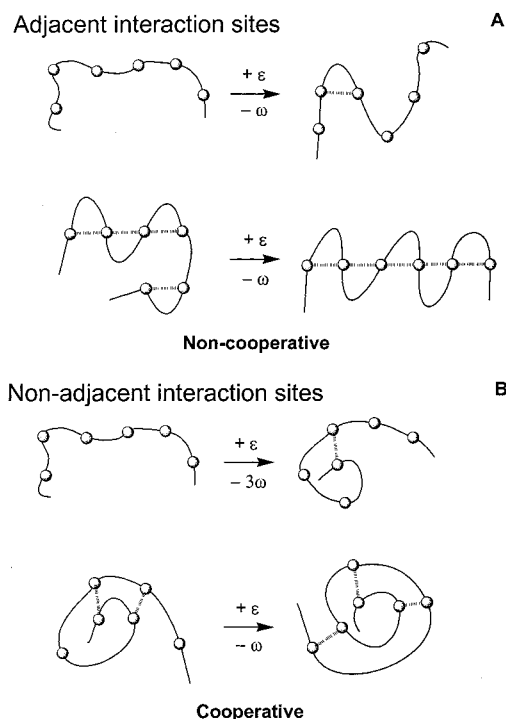


Figure 4. Origin of cooperativity. (A) Formation of a "trivial sheet", and (B) formation of a "trivial helix." Enthalpy change is shown above each reaction arrow and entropy change below. Trivial sheets do not require nucleation.

unfolded and folded states or at which $\Delta G = 0$, called the folding (or melting) temperature (eq 5).

$$T_{\text{fold}} = \frac{-\epsilon}{kN \ln \omega} \quad (5)$$

Thus, the TTM free energy of folding becomes negative at a temperature where $kT \ln 3$, the entropy of the chain lost during folding, equals the enthalpic gain of folding, the energy gap between the folded state and all other states. A plot of the fraction of the population that is in the unfolded state as a function of temperature shows a sigmoidal curve that is indicative of the cooperative nature of this transition (Figure 3). Although the very term indicates the cooperation of two or more interactions, the transition of this small single-interaction system is cooperative in the sense that the system has a tendency to be either completely unfolded or completely folded. Such transitions are observed for biopolymers, especially small, rapidly folding globular proteins.⁴⁷

Cooperativity cannot be achieved for systems that fold exclusively from noncovalent interactions between repeat units held adjacent by covalent bonds or more specifically interacting sites held adjacent by covalent bonds. Such chains fold to "trivial sheets". Conformations that result exclusively from adjacent interacting sites such as that schematically depicted in Figure 4A will not exhibit cooperative folding. As the trivial sheet folds, the ΔH and ΔS of each contact formation is the same. In other words, making the last contact is no easier than making the first. The situation for nonadjacent interacting sites is different (Figure 4B). Folded states stabilized by nonadjacent interacting sites can exhibit cooperativity. For the

model system here, forming the last contact is easier than forming the first. For simplicity throughout the rest of the review, "nonadjacent interacting sites" will be referred to as simply "nonadjacent repeat units", since for many foldamers each repeat unit has the potential to form a favorable chain-chain interaction.

The simple TTM model captures some of the essential features of the folding reaction and a key requirement of the folding system, namely, the large energy gap between the folded and unfolded states. Notice that the larger (and more negative) the value of ϵ , the more negative the free energy of folding will be. More detailed studies of a 27-mer on a 3-D lattice led Sali et al.⁴⁸ to propose that this energy gap was the definitive parameter for determining foldability. Again, further considerations of the kinetics involved in tyligomer folding suggest that this parameter is necessary but not sufficient to determine general foldability.

This is clearly only a gross view of the folding reaction, which despite its complexity is just the process of going from a large number of relatively high-energy conformers to a very small number of low-energy conformers. This model assumes that each state has equal accessibility from every other, implying that the kinetic barriers between each of the states are equal. Further consideration of the kinetics of this model is described below and obviates the need for a more complex description.

Given the requirement of a large energy gap, it then becomes important to determine the structure of the global minimum energy conformation and if its energy is sufficiently lower than the unfolded ensemble to be highly populated under some set of environmental conditions. The design of any foldamer will have to begin with the answer to these questions, which may be provided by intuition or by various computational techniques that can determine the global minimum energy structure efficiently.

c. Folding Reaction Free Energy Surfaces.

The folding reaction, in which the members of the unfolded ensemble converge to the folded state ensemble, is difficult to describe in the detail usually afforded to small molecule reactions. The reactant, product, and transition structures in small molecule reactions are often unique, structurally defined points in a space defined by the $3n - 6$ degrees of molecular freedom, where n is the number of atoms in the system. Because of the relatively small number of relevant structural parameters usually involved for small molecules, the potential energy can be represented as a function of those parameters—a potential energy surface (PES). Given a complete description of the potential energy surface along the degrees of freedom relevant to the reaction, the kinetics and thermodynamics of the reaction, and indeed its mechanism, are described by the set of trajectories along that surface connecting the reactant and product. The average path of these trajectories then suggests a reaction progress variable known as the reaction coordinate.

Such an analysis is impractical, indeed impossible, for the folding reaction because many more degrees of freedom are involved and because the folding

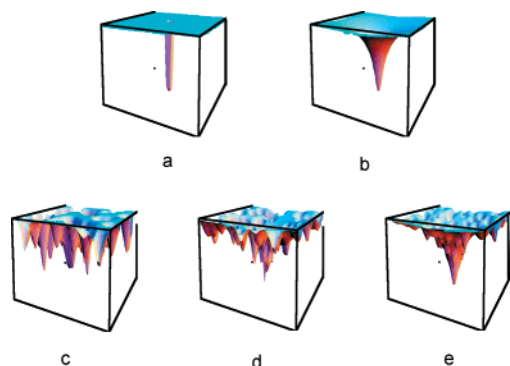


Figure 5. Free energy surfaces or “landscapes”. (a) The “golf-course” energy landscape, (b) the smooth funnel, and (c–e) rugged surfaces where c has no energy gap and e has a large energy gap.

reaction generally involves reactants, transition states, and products that are not single, well-defined structures. It is therefore much more difficult to define a reaction coordinate in terms of the internal coordinates of the chain. The situation is also more complex because a very large number of trajectories connect the many members of the unfolded ensemble with the folded state, often through an ensemble of transition structures. Because of these extra degrees of freedom in the reactant and transition-state ensembles, consideration must be given to the system's entropy, which is comparatively unimportant or easily deconvoluted in small molecule reactions. In addition, the role of the solvent is often significant in determining the energy of any given conformation; the exact structure of the solvent shell constitutes another large number of degrees of freedom, or structural variations, that must be taken into account.

For these reasons, the folding reaction is often described with a free energy surface (FES), or landscape. The FES is analogous to the PES drawn for small molecule reactions but includes a summation over the extra degrees of freedom, including those of the solvent, as a function of the internal coordinates of the oligomer. The effect of this summation at each point on the surface is the inclusion of the entropy at that point; the more degrees of freedom at that point, the larger the number of states at that point and the larger the entropy. Usually, the enthalpy and the entropy are evaluated over one or more progress variables, which are usually measures of structural similarity to the folded state, such as the degree of collapse or the fraction of interresidue ‘contacts’ that are present in the folded structure. Since FESs incorporate entropy, their shapes are very temperature dependent, unlike their PES counterparts.

Some examples of representative FESs are shown in Figure 5, including that for the lattice model (Figure 5a) examined above. This particular surface, consisting of a single, low-energy conformer distinct from the ensemble of nearly isoenergetic unfolded conformers is often referred to as the ‘golf-course’ landscape. If a more realistic description is used in which the unfolded conformers start taking on different energies, barriers between different minima

can become large enough such that examination of the kinetics across this surface is required.

Each accessible conformation lies at the bottom of local vibrational and torsional energy wells, and their energies will also be dependent on nonadjacent interactions such as electrostatic and van der Waals forces between nonneighboring chain segments and side chains. These nonadjacent interactions can be both energetically favorable and unfavorable. The folded state of a well-designed foldamer minimizes the unfavorable interactions and maximizes the favorable ones. Because small changes in local structural parameters, such as rotation around a bond, can bring previously separated parts of the molecule together, thereby introducing many new contact energies, the FES can be very rugged. This is not usually the case for small homooligomeric systems because of the relatively small number (compared to a biopolymer) of random intrachain interactions that generate the ruggedness. These systems have FESs such as that in Figure 5b, a smooth funnel. Longer chains, however, are capable of great ruggedness. Figure 5c depicts a completely rugged landscape with no single conformation dominating the thermal equilibrium mixture. Such rugged surfaces are typical of random heteropolymers, and an extremely poorly designed polypeptide would be expected to exhibit such an FES. Figure 5d shows a very rugged funnel, while Figure 5e depicts a classical rugged funnel typical of good folders having tertiary structure, such as globular proteins. Those systems having FESs such as Figure 5d might be expected to fold but more slowly than those having funnels such as Figure 5e since the greater depth of nonnative wells slows eventual escape to the folded state.

d. Kinetics of Folding. While the thermodynamics of some simple proteins and secondary structure domains are well modeled by the simple picture described above, the folding kinetics of chains can be more complex. The simple golf-course model (Figure 5a) grossly overestimates the amount of time necessary to reach the folded state, and this overestimation is often referred to as Levinthal's paradox.⁴⁹ For example, a protein containing 100 residues, each able to access only two local minima on the Ramachandran plot, has 2^{100} conformations. If it only took a picosecond to interconvert between conformers, it would take 10^{11} years to randomly search through all 2^{100} conformations before the system arrived at the folded state. This argument has been called a paradox because a concrete mathematical analysis gives an obviously erroneous result; the majority of globular proteins that exhibit simple two-state behavior fold on the timescale of a second or less.⁴⁷ However, the initial assumption that all 2^{100} conformers are equally thermally weighted is unfounded, despite the fitness of the model in describing the thermodynamics of folding. To accurately model the kinetics then, the loss of entropy that accompanies folding must be dealt with. Clearly, the FES of a foldamer cannot be described by a golf-course landscape if it is to fold reliably in a way that reproduces observation. It also suggests that more is required than simply the existence of a large energy gap for

the folded structure if the system is to fold on a reasonable time scale.

It is conceivable that the unreasonably long search time predicted by Levinthal could be reduced by decreasing the number of conformations involved in the random search. Discarding the conformations whose chains fold back on themselves and are therefore sterically disallowed reduces the number of conformers from 10^{60} to 10^{43} for a 2-D square lattice 100-mer,^{50,51} a number that still requires an unrealistic amount of search time.⁵²

If, however, the number of compact structures (those present after a solvophobic collapse) is considered, the size of the search drops further to 10^{17} conformers,⁵³ a much smaller number but one that is still too large for a truly random search to approximate real folding times. While the collapsed ensemble is still too large, it should be noted that the process of collapse reduces both the entropy and enthalpy of the system. This suggests a possible solution to Levinthal's paradox. Certain FESs can be described as funnels in which the energy generally decreases as the structure more closely resembles that of the folded state. Just as importantly, this lowering of the energy is accompanied by a concurrent loss of entropy. That is, the width of the funnel narrows and the energy goes down as the folded state is approached. Tyligomers must have FESs that are funnel-like, such that the overall free energy gradient favors movement of the system toward the folded state from any starting geometry or point of the multidimensional FES.

e. The Funnel Picture. For those systems with FESs resembling that in Figure 5c, that is, rugged surfaces with many deep minima and no single dominant folded state, any cooling will simply result in relaxation to the nearest well. If the temperature becomes low enough, the interconversion between these traps, or other deep minima structurally distinct from the folded state, will become very slow, even if one state is lower in energy than all the rest. Such conditions would lead to the observation of non-Arrhenius kinetics, as is observed for some polypeptides.⁵⁴ When this interconversion is slowed to the point that it is effectively nonexistent, a glass transition has taken place. At this point, it becomes very unlikely that the folding reaction, or indeed any further progress toward a global minimum structure, will proceed any further. Most folding biopolymers lie between the two extremes of the flat, rugged landscape and the smooth funnel, thereby exhibiting a range of thermodynamic and kinetic behaviors.

For systems with smooth funnel FESs such as that in Figure 5b, a cooling of the system will lead smoothly and rapidly to a relaxation to the bottom of the funnel. Such is the case for reliably folding helical oligomers. Again, small oligomers are more likely to have smooth funnels because shorter chains have fewer nonadjacent interactions that can contribute to ruggedness. The FES of an oligomer can be considered as a small section of a polymer's FES that immediately surrounds the folded state. Thus, the only ruggedness present in the oligomer FES will be that present near the folded state. Additionally,

the energy gap is already enhanced by the high symmetry of secondary structures. For instance, helices offer a minimally frustrated way of packing side chains to avoid unfavorable van der Waals forces while maximizing some favorable intrachain contacts, often hydrogen bonds. Small helices and sheets are thus well-designed folders, because of the smoothness of the FES and their energy gaps. Their thermodynamics are very similar to those for the golf-course model, as reflected in the similarity in the overall topology of the two funnels.

2. Foldamers: Secondary Structure

Since many of the foldamers described in this review have helical folded structures, the FES as well as the thermodynamics and kinetics of folding to a helical geometry will be considered in some detail. It should be noted that sheets, having regions of segments of the same dihedral angles, are themselves helices or bundles of two or more interacting helices. As a result, the mechanism of sheet folding is related to that for helices. It involves potential cooperativity in two dimensions, both along the strand and between strands.^{55,56} As it is slightly more complicated, it will not be treated in detail.

a. Folding of Helices: Thermodynamics of the Helix-Coil Model. Since the FES that describes helix folding, the smooth funnel, is topographically similar to that of the golf-course landscape, it represents a cooperative transition. There exists one transition between the higher energy unfolded state and the lower energy folded state. The statistical thermodynamics of the helix-coil transition were first described by Zimm and Bragg⁵⁷ as a one-dimensional problem. Cooperative phase transitions can be described in terms of a nucleation/propagation model,⁵⁸ a description of which follows.

Consider an oligomer that forms a helix with N_i segments per turn, again with ω conformations available to each chain segment. If the favorable intrachain contacts each contribute an energy ϵ to the system (usually called ϵ_H because a hydrogen bond is often responsible), the change in entropy and energy for each step of helix formation can be considered. Since each conformational choice along the chain—helical or nonhelical—is dependent only on the immediately previous step, the problem is essentially one-dimensional. That is, the free energy change of a residue as it progresses from a random-coil geometry to that of the helix is dependent only on the state of its neighbors. Figure 6 shows ΔH (ΔE) and ΔS for the coil-to-helix change for a segment adjacent to a helical segment and to a coil segment. Each situation involves the loss of $k_B \ln(\omega)$ conformational entropy. Only when $N_i + 1$ adjacent helix segments are formed does the system gain the ϵ interaction energy. Thus, for the first N_i coil-to-helix steps, there is a total loss of entropy of $N_i k_B \ln(\omega)$ but no gain in energy; this is called the nucleation of helix formation. Once this helix nucleation has occurred, each subsequent conversion of a segment from coil to helix geometry, i.e., propagation, involves the loss of $k_B \ln(\omega)$ entropy and a gain of energy ϵ .

The free energy change in going from a random coil to a helix where n is the number of segments in the

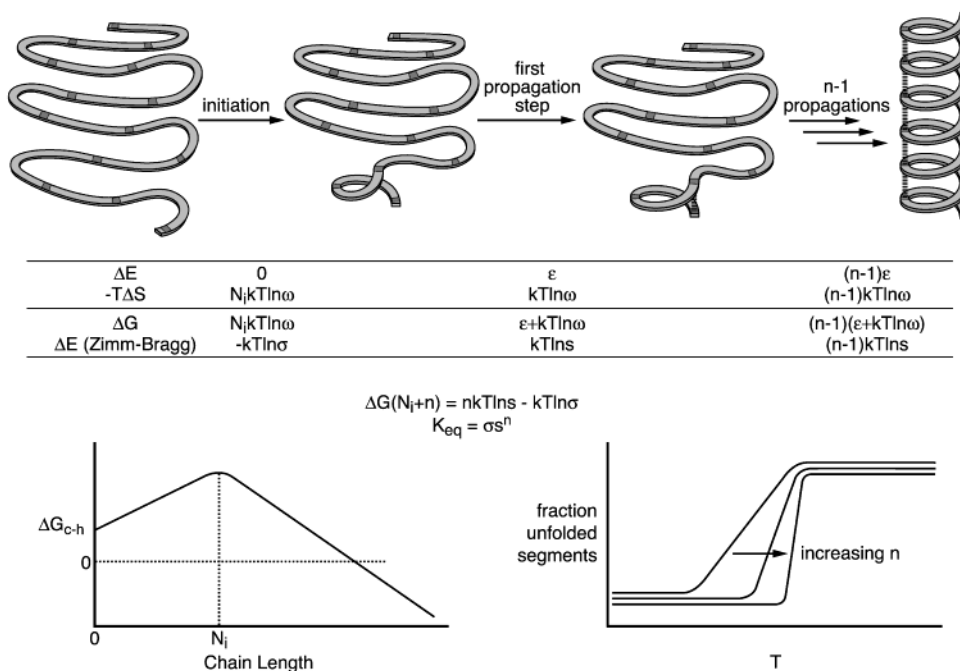


Figure 6. Helix–coil transition. (top) The initiation and propagation steps and their attendant changes in enthalpy and entropy. (lower left) The free energy of folding as a function of chain length, and (lower right) the sharpness of the transition as a function of chain length.

helix minus the number required to form the first turn is given by eq 6 and is plotted in the lower left of Figure 5.

$$\Delta G_n = \Delta G_{\text{nuc}} + n(\Delta G_{\text{prop}}) = N_i kT \ln \omega + n(kT \ln \omega - \epsilon) \quad (6)$$

There is a free energy cost upon folding until the chain reaches a length at which the enthalpic gain of the intrachain interactions outweighs the entropic cost of constraining the chain in the folded conformation. It can then be seen that a cooperative transition takes place when the change in free energy between helix and coil states becomes negative at the folding temperature, T_f (eq 7). The sharpness of this transition is dependent on the number of residues required for initiation, as can be seen from eq 2 and is shown in the lower right of Figure 6.

$$T_f = \frac{n\epsilon}{(N_i + n)k \ln \omega} \quad (7)$$

These quantities are often cast in the form of an equilibrium constant, with σ and s representing the equilibrium constants for the nucleation and propagation steps, respectively (eq 8)

$$K_{\text{eq}} = e^{-\Delta G/kT} = e^{-N_i \ln \omega} (e^{\epsilon/kT} e^{-\ln \omega})^n = \sigma s^n \quad (8)$$

where $\sigma = \omega^{-N_i}$ and $s = e^{\epsilon/kT} \omega^{-1}$.

Zimm and Bragg showed that the fraction of segments in a helical conformation exhibits a sharp cooperative transition as s is increased, which is equivalent to increasing the interaction energy ϵ or decreasing the temperature. The interaction energy is designed into the system based on the chemical

structure of the segments, but since it is a free energy it may also be changed by the environmental factors over which the free energy is evaluated. For instance, if the interaction arises from a solvophobic force, it can be made stronger by making the solvent more polar. Likewise, a hydrogen bond interaction can be made stronger by making the solvent less polar or weaker by adding competitive, protic solvents. Changing the net strength of the intrachain interactions shifts the folding temperature; this is the principal underlying solvent denaturation experiments. Rather than changing the temperature while keeping ϵ constant, the reverse may be done in order to see the transition.

Foldamers that adopt helical conformations are reliable folders because they lie on a smooth funnel FES. The folding to these highly symmetrical structures can be described by the two parameters ϵ and ω , both of which can be controlled by the foldamer chemist in the design of the oligomer.

b. Folding of Helices: Kinetics. Since helices have experimentally been shown to fold on a time scale in the milliseconds to microseconds,^{59,60} there do not seem to be serious kinetic issues that must be considered in their design. This is consistent with a smooth-funnel FES, with little ruggedness to slow the progress of the system down the funnel to the folded state. There is some evidence that the little ruggedness present does lead to the presence of folding intermediates for some helices,^{61,62} and in some cases the pathways between these intermediates can be enumerated,⁶³ but in general the folding should be rapid enough that (a) changes in the design will make only small differences in the absolute folding rates and (b) small helices with a thermodynamic propensity to fold will do so rapidly enough to demonstrate ideal foldamer properties.

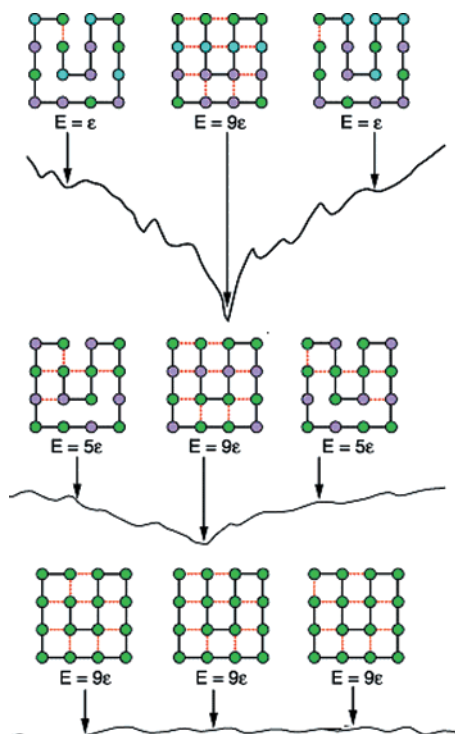


Figure 7. Effect of heterogeneity on energy gap. Homopolymers have degenerate folded structures, but increased heterogeneity leads to a larger energy gap between the lowest energy structure and the rest. (Adapted from ref 65.)

3. Tylligomers: Secondary and Tertiary Structure

This review covers the topic of foldamers, those oligomers that can fold, but since it is a natural goal of this field to be able to design and construct larger, more complicated molecules capable of folding to a greater variety of more complex structures, the issues of design of these tylligomers should be considered. Many of the aspects of folding are the same as those described above, but there are additional design issues that arise for tylligomers. Because such molecules have many more possible nonadjacent contacts and exponentially more conformations available, the FES can become much more rugged. There is also the need to construct heteropolymers of specific sequence to break the symmetry of the homopolymer.

a. Homopolymers vs Heteropolymers: Widening the Energy Gap. The high symmetry of helices is responsible for making them the lowest energy structures available to many of the short foldamers discussed below. Their existence belies the fact that homopolymers do not, in general, have unique low-energy folded states. This can be illustrated with a 2-D square lattice model in Figure 7. All of the compact homooligomers have the same energy. One way to reduce this degeneracy, and the way that has been employed by nature in the case of proteins, is to use several different residues in the chain. These different residues can have different interaction energies with each other and thus reduce the symmetry of the FES. For instance, using two different monomers in the oligomer, both of which interact with alike monomers much more strongly than with dissimilar monomers, will lower the relative energy

of some conformations as in Figure 7. The use of a three-letter code provides an even greater energy difference; the more information-rich the sequence, the more information-rich the FES.

While proteins are able to form very specific structures and perform very specific functions by employing 20 different types of monomers, or a 20-letter code, it is of great interest whether such a large number, and indeed such a large and complex set of sequences, is necessary for such specificity. Since the design and perhaps even synthesis of a foldamer with specific structure and function will be simpler with a smaller set of structural units, it would be advantageous to determine how small a set of these monomers can give rise to specificity of structure and, ideally, function.

Screening of combinatorial libraries of simplified proteins has recently revealed that as few as five amino acids can be necessary to generate a specific structure.⁶⁴ These same experiments suggested that when only three different residues are included, reliable folders are not made. The folding funnel can be used to interpret these results, as demonstrated in Figure 7.⁶⁵ Assuming a model in which interactions between similar residues are more stabilizing than those between different residues, it can easily be seen how a folded state with a large energy gap can be designed.

Simulations on a 2-D square lattice with a two-letter alphabet have been performed to determine what fraction of possible sequences have a unique ground state and how this fraction changes as a function of the number of residue types along the chain. Chan and Dill⁶⁶ enumerated all of the conformations of each possible HP heteropolymer of length less than 18, while Thirumalai and Camacho⁵³ did the same for $N < 23$. They reported that the average number of lowest energy conformations for a chain of length N converged to approximately 13 as N increased. They also reported that the average number of lowest energy structures had a minimum when the fraction of nonpolar monomers in the chain was around 0.6, which is approximately the same ratio as that found in proteins.⁶⁷ Chan and Dill earlier reported similar results and further calculated the percentage of sequences with unique ground states to be between 2.1% and 2.6% for sequences with $N = 12$ to $N = 17$. While they were not able to extrapolate this percentage to longer chains, they did estimate that the fraction of 100-mer sequences with a ground-state degeneracy of 5 or less to be on the order of 10^{-3} to 10^{-5} . Both of these studies suggest that even a very simple set of monomers may have a very good chance of exhibiting protein-like behavior by virtue of having a natively unique ground state.

Chan and Dill also evaluated the percentage of residues that existed in a secondary structure, either helix-like, sheet-like, or turn-like. They found that an average of ca. 40% of all monomers were part of a secondary structure over all conformations, a number that is in good agreement with the experimental observation that random heteropolypeptides exhibit 46% helicity, as measured by circular dichroism.⁶⁸ This percentage increased to over 60% for

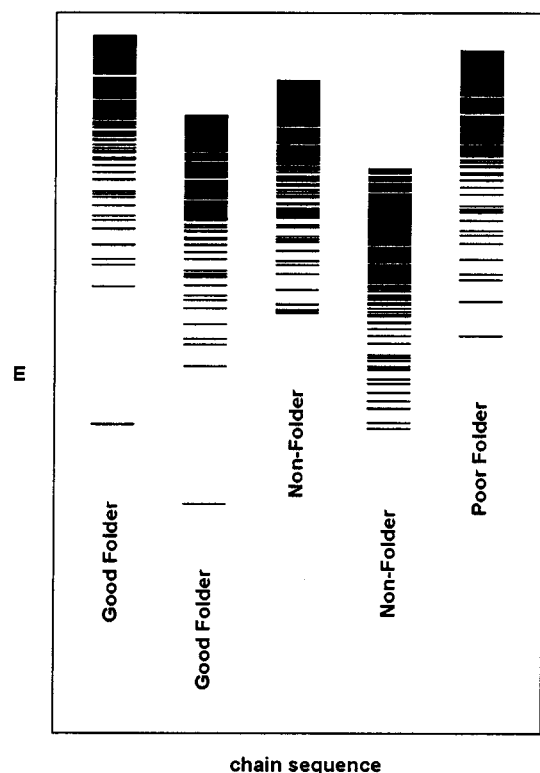


Figure 8. Energy spectra (density of states) for several 3-D 27-mer HP heteropolymers and the fraction of MC runs which resulted in folding. Larger energy gaps lead to greater foldability. (Adapted from ref 48.)

compact homopolymer conformations⁶⁹ and suggests that the formation of highly symmetric secondary structures is not sequence-specific nor only a property of reliable folders. The existence of these locally organized low-energy structures suggests a self-similarity of the FES that enhances its funnel-like shape even if helices or sheets that are not present in the folded state are formed during folding.

Similar studies were performed on 3-D 27-mer HP heteropolymers,⁴⁸ but because of the much larger number of possible conformations, the sequence space was sampled randomly. The likelihood of folding for several randomly generated sequences was evaluated by measuring the number of random Monte Carlo steps required for the sequence to find the folded state.^{70–72} Figure 8 represents the energy spectra of several of these sequences and the folding efficiency, which was measured as the fraction of MC runs that led to folding. Each individual line represents an individual conformation and its height the energy of that structure. Degeneracy of conformations is represented by the dense packing of states, which appear as regions of solid continuum. It can be seen that although each of the sequences had a nondegenerate ground state, only those with a large energy gap were reliable folders. Again, this indicates that a large energy gap, which will be referred to below as δE_s , between the native state and the rest of the non-native states is at least necessary if a chain is to fold.

b. The REM Analysis of the Rugged Funnel. It has been noted that the stability gap alone does not indicate whether a polymer will fold. If the barriers to interconversion between the states shown

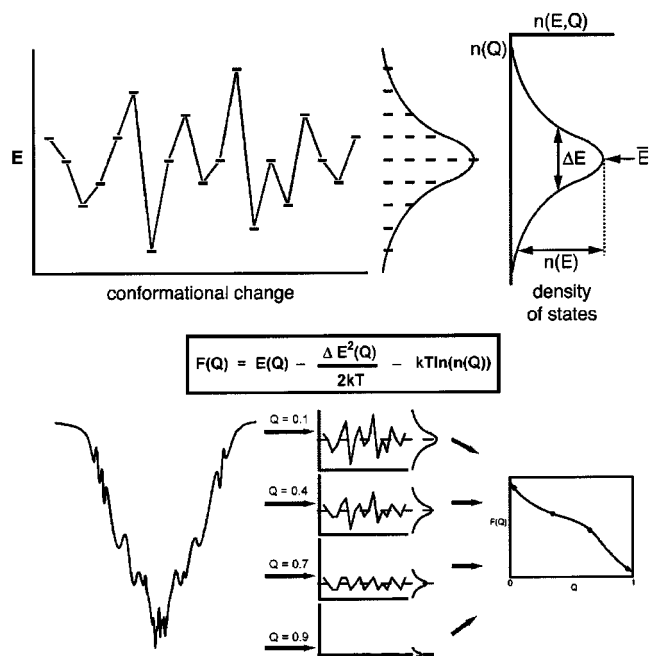


Figure 9. REM analysis of the rugged funnel. Free energy diagrams can be generated by examining the density of states at every level of the funnel.

in Figure 8 are taken into account, it is possible to imagine a system that becomes trapped in a non-native state, below the glass transition temperature, even if the folded state lies far below the trap. The kinetics and thermodynamics of rugged folding funnels have been analyzed by Wolynes and co-workers⁷³ using a random energy model (REM) developed by Derrida.⁷⁴ The large number of states and pathways between the states complicates a complete, explicit analysis of the free energy surface but is well-suited to a statistical description.

The key assumption of the generalized random energy model is that the energies of any two conformations are independent of each other. This leads to a distribution of states that can be described as a Gaussian function. This approximation can be made less stringent by assuming that there will be some correlation of energies, which will be dependent on the proximity of the two conformations to the folded structure. This similarity measure, called Q , is a function of certain internal geometrical coordinates of the foldamer that describe the folded state, such as those between nonbonded residues that become proximate after folding. The rugged funnel, shown in Figure 5e, is intermediate between the completely rugged surface, shown in Figure 5c, and the smooth funnel, shown in Figure 5b. The parameter Q on the rugged funnel roughly indicates the energy of a conformation arising from the smooth funnel component. The closer Q is to 1, the more the conformation resembles the folded state and the lower the energy will be in general. Within each strata of Q on the funnel, however, the energy level distribution will be given by a Gaussian function, in that it represents the smooth funnel component of the FES (Figure 9). This density of states, or the probability that a given state will have a structure parameter Q and an energy E , is given by eq 9. Here $\overline{E(Q)}$ is the average

energy of all structures having a structure parameter of Q . $\Delta E^2(Q)$ corresponds to the width of the Gaussian distribution for all of the structures at Q ; this value is a measure of the roughness of a section of the FES that contains all of the structures at Q .

$$P(Q, E) = \frac{1}{\sqrt{2\pi\Delta E^2(Q)}} \exp\left\{-\frac{[E - \overline{E(Q)}]^2}{2\Delta E^2(Q)}\right\} \quad (9)$$

To describe the thermodynamics, the free energy can be evaluated. Assuming that the folding reaction is taking place at constant temperature and pressure, the free energy is given by eq 10, where E_{mp} is the thermally most probable energy and S the entropy.

$$F(Q) = E_{mp}(Q) - TS(E_{mp}, Q) \quad (10)$$

The entropy can be calculated by taking the logarithm of the amplitude of the density of states (the height of the Gaussian distribution). The energy can then be evaluated by determining the value at which the density of states function reaches its maximum value.

Substitution and simplification gives the following expression for the free energy of the system as a function of Q in terms of the average energy along the funnel (equivalent to its slope) and the ruggedness or width of the Gaussian probability distributions at each strata of the funnel (eq 11). The derivation of this result is depicted graphically in Figure 9.

$$F(Q) = \overline{E}(Q) - \frac{\Delta E^2(Q)}{2kT} - TS_0(Q) \quad (11)$$

A significant feature of this model is that it predicts a glass transition, that is, a point below which the entropy of the system goes to zero. The entropic part of the free energy expressed in eq 11 is clearly given by the last two terms divided by the temperature (eq 12).

$$S(Q) = S_0(Q) - \frac{\Delta E^2(Q)}{2kT^2} \quad (12)$$

The temperature at which the entropy becomes zero and therefore at which no other structures are kinetically accessible is then given by eq 13 and is called the glass transition temperature.

$$T_g(Q) = \sqrt{\frac{\Delta E^2(Q)}{2kS_0(Q)}} \quad (13)$$

Below this temperature, the system becomes trapped as the barriers to interconversion between states become thermodynamically insurmountable. The larger the roughness of the surface, represented by the width of the Gaussian that describes the energy distribution function, the higher this T_g occurs. Thus, the roughness of the surface can be identified as another parameter that determines the foldability of a chain because it is this roughness that determines how likely the chain is to become frozen

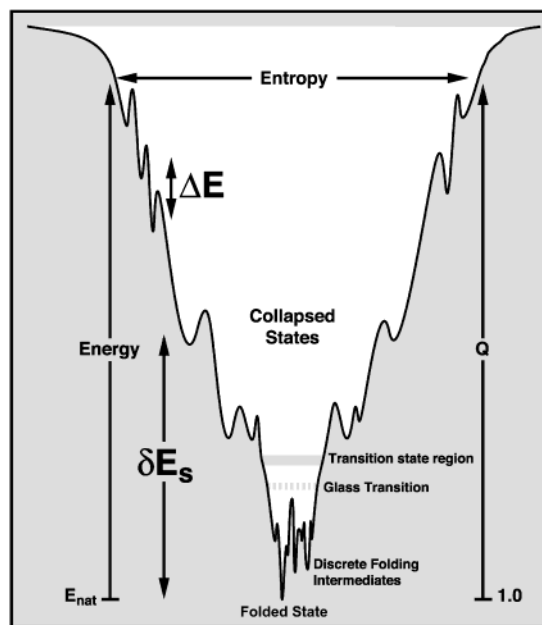


Figure 10. Folding funnel.

into a nonnative state before it can reach the global minimum. While T_g is the primary kinetic parameter of this analysis, T_f , or the folding temperature, is the primary thermodynamic one and has the same meaning and derivation as that discussed previously. It can be shown that $T_f \approx \delta E_s/S_0$, which describes the slope of the folding funnel in terms of the energy gap between the folded and unfolded populations, δE_s . As would be expected, the larger the energy gap, the higher the folding temperature will be.

These parameters can be illustrated on a more detailed schematic of the folding funnel (Figure 10). The height of the funnel FES corresponds not only to the energy but also approximately to Q , the folding reaction coordinate. These are E_{nat} (the energy of the folded state) and 1 at the bottom of the funnel, respectively. The width of the funnel is approximately the entropy or the density of states at that level of the funnel. As the system progresses down the funnel, it has the possibility of passing through a collapsed state, a transition state, and a glass transition. The degree of ruggedness also changes as the system progresses down the funnel.

It has been shown by Wolynes and co-workers^{75,76} that maximizing the ratio of T_f to T_g produces the most reliable folders, and this ratio is related to the ratio of the energy gap to the ruggedness (eq 14).

$$\frac{T_f}{T_g} \approx \frac{\delta E_s}{\Delta E} \sqrt{\frac{2k}{S_0}} \quad (14)$$

It should be noted that reducing the ruggedness measure $(\Delta E)^2$ to zero gives the same result as that obtained for the smooth funnel that models the folding of a helix. The possibility of another transition, the glass transition, reveals the complexity possible in the tylogomer folding mechanism. Tylogomers with particularly smooth FESs may never encounter this second-order phase transition and exhibit simple and cooperative Arrhenius kinetics. As the ruggedness is increased, the likelihood of encoun-

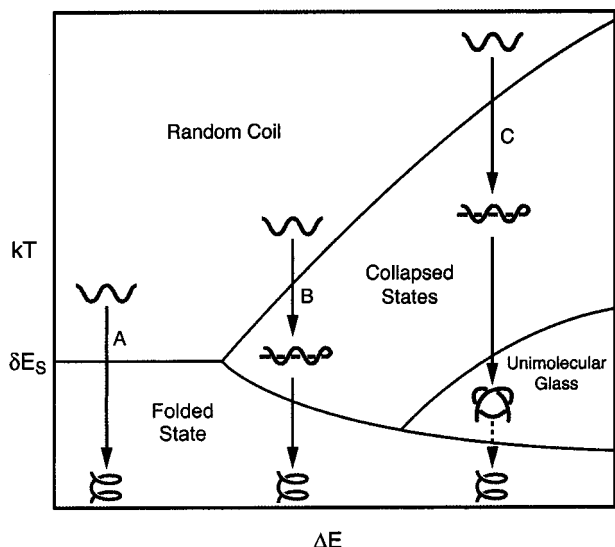


Figure 11. Phase diagram of foldamers. The ruggedness of the FES is ΔE . Small, two-state foldamers exhibit only a single cooperative transition (A). Tylligomers, both longer and having more rugged FESs, undergo a preliminary collapse transition which then folds to the folded state (B). Increasing the ruggedness further leads to a glass transition (C) where subsequent formation of the folded state may be extremely slow.

tering a second transition and complex dynamics increases. This is illustrated in the folding “phase diagram” (Figure 11), which has been generated by enumeration of a 2-D lattice model⁷⁷ and corroborated by other theoretical and experimental results. Along the x -axis is the ruggedness, and the y -axis represents the temperature. The smoothest funnels will undergo collapse and folded structure formation at the same time in a very cooperative process (pathway A), which is reminiscent of a two-state cooperative system. As the $(\Delta E)^2$ increases, a transition to the collapsed state may be observed (pathway B), followed by folding to the folded state. This collapse transition has been observed in homo-⁷⁸ and heteropolymer⁷⁹ lattice simulations. In both studies, the collapse transition was sometimes accompanied by folding fully to the folded state, especially when the intrachain contact energies were large. Of course, increasing these energies raises the folding temperature and in effect decreases the relative ruggedness. When the ruggedness is increased still further, the possibility of a glass transition (pathway C) exists.

A ratio of T_f/T_g of greater than 1 is required for a polymer to be a reliable foldamer, and this analysis provides some parameters that must be considered in the molecular design. Just as lattice simulations and simpler thermodynamic models suggested, maximizing the energy gap produces a more reliable folder. Minimizing the ruggedness to avoid the slowing of interconversion of conformers on the way down the funnel also gives a better folder. The last parameter, S_0 , is related only to the number of possible conformations available to the system. It is shown that the smaller this number, the better the folder will be. Thus, the conformational flexibility of each residue must be taken into account when designing a tylligomer and is possibly the most easily controlled of the parameters generated by the REM funnel

analysis. The readers are directed to excellent reviews^{39,80} of the folding funnel for further details.

4. Designing Folding Molecules: Toward Tylligomers

a. Designing Foldamers: Helices and Sheets.

The design of helical oligomers, then, is a fairly simple task, compared to the design of tertiary folds. Of course, any design must take into account the synthetic feasibility of the chain, and this is addressed in the next section. Since helices appear to fold on a very small time scale along a smooth funnel, an oligomer that folds to a helix or a small sheet (usually called a turn) must meet only thermodynamic criteria, namely, the δE_s , and S_0 parameters discussed in the rugged funnel analysis above. Since the funnel is indeed smooth, we can consider the ruggedness ΔE for oligomeric systems to be negligible.

The simpler of these parameters is the conformational entropy, S_0 , which is a function of the chain length and conformational entropy of each chain segment. The chain length may be tuned by the synthetic chemist, either by the traditional methods available for polymerizations or by the synthesis of discrete oligomer lengths. As discussed above, the conformational entropy of the chain segments can be determined by a simple Ramachandran-like analysis of the segment’s potential energy surface. A greater number of conformations available to each segment will tend to reduce the foldability simply by increasing the conformational phase space through which the ‘search’ for the folded state takes place. In other words, increasing ω increases the entropy that must be lost to achieve folding, thereby lowering the folding temperature. Of course, lowering ω too far can result in raising the folding temperature to the point that the unfolded state will never be observed at relevant temperatures. This is problematic for foldamers whose function depends on the reversibility of folding.

Chemically, of course, the segments must be joined in such a way that a helix or a turn is at least a plausible sterically allowed structure among many nonordered conformations. Simple chemists’ intuition or molecular modeling should be adequate to determine this criterion. Second, the turns of the helix or the strand-to-strand contact must be stabilized by some interaction that is long range or not on adjacent monomer units. Several analyses have indicated that the energy gap δE_s must be maximized for a reliable folder, but how is this related to the actual physical parameters of oligomers? Larger intrachain interaction energies and greater heterogeneity of residues (and thus interaction energies) tend to maximize the energy gap, as does the minimization of geometrical frustrations arising from sterically unfavorable backbone or side-chain interactions in the folded state. (Adjacent contacts may result in noncooperativity.) The orientation and strength of these interactions is the key factor that will stabilize the folded state. The strength of the interactions may be difficult to predict since they will be dependent on extrinsic factors such as the solvent and may be enhanced or diminished by nonspecific, nondirectional forces in the molecule, such as the solvophobic force. It could be considered

that the stronger these interactions are, the “better” the foldamer would be. However, this may not be the case; one must always consider the strength of all of the interactions in the folded state relative to the entropy of the chain that is lost upon folding. Again, interactions that are too strong will lead to a structure that will never unfold. It should be noted that stronger interactions may be required for the folding of multistranded systems to overcome the greater entropy loss that must occur from bringing two noncovalently connected pieces of the foldamer together.

Ideally, to be able to observe a folding reaction, the entropy must be balanced with the enthalpy of the intrachain interactions over some reasonable temperature range that allows observation, characterization, and utilization of the two states.

b. Toward Designing Tyligomers. The analysis of the rugged funnel landscape indicates the properties the FES of a chain should have in order to be a reliable folder. Rational design of a foldable tyligomer, then, depends on being able to control not only the thermodynamic parameters discussed above, δE_s , and S_0 , but also the kinetic parameter, ΔE , or FES ruggedness.

It has been noted that while in general homopolymers do not exhibit unique ground-state structures, many of the homopolymers described in this review do exhibit structurally unique folded states reminiscent of small proteins or at least of highly symmetrical secondary substructures of protein segments. The apparent contradiction results from the symmetry of the folded conformations of these relatively short homopolymers and of the smoothness of their funnels. Just as atomic clusters exhibit magic numbers,⁸¹ that is, structures of certain sizes which possess a high symmetry exhibit larger than expected stabilities, so too do proteins. It has been found that certain numbers of residues⁸² and secondary structures⁸³ occur more frequently than others in the set of known proteins. There is no reason to suppose that the high symmetry of helices should not also reduce the degeneracy of homopolymers as well.^{84–86} This does point to the need for further heterogeneity in future tyligomers if less symmetric folded structures are to be realized. It also suggests that the inclusion of these symmetric domains in a complex tyligomer may result in a smoother, steeper funnel.⁸⁷ Nature has made full use of these symmetric domains in biopolymers, not only as structural motifs, but also as easily foldable, funneled domains in the overall folding funnel.^{88,89} While such secondary domains may not be necessary to ensure a foldable oligomer, they may provide a simplifying shortcut from the design perspective. Lattice model tertiary structures containing high helical content have been shown to be highly foldable.⁹⁰ Indeed, the de novo protein designs to date rely heavily on the presence of secondary structures.⁹¹ Lattice model studies have shown that strong short-range chain–chain interactions provide a large energy gap with cooperativity.^{92,93} On the other hand, tyligomer designers must also take care to include a sufficient number of longer range chain–chain interactions. Lattice model stud-

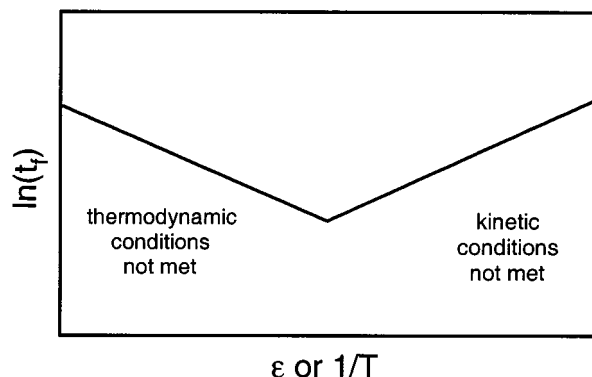


Figure 12. Non-Arrhenius folding kinetics. The folding time as a function of the intrachain interaction energy or equivalently temperature.

ies⁹⁴ indicate that longer range interactions speed up the folding reaction as well as make it more cooperative.⁹⁵

The heterogeneity of the chain can be controlled completely by discrete synthesis, and the strength of the intrachain interactions can be controlled by the choice of chemical moieties present in each monomer. It should be noted that increasing the strength of the interactions that hold the compact folded state together is equivalent to raising the folding temperature or lowering the ambient temperature. All of these serve to increase the thermodynamic likelihood of folding. However, it should also be noted that increasing the interaction magnitudes too much could lead to a decrease in the folding rate, even for homooligomers. This leads to a consideration of the ruggedness parameter, ΔE .²

Ruggedness is a property of the FES that should be minimized in a reliably folding tyligomer. If the favorable interaction energies that keep the chain in a compact conformation become too large, then interconversion among these compact states will become too slow. Deep energy wells will have large barriers to interconversion. In fact, the incorporation of secondary structures that are too strongly stabilized may increase the ruggedness and slow the folding rather than facilitate it.

Thus, increasing the magnitude of this intrachain interaction energy will potentially increase the energy gap by deepening the funnel, but it can also increase the ruggedness. A plot of the folding rate versus the interaction energy, or equivalently the temperature, has a shape such as that in Figure 12. This non-Arrhenius dependence of the rate on the temperature has been observed in experimental measurements of the folding rate⁹⁶ as well as several lattice simulations,^{97–99} where the rate measured by the number of MC steps before the simulation arrives at the folded state. The reason for this behavior is that at temperatures higher than ideal or interaction energies lower than ideal, folding is not favored enthalpically, whereas at temperatures lower than or interaction energies higher than ideal, folding is slow because of slow passage over the barriers between local minima.

c. Predicting Foldability. It is relatively straightforward to determine if a certain tyligomer sequence will indeed possess a unique folded state that is

kinetically accessible from the unfolded ensemble. The rigorous approach is to simulate the folding funnel, which involves determining the energy gap and the ruggedness. Finding the magnitude of the energy gap requires the identification of the global minimum, the folded structure, which has been proven in information theory to be an NP-hard problem. That is, there does not exist an algorithm with a difficulty and average time of completion that scales polynomially with the size of the problem. Thus, essentially the only way to ensure location of the global minimum is to exhaustively search all of phase space, a prohibitively long procedure for the reasons that Levinthal illustrated. However, algorithms have been developed that stand a very good chance of locating the global minimum, often taking advantage of the properties of funnels just as real biopolymers do. Once the global minimum has been found as a likely candidate for the folded structure, the gap can be measured by comparing its energy to the energies of the next lowest lying states. While the presence of a sizable gap does not guarantee folding behavior, it does favor it, and the presence of degenerate states that are not similar in structure would be sufficient to screen out a polymer sequence as a folding candidate.

The characteristics of the funnel can also be measured, and given a knowledge of the ruggedness and slope as a function of Q , the free energy can be determined for each strata of the funnel by the equations given above.^{100,101} This can be accomplished by sampling the FES using Monte Carlo algorithms or by sampling during molecular dynamics simulations. Once enough structures are sampled for each strata of the funnel, a plot of the free energy as a function of Q can be made, which is very reminiscent of a potential energy diagram of the type used to picture the mechanisms of small molecule reactions. T_f and T_g can also be determined from this simulation data and the likelihood of folding evaluated.

d. Designing Tylogomeric Folded Structures.

It may be enough to simply show that a single structure can be obtained; if the goal is simply to design a chain that folds, this is sufficient. However, designing tylogomers that are capable of carrying out certain functions such as binding or catalysis will involve the much more complicated task of designing heteropolymers that fold to specific folded structures. Forward engineering is much easier if one knows the rules of design, which can be learned from extensive reverse engineering. There has been some progress made on the reverse engineering of proteins, that is, the *ab initio* prediction of protein structure given the amino acid sequence. Unfortunately, most of this progress has been specific to the polypeptide chemical system and, as such, is parametrized for these particular biopolymers. Some theoretical work on this problem has been done, as well as lattice simulations, but there are few results that can guide the foldamer designer at present.

The forward engineering problem may be even more difficult for real systems, but there has been some illuminating work done using lattice models that helps to identify the challenges involved. Lattice

simulations have demonstrated that not all structures are equally designable. An exhaustive enumeration of all of the possible 3×3 3-D lattice two-letter alphabet structures and sequences was performed.¹⁰² All of the sequences that had a high foldability were considered, and it was found that there were some structures to which many sequences folded and some structures to which no sequences folded. Earlier studies of 2-D lattices revealed the same result.¹⁰³ These structures that kept turning up were considered to have a high "designability". If one were to try to design a sequence that would fold to such a structure, one's chances of success would be relatively high. Additionally, such structures are more stable to mutations of the sequence and can be considered more evolutionarily robust.

Since there are some structures that are easier to design than others, their nature and structural properties should be considered. These highly designable 3-D lattice structures have high symmetry and often have high proportions of secondary structure-like motifs.^{104,105} Thus, there seems to be a correlation between those structures that are highly designable and the highly foldable sequences that fold into them. These design principals must be tested for the backbones and structural motifs that are described below. We must first learn to design synthetic foldamers that will simply fold before we can learn to design tylogomers that are endowed with the same specific functionality found among the biopolymers.

B. Foldamer Synthesis and Purification—The Chemistry of Oligomers

As discussed in the Introduction, one goal is the generation of high molecular weight tylogomers with discrete chain lengths and primary sequences. Yet, chemists' inability to prepare high molecular weight substances in pure, monodisperse form precludes their current study. Thus, the field is currently restricted to the size regime of oligomers. Even here the synthetic challenges are significant. It has been stated, "despite much methodological progress, the synthesis and purification of monodisperse oligomers often remains quite tedious."¹⁰⁶ Three approaches to heteromeric chain molecules have been developed: step-by-step, iterative, and polymeric growth. Step-by-step growth is the extension of a chain one monomer at a time and allows for high sequence control at the cost of slow chain growth. Iterative approaches permit more rapid chain lengthening, especially through split pool divergent/convergent methods, while imposing some limits on sequence control.¹⁰⁷ For instance, an orthogonally diprotected dimer, A–B, can be coupled to a tetramer, A–B–A–B, doubling chain length but limiting sequence variability. Solid-phase methodologies in foldamer synthesis have utilized both step-by-step and iterative growth.^{107–111} The third approach, polymeric growth, provides rapid but statistical chain lengthening to a heteropolymeric mixture with minimal control over length or sequence and, therefore, has been avoided for the generation of foldamers. Though modifications of polymeric growth methodologies to narrow chain-length distribution have been proposed, a reliable

approach to generation of heteromeric tylogomers remains unidentified. Furthermore, while methodologies for the separation and purification of polymers exist, strategies for isolating one component from a high molecular weight heteropolymeric mixture are lacking and may limit this approach toward the generation of sequence-specific chains.

C. Foldamer Characterization—Experimental and Instrumental Methods

Foldamer characterization is approached in two stages: determining the properties of covalent synthesis (structure and purity) and conformational analysis of the folded state. Although established methods for organic synthesis, such as NMR, HPLC, and mass spectrometry, are employed in foldamer research routinely, various techniques must be drawn upon in order to *infer* the state of aggregation and the solution conformation of a chain molecule. This first aspect mostly involves using conventional methods of organic and polymer analysis while the second is much more difficult, since most new foldamer backbones do not have established spectroscopic signatures of secondary structure. Table 1 shows representative examples of common approaches to foldamer characterization. In addition, there are three powerful approaches to ascertain the stabilizing forces responsible for the folded state: variation in oligomer length, stoichiometry (and concentration), and environmental conditions. Through the use of chain-length studies, information about the critical chain length in cooperative folding and the Zimm–Bragg equilibria, σ and s , can be determined.¹¹² Concentration effects are known to impact foldamer architectures¹¹³ and require scrutiny when attempting to characterize the folding transition of a particular foldamer. In a single-stranded chain, the folding process is driven by intramolecular association and, therefore, concentration must be kept low enough to avoid aggregation, which can disrupt the ability of the oligomer to fold into the most thermodynamically stable conformation. In multistranded foldamers, both concentration and stoichiometry must be controlled since subtle changes in either can promote the formation of deleterious assemblies. Additionally, titrations of multicomponent systems allow for the determination of the stoichiometric ratios of the assembly. Elucidation of specific interactions by investigating solvent, temperature, and pressure effects can reveal driving forces present in the folding reaction.

III. Foldamer Research

A. Overview

As implied in the Introduction, both proteins and (deoxy)ribonucleic acids can be viewed as ideal tylogomers—that is, the archetypal biological examples of discrete, high molecular weight macromolecules of mixed sequences with compact solution conformations assembled from many subunits of secondary structure. In our assessment of the literature, we have organized foldamer systems into four

categories: peptidomimetics, single-stranded abiotics, nucleotidomimetics, and multistranded abiotics. In general, single-stranded abiotics are unnatural backbones that mimic secondary structures, such as helices and sheets, while multistranded abiotics commonly emulate double- and triple-helical conformations seen in oligomeric nucleic acids. When examining those systems that fit within our definition of a foldamer, a subtle disparity in *motivation* and *method* for mimicking biomacromolecules is uncovered. This disparity has dictated the inclusion and exclusion of specific examples of foldamers in past reviews, with the single-stranded abiotics being predominantly identified as foldamers. Therefore, a short discussion of these distinctions is helpful to understand our delineation of the literature.

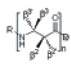
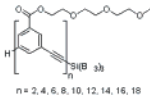
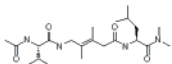
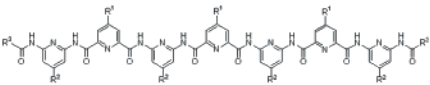
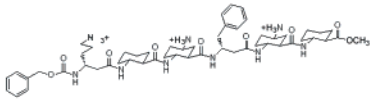
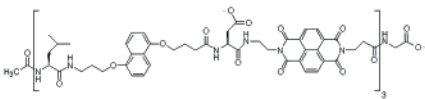
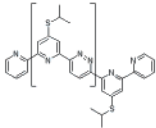
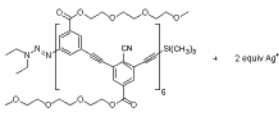
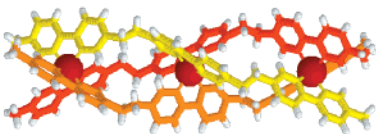
B. Motivation

The motivation for foldamer research will function as our first classification for this article. Specifically, we wish to call attention to the difference between “foldamer research” (the purposeful development of chain molecules that exhibit ordered conformations in solution predominantly determined by noncovalent interactions within or between nonadjacent monomer units) and “research on molecules that are foldamers” (the study of such molecules predominantly for their functional attributes). A myriad of functions have been sought in the study of foldamers, from information storage and antibiotic properties to gene therapy and materials applications. However, no matter what the final aim, there exists a clear disproportionality between the *basic* research of designing, synthesizing, and characterizing the secondary structures of unnatural oligomers and the *targeted* research of generating such molecules purely for their functional properties. More for historical than conceptual reasons, these motivations led to our first division of the literature into single- and multistranded foldamers, where single-stranded systems have predominantly been identified in the literature as foldamers.

C. Methods

Additionally, these two research motivations can be further categorized as being a part of either “top-down” or “bottom-up” foldamer design methods. Considerable progress has been made in the modifications of biological systems whose design is primarily based on a top-down approach, where logical extensions of either peptidic or nucleic backbones to enhance, elucidate, or mimic their structure and properties have led to related families of backbones, referred to here as peptidomimetics and nucleotidomimetics. Alternatively, supramolecular chemists have been interested in mimicking biological structures and properties from a bottom-up design, where analogous architectures to biomacromolecules are obtained by backbones that bear little resemblance to natural chains. Both design methods aim to develop unique structures that exhibit similarity to the components and the mechanisms of biochemical systems. Overall, we have chosen to arrange our specific examples not by application, but by the

Table 1. Foldamer-Specific Characterization Techniques, Possible Secondary Structure Data Thereof, General References Regarding Their Usage, and a Representative Reference, Structure, and Type of Foldamer from Each Field

Technique	Structural Information	General Reference	Representative Oligomer Reference	Structure and Type of Representative Oligomer
<i>Spectroscopic Methods</i>				
Circular dichroism (CD)	Chromophore interactions; local conformation of chromophore	902	223	 helical β -peptides
Fluorescence	Chromophore interactions; local conformation of chromophore	903	112	 helical oligo(<i>m</i> -phenylene ethynylene)
Infrared (IR)	Aggregation; H-bonding	904	342	 <i>trans</i> -5-amino-3,4-dimethylpent-3-enoic acid (ADPA) β -turn mimic
NMR (1D)	Aggregation; H-bonding; aromatic interactions	905	448	 helical oligo(2'-pyridyl-2-pyridinecarboximide)
NMR (2D)	3D arrangement of structured backbone in solution	905	239	 helical <i>trans</i> -2-amniocyclohexane-carboxylic acid (ACHC) β -peptide
Ultraviolet-Visible (UV-vis)	Chromophore interactions; local conformation of chromophore	906	391	 donor-acceptor stacked aedamer
<i>Non-Spectroscopic Methods</i>				
Electron Microscopy	Real-space visulation of morphology and chain packing in the solid state	907	382	 helical oligo(pyridine-pyridazine)
Microcalorimetry (μ -cal)	Thermodynamics of folding and association	908	476	 helical oligo(<i>m</i> -phenylene ethynylene)
X-ray crystallography	3D arrangement of atoms in the solid state	909	815	 Helicate triplex

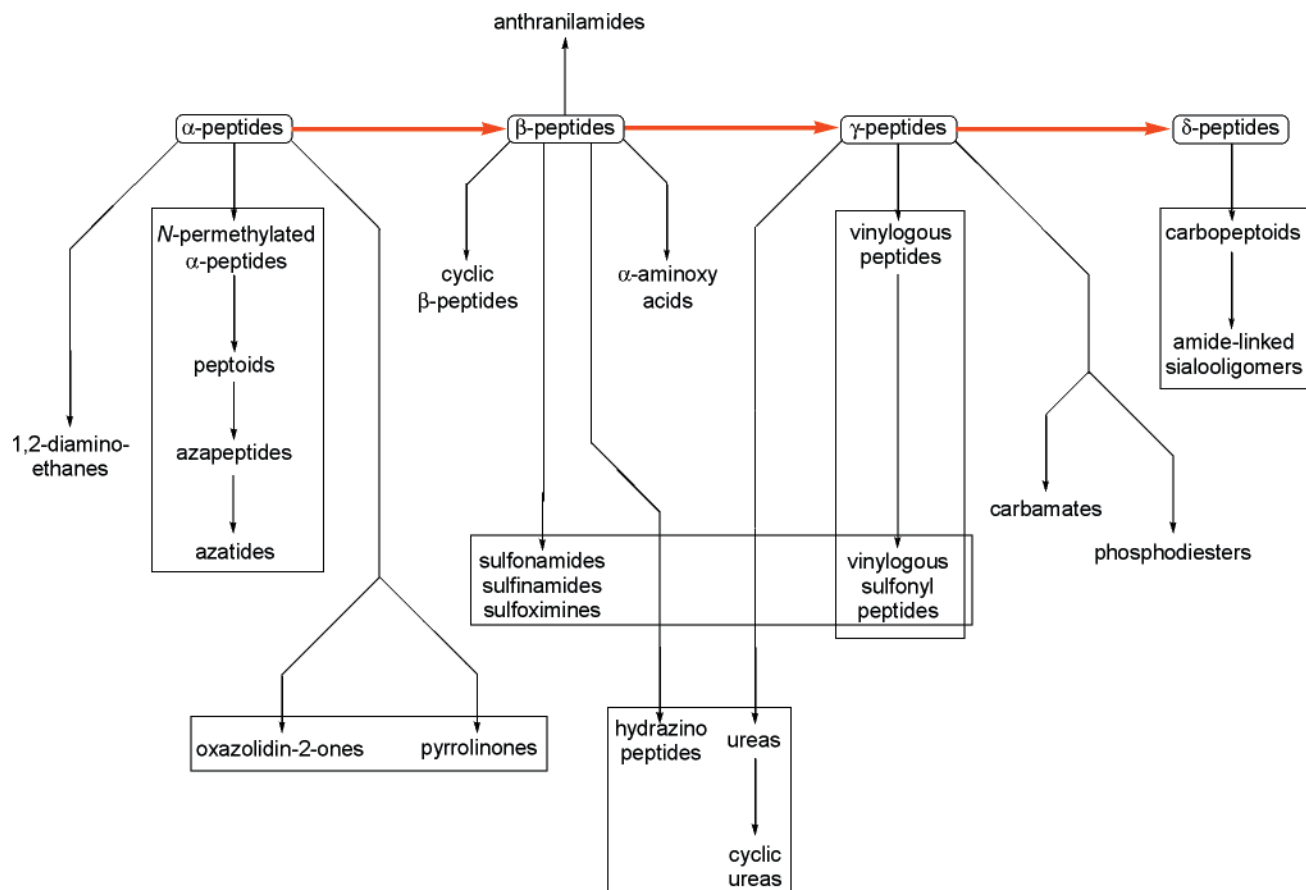


Figure 13. Structural lineage of peptidomimetic backbones.

structure of the backbone repeat unit, thereby casting a reasonably wide net of coverage. For these reasons, we partitioned the literature into peptidomimetics, nucleotidomimetics, and abiotic variations of each.

D. General Scope

Our foremost criterion for inclusion of specific examples from foldamer research in this section is as follows: was conformational analysis performed on the molecules in question through studies on discrete oligomers? We chose “interesting examples” from the literature to demonstrate the basic character of foldamer research and have been as exhaustive as possible within this definition of the field. Additionally, we limited our treatment of more extensive areas to suit the length of this review. While many of the following might technically fit our definition of foldamers, they will not be covered here: oligo(α -amino acid)s, oligo(deoxy)ribonucleotides, simple ligand–metal complexes, non-oligomeric synthetic receptors,^{114–119} non-oligomeric chemosensors,^{120–123} transition-metal-assembled three-dimensional cyclic nanostructures¹²⁴ and two-dimensional grids,¹²⁵ hydrogen-bonded networks and tapes,¹¹⁸ supramolecular polymers,^{33,126} dendrimers,¹²⁷ and oligomers mentioned in the Introduction. We will also not be inspecting the abundance of molecules that adopt helical conformations *only* in the solid state, as this defies our definition of having discrete solution structure.

IV. Peptidomimetic Foldamers

The field of peptidomimetics aims at mimicking peptide structure through substances having controlled spatial disposition of functional groups. Peptidomimetics have general features analogous to their parent structure, polypeptides, such as amphiphilicity. They have been developed, to a large extent, for the purpose of replacing peptide substrates of enzymes or peptide ligands of protein receptors.^{128–133} Peptidomimetic strategies include the modification of amino acid side chains, the introduction of constraints to fix the location of different parts of the molecule,¹³⁴ the development of templates that induce or stabilize secondary structures of short chains,^{135,136} the creation of scaffolds that direct side-chain elements to specific locations, and the modification of the peptide backbone. Of these strategies, systematic backbone modifications—structural alterations of the repeat unit—are most relevant to the field of foldamers. Backbone modifications may involve isosteric or isoelectronic exchange of units or the introduction of additional fragments. Efficient monomer preparations and repetitive synthetic methods for oligomer constructions have recently been developed for many biologically inspired, unnatural chain molecules.¹³⁷ To summarize progress to date on these systems and structurally organize them, a family tree of peptidomimetic backbones is shown in Figure 13, organized from left-to-right by the number of atoms separating peptide (or peptide-like) units and top-to-bottom by the functional group classes.

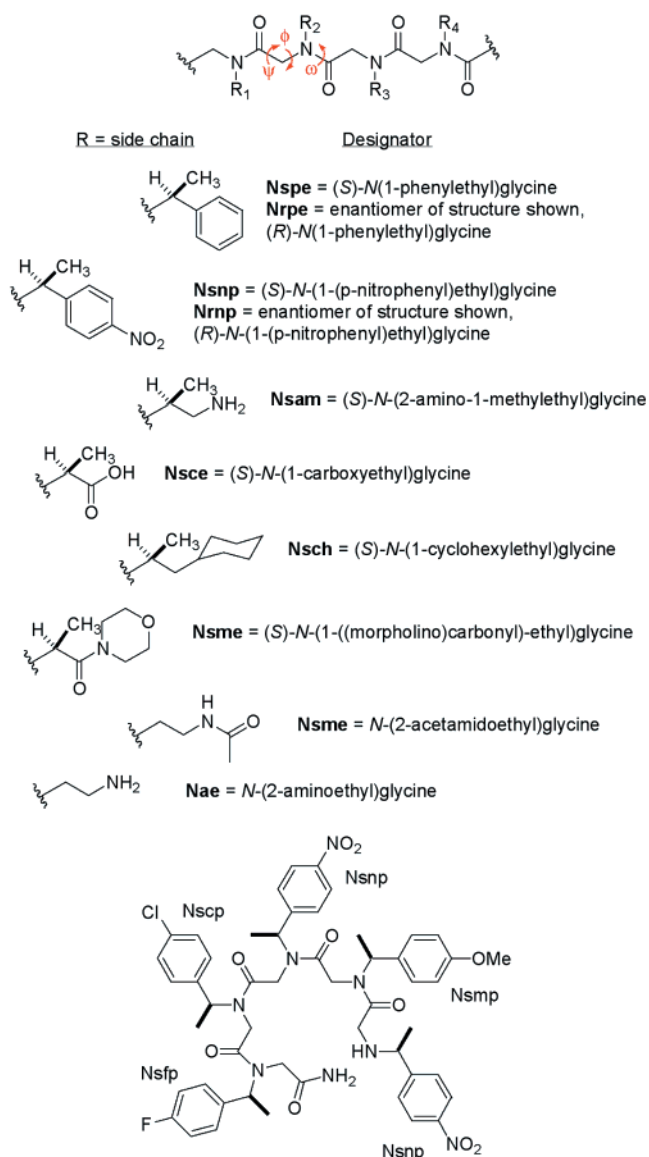


Figure 14. General peptoid backbone, representative chiral side chains, and a peptoid pentamer that adopts a helical secondary structure.

Our focus here is on peptidomimetic oligomers whose secondary structure has been well characterized. For some of these backbones, monomers and sequences giving rise to helical, extended (i.e., “strand”), and turn conformations have been identified. These will be discussed in greatest detail. Other systems included in this section are considered either as potential foldamers or systems that have been discussed within the context of foldamer research but for which only limited information about their secondary structures is presently available. In these cases we will restrict our discussion to brief summaries.

A. The α -Peptide Family

1. Peptoids

Poly-N-substituted glycines or “peptoids”¹³⁸ belong to the α -amino acid lineage, differing from their genitor in that the pendant groups are attached to the amide nitrogen rather than C_{α} (Figure 14).

Although these peptidomimetic oligomers lack stereochemistry in the backbone, their side chains are spaced apart by a distance similar to that of the natural backbone. The absence of amide hydrogens precludes the possibility of intramolecular $CO\cdots H-N$ H-bonds. Moreover, low energy conformations for tertiary amides include both *cis* and *trans* states about the peptide bond (*cis* amide refers to geometries where the main-chain C_{α} atoms are *cis* to one another). Calculations on dipeptoids^{138,139} reveal significant twisting about the peptide bond owing to steric interactions that involve the nitrogen substituents. These steric interactions limit the set of energetically accessible conformations about the other two backbone torsions. The lack of H-bond constraints and the presence of both *cis* and *trans* peptide bonds are reasons to expect the conformational diversity of peptoids to be greater than α -peptides. However, peptoid sequences as short as five residues adopt stable helical secondary structures in a variety of solvents, and the unfolding process is both reversible and cooperative.¹⁴⁰

Calculations predicted that peptoids bearing side chains with stereocenters adjacent to the main-chain nitrogen have a limited number of energetically accessible conformations.¹⁴¹ On the basis of this prediction, longer oligomers were postulated to adopt a helical conformation with *cis* amide bonds, similar to the polyproline type I helix. To test this idea, a series of peptoid sequences were prepared from monomers bearing chiral, nonracemic side chains (Figure 14).¹⁴⁰ The shape of the CD band changed from the monomer up to the pentamer, beyond which the CD band shape remained constant with increasing chain length, resembling the α -helical conformation of the α -peptide backbone. Moreover, beyond the pentamer, the intensity of the CD signal, on a per-residue basis, did not increase.^{140,142}

A pentamer sequence that exhibited good dispersion and sharp 1H NMR signals was used in a detailed conformational study.¹⁴³ On the basis of ROE cross-peak data obtained in methanol, all of the amide bonds of the major species were of *cis* geometry. Although multiple species in slow exchange were apparent from the NMR spectra, the major species was determined to be a regular helix with three residues per turn and a pitch of ca. 6 Å, in good agreement with molecular modeling predictions. The minor species were postulated as resulting from slow exchange of *cis* and *trans* isomers.

The conformation of the major species identified by 1H NMR was presumed to give rise to the observed CD signal. To verify this, the conformational transition was studied by CD as a function of both pH and temperature for peptoids bearing ionizable carboxylic acid side chains.¹⁴⁰ Over the pH range of 7–3, the CD signal intensity of a 30-mer changed very little. At pH 2, the CD signal was greatly diminished and interpreted to signify complete unfolding. At pH 4.1, this oligomer exhibits a complete, reversible loss of the helix-like CD signal over a 40 °C temperature range. Although it is not clear what causes helix destabilization at low pH, the behavior was characterized as highly cooperative as compared to α -peptides of similar length.

Recent studies by Barron et al. helped refine details on the sequence¹⁴⁴ and chain-length¹⁴² requirements for stable peptoid helices. A systematic study using a series of discrete homooligomers of (*R*)-*N*-(1-phenylethyl)glycine ranging from 3 to 20 residues in length showed that there is a length-dependent shift in the relative population of *cis*-amide helices. The spectrum of the nonamer is unlike any of the other members in the series, suggesting that this sequence adopts a different conformation. However, the unusual behavior of this particular chain length is presently unexplained. When the oligomer length exceeds 12 residues, a helix with *cis* amide bonds becomes the most favored conformation by a significant degree, and no changes are noted in the CD of longer chains up to the 20-mer. In an effort to better understand factors that contribute to helix stability, a series of 30 heterooligomers was prepared and their solution conformation studied by CD and NMR.¹⁴⁴ On the basis of these results, it was concluded that a stable helix results from (1) a monomer composition in which at least 50% side chains bear *N*- α -stereocenters and aromatic substituents, (2) placement of one or more α -chiral substituents on the carboxy-terminus to prevent helix fraying, and (3) a sequence that maximizes the number of aromatic–aromatic interactions along the direction of the helix axis. While these factors contribute significantly to the stability of short peptoid helices, they are less important for peptoids containing more than 12–15 monomers, as the chain length itself contributes significantly to helix stability.

Protease enzymes do not degrade *N*-substituted glycine oligomers.¹⁴⁵ This observation together with the fact that peptoids are readily synthesized¹⁴⁶ by standard solid-phase methods and the fact that many display good solubility in water make them prime candidates for pharmaceutical and agrochemical research. Peptoid analogues of peptide ligands were identified in the initial studies supporting the feasibility of this idea.¹³⁸ More recently, cationic peptoid sequences were shown to be efficient reagents for gene delivery.¹⁴⁷ A combinatorial approach that varied chain length, frequency of cationic side chain, hydrophobicity, and shape of side chain produced a small subset of sequences that were active at condensing DNA and offering nuclease protection. One member of the peptoid library, a 36-mer, was found to have good transfection activity for many cell lines, apparently as the result of a spherical nanostructure complex that it formed with DNA.

2. *N,N*-Linked Oligoureas

In 1992, Nowick and co-workers began a program of study on acyclic oligomers whose conformations are stabilized by intramolecular H-bonds. As part of this effort, they investigated the solution and solid-state structures of a family of *N,N*-linked oligoureas having the repeat unit $[-N(\text{CONHR})-(\text{CH}_2)_m-]$,¹⁴⁸ the $m = 2$ member of this family belongs to the α -peptide family of peptidomimetics (Figure 15). This particular chain molecule has interesting conformational characteristics in solution, in part owing to the **S(9)** H-bond between side chains of adjacent units. (Throughout this review we use Etter's graph set convention to describe H-bond interactions:^{149–151}

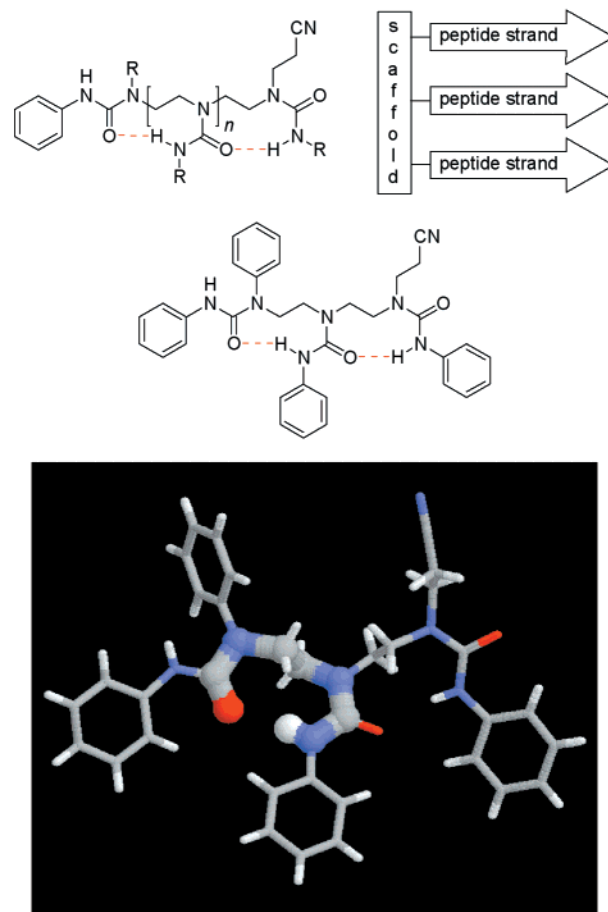


Figure 15. *N,N*-Linked oligoureas. X-ray crystal structure of a triurea derivative.¹⁵³

S(*n*) stands for “self” and denotes an intramolecular hydrogen bond involving *n* atoms; **C(*n*)** stands for “chain” and denotes a repetitive motif whose repeat unit contains *n* atoms). Detailed infrared and ¹H NMR studies have indicated that the dimer and trimer are fully hydrogen bonded in CHCl₃ solution.^{152,153} The ¹H NMR chemical shifts of the NH groups did not vary with concentration over the range from 1 to 10 mM, suggestive of intramolecular H-bonding.

The crystal structure of a triurea derivative revealed a conformation in which **S(9)** H-bonds orient the side-chain residues in roughly parallel directions, thus resembling peptide β -turns (Figure 15).¹⁵³ Thus, as originally envisioned,^{148,152} these peptidomimetics are well-suited as molecular scaffolds to template multistrand artificial β -sheets.^{154–157} It should be noted that if only simple urea pendant groups were attached to the oligomeric backbone, the nonadjacency criterion would place these structures outside of our foldamer definition. Given the collection of H-bonding interactions that comes with pendant β -strands, the conformation of these more complex *N,N*-linked oligoureas are stabilized by long-range noncovalent interactions, and therefore, they likely possess cooperativity and other characteristics expected of foldamers. We return to some of these aspects in the section of this review on multistranded abiotic foldamers.

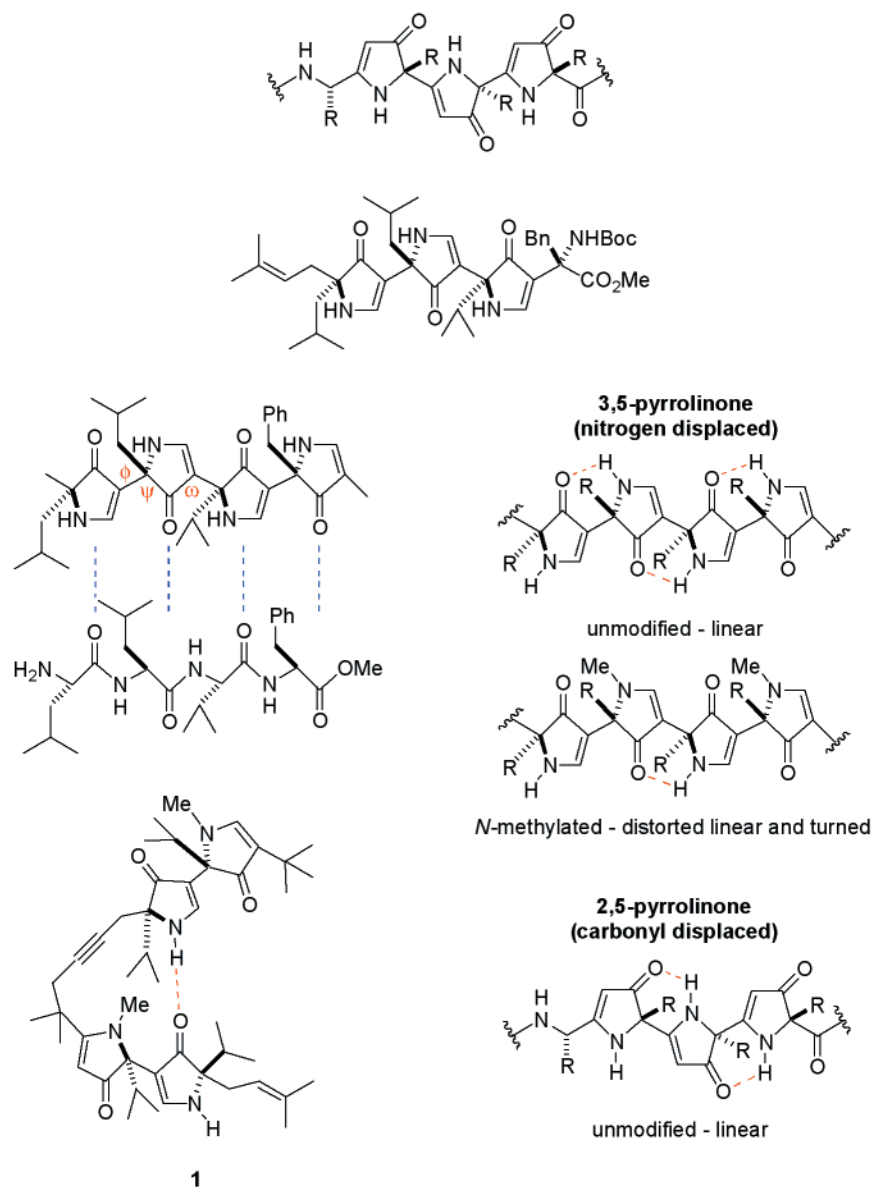


Figure 16. Oligo(pyrrolinone) backbones linked through the 2,5- and 3,5-positions. The correlation between the 3,5-linked pyrrolin-4-ones and α -peptide β -strands. The **S(6)** hydrogen-bonding interaction is indicated in red. *N*-Methylated 3,5-linked pyrrolin-4-one sequence **1** adopts a helical conformation in the solid state and in solution.

3. Oligopyrrolinones

Oligopyrrolinones (Figure 16) are best classified as members of the α -peptide backbone, even though their vinyllogous amide bond is not a part of the primary chain. With the initial intention of creating a non-peptide β -strand mimic,¹⁵⁸ Smith and Hirschmann originally conceived two backbone types (Figure 16).¹⁵⁹ The first is based on 3,5-linked pyrrolin-4-ones having an all carbon primary backbone in which the nitrogen is displaced relative to the α -peptide chain. The second is based on 2,5-linked pyrrolin-4-ones in which the primary backbone contains a nitrogen atom and the carbonyl is considered displaced relative to the α -peptide chain. Thus far, only the nitrogen-displaced backbone has been reported, although the other scaffolds still appear to be under consideration.¹⁶⁰

Peptidomimetics based on 3,5-linked, 5-substituted pyrrolin-4-ones have many structural features common to α -peptide chains (Figure 16). The carbonyl

group is spaced every three atoms with an orientation similar to that of carbonyl groups in β -pleated strands,¹⁶¹ while the nitrogen is displaced with respect to its usual location in the α -peptidic backbone. Incorporation of the nitrogen atom as a vinyllogous amide into the pyrrolinone ring provides rigidity and constrains the ψ and ω angles of the corresponding α -peptide chain. An **S(6)** intramolecular hydrogen bond between the $C=O \cdots H-N$ groups of adjacent residues helps to constrain the ϕ dihedral and ensure an extended conformation. By the non-adjacency criterion in our definition, this example is technically not a foldamer; it is simply an oligomer whose conformation is fixed by intramolecular non-covalent interactions. In other words, the chain's conformation can probably be described as a collection of independent units rather than as a cooperative group. Nonetheless, the oligomer is interesting because side chains added to the ring's 5-position are oriented similarly to those of an α -peptide chain that

adopts an extended β -strand conformation. A drawback to this design, however, is the difficulty of monomer and oligomer syntheses, which has been improved with a more general synthetic scheme, allowing the incorporation of functionalized side chains.¹⁶²

Molecular modeling and X-ray crystallographic studies¹⁵⁹ showed that side chains in the 5-position take on the alternating above-plane, below-plane orientations as found in β -pleated sheets. The pyrrolinone NH protons were observed to form hydrogen bonds both intramolecularly to stabilize the β -strand and intermolecularly to produce sheets. These observations suggest that the disposition of vinylogous amide carbonyls retain H-bond acceptor characteristics and closely correspond to the α -peptide chain. Furthermore, the pyrrolinone NH groups, while vinylogously displaced from the backbone, engage in H-bonding, presumably owing to their comparable basicity (pK_a ca. 2–3)¹⁶³ with amide NH groups (pK_a ca. 0–1).¹⁶⁴ Parallel and antiparallel strand orientations were observed in the solid state, depending on the presence or absence of protecting groups on the terminal nitrogen.

The oligopyrrolinone scaffold has been used as a protease inhibitor and a ligand for hormone and other protein receptors. The main idea is that these sequences can adopt bioactive conformations of endogenous peptide ligands while exhibiting good pharmacokinetic properties. This strategy was used to design pyrrolinone-based inhibitors of renin¹⁶¹ and HIV-1¹⁶⁵ proteases that are known to bind their substrates in an extended β -strand conformation. Similarly, this strategy was used¹⁶⁶ to design a bispyrrolinone-peptide hybrid ligand that binds class II MHC receptors, where the antigenic peptide ligands adopt extended, polyproline type II conformations with twisted backbones projecting side chains every 120° . The crystal structure of this complex shows that the bispyrrolinone unit adopts a polyproline type II-like conformation with the side chains projecting into the same places as the peptide side chains they replace. Moreover, the bispyrrolinone backbone forms H-bond contacts with the receptor in much the same way as the natural ligand.

N-Methylated bispyrrolinones adopt a twisted dihedral about ϕ which opens the way to helical conformations in longer oligomers.¹⁶⁰ This idea was supported by crystallographic observations that revealed an extended helical array in the solid state, based on intermolecular hydrogen bonding from O(1) of one molecule to the hydrogen on N(2) of a second. This led to the design of 3,5-linked pyrrolinone sequence **1** in which an alkynyl tether was used to join a pair of bispyrrolinone units (Figure 16), designed from the geometry of the solid-state helical array. The crystal structure of this tetrapyrrolinone shows a twisted conformation that resembles a short helical stretch, stabilized by an **S(14)** intramolecular H-bond. In chloroform solution, ¹H NMR and IR data indicate that this H-bond is maintained, suggesting that a similar conformation exists in solution and the solid state. These results show that the pyrrolin-4-one unit is a versatile building block that may be used to generate both extended and helical secondary structures.¹⁶⁰

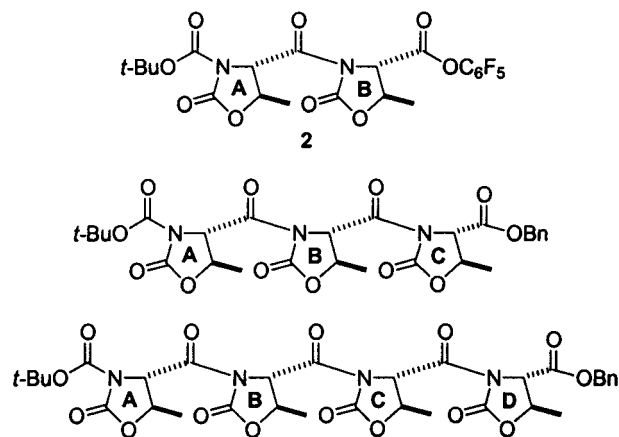


Figure 17. Oligomeric oxazolidin-2-ones synthesized and studied as possible foldamers.¹⁶⁷

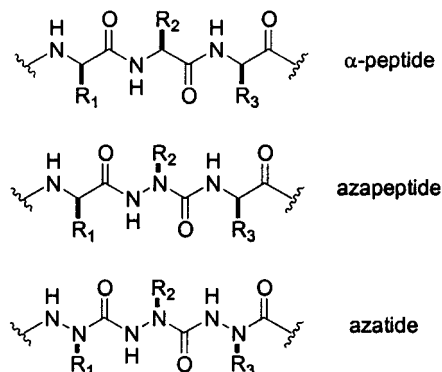


Figure 18. Comparison of the α -peptide, azapeptide, and azatide peptidomimetic backbones.

4. Oxazolidin-2-ones

Oligomers based on oxazolidin-2-ones (Figure 17) belong to the α -peptide genre and recently have been discussed in the context of foldamers.¹⁶⁷ This backbone can be considered as a pseudoproline structure. On the basis of ¹H NMR chemical shift data, shifts, and AM1 calculations, the bisoxazolidinone **2** was believed to adopt a conformation in which the two rings are approximately orthogonal to one another. A trimer and tetramer exhibited similar ¹H NMR behavior that led the authors to conclude that both oligomers fold into ordered structures. However, given the lack of supporting evidence and the apparent noninvolvement of conformationally stabilizing intrastrand noncovalent interactions, we hesitate to categorize these oligomers as foldamers at present.

5. Azatides and Azapeptides

Azatides and azapeptides are α -peptide relatives in which one or more of the α -carbons have been replaced by a trivalent nitrogen atom (Figure 18). While azapeptides (α -peptides in which only a portion of the C_α atoms are substituted with nitrogen) have long been known,¹⁶⁸ only recently have all-aza chains, or what has been termed azatides,¹⁶⁹ been synthesized.¹⁷⁰ The conformational properties of these oligomers have not yet been thoroughly explored, although they have interesting characteristics, which makes them appropriate for discussion here. Until more definitive studies are completed, we consider them as potential foldamers.

High-level *ab initio* calculations show that diacylhydrazines are intrinsically nonplanar with respect to the CO–N–N–CO torsion, and the corresponding rotational barriers are high.¹⁷¹ The global minimum finds the nitrogen lone pairs approximately perpendicular to one another. Thus, their conformational properties are essentially determined by the conformation of their hydrazine and urea constituents. As a result of restricted rotation about the N–N bond, azapeptides cannot adopt extended conformations. This is likely the reason that they are resistant¹⁷² to chymotrypsin-like proteases, which bind their substrates in extended forms.

X-ray data on azapeptides confirm their tendency to adopt turn conformations.^{170,173} For a variety of proteinogenic side chains, the most stable conformation is nearly identical to the calculated one. Although no azapeptides foldamers are presently known, they have been suggested as being strong inducers of secondary structure.¹⁷⁴ However, as their conformation is dominated by the intrinsic torsional characteristics of the hydrazine and urea constituents, it is unclear what role intrastrand noncovalent interactions will play in determining chain conformation. Consequently, the suitability of this unit as an ideal building block for foldamer research is called into question. More work is needed to determine the aptness of this subunit.

B. The β -Peptide Family

1. β -Peptide Foldamers

a. Introduction and General Considerations.

Considerable effort has been invested into studies on β -peptide backbones, a sensible starting point for foldamer research given the close relationship to the ubiquitous α -peptide^{175–178} chain. On the basis of the known high flexibility of glycine-rich peptides, one might expect β -peptides to possess greater conformational flexibility and, therefore, to be entropically disfavored from acquiring ordered solution conformations (Figure 19).^{179,180} In contrast to this intuitive view, certain substitution patterns in the β -amino acid family^{181,182} impart a strong bias to the torsional potential energy surface, enabling the formation of a rich variety of regular conformations.^{183–186}

b. β -Peptide Homopolymers. For more than 40 years, systematic studies on β -amino acid homopolymers in solution and the solid state have been conducted, revealing their potential to adopt well-defined conformational states (Figure 20).^{187–190} The first suggestion that poly(β -amino acids) take on helical conformations in solution appears to have been put forth in 1965 by Kovacs et al.¹⁸⁸ based on studies with poly(β -L-aspartic acid) [poly(β Asp)]. They proposed a 14-helix consisting of 3.4 residues per turn with H-bonding between each C=O and the third N–H group toward the N-terminus (i.e., a repetitive **S(14)** motif). Subsequent investigations^{191,192} raised doubts about this initial claim since it was found that poly(β Asp) is synthesized as a mixture of α - and β -linkages. These and studies with other poly(β -amino acids) suggested that β -peptides adopted disordered solution conformations^{179,193} or extended β -sheet structures^{189,194} rather than helical conformations.

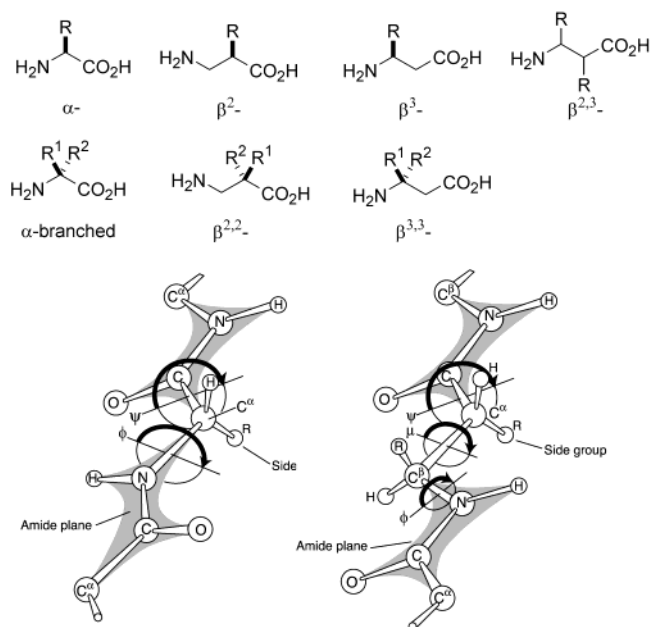


Figure 19. Labeling of atoms and dihedral angles in the α -peptide backbone according to the 1969 IUPAC–IUB Commission on Biochemical Nomenclature⁸⁹⁹ and the analogous scheme for β -peptides. In the text that follows, the abbreviated nomenclature introduced by Seebach is adopted,²²⁸ referring to β -amino acids as homologues of the natural α -amino acids bearing the same side chain by adding the letter “H” preceding the three-letter code of the natural amino acid. Thus, β^2 -HXaa and β^3 -HXaa are used to designate a homologue of the α -amino acid Xaa with the “natural” side chains in the 2- or 3-position, respectively.

Over the next decade, however, further work on poly(β -amino acids) continued to reveal evidence for ordered conformations in solution and the solid state. In 1972, on the basis of chiroptical data, viscosity, and NMR spectroscopy, Yuki et al. asserted that the poly- β -peptide poly- β -(α -isobutyl-L-aspartate) [i.e., poly(*S*- β AspOiBu)] adopts a helical conformation in solution and exhibits a helix–coil transition analogous to poly- α -(γ -benzyl-L-glutamate).¹⁹⁵ However, on the basis of X-ray diffraction and polarized IR spectroscopy of the stretched film, these authors reinterpreted the conformation as a type of β -sheet structure.¹⁹⁶ In solution, they proposed that the ordered state consisted of intramolecularly H-bonded β -sheets. Systematic studies with discrete β -peptide oligomers¹⁹⁷ determined the critical chain length for the putative β -sheet formation to be eight units.¹⁹⁸ In due course, however, the conformational structure of this polymer was once again reinterpreted as helical both in the solid state and in solution.¹⁹⁹ The uncertainty in being able to definitively establish the solution conformation of poly(β -amino acids) is characteristic of the field in decades past and illustrates the difficulties of determining the solution conformation of chain molecules.

It is interesting to note that as early as 1968, Bestian¹⁸⁹ and Schmidt¹⁹⁰ showed that the substitution pattern at the α - and β -carbons can dramatically influence the properties of the resulting polymers (Figure 20). Even though Bestian’s studies were conducted on polymers derived from racemic β -lactams, the observations foreshadowed many of the findings made recently.^{200,201} For example, the *threo*-

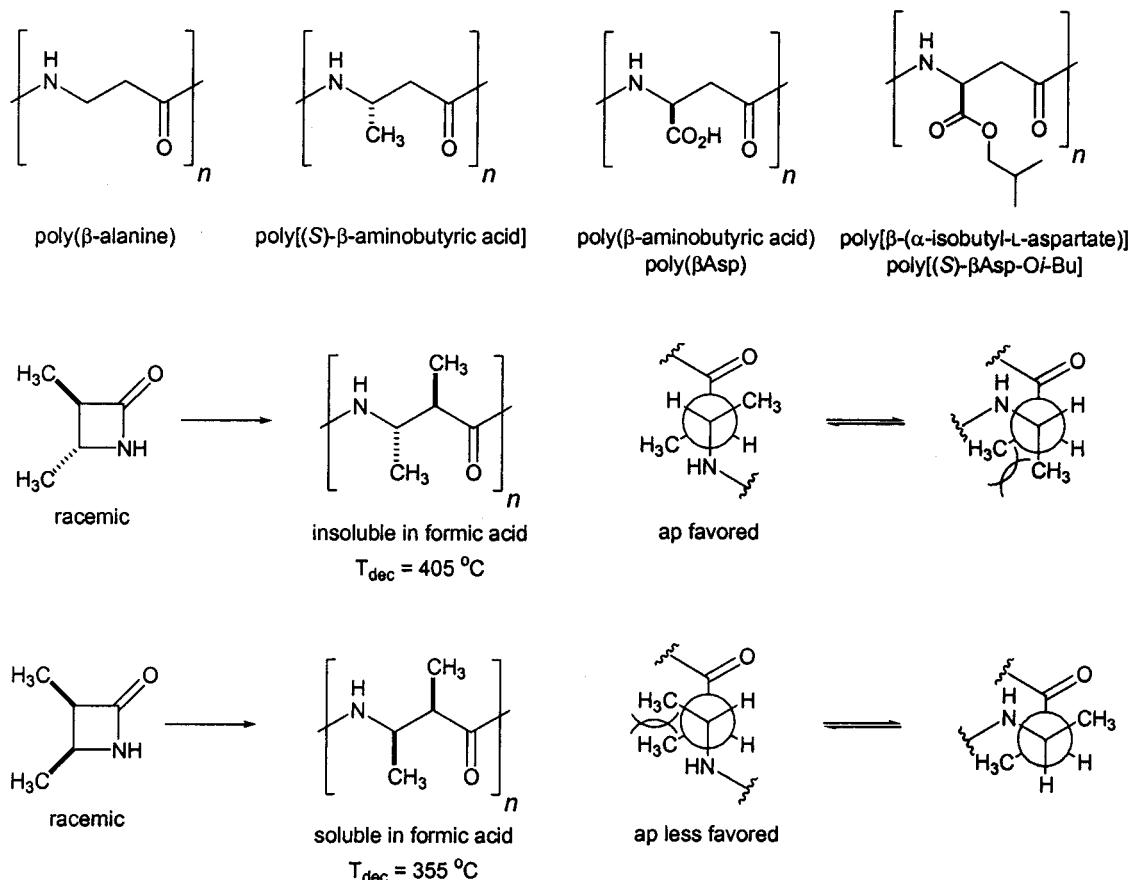


Figure 20. Examples of β -amino acid homopolymers from racemic lactams and the conformational preferences as rationalized in 1968 by Bestian.¹⁸⁹

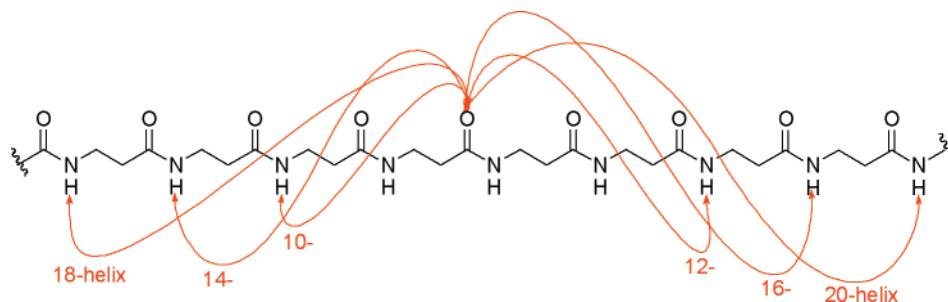


Figure 21. Possible intramolecular H-bond arrangements in β -peptides.

disubstituted monomer produced a highly stable, insoluble backbone, while the corresponding *erythro*-disubstituted monomer resulted in a polymer that was much more soluble and had lower thermal decomposition. This was explained¹⁸⁹ by the preference for antiperiplanar (*ap*) torsion angles with the *threo* isomer and hence extended chains in this case, while the *erythro* isomer was more prone to adopt synclinal (*sc*) torsion angles. Although detailed structural studies were not performed, powder X-ray diffraction and IR spectroscopic studies supported these assertions. Solubility was a serious problem that hampered these early investigations.

In 1984, Fernández-Santín et al. reported¹⁹⁹ that poly(*S*- β AspOiBu), the poly- β -peptide first described by Yuki,¹⁹⁵ does indeed exist in helical conformations when fibers are spun or films are cast from chloroform solutions. This work claimed to be the first report of helical conformations in a polyamide backbone other than chains of α -amino acids. Depending

on sample preparation, two types of helical structures were found in the solid state. Fibers pulled from a concentrated solution of chloroform showed hexagonal packing, while chloroform solutions precipitated with ethanol produced a tetragonal crystal habit. Systematic consideration of the possible helical conformations (Figure 21) led to four models. The tetragonal crystal was initially thought to consist of a right-handed helix in which 4 residues are present in one turn and hydrogen bonding involves a 20-membered ring. On the other hand, the hexagonal crystal was initially thought to consist of a left-handed helix in which 13 residues are present in 4 turns and H-bonding occurs through a 16-membered ring. Helical conformations were also believed to be stable in helicogenic solvents. Solvent denaturation experiments followed by ¹H NMR and solution viscosity showed evidence²⁰² of a helix-coil transition similar to that seen in helical poly(γ -benzyl-L-glutamate).²⁰³ However, experimental evidence²⁰⁴ and

molecular modeling studies^{205–207} now strongly support a right-handed 14-helix (similar to that originally proposed by Applequist¹⁸⁸) in the hexagonal crystal and a right-handed 18-helix in the tetragonal crystal. Predictions based on matching calculated and observed CD spectra, however, while qualitatively consistent with helical conformations, are unable to distinguish between the possible helical conformations.²⁰⁸

Studies with other poly(β -L-aspartate)s demonstrate that these polymers not only adopt conformational patterns that are similar to poly(α -amino acids), but that they exhibit greater conformational versatility. The range of conformations now include extended chain structures, arranged as antiparallel packings that come about by stretching poly(α -methyl- β -L-aspartate) films in boiling water.²⁰⁹ In solution, the helix-coil conformational transition is a phenomenon common to the whole family of poly(α -alkyl- β -L-aspartates).²¹⁰ The ordered conformation is responsive to environmental factors such as temperature and solvent in much the same way as for poly(α -peptides).

Methods for the facile preparation of high molecular weight poly(β -homopeptides) are not common and limited to specific cases such as poly(α -alkyl- β -aspartates). By analogy to the preparation of poly(α -homopeptides) by ring opening polymerization of α -amino acid-*N*-carboxyanhydrides, Cheng and Deming recently attempted to polymerize β -amino acid-*N*-carboxyanhydrides using either NaO^tBu or a nickel amido amidate complex as the initiator.²¹¹ The molecular weights achieved were generally low ($8 \leq$ degree of polymerization ≤ 20) due to precipitation of these poorly soluble macromolecules. The benzyl carbamate-protected oligo(β -homolysine) adopted a helical conformation in hexafluoro-2-propanol (HFIP). In direct analogy to poly(α -homolysine),²¹² the deprotected oligo(β -homolysine) exists in a disordered conformation at low pH due to electrostatic repulsion. As the pH was raised from 10 to 11.2, a strong Cotton effect was observed, suggesting a transition to a helical conformation. This transition was shown to be reversible. A similar pH-induced transition was found for oligo(β -homoglutamate) in aqueous solution. These examples show that polymerizations can be used as a rapid screening method to bypass the slow and tedious step-by-step preparation of oligomers.

c. β -Peptide Oligomers. Systematic studies on cyclic oligomers and small β -peptides have provided valuable insight into the conformational preferences of their long-chain linear counterparts. This approach has been extensively used to study conformations in α -peptides,²¹³ where a wide variety of folded forms has been observed. The geometric constraints in cyclic structures greatly reduce the conformational degrees of freedom, thus making it possible to observe turns and noncovalent interactions that may otherwise not be present in small linear analogues. The shapes of α -peptides have been described as sinusoidal, saddle, elongated loop, disk, pleated sheet, and helical. The general conclusion from crystallographic studies with small α -peptides is that the folding

resembles aspects of protein secondary structure, but overall it is quite unpredictable.²¹³

Although many fewer cyclic β -peptides have been crystallographically examined in comparison to α -peptides, a similar conclusion can be made: many of the observed conformations hint at features found in β -peptide oligomers and polymers. For example, systematic studies on cyclic oligomers that incorporated β -amino acids have revealed that these units readily adopt turned motifs.^{214–218} Using molecular models, Pavone et al. hypothesized²¹⁴ that cyclic peptide oligomers containing the β -HGly dipeptide sequence are able to adopt conformations that permit transannular H-bonds between the amide groups of the β -HGly residue. To test this idea and its generality, a variety of cyclic peptides were synthesized and their crystal structures obtained. Indeed, many turn types were observed depending on the number of β -peptide residues, their placement in the sequence, and the total number of residues in the cyclic structure. As a representative example, the structure of the **S(13)S(10)**²¹⁹ containing *cyclo*-(L-Pro-L-Pro-L-Phe- β -HGly- β -HGly) is shown in Figure 22.²¹⁵ A transannular H-bond between the carbonyl of the β -HGly and the N-H of Phe is clearly evident. Starting from the H-bond donor and tracing through the β -HGly dipeptide segment to the H-bond acceptor (i.e., the thick bonds in Figure 22), it can be seen that 13 atoms are involved in the H-bond circuit. The second hydrogen bond circuit involves 10 atoms tracing from donor to acceptor through the L-Pro-L-Pro segment. It can be seen from Figure 14 that the C $_{\alpha}$ -C $_{\beta}$ bonds of both β -HGly units adopt a gauche (i.e., *sc*) dihedral angle to form corners of the covalent ring and to orient the H-bond donor and acceptor for transannular interaction. An example of a crystallographically characterized macrocycle that incorporates a β^3 -substituted residue is also shown in Figure 22.²²⁰ The interesting features of this pentapeptide are the **S(12)S(10)** transannular H-bond interaction, the *cis* amide conformation, and the *sc* torsion about the C $_{\alpha}$ -C $_{\beta}$ bond (Figure 22). A similar dihedral arrangement is found in many of the β^3 -peptide oligomers as noted below.

Seebach and co-workers studied macrocycles composed entirely of β -amino acid residues.^{221,222} Three different stereoisomeric tetracycles of β -HALa were synthesized by cyclization of their pentafluorophenyl esters. The ease with which β -cyclopeptides were formed relative to α -cyclopeptides of similar size was noted as a tendency for the β -peptide backbone to favorably adopt turn structures.^{221,223} Poor solubility and high melting points characterized the physical properties of these compounds. Their solid-state structures, as shown in Figure 23, were determined by refinement of powder X-ray data.²²² It can be seen that the C=O and N-H bonds are approximately oriented in a direction perpendicular to the average macrocyclic plane (Figure 23). This in turn leads to tubular stacks held strongly together by intermolecular **C(4)** H-bond chains. These H-bond arrangements qualitatively resemble the intramolecular H-bonding motifs in helical β -peptide oligomers.

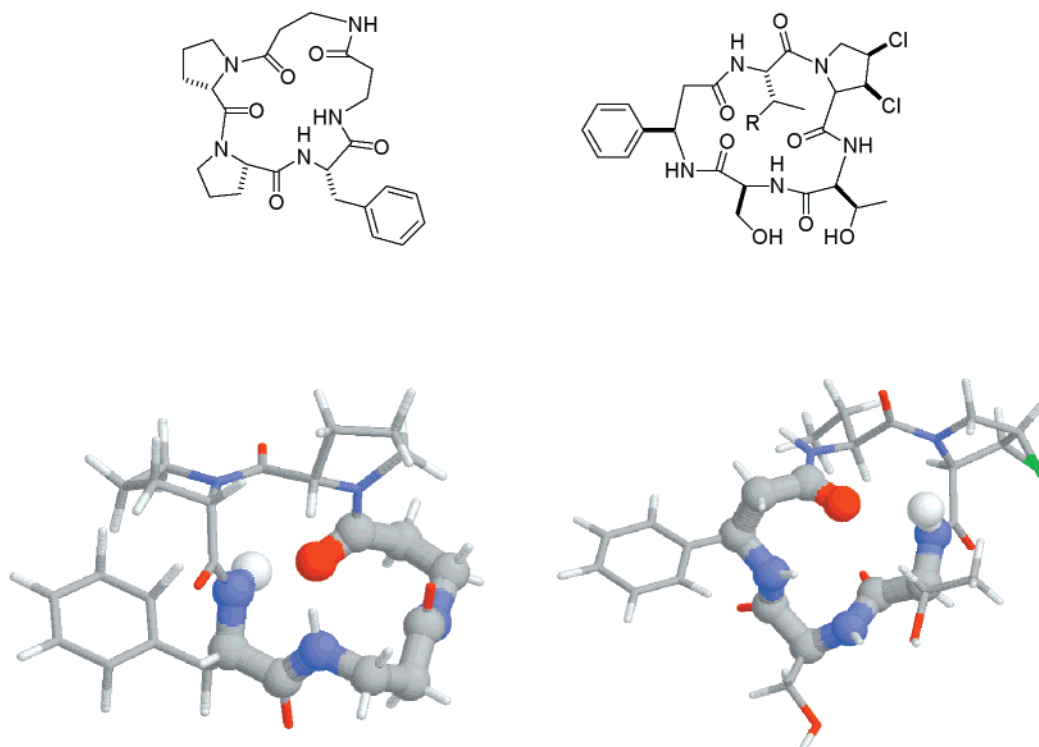


Figure 22. Crystal structures of *cyclo(L-Pro-L-Pro-L-Phe- β -HGly- β -HGly)*²¹⁵ showing H-bond patterns and another cyclopentapeptide.²²⁰ The β -peptide segments involved in **S(13)S(10)** and **S(12)S(10)** transannular H-bonds are rendered as thick cylinders. Newman projections about the C_{α} - C_{β} bonds of the β -amino acid residues show a *sc* conformational preference.

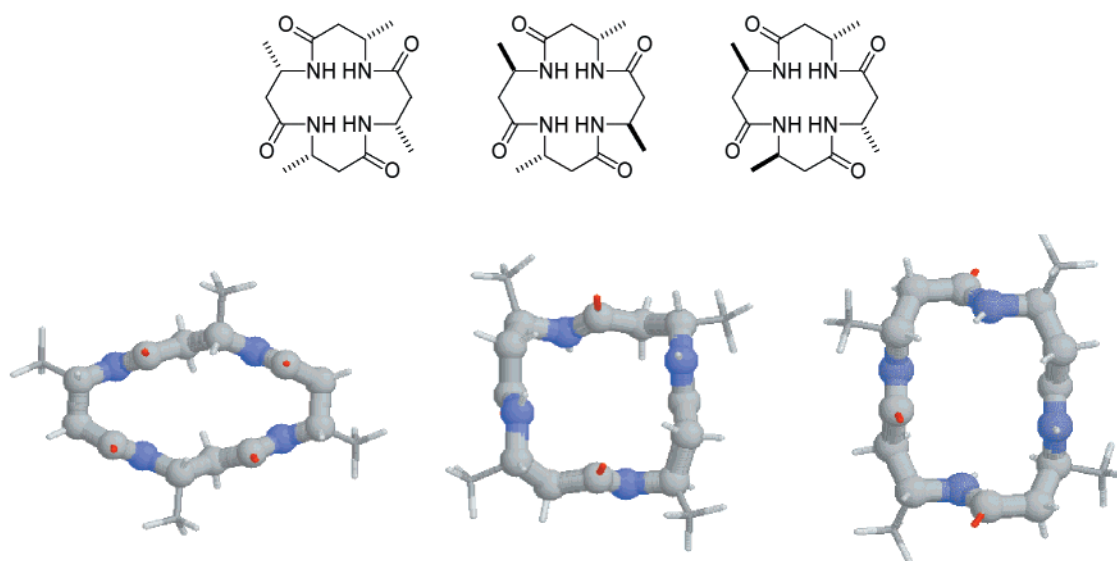


Figure 23. Chemical and crystal structures of three different stereoisomeric tetracycles of β -HAla.²²²

While the studies of Pavone and others with cyclic peptide oligomers showed that next-nearest-neighbor amides can engage in H-bonding interactions, the contribution of cyclic constraints raises the question of whether such interactions could readily occur in acyclic systems. In 1992, the crystal structure of the linear tripeptide *t*-Boc-Aib-Aib- β -HGly-NHMe (where Aib is α -aminoisobutyric acid) was reported, showing that intramolecular H-bonding interactions form even in short chains void of macrocyclic constraints.²²⁴ The *sc* dihedral about the C_{α} - C_{β} bond together with the sharp bend at the Aib C_{α} carbon form corners that

contribute to a next-nearest-neighbor **S(11)** H-bonding motif (Figure 24).

It is interesting to consider whether intramolecular H-bonding interactions or the dihedral preferences of the β -peptides dictate the conformations of these short β -peptides. Although this is difficult to deconvolute from X-ray structures, the importance of torsional bias can be inferred from the crystal structure of the β -tripeptide *t*-Boc- β^3 -HVal- β^3 -HAla- β^3 -HLeuOMe reported by Seebach in 1996 (Figure 25).²²³ No intramolecular H-bonds were observed in **3**; yet, it is apparent that one of the β -peptide

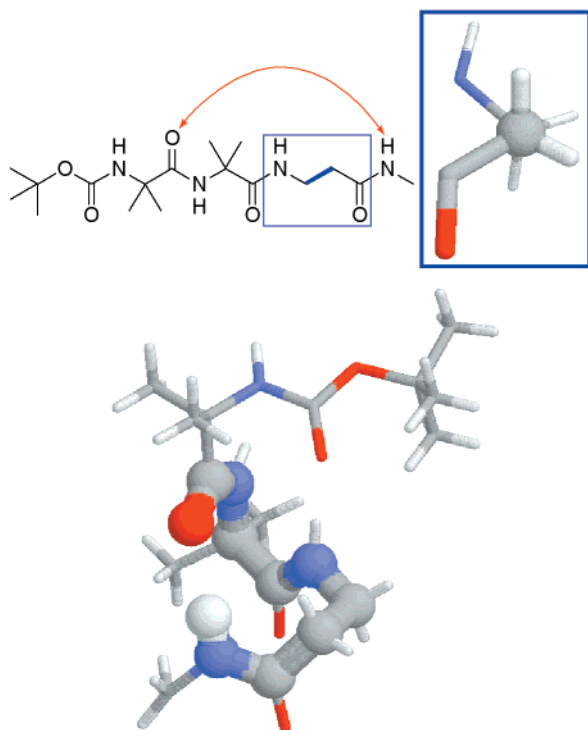


Figure 24. Crystal structure of the linear tripeptide *t*-Boc-Aib-β-HGly-NHMe (where Aib is α-aminoisobutyric acid).²²⁴ The **S(11)** H-bond segment is rendered in thick cylinders. The *sc* dihedral angle about the C_{α} - C_{β} bond of the β-peptide residue is also indicated.

residues makes a tight turn due to a *sc* C_{α} - C_{β} torsion. It is noteworthy that the *sc* dihedral angle is located in the residue bearing the largest substituent, possibly hinting that β-peptides, especially those

with bulky substituents, have a torsional potential energy surface that can easily accommodate turned conformations. On the basis of quantum mechanical calculations, Wu and Wang argued that an internal electrostatic interaction causes this *sc* C_{α} - C_{β} dihedral preference.¹⁸⁴

Dado and Gellman addressed the possibility of nearest-neighbor interactions between amides in β- and γ-peptides.²²⁵ Nearest-neighbor interactions, should they be common, could dominate the potential energy surface and work against the formation of long-range conformational order in β-peptides. To address this issue, the folding behavior of β-alanine and γ-amino butyric acid derivatives **4–9** were studied in solution by IR spectroscopy in methylene chloride (Figure 26). These studies concluded that nearest-neighbor H-bond formation in β-peptides is not a favorable process. The absence of intramolecular H-bond formation in **4** and **6** indicates that neither the six- nor the eight-membered cyclic H-bond is favorable. However, tertiary amide **5** did adopt an intramolecular H-bonded conformation. This observation with **5** is believed to result from at least two effects: first, an $A^{1,3}$ -like interaction between nitrogen substituents and, second, the stronger H-bond acceptor ability of tertiary amides over secondary amides. The important conclusion from Gellman's study was the recognition that since H-bonds between nearest-neighbor amides are not favorable in β-peptides, this backbone could likely be an unnatural amide-based polymer that is able to adopt compact and specific folding patterns. γ-Peptides **7–9**, on the other hand, which were also studied, were suggested to be less suitable since they

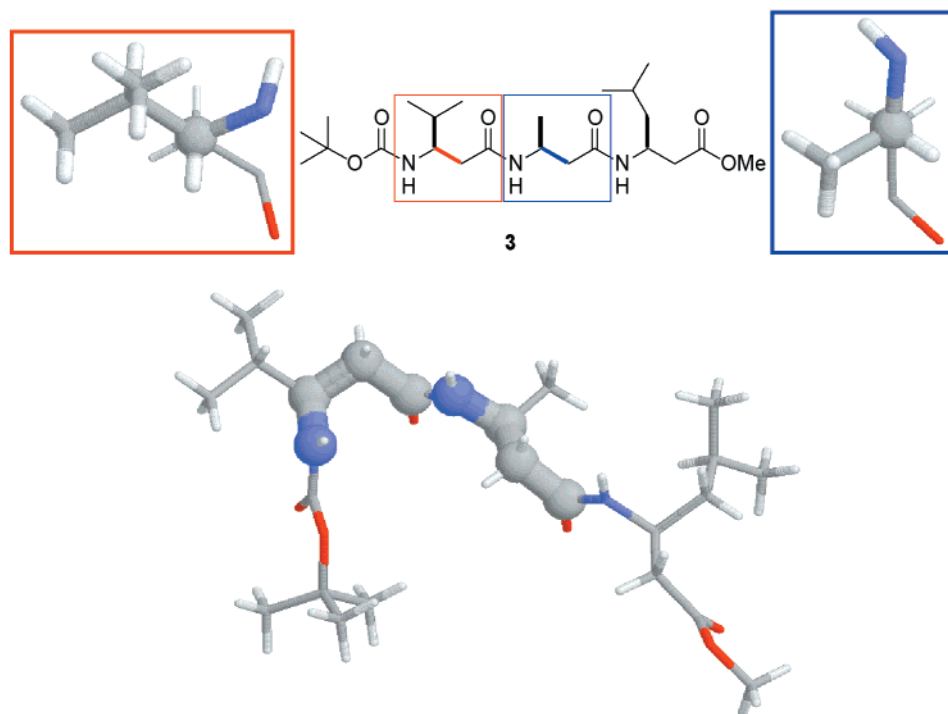


Figure 25. Crystal structure of the β-tripeptide *t*-Boc-β³-HVal-β³-HAla-β³-HLeuOMe (**3**) reported by Seebach²²³ showing an intrinsic preference for a turned conformation. Two of the β-peptide residues are rendered as thick cylinders. The Newman projections about the C_{α} - C_{β} bonds for these residues are shown, indicating the apparent preference of the β³-substituted residue bearing the bulky substituents to adopt a *sc* conformation while the residue with the smaller methyl substituents takes on an *ap* conformation.

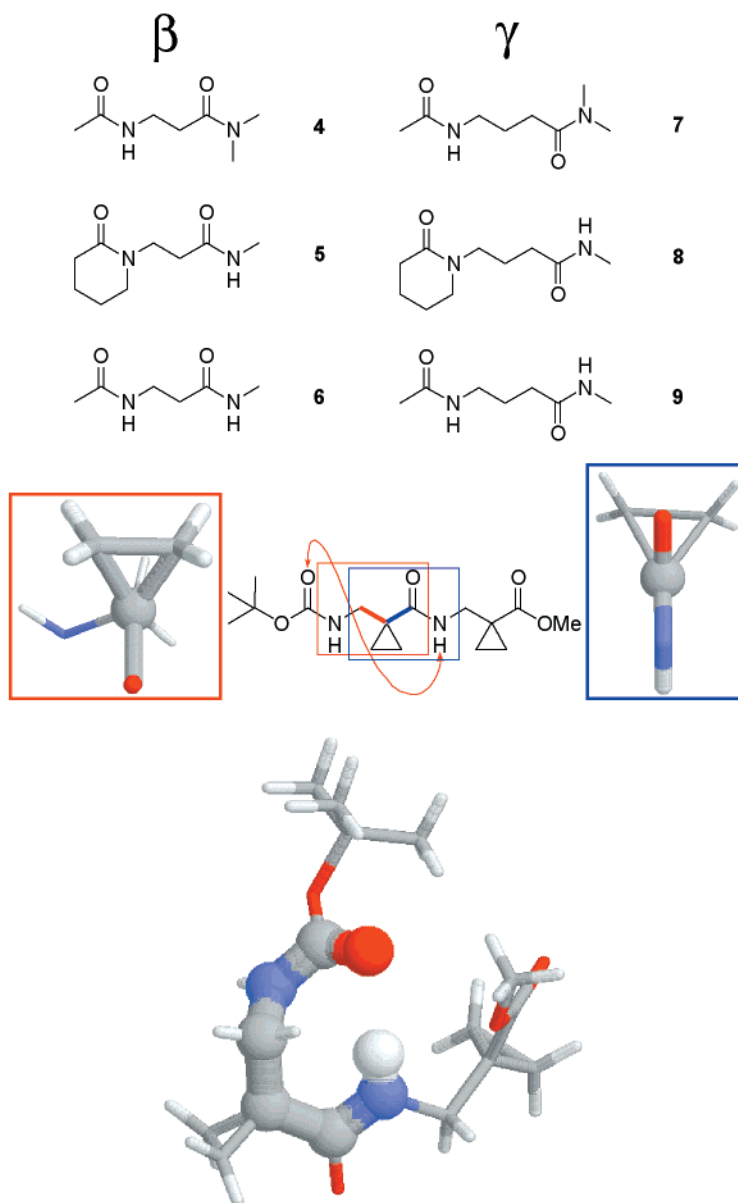


Figure 26. Nearest-neighbor H-bonds observed in β -peptides synthesized from 1-(aminomethyl)cyclopropanecarboxylic acids.²²⁶ This **S(8)** pattern is an example of residue-induced turn formation, resulting from the dihedral and bond angle constraints introduced into the $\beta^{2,2}$ -backbone by the cyclopropyl substituents. The crystal structures show a dipeptide and tripeptide in which the **S(8)** H-bond segments are rendered in thick cylinders. For the dipeptide, Newman projections are shown looking down the $C_\alpha-C_\beta$ bond and the $C(O)-C_\alpha$ bond.

were conducive to nearest-neighbor hydrogen bonding. It should be noted that following Gellman's studies, the special case of β -peptides synthesized from 1-(aminomethyl)cyclopropanecarboxylic acids was reported in which nearest-neighbor H-bonding interactions are observed.²²⁶ Hyperconjugation between the cyclopropane σ orbitals and the π^* orbital of the $C=O$ bond impart preference for the bisected or *s-cis* conformation. This together with bond angle deformations caused by the cyclopropyl substituent provide sufficient backbone constraints to induce nearest-neighbor **S(8)** H-bonding, as seen in the crystal structures of the β -peptide dimer and trimer (Figure 26).

d. Helical Secondary Structures in Oligomeric β -Peptides. *i. Background and General Considerations.* At least 15 α -amino acid residues are required for formation of stable α -helix secondary

structures in protic solvents.²²⁷ Given the seemingly greater flexibility of β -peptides, one might expect that even longer stretches of β -peptide oligomers would be required before stable helices form. However, this turns out not to be the case. As hinted from the observations highlighted above, short β -peptide backbones are poised to adopt ordered conformations. In 1996, two groups independently reached this conclusion: short β -peptide oligomers form surprisingly stable helices in solution and the solid state.^{32,223} Seebach^{221,228,229} approached the problem from the context of amide analogues of oligo-(*R*)-3-hydroxybutanoates (i.e., oligo-HBs) to address the question of whether replacing the oxygen in the HB backbone with the N–H hydrogen bond donor would stabilize helical conformations analogous to those observed for oligo-HBs.^{230,231} Gellman⁴ studied hydrogen bonding in model amides and on the basis of their previous

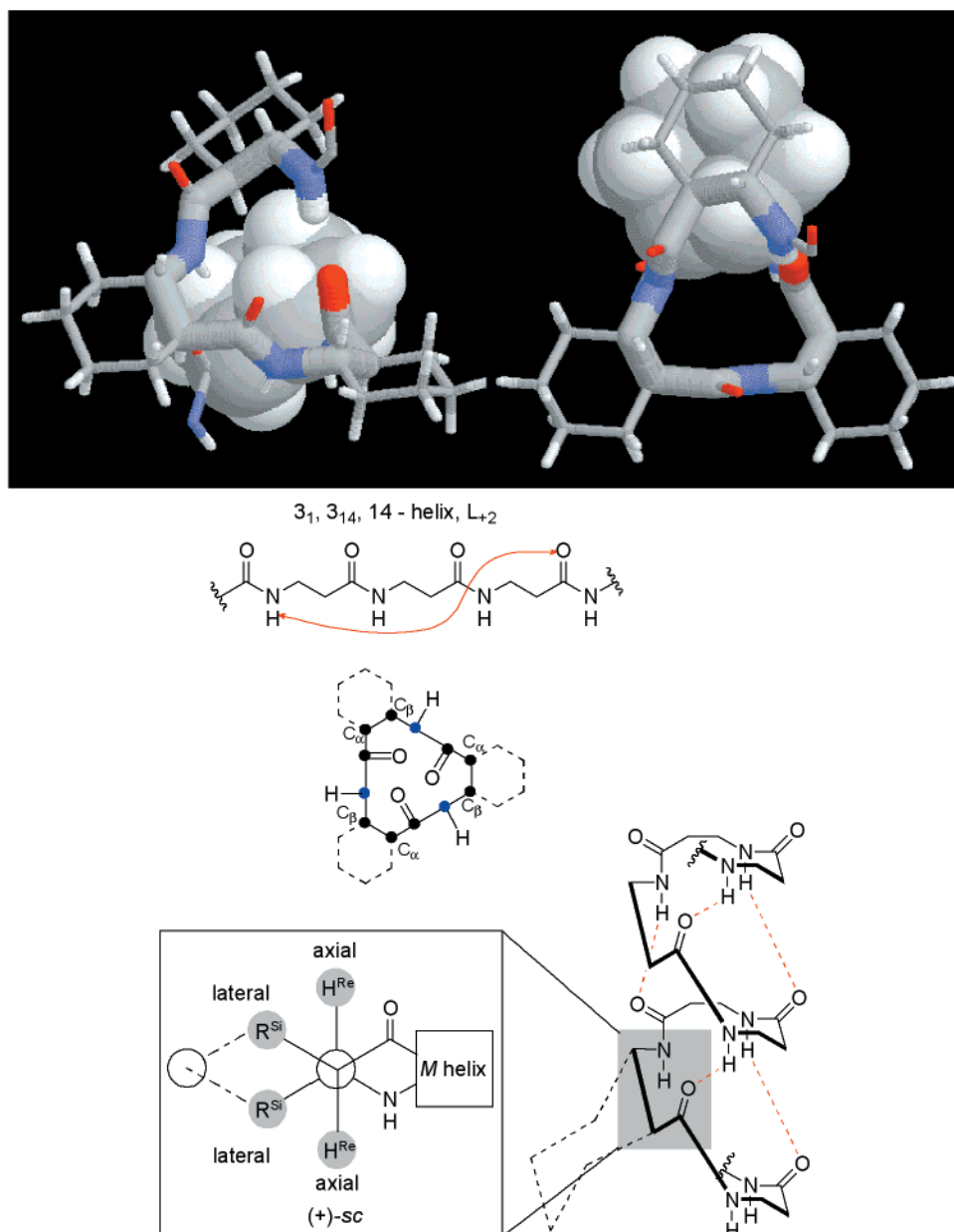


Figure 27. Side and top views of ca. one turn of the 14-helix extracted from the crystal structure of Gellman's *trans*-ACHC hexamer.²³⁹ A single **S(14)** H-bond circuit in the peptide backbone has been rendered as thick cylinders. Additionally, one residue has been rendered as a space-filling model to provide a frame of reference between the two views and to more clearly show the spatial relationship between cyclohexyl groups.

results predicted²²⁵ that β -peptide oligomers could adopt long-range conformational order.

Prompted by questions that arose from structural modification of oligo-HBs,^{221,229} Seebach's group investigated homologues of natural L-amino acids, beginning with a hexapeptide H-(β^3 -HVal- β^3 -HAla- β^3 -HLeu)₂-OH. The above-mentioned hexamer is considered as a β^3 -peptide since all of the side chains are in the 3-position. The particular sequence selected is reminiscent of the arrangements observed in the dimer-forming leucine zipper region of DNA binding proteins,²³² and the fragment Val-Ala-Leu has previously been used as a building block to study the influence of α,α -disubstituted amino acids on peptide conformation.²³³ The apolar side chains afforded β -peptide sequences that were soluble in organic solvents. In subsequent studies, functional-

ized sequences were also investigated.²³⁴ It is increasingly clear that functionalization with polar appendages can have a dramatic impact on the secondary structure.²³⁵ Extension to γ -peptides (see below),^{236,237} which were shown to adopt a stable right-handed helix, gave the surprising result that of the three backbones, the α -peptides are the least prone to adopt stable secondary structures.

Gellman's approach focused on conformationally rigidified residues that limited the degrees of freedom about the C $_{\alpha}$ -C $_{\beta}$ bond, with the intention of observing ordered conformations from the fewest possible residues. They approached the design of helical oligomeric β -peptides with the aid of systematic molecular modeling studies.³² The candidates were selected from β -amino acids in which the backbone carbons were embedded into carbocycles containing

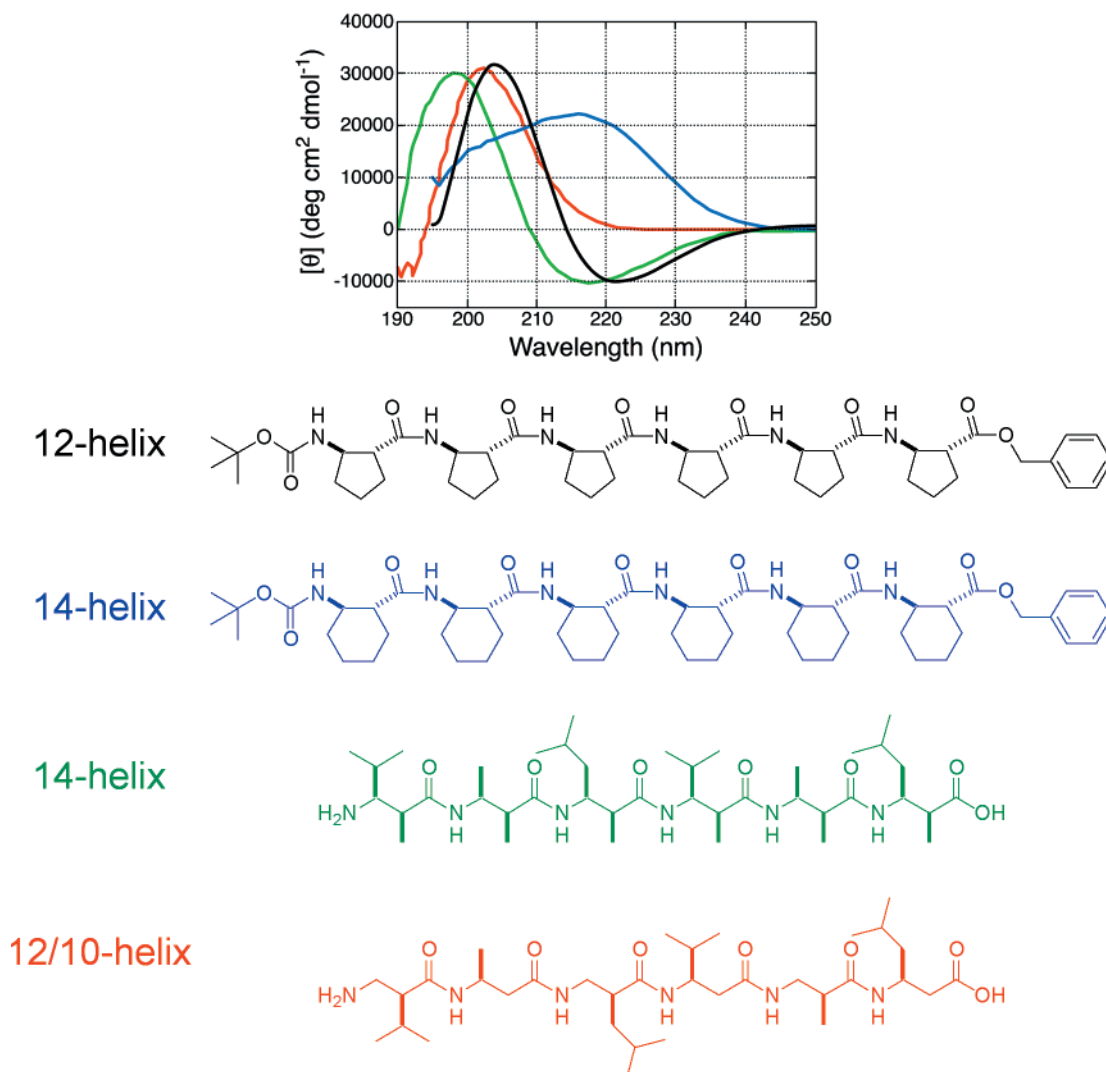


Figure 28. Circular dichroism spectra of four different β -peptide sequences in methanol: black,²⁴¹ blue,²³⁹ green,²⁷³ and red.²⁴⁹

three, four, five, or six atoms. Both *cis* and *trans* ring stereochemistries were considered, and for the *cis*-containing peptides, both orientations of the ring with respect to the helix were examined. Helical conformations were modeled for each of these 12 different sequences using the six smallest H-bonded cyclic patterns: the 12-, 16-, and 20-helix corresponding to H-bonds from carbonyls to N–H groups in the C-terminal direction and the 10-, 14-, and 18-helices corresponding to H-bonds from carbonyls to N–H in the N-terminal direction (Figure 21). Molecular mechanics studies of the resulting 72 structures led to the conclusion that the 14-helical form of *trans*-2-aminocyclohexanecarboxylic acid (*trans*-ACHC) would be the most stable among these hypothetical helices. These studies also predicted that *trans*-2-aminocyclopentanecarboxylic acid (*trans*-ACPC) would adopt the 12-helix,²³⁸ a surprising result in that there had been no example of this conformation in the β -peptide field. As mentioned below, both of these structure types were observed as predicted.

The helical conformations of Gellman's oligomers were firmly established by a battery of experimental techniques. The crystal structure of the *trans*-ACHC hexamer (Figure 27) revealed that all four of the

possible 14-membered ring H-bonds were present in the solid state.^{32,239} In solution, the β -peptides were established to be monomeric under the conditions used for NMR and CD studies.²⁴⁰ Amide proton NH/ND exchange experiments suggested that in methanol the hexamer adopts a very stable intramolecularly hydrogen-bonded conformation, presumably the 14-helix. A solution structure for the *trans*-ACHC hexamer based on NMR-derived constraints was hampered by severe overlap of signals in the $C_{\alpha}H$ and $C_{\beta}H$ regions in this case.²⁴⁰ The CD spectrum in methanol shows a single peak above 200 nm with a maximum at 217 nm (Figure 28). The intensity at the maximum increased as the chain lengthened, presumably the result of a growing population of the 14-helical state.²³⁹ This behavior was suggested to be an indication that the 14-helix formation involves a cooperative process (see below).

As predicted computationally, the *trans*-ACPC oligomers revealed a different type of helical conformation in both solution and the solid state. Crystal structures of the *trans*-ACPC hexamer and octamer displayed the 12-helical conformation (Figure 29).^{238,241} The spectral data of the ACPC oligomers in solution are consistent with the crystallographic observations.

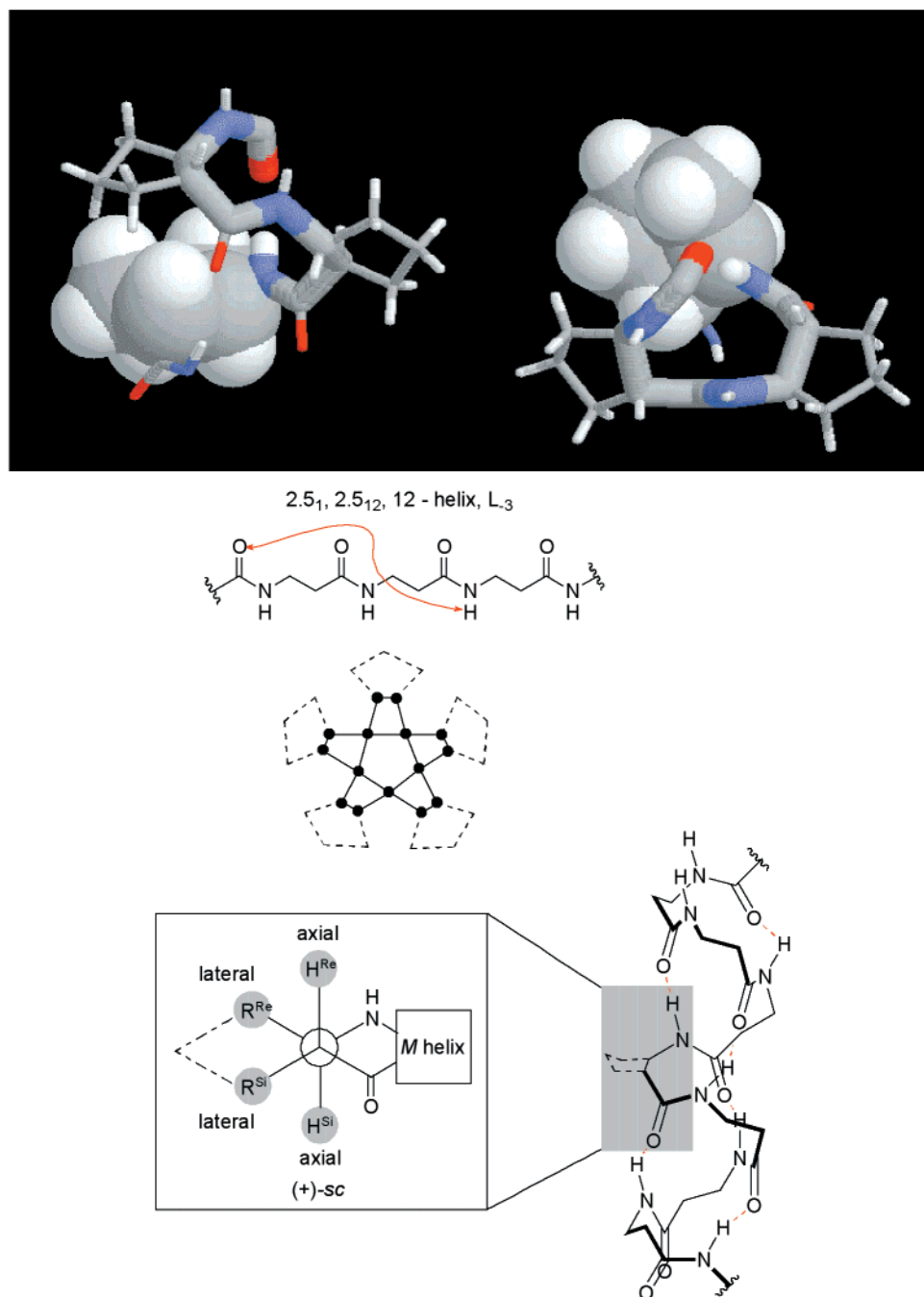


Figure 29. Side and top views of ca. one turn of the 12-helix extracted from the crystal structure of Gellman's *trans*-ACPC hexamer.²⁴¹ A single **S(12)** H-bond circuit in the peptide backbone has been rendered as thick cylinders. Additionally, a residue has been rendered as a space-filling model to provide a frame of reference between the two views and to more clearly show the spatial relationship between cyclopentyl groups.

Circular dichroism spectra of the ACPC oligomer series in CH₃OH vary significantly with chain length. While the trimer and tetramer show no maxima above 200 nm, the CD pattern of the pentamer and hexamer begin to converge and the magnitude of the Cotton effect increases as the chain lengthens. This behavior is interpreted as an increasing population of the 12-helical conformation with increasing chain length, reflecting cooperativity in the 12-helix formation. The CD spectrum of the ACPC hexamer is clearly distinct from the 14-helical β -peptides (Figure 28), displaying a maximum around 207 nm and a minimum at 222 nm. The observed CD spectrum agrees well with theoretical spectral predictions for

the 12-helical conformation.²⁴² In pyridine-*d*₅, the ACPC hexamer and octamer displayed sufficient ¹H NMR dispersion to afford solution structures calculated from NMR-derived distance constraints.²⁴⁰ The NMR-determined conformations of these oligomers were similar to the conformations found from crystallography. Correlations established by NOE data were observed for all C _{β} H(*i*)–NH(*i*+2) proton pairs along the backbone as expected for a fully formed 12-helix. However, the data suggested the lack of a high degree of conformational order in the chain ends, indicative of fraying.

The switch in H-bonded patterns for the ACHC and ACPC β -peptides teaches that foldamer conforma-

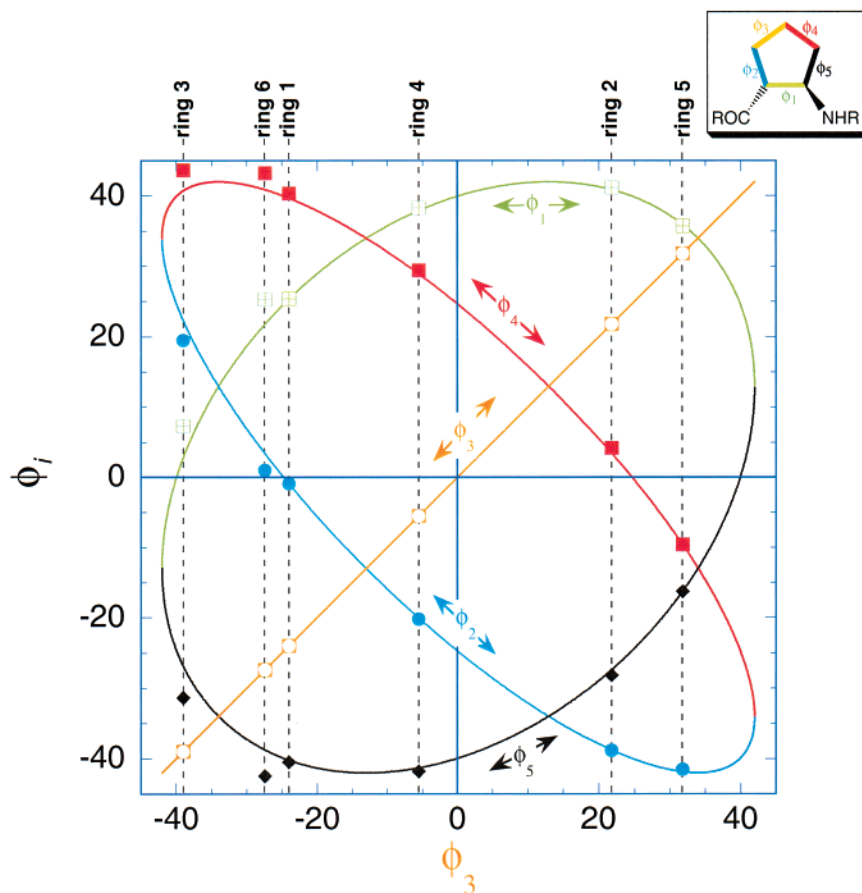


Figure 30. Data from the crystal structure of the ACPC hexamer show that the five internal torsions within each of the six cyclopentyl residues are superimposed on the cyclopentyl pseudorotation circuit as revealed in a correlation plot of ϕ_i vs ϕ_3 .

tions can be controlled by small residue changes, a concept not common to α -peptides. It is interesting to understand what specific residue-based changes bring about this conformational switch. The internal ring torsion across the $C_\alpha-C_\beta$ bond in the ACHC hexamer varies little among the six residues, spanning the range from -55.0° to -58.8° . In contrast to cyclohexyl rings, five-membered carbocyclics are considerably more flexible. The coupling of small bond angle deformations to internal rotational angles gives rise to an equipotential energy surface known as the pseudorotation circuit.^{243,244} The five internal dihedral angles, ϕ_i , are highly correlated to one another because of geometric restrictions from ring constraints. This correlation is apparent in a plot of ϕ_i vs any one of the internal angles (e.g., ϕ_3), whereby elliptical paths of the pseudorotation circuit connect equipotential points between torsional extremes of $\pm 42^\circ$ (Figure 30).^{245,246} From the crystal structure of ACPC hexamer, the five internal torsions within each of the six cyclopentyl residues are superimposed on the cyclopentyl pseudorotation circuit in Figure 30. It can be seen that nearly all of the ring dihedrals conform very well to the cyclopentane pseudorotation circuit. Only rings 3 and 6 show minor deviations from the expected correlations, suggesting either a slight deformation away from ideality or possibly limitations in the X-ray refinement of these two rings. In great contrast to the ACHC case, the $C_\alpha-C_\beta$ torsional angles (ϕ_1) in ACPC are significantly more

variable, taking on a range of values from 7.3° to 41.2° . Traversing along the helical backbone from one ring to the next, no obvious pattern in dihedral values emerges, which is somewhat surprising given the regular backbone conformation. In addition to the noted variability in ϕ_1 , the ring substituents deviate significantly from the nearly ideal gauche conformation of ACHC. The greater flexibility about ϕ_1 and the deviation from gauche geometry are apparently the major factors responsible for the tighter 12-helix in ACPC oligomers.

Recently, β -peptide oligomers from *cis*-substituted oxetane rings have been synthesized and studied.²⁴⁷ Molecular modeling and NMR NOE data in $CDCl_3$ and C_6D_6 on the hexamer have identified a helical secondary structure stabilized by four **S(10)** H-bonding interactions. Although **S(10)**-stabilized turns are known in β -peptides,^{248,249} this is the first example of the repetition of this pattern to generate a 10-helix. Thus, while the cyclopentane and cyclohexane β -amino acid oligomers adopt the 12- and 14-helix, respectively, and **S(8)** interactions produce a ribbon structure in cyclopropane-based β -peptides,²²⁶ the *cis*-oxetanes take on the intermediate **S(10)** H-bond ring size, giving a consistent trend. These latest results build on the general theme, previously mentioned, that foldamer conformations are sensitive to small residue changes. Finally, it should be mentioned that furanose²⁵⁰ and pyranose²⁵¹ carbopeptides having a β -amino acid repeating unit are under development,

but thus far, no information is available on the secondary structures of these presumably water-soluble backbones.

The 14-helix conformation of the β -peptide oligomers prepared by the Seebach group was also rigorously established in solution and the solid state. The first clues about solution structure for these β -peptides were revealed by the dramatic changes in CD spectra that accompanied an increase in chain length. The β -dipeptide and β -tripeptide showed CD traces that resembled that of the unstructured α -hexapeptide Val-Ala-Leu-Val-Ala-Leu-OMe in MeOH. In contrast to the CD spectrum of the unstructured α -hexapeptide, the corresponding β -hexapeptide exhibited a strong, broad minimum at 216 nm, a zero crossover at 207 nm, and a maximum at 198 nm (Figure 28).²²³ The spectrum of the β -hexapeptide was independent of concentration and, with the exception of sulfuric acid, independent of solvent. As noted above, the crystal structure of Boc- β -tripeptide **3** shows a turn-like conformation as a consequence of adopting a *sc* dihedral angle about one of the C_{α} - C_{β} bonds (Figure 25). This turn was envisioned as the starting point of a helix that could arise in longer sequences. ¹H NMR data was used to study the solution structure of the β -hexapeptide in pyridine-*d*₅ (a NMR structure in MeOH was later elucidated to corroborate the pyridine-*d*₅ NMR solution structure and CD data).²⁵² An analysis of coupling constants revealed hindered rotation around the C_{α} - C_{β} bond on the NMR time scale, while prevalent NOE's were observed between $NH^i-C_{\beta}H^{i+2}$ and $NH^i-C_{\beta}H^{i+3}$. The corresponding distance and bond angle restraints from coupling constants were used to compute a set of solution structures. The spiraling conformation of this β -hexapeptide is a 14-helix, similar to that identified for *trans*-ACHC. This finding was rather surprising given the short, hexameric chain length and the intuition that β -peptide backbones without rigidification are more flexible than α -peptides, which are typically unstructured if they possess less than 15–20 residues.

The CD data of Seebach's β -peptides differ somewhat from the 14-helix ACHC hexamer of Gellman (Figure 28). Although ¹H NMR data establish that the 14-helix conformation is adopted by H-(β^3 -HVal- β^3 -HAla- β^3 -HLeu)₂-OH, the differences at lower wavelengths are not easily explained. Gellman interpreted this to mean that the Seebach β -peptides and the *trans*-ACHC oligomers equilibrate between the 14-helix and other conformations in solution.²³⁹ The recorded CD may thus reflect averages of the various conformations, and therefore, the observed variations could indicate different populations of the 14-helix by these two classes of β -peptides. Longer β^3 -peptides, up to 15-mer, exhibited a very similar CD pattern, although the signal intensity increased significantly.²⁵³ It can be assumed, based on the magnitude of the Cotton effect, that longer chains contribute to greater conformational stability by increasing the set of ordered conformations relative to the ensemble of disordered conformations. However, the consistent CD pattern suggests that the distribution of conformations among those in the set

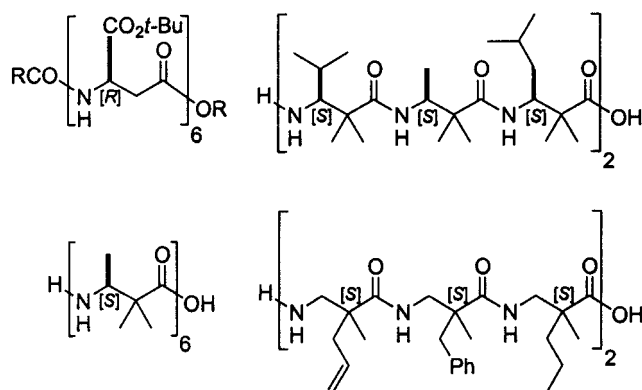


Figure 31. Examples of β -peptides that exhibit strong Cotton effects but whose structures are presumably incompatible with 14-helix conformation.

of ordered structures does not depend on chain length. An even greater mystery with regard to the CD spectra has emerged recently following studies of β -peptides that are presumably (vide infra) unable to adopt the 14-helix conformation (Figure 31).²⁵⁴ Surprisingly, these oligomers still exhibited strong Cotton effects with CD spectra matching that of the 14-helix. A compilation of CD data for a large number of β -peptides showed little variation despite putative differences in their secondary structures.²⁵⁴ The authors concluded that an interpretation of the CD spectra will have to wait until NMR solution structures become available. They went on to claim that at the present stage of knowledge, there is little structural information in CD spectra and CD is not a conclusive tool for determining β -peptide structures.

ii. Systematic Backbone and Sequence Variations in β -Peptides. Systematic backbone and sequence modification constitutes a powerful approach to learn about the fundamental interactions that contribute to the stability of secondary structure. For example, disulfide linkages have proven to be a valuable tool in the study of α -peptides by introducing conformational restrictions in order to verify the spatial relationships of side-chain positions. Jacobi et al. applied this technique to β -peptides to demonstrate the relationship of side chains in sequences prone to adopt the 14-helix conformation (Figure 32).²⁵⁵ For the 14-helix, a disulfide bridge is possible between lateral positions *i* and *i*+3 but not between *i* and *i*+4. In the former case, disulfide formation will prevent the helix from unwinding, while in the latter case, macrocycle formation can only occur if the helix unwinds. Air oxidation of β^3 -peptides with cysteine (CH_2SH) and homocysteine (CH_2CH_2SH) side chains gave the corresponding disulfide-containing macrocycles. Macrocycles from the *i* and *i*+3 positioned cysteine residues give CD spectra characteristic of the 14-helix in MeOH and H₂O. The ¹H NMR solution structure of this macrocycle has been determined to be that of the expected helical conformation.²⁵⁶ The corresponding macrocycles that result from linking the *i* and *i*+3 homocysteine units give weaker CD spectra in MeOH, while in H₂O, all evidence of helical secondary structure was absent. As expected, macrocycles from the joining of *i* and *i*+4 cysteine or homocysteine units gave CD spectra that do not match the 14-helix.

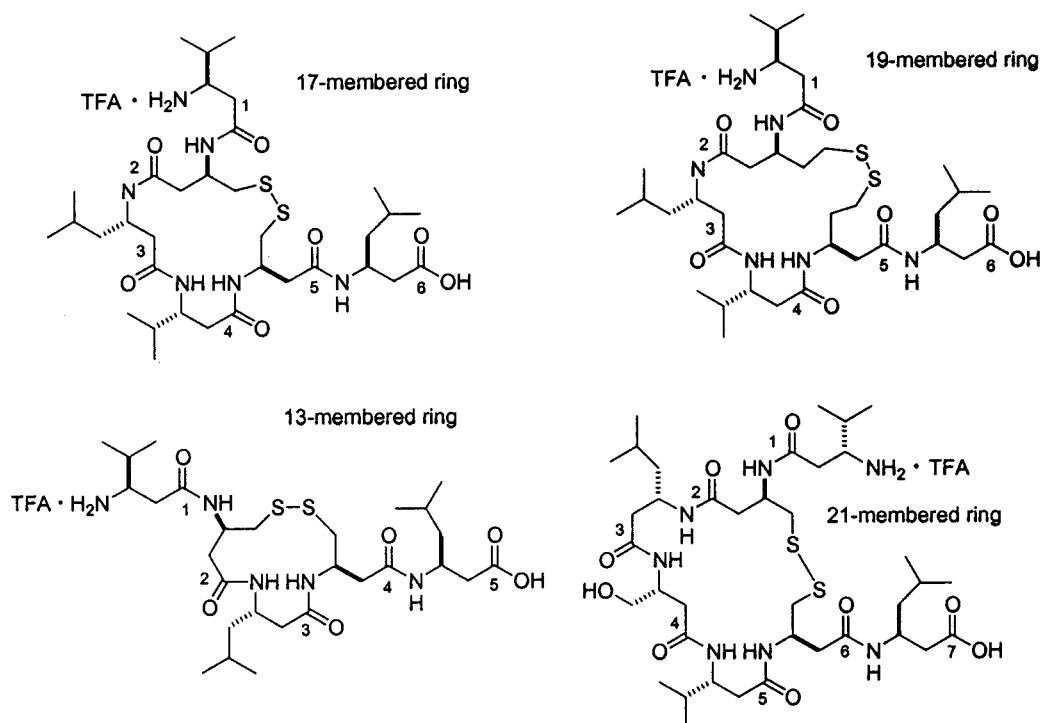


Figure 32. β -Peptides with β -HCys residues to demonstrate the side-chain relationship in sequences prone to adopt the 14-helix conformation through disulfide formation.

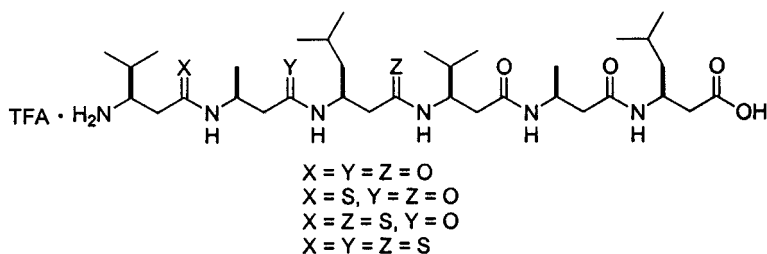


Figure 33. Backbones of monothio-, dithio-, and trithio- β -hexapeptides.

Thioamide replacement (i.e., thionation) introduces the C=S function as an isosteric substitution for C=O, perturbing H-bond donor and acceptor tendencies, and altering the geometry through a longer C=S bond length and a higher torsional barrier in the thioamide bond. Systematic studies on β -thiopeptides, while interesting, have yet to shed much light on the role of H-bonding or backbone rigidity on secondary structure stability in β -peptides.²⁵⁷ Monothio-, dithio-, and trithio- β -hexapeptides were prepared and studied (Figure 33). The solubility of the hexapeptides in organic solvents increased dramatically with the introduction of each C=S group. The CD spectra of these derivatives were difficult to interpret, but they suggest the presence of more than one secondary structure under various conditions. The β -trithiohexapeptide exhibited a pronounced exciton splitting of the $\pi \rightarrow \pi^*_{C=S}$ band, and the ^1H NMR solution structure in MeOH revealed the 14-helix to be the dominant conformation.

Although H-bonding interactions are typically invoked as a major contribution to secondary structure formation in β -peptides, the extent to which these interactions contribute to conformational stability is unclear.²⁵⁸ Should the monomer's torsional potential energy surface be sufficiently biased or solvophobic

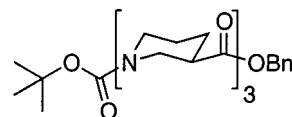
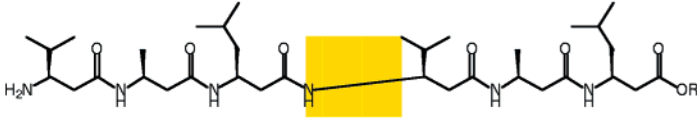
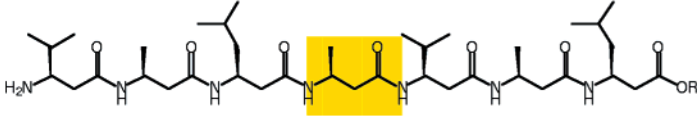
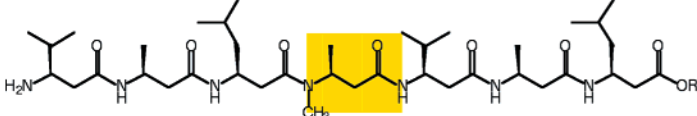
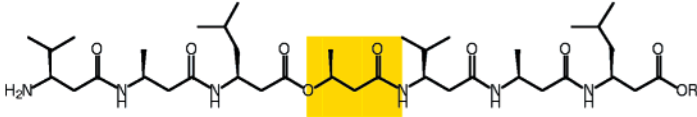
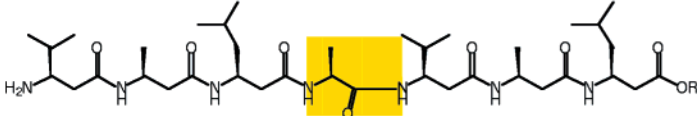
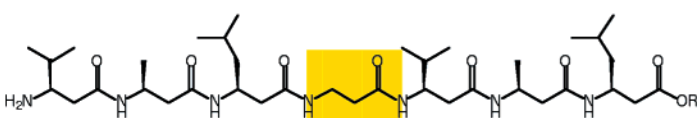


Figure 34. Structure of the β -tripeptide from β -HPro.

forces dominate secondary structure formation, one might expect that H-bond interactions could be eliminated without significant consequence. Surely in a solvent like MeOH, there is only a small energy difference between an intramolecular H-bond and a MeOH-amide H-bond. The fact that oligomers and polymers of proline²⁵⁹ as well as peptoids¹⁴⁰ adopt discrete secondary structures is clear evidence that H-bonds are not essential to ordered solution conformations of amide backbones.²⁵⁸ In 1999, Gellman²⁶⁰ and Seebach²⁶¹ both reported non-hydrogen-bonded secondary structure formation in β -peptides by preparing and studying analogues of proline (Figure 34). Complex mixtures of *cis* and *trans* amide rotamers were detected by ^1H NMR spectroscopy,²⁶¹ and this complexity has hampered conformational studies in solution. Nonetheless, CD spectra of these oligomers display intense and distinct patterns. Systematic studies of CD spectra as a function of chain length provided clues that these oligoproline analogues

Table 2. Single Residue Mutants Used To Probe the Structure of β -Peptides²⁵²

Sequence	Mutant	CD
	Original sequence	14-helix
	Original sequence extended by one internal β^3 -HAla	14-helix
	N-methylation (steric and H-bond perturbations)	Loss of CD pattern corresponding to 14-helix
	Replacement of NH by O (H-bond perturbation)	Loss of CD pattern corresponding to 14-helix
	Removal of one methylene group	Loss of CD pattern corresponding to 14-helix
	Omission of substituents.	Solvent dependent CD. MeOH: 14-helix H ₂ O/MeOH: loss of CD pattern corresponding to 14-helix

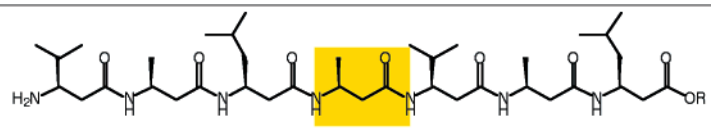
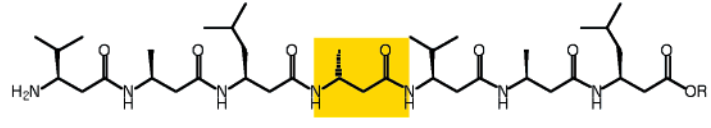
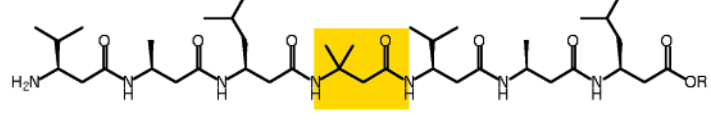
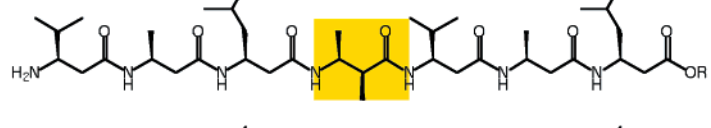
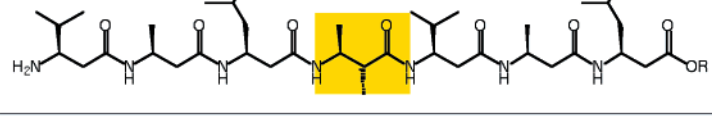
adopt regular secondary structure in MeOH and that the extent of secondary structure formation is maximal once four residues are in place.²⁶⁰ On the basis of the β -tripeptide crystal structure, ¹H NMR coupling constants, and assumptions based on conformational analysis, Seebach proposed a 10₃ right-handed helix for the (*S*)- β^3 -homoproline chain. This extended conformation is a further example that illustrates how the preferred backbone conformation around the central C _{α} -C _{β} bond dominates the secondary structure of β -peptides.

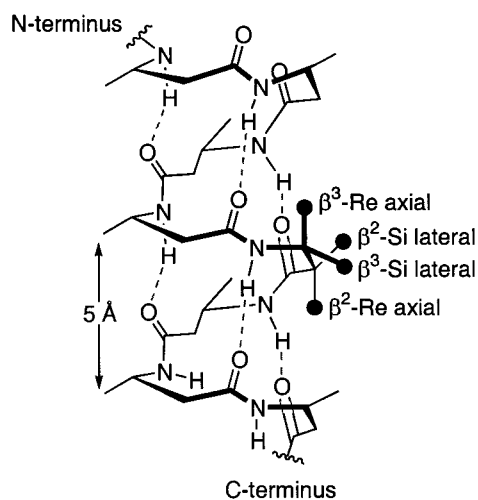
Seebach's helical molecular model led his group to test how variations in backbone constitution and stereochemical modifications stabilized or destabilized the secondary structure.²⁵² Incorporation of a single amino acid residue into the center of the original β^3 -hexapeptide HVal-HAla-HLeu-HVal-HAla-HLeu-OMe sequence generated a series of single point mutations (Table 2). As predicted by Seebach's model,²²³ many relatively minor structural changes to the central residue were incompatible with the 14-helix, resulting in sequences that did not show the characteristic CD pattern of the 14-helix. These included *N*-methylation (i.e., an *N*-Me β -amino acid), replacement of NH by O (i.e., a β -depsipeptide), and removal of the CH₂ group (an α -amino acid). These observations suggested that proper dihedral angles, H-bonding, and a periodic backbone are necessary in order to maintain conformational integrity. The absence of side-chain substituents on the central β -amino acid residue also destabilized the helical

secondary structure. Specifically, a sequence containing the 3-aminopropanoyl unit (β -HGly, i.e., loss of single methyl side chain) gave a CD spectrum that became highly dependent on solvent. In MeOH the CD spectrum of the β -HGly mutant was characteristic of the 14-helix, while in 1:1 MeOH:H₂O an entirely different and yet uncharacterized pattern emerged. These results pointed to a strongly biased torsional potential energy surface for β -peptides bearing side chains in the 2 or 3 position.²⁵² This is consistent with the subsequent observation that the helix to random conformation transition in β -peptides is a noncooperative process.²³⁴

A series of mutants having stereochemical variations in the central β -amino acid position revealed additional information (Table 3). According to Seebach's original model,²²³ the short pitch of the β -peptide helix and the equatorial orientation of the side chains with respect to the helical axis both place limits on substitution patterns that can sustain the helical secondary structure (Figure 35). Thus, lateral non-H-substituents in the 2- and 3-positions on the 3-amino acid residues of the helix were predicted not to interfere with the secondary structure, while axial ones were expected to disrupt the helix. This is borne out by the data in Table 3.²⁵² Incorporating a single mismatched residue in the central position of the β -heptadepsipeptide caused the CD pattern to disappear, while detailed NMR and CD data confirm the helical structure in mutants that have lateral substituents. The geminal dimethyl mutant is also

Table 3. Single Residue Mutants Used To Probe How Substituents on the β -Peptide Effect the 14-Helix Conformation²⁵²

Sequence	Mutant	CD
	Original sequence	14-helix
	Inversion of configuration at β^3	Loss of CD pattern corresponding to 14-helix
	Geminal dimethyl substitution at β^3	Loss of CD pattern corresponding to 14-helix
	<i>like</i> - $\beta^{2,3}$ -dimethyl substitution (methyl groups occupy lateral positions in the 14-helix)	Strong 14-helix signal
	<i>unlike</i> - $\beta^{2,3}$ substitution (methyl groups occupy a lateral and an axial position in the 14-helix)	Loss of CD pattern corresponding to 14-helix

**Figure 35.** Side view of the β -peptide 14-helix with 5 Å pitch. The black circles correspond to unspecified side chains.

consistent with this prediction since one of the methyl groups would be in the axial position. Here, the behavior is in contrast to α,α -disubstituted α -amino acids that are known to stabilize helical structures. Results based on NMR and CD data fully confirmed the predictions.

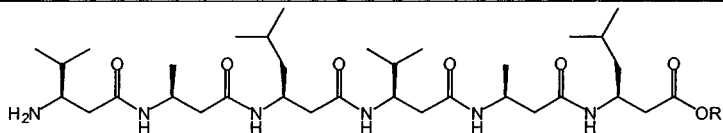
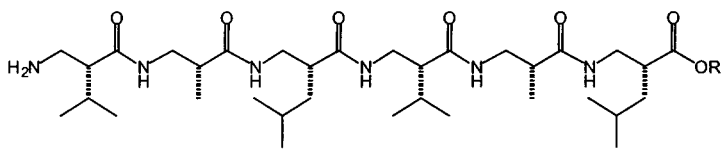
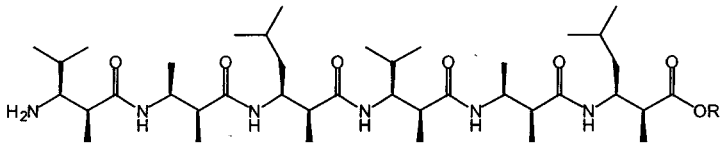
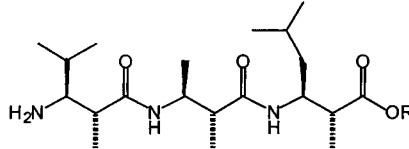
Noticeably absent from Table 3 are β -peptides from β -amino acids with side chains only in the 2-position (β^2 -amino acids). The isomeric β -peptide carrying the same side chains in the α - rather than β - position was predicted to also give the 14-helix secondary structure, but for the particular stereochemistry, shown in Table 4, the handedness was expected to be opposite of the previously studied β^3 -peptide. CD measurements on various β^2 peptide oligomers supported this prediction.^{253,262} Curiously, the magnitude

of the Cotton effect was relatively weak and strongly dependent on solvent and temperature, suggesting a less stable secondary structure for the β^2 vs β^3 sequence. This notion is consistent with calculations of the conformational potential energy surface of β -peptides.¹⁸⁵ These calculations show that β -substitution is more efficient than α -substitution in reducing the flexibility of the β -peptide backbone.

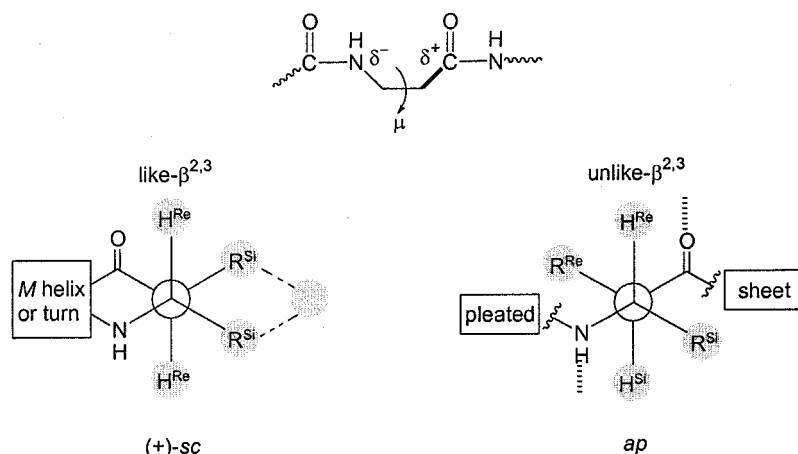
The strong CD signal from the stereochemical mutant carrying substituents in both the 2- and 3-positions (Table 3) suggested that this stereochemistry should favor the 14-helix. Indeed, a hexameric sequence made entirely from *like*- $\beta^{2,3}$ residues (Table 4) exhibited the characteristic CD pattern of the 14-helix, although the spectra recorded were not independent of concentration, suggestive of an aggregation phenomenon.²⁴⁹ Interestingly, the ¹H NMR solution structure and NH proton exchange studies on this sequence revealed that the peptide backbone is sterically protected by the many hydrophobic substituents, possibly to such a degree that crowding destabilizes the helix and causes it to unwind.

The simple “at-a-glance” predictive correlation that emerges from Tables 3 and 4 is as follows: with the peptide backbone drawn in the plane of paper, substituents in the same “half space” (i.e., *like*-configuration) are all matched to the same helical handedness. This correlation can be rationalized by analyzing the basic conformers in β -amino acids.^{183,184,263,264} Such an analysis reveals a strongly preferred backbone torsion around the C_α - C_β bond, driven in part by the tendency to minimize repulsive vicinal interactions (Figure 36)²⁴⁹ and possibly by internal electrostatic considerations.¹⁸⁴ The *sc* conformation, favored for monosubstituted β^2 - or β^3 -residues (especially if the substituents are bulky)²⁶³

Table 4. β -Peptide Amino Acid Sequences Probing the Effects of Stereochemistry and Substitution of the 14-Helix Conformation

Sequence	Sequence description	Assigned Structure
	Original sequence – a β^3 -amino acid	14-helix (<i>M</i>) ^a
	A β^2 amino acid sequence	14-helix (<i>P</i>) ^b
	A like- $\beta^{2,3}$ -amino acid sequence	14-helix; forms aggregates ^c
	An unlike- $\beta^{2,3}$ amino acid sequence	Extended strand ^d

^a Reference 223. ^b Reference 262. ^c Reference 249. ^d Reference 201.

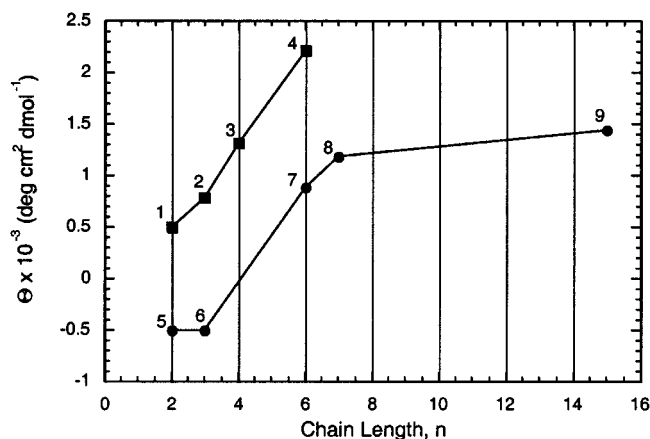
**Figure 36.** *sc* and *ap* conformations about the C_{α} – C_{β} bond of β -amino acid residues. Schematic depiction of the electrostatic considerations that favor the *sp* conformation.

and like- $\beta^{2,3}$ disubstituted residues, promotes helical or turn conformations. The *ap* conformation, favored for unlike- $\beta^{2,3}$ disubstituted residues, promotes an extended, strand-like structure (vide infra). Geminally disubstituted residues have no preferred conformation about the C_{α} – C_{β} bond, although axial positions in a helical conformation would destabilize a 14-helix (Figure 35).

iii. Cooperativity. Cooperative conformational order results from multiple noncovalent interactions between nonadjacent chain segments. A critical chain length and sigmoidal transitions are the hallmarks of cooperative ordering mechanisms. In the specific case of helical conformations, this behavior can be understood^{265–267} as resulting from a minimum number of residues required to nucleate stable helix propagation. Since the propagating helix is stabilized by noncovalent interactions between nonadjacent

repeat units, the critical nucleus size generally corresponds to a chain length of at least one turn. Experimental observations^{268,269} on helix-forming α -peptides are in good agreement with theory, although a deeper understanding of the specific interactions responsible for this cooperativity is still developing.^{258,270,271}

For β -peptide secondary structures, cooperative formation has been investigated in various ways. One test of cooperativity involves examining the onset of conformational order as a function of chain length. The earliest study of this sort for discrete β -peptide oligomer appears to date back to 1979 on poly(*S*- β AspOiBu).¹⁹⁸ However, at that time the structure of the ordered conformation was not understood. Clues about cooperativity in forming the 14-helix with β -peptides can be found from CD studies. Figure 37 shows a plot of CD intensity (normalized per



Data Point	Sequence	Conc.	Ref.
1	Boc-(ACHC) ₂ -Bn	0.3 – 1.0 mM	239
2	Boc-(ACHC) ₃ -Bn	0.3 – 1.0 mM	239
3	Boc-(ACHC) ₄ -Bn	0.3 – 1.0 mM	239
4	Boc-(ACHC) ₆ -Bn	0.3 – 1.0 mM	239
5	Boc-β ³ -HAla-β ³ -HLeu-OMe	0.2 mM	223
6	Boc-β ³ -HVal-β ³ -HAla-β ³ -HLeu-OMe	0.2 mM	223
7	CF ₃ CO ₂ H-(H(β ³ -HVal-β ³ -HAla-β ³ -HLeu) ₂ -OMe	0.2 mM	223
8	CF ₃ CO ₂ H-H-β ³ -HVal-β ³ -HAla-β ³ -HLeu-β ³ -HAla-β ³ -HVal-β ³ -HAla-β ³ -HLeu-OH	0.2 mM	254
9	CF ₃ CO ₂ H-H-β ³ -HLeu-β ³ -HAla-β ³ -HVal-β ³ -HPhe-β ³ -HVal-β ³ -HAla-β ³ -HLeu-β ³ -HPhe-β ³ -HLeu-β ³ -HAla-β ³ -HVal-β ³ -HPhe-β ³ -HVal-β ³ -HAla-β ³ -HLeu-OH	0.02 mM	253

Figure 37. Intensity of the CD maximum in the vicinity of 215 nm normalized per backbone amide bond as a function of the chain length. All of the spectra were taken in methanol. The sequence and concentration of the individual points are listed in the table. The signs of the CD signals were chosen such that all sequences have the same stereochemical configuration in the β³-position.

amide) vs the number of residues for Gellman's and Seebach's 14-helix forming β-peptides. In the Gellman series,²³⁹ a significant CD intensity is already present in the dimer, even though such a chain is too short to form a complete turn. The steady rise in CD intensity from dimer to hexamer suggests a continuous growth in 14-helix population, which presumably in the long chain limit will reach an asymptotic value. On the basis of this behavior, the backbone appears to be highly preorganized for the helical conformation and is reminiscent of helically templated polypeptides.²⁷² Although the steady rise of CD intensity was claimed by Gellman to be evidence that formation of the 14-helix involves a cooperative process,²³⁹ the dihedral angles of these β-peptides are highly constrained, possibly precluding this backbone from exhibiting cooperative conformational transitions.

In comparison to Gellman's conformationally constrained β-peptides, the Seebach β³-peptides display chain-length dependence^{223,253,273} more typical of α-peptides (Figure 37). The dimer and trimer show weak Cotton effects, uncharacteristic of the 14-helix. Beyond the trimer, a rapid rise in CD intensity is observed, and a plateau is reached for chains of sufficient length. Thus, a threshold chain length seems necessary to initiate conformational order and an asymptotic limit appears to exist. Although the behavior of Seebach's β-peptides shown in Figure 37 appears characteristic of cooperative helix formation,

temperature-dependent CD and ¹H NMR studies reveal that the dominant contribution to helix stability in these β-peptides is related to the preferred conformation about the C_α-C_β bond.²⁷⁴ The intensity of CD signals and ¹H NMR chemical shifts changed linearly with temperature over the range from 100 K up to 393 K. This temperature spans the theoretically predicted melting temperature of ca. 340 K.²⁷⁵ A cooperative melting transition in which the whole structure is lost all at once would be expected to show a sigmoidal rather than linear temperature dependence. Thus, rather than displaying all-or-none behavior characteristic of two-state phenomena, the 14-helix gradually populates nonhelical conformations as the temperature is raised. If the predominant stabilizing force were a collection of long-range, noncovalent interactions (e.g., hydrophobic interactions or H-bonds between nonadjacent segments), cooperative behavior would be expected. In contrast, conformational changes that result from a redistribution of the populations of localized torsional states will gradually become depleted in the helical conformation. Such a process cannot be considered cooperative. This noncooperative behavior is consistent with the lack of observed melting in β-peptides.²⁷⁴ On the basis of these results, it seems that the β-peptide derives its helix-inducing propensity from its torsional potential energy surface.¹⁸⁵

iv. Heterosequences. Heterosequences incorporating both β² and β³ amino acids were also synthesized and with appropriate matching of stereochemistry (i.e., like-configuration) were expected to exhibit the 14-helix. However, their behavior was found to be surprising (Table 5).²⁴⁹ The CD spectra of many coligomer sequences did not show the usual 215/200-nm CD pattern in MeOH, but rather a CD spectrum with an intense single peak at ca. 205 nm was observed (Figure 28). Complicating matters further, this behavior depended somewhat on the terminal protecting groups.²⁴⁹ With *N*-Boc and benzyl ester protecting groups intact, the unusual CD pattern was generally observed, while deprotection mostly gave CD spectra characteristic of the 14-helix. The extreme intensity of the CD signal for the protected forms together with the very long half-lives of the NH/ND exchange rates suggested a new ordered conformation. This was confirmed by detailed ¹H NMR solution-structure analyses which revealed a novel irregular helix consisting of three H-bonded turns: a central 10-membered ring and two 12-membered H-bonded rings (designated 12/10-helix). Molecular dynamics studies have simulated reversible folding into this unique conformation.²⁷⁶

Direct structural evidence for the 10-membered H-bonded ring was found in the crystal structure of a geminally disubstituted tripeptide.²⁷⁷ The *N*-terminal carboxy group and the amide NH of the second amino acid H-bond form a tight turn. This ring is quite similar to the central 10-membered H-bonded ring of the 12/10-helix. Interestingly, even tighter turns could be generated in sequences derived from 1-(aminomethyl)cyclopropanecarboxylic acid.²²⁶ As mentioned above (Figure 26), the conformational constraints in this β-amino acid induce the **S(8)**

Table 5. Role of Sequence Variation and End Groups on the Solution Conformation of β -Peptides

Sequence	Description	End groups	Assigned Structure ^a
	A β^2 -block- β^3 -sequence	R=Boc R'=Bn	12/10-helix
		R=H R'=H ^b	14-helix
	A β^2 -alternating- β^3 sequence	n=1, R=Boc, R'=Bn	12/10-helix
		n=1, R=H, R'=H ^b	12/10-helix ^c
		n=2, R=Boc, R'=Bn	12/10-helix
		n=2, R=H, R'=H ^b	14-helix
	A β^2 - β^3 heterosequence	R=Boc R'=Bn	12/10-helix

^a On the basis of CD spectra in MeOH. ^b Trifluoroacetate salt. ^c Also based on NMR structure determination.

H-bonding pattern between next neighbors. This is an example of residue-controlled or substituent-induced turn formation, and it illustrates how the monomer's torsional potential energy surface can be biased to regulate backbone conformation.

The 12/10 secondary structure was rationalized on the basis of solvophobic interactions.²⁴⁹ Whereas the 14-helix conformation of the β^2 -alternating- β^3 sequence does not provide close interactions between side chains in successive turns, in the 12/10-helix they are directly atop one another. Solvophobic interactions with the terminal protecting groups explained why the protected forms were more prone to adopt the 12/10-helix. In the unprotected form, the dipole moment of the 14-helix may add stability through charge–pole interactions.^{234,249} An alternative rationalization is one that illustrates negative design principles. Whereas many patterns of alkyl substitution disrupt the 14-helix, they only cause mild destabilization of the 12/10-helix pattern.¹⁸⁵ Thus, it is possible to destabilize (i.e., design away) the 14-helix in favor of the 12/10-helix. Regardless of interpretation, in 1997, when Seebach's group communicated their initial findings on the β^2 - β^3 -co-oligomers, it became apparent from this work²⁴⁸ and the related studies by Gellman²³⁸ that the β -peptides are likely to have a high degree of variability in secondary structure type.

v. Water-Soluble β -Peptide Foldamers. Following earlier observations,^{278,279} Seebach's initial paper on β -peptide oligomers showed that this backbone is remarkably resistant to proteolytic digestion and, hence, potentially useful as a candidate for new drugs.²²³ Consequently, there has been considerable activity on the development of β -peptides that are both highly water soluble and conformationally structured in aqueous solution. Several groups have

contributed to the discovery of stable secondary structures from β -peptides in aqueous solution. Some of the oligomers examined for this purpose can be found in Figure 38. To enhance water solubility, β -peptides containing polar serine and lysine side chains were synthesized and studied.^{253,280} While in MeOH these oligomers exhibited the CD profile typical of the 14-helix, in aqueous solution fewer of the oligomers studied maintained this pattern. Those that did exhibit spectral characteristics of the 14-helix in water did so with much reduced intensity. Moreover, in both organic as well as aqueous solvents, the presence of a large number of neighboring cationic side chains destabilizes the secondary structure, consistent with the well-known behavior of poly-(α -homolysine).²¹² It was concluded that oligomers with neutral serine-derived side chains have a smaller helix-disrupting effect in water than the charged lysine derivatives. However, β -peptides that are hydroxylated in the α -position appear to be void of helical secondary structure.²³⁵

To reduce the disruptive consequences of several charged groups, β -peptide sequences having just one polar side chain (either homoglutamate or homolysine) were studied by Gung and Zou (Figure 38).²⁸¹ However, these heptamers were poorly soluble in water. Heptamers bearing two β -HGLu or one β -HGLu and a C-terminal aspartate (D-Asp) were synthesized next and found to be soluble in water up to concentrations from ca. 5 to more than 15 mM (without significant aggregation). However, in going from MeOH to H₂O, the helical content decreased as judged by CD, and no NOE cross-peaks characteristic of the 14-helix were observed in water. It is interesting to note however, that the peptide sequence with the D-Asp C-terminus gave considerably greater CD intensity at 216 nm than the sequence differing by

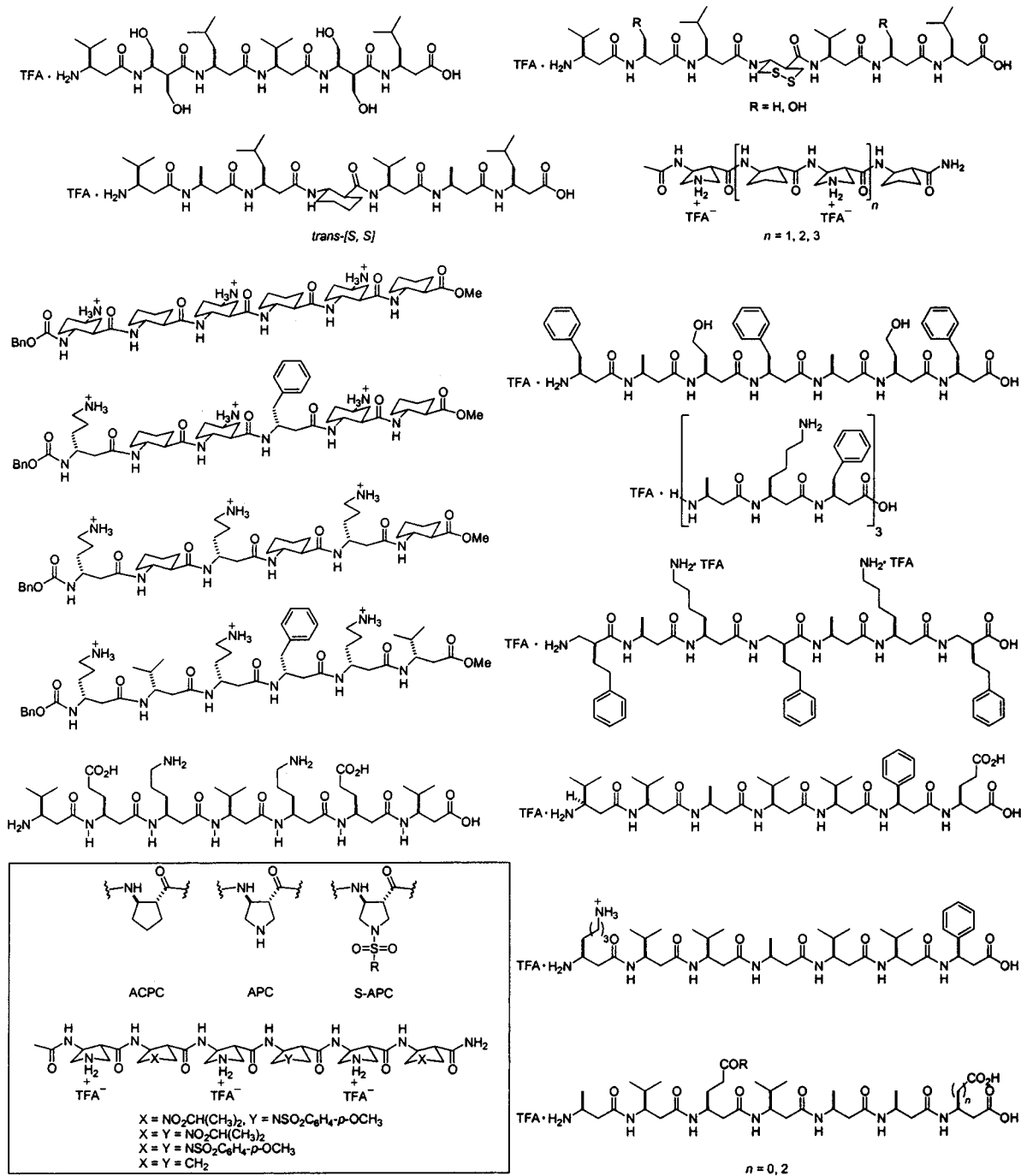


Figure 38. Water-soluble β -peptide oligomers.

only two CH_2 units, suggesting that D-Asp may provide some type of stabilizing C-capping interaction.

Gellman showed that by limiting backbone flexibility it is possible to overcome the poor stability of the 14-helix in aqueous media.²⁸² His group performed systematic studies on oligomers having varying proportions of rigidifying cyclohexyl and acyclic β -amino acid residues (Figure 38). To promote water solubility and reduce aggregation tendencies, an additional amino group was added to the cyclohexane ring of *trans*-2-aminocyclohexanecarboxylic acid (*R,R*,*R*-2,5-diaminocyclohexanecarboxylic acid, DCHC).²⁸³ In aqueous solution, all of the DCHC-containing hexameric oligomers displayed a broad CD spectrum with a maximum at 215 nm, characteristic

of the 14-helix. The intensity at 215 nm decreased by ca. 20% upon replacement of two cyclohexyl residues for acyclic residues. 1H NMR studies on this oligomer in water provided NOE data to corroborate the postulated 14-helix. However, with each successive replacement of a cyclic for an acyclic unit, a further decrease in CD intensity was observed, suggesting diminished stability of the 14-helix in H_2O with increasing acyclic content. Similarly, Gellman and co-workers showed that β -peptides containing four to eight pyrrolidine-based residues (APC) provide water-soluble oligomers that acquire the 12-helix conformation in aqueous solution as determined by CD and 1H NMR (Figure 38).²⁸⁴ A recently reported modification of this backbone involves *N*-sulfonylation (S-APC) that enables the modular introduction

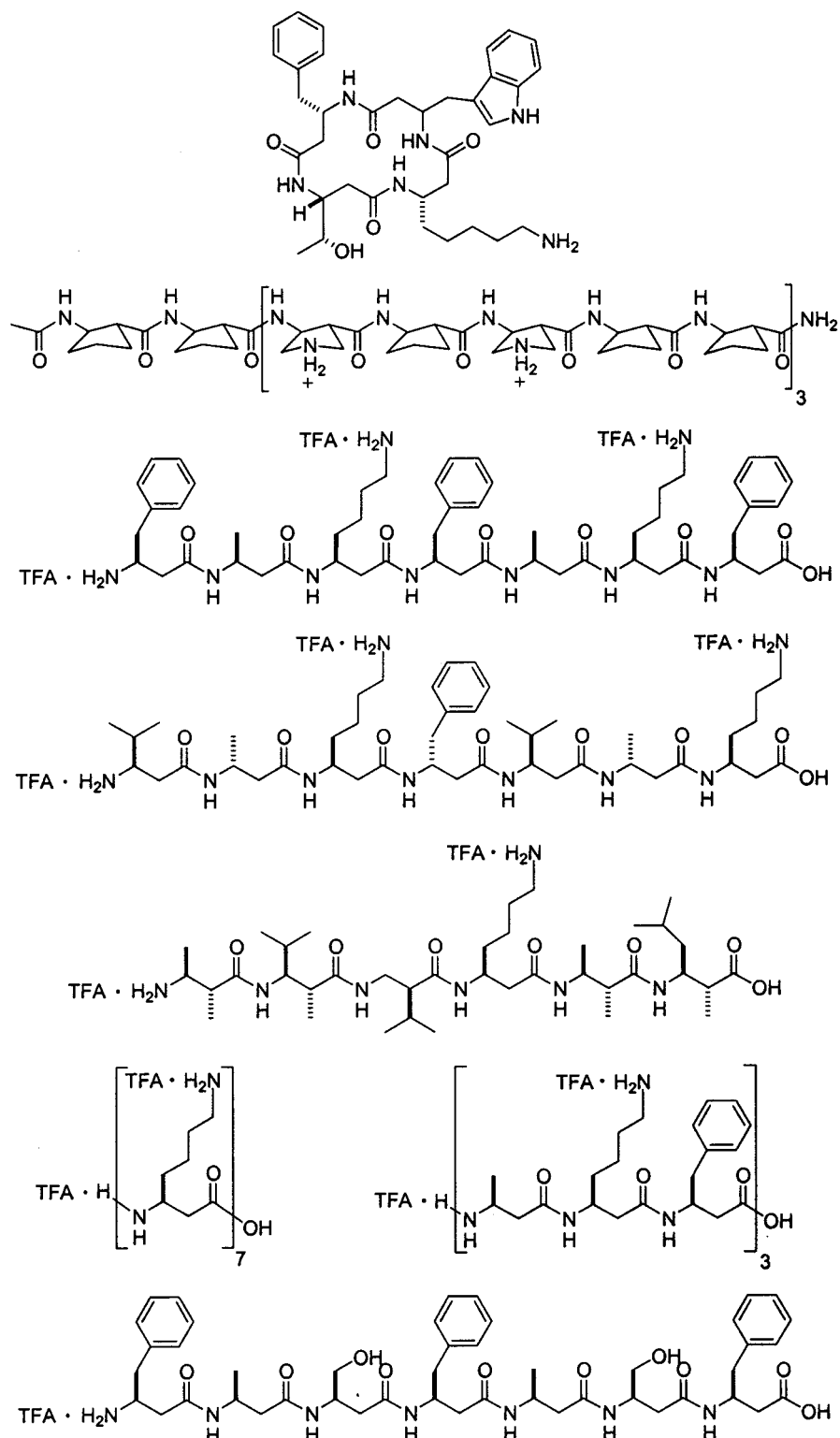


Figure 39. β -Peptide oligomers studied for their biological activity.

of a wide range of side chains onto the APC unit.²⁸⁵ Despite the change in the geometry of the five-membered ring upon sulfonylation, the 12-helix persists, although somewhat more tightly wound.

Seebach further pursued the design of water-soluble helical β -peptides based on sequences having minimal conformational constraints.²⁸⁶ Following on their observation that *like-2,3*-disubstituted β -amino acids increase the stability of the 14-helix conformation, they prepared monomers carrying two serine or

two cysteine side chains and incorporated these into β -hexa- and β -heptapeptides (Figure 38). Ionic side chains were excluded on the basis of their tendency to destabilize the 14-helix conformation. Deprotection of the thiol groups resulted in cyclic disulfide formation in the case of cysteine-containing sequences. To study the CD contribution of the disulfide chromophore, the carbocyclic analogue was also prepared. All of these sequences including the hexapeptide showed a CD spectrum in H_2O characteristic of the

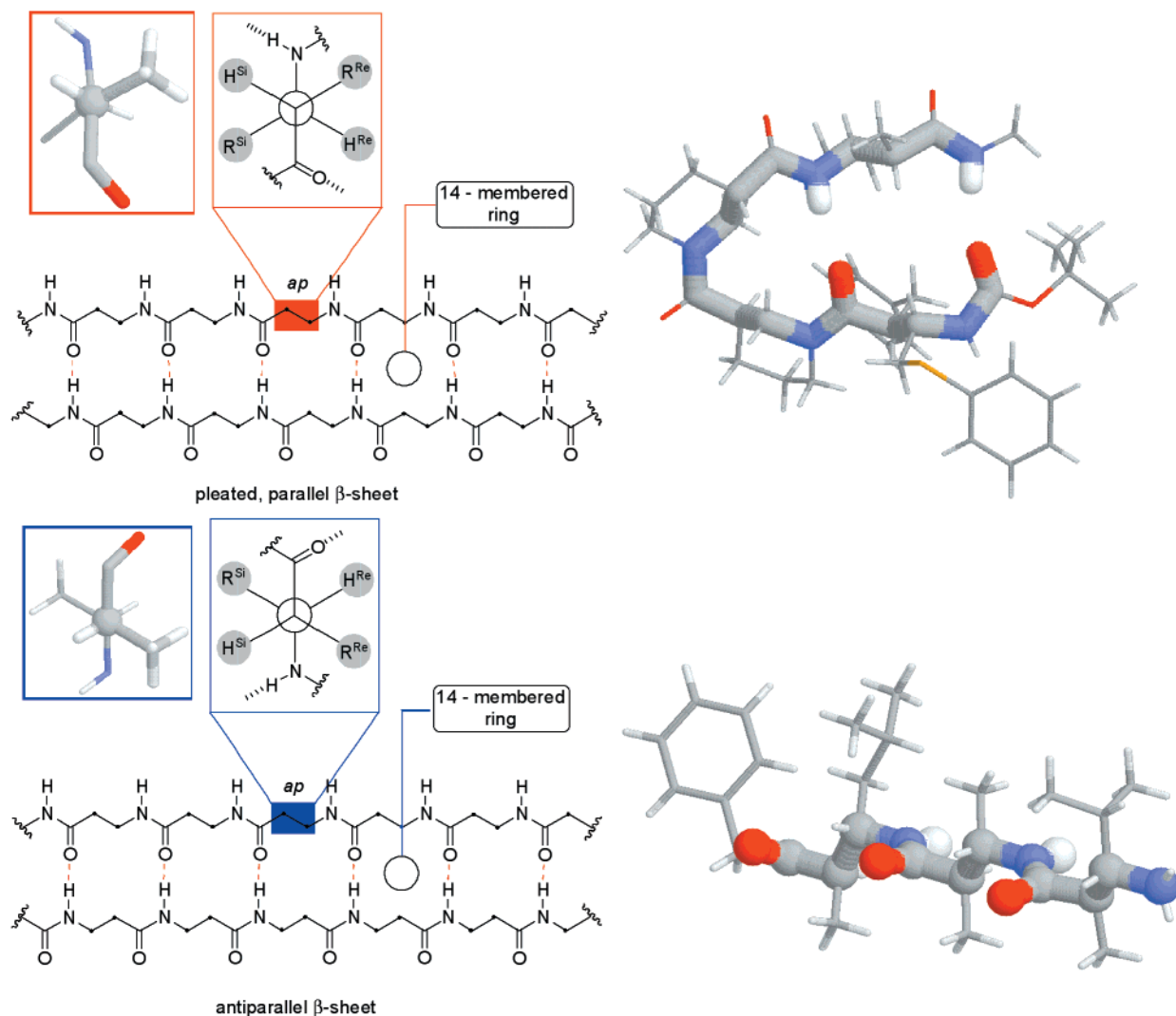


Figure 40. Crystal structures of β -peptide sequences with antiparallel and parallel β -sheetlike structures.²⁰¹ The backbone is rendered in thick cylinders. Newman projections show representative C_{α} - C_{β} dihedral angles in the *ap* conformation.

14-helix. Whereas the hexapeptide without conformational restriction gave no NOE cross-peaks indicating little helical content in water, the heptapeptide containing the cyclic disulfide showed NOEs characteristic of the 14-helix. The low intensity of these cross-peaks suggested that only partially helical conformations, or a mixture of helical and non-helical chains, exist for this sequence under these conditions.

The successful development of water-soluble β -peptides having helical conformations from sequences that do not contain any constrained monomers was achieved using salt-bridge stabilization strategies (Figure 38). This approach was realized independently by Seebach²⁸⁷ and DeGrado.²⁸⁸ Both of these studies showed, by NMR and CD methods, that electrostatic interactions between the side chains of acyclic β -amino acids produce a well-defined 14-helix in aqueous media. Since charged groups resulted from deprotonated acidic and protonated basic residues, the stability of the helical conformation was expected to be pH dependent. Indeed, the CD intensity was shown to reach a maximum at an intermediate value of pH in which the salt bridge would exist. DeGrado showed that the CD intensity depends

markedly on the concentration of added electrolyte. A plot of CD intensity versus the square root of NaCl molality is approximately sigmoidal, with a midpoint near 0.4 M (according to Debye-Hückel theory, the energy of electrostatic interactions between ions scales as the square root of $[\text{NaCl}]$).

vi. Biological Activity of β -Peptide Foldamers. The availability of conformationally structured, water-soluble β -peptide sequences, together with their known stability and resistance to enzymatic degradation,^{289,290} has led to some early observations regarding the biological activity of this oligomer class. Seebach and co-workers designed cyclic β -peptides containing only four residues that bind to the somatostatin receptor with micromolar affinity (Figure 39).²⁹¹ Hexa-, hepta-, and nonameric β -peptides carrying one to seven water-solubilizing groups have also been shown to be inhibitors of small intestinal cholesterol and fat adsorption.²⁹² A correlation was found between the ability of β -peptides to form an amphipathic 14-helix in MeOH and their inhibitory effect. DeGrado^{293,294} and Gellman²⁹⁵ used similar designs in mimicking natural membrane-active peptide toxins and antibiotics. A strong correlation exists among the sequences studied between the helical

content and antibacterial activity. To be therapeutically useful as antibiotics, they must function in the presence of human cells. Interestingly, favorable selectivities have been noted. These studies are clearly in their infancy but point to the likelihood that the β -peptide scaffolding holds much promise as a candidate for the molecular design of bioactive agents.

e. Strands and Turns: Artificial Sheets from β -Peptide Foldamers. There is currently considerable activity in the design and study of peptide sequences that serve as models of β -sheet secondary structures.^{136,156,296} Understanding how the substituent stereochemistry of β -amino acids influences backbone conformation has guided the design of β -peptide sequences with parallel and antiparallel β -sheetlike structures (Figure 40).²⁰¹ The *unlike- $\beta^{2,3}$* residues were predicted to adopt an extended conformation, and indeed, this has now been observed in several cases (Table 4). Although early studies on poly(β -peptides) suggested β -sheet formation from *unlike- $\beta^{2,3}$* residues,¹⁸⁹ the first oligomeric example of a β -strand from β -peptides appeared from Gellman's lab.²⁰⁰ The crystal structure displays the expected antiparallel sheet formation including a β -turn-like conformation stabilized by a 10-membered-ring hydrogen bond. This particular turn unit was based on earlier studies from Gellman's lab on the development of minimal hairpin structures in which it was found that the L-proline-glycolic acid segment functioned effectively.²⁹⁷ In contrast to the *unlike- $\beta^{2,3}$* disubstituted residues, Gellman showed that residues bearing only a single substituent did not lead to a well-ordered solution conformation.²⁰⁰

Whereas Gellman's original artificial β -sheet sequence utilized α -amino acids to fix the turn conformation, he later developed a β -peptide reverse turn that promotes hairpin formation.²⁹⁸ The design was based on nipecotic acid residues but required a heterochiral dipeptide sequence to stabilize antiparallel sheet structures.^{299,300} Seebach showed in 1999 that sequences consisting entirely of β -amino acids could be designed to achieve both turn and strand components.²⁰¹ To enforce an antiparallel pleated sheet arrangement, a turn segment was added between a pair of *unlike- $\beta^{2,3}$* residues. The turn design was based on the sequence that promoted the 12/10-helix. The introduction of the turn motif resulted in significantly enhanced solubility. ¹H NMR structure determination in methanol-*d*₄ showed that this β -peptide adopts both a hairpin arrangement and the expected antiparallel β -sheet. When no turn segment was present, the crystal structure of a tripeptide consisting of *unlike- $\beta^{2,3}$* residues showed 14-membered H-bonded rings in parallel pleated sheets (Figure 40). It can be seen that all of the carbonyl groups are aligned, leading to a polar sheet. Solubility decreased with increasing chain length. Other examples of reverse turns³⁰¹ and β -strands³⁰² from β -amino acids have appeared recently.

2. α -Aminoxy Acids

Another member of the β -peptide family is the α -aminoxy acid repeat, first discussed in the context of peptidomimetics by Yang et al.³⁰³ These authors

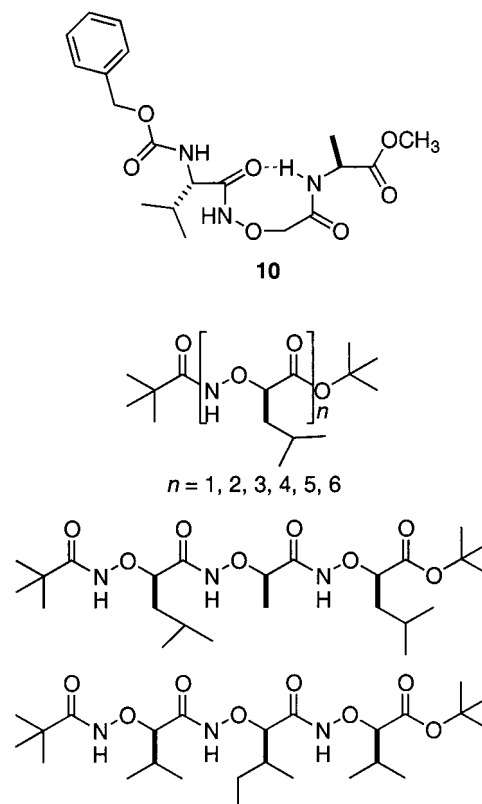


Figure 41. Representative examples of α -aminoxy peptide oligomers.

reasoned that the unusual torsional characteristics of the N–O bond in hydroxylamine resulting from lone-pair electron repulsion would help rigidify the β -peptide backbone. IR and ¹H NMR spectroscopic studies on a series of model compounds showed that an **S(8)** hydrogen bond is favorable, giving rise to a conformation analogous to the γ -turn motif found in proteins. In particular, the O–C bond of N-oxy amides strongly prefers out-of-plane orientations, and the barrier for rotation about the N–O bond is calculated to be about 7 kcal·mol⁻¹. The **S(8)** hydrogen bond between Val–C=O···H–N–Ala was evident in tripeptide **10** (Figure 41), leading to the suggestion that the “N–O turn” can be used as a novel type of backbone fold.

Peptides of α -aminoxy acids, i.e., oxa-peptides, are analogues of β -peptides, with C _{α} replaced by O. Extension of the model studies to higher oligomers from chiral α -aminoxy acid peptides resulted in a helical conformation owing to consecutive, right-handed N–O turns and **S(8)** hydrogen bonds (Figure 41).³⁰⁴ This conformation was supported by a combination of X-ray crystallography, NMR, CD, and computer simulation. Computer simulations predicted a conformation in which each turn consisted of 1.8 units.³⁰⁵ The helical structure was observed in oligomers as short as the trimer and was independent of side chains.

3. Sulfur-Containing β -Peptide Analogues

Several sulfur-containing β -peptide analogues have been generated (Figure 42). Oligomers in which the peptide bond has been replaced by the sulfonamide (i.e., β -sulfonopeptides),^{306–309} sulfonamide (i.e., β -sulfi-

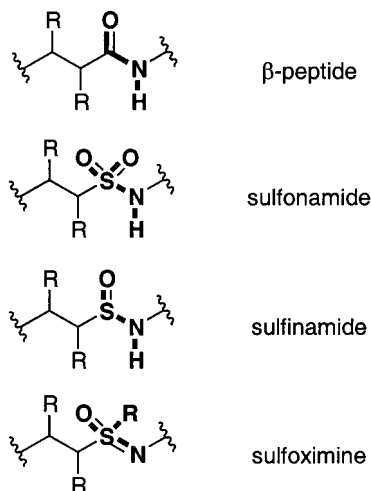


Figure 42. Structural comparison of sulfur-containing β -peptide analogues: oligomers in which the peptide bond has been replaced by sulfonamide (i.e., β -sulfonopeptides),³⁰⁶ sulfinamide (i.e., β -sulfinopeptides),³⁰⁷ or sulfoximine³¹⁰ functional groups.

nopeptides),³⁰⁷ or sulfoximine³¹⁰ moiety have been synthesized and are presently under consideration as possible foldamers. Replacement of the peptide bond with a secondary sulfonamide has two important conformational consequences.^{311,312} First, the barrier to rotation about the S–N bond is much lower than that of the peptide C–N bond. Second, the most favored dihedral angle defined by H–N–S=O is approximately 0° rather than 180° for the H–N–C=O unit.

At this time, relatively little solution characterization work has been performed to show that these oligomers adopt regular secondary structures. Evidence for **S(12)** hydrogen bonding in dipeptides of unsubstituted³⁰⁶ or chiral, β -substituted^{308,313} β -sulfonamides has been found by IR and ^1H NMR spectroscopies. However, in each case, terminal unit

carbamate or amide carbonyl oxygen atoms serve as the H-bond acceptor, owing to the very poor hydrogen-bond acceptor ability of the sulfonamide group.³¹³ It is unclear if these H-bonding interactions will be important in oligomers where the terminal groups play a minor role. To begin to address this issue, Gellman recently evaluated the possibility of two-point hydrogen bonding between a secondary sulfonamide and an α -amino acid residue.³¹⁴ Evidence for intramolecular N–H \cdots O=S and N–H \cdots O=C interactions in chloroform was found from IR and ^1H NMR studies in a molecule containing a sulfonamide linked to a valine by a turn-forming segment.

Very little information is available on the solution conformations of sulfinamide or sulfoximine peptides. These examples clearly show how synthesis can far outpace structural studies in foldamer research, stemming from the difficulties of characterizing solution conformations for each new backbone type.

4. Hydrazino Peptides

Replacing the C_β atom in β -amino acid residues of β -peptides with nitrogen leads to hydrazino peptides.³¹⁵ As a result of this substitution, another H-bond donor and H-bond acceptor are contained within the backbone. Consequently, there is a fairly significant increase in the number of possible secondary structures that could be adopted by this repeat unit including H-bonded rings containing either odd or even numbers of atoms (Figure 43). Several helical and turn motifs were calculated to be stable,³¹⁵ some of which were analogous to their β -peptide counterparts, but there is as of yet no experimental data to support these predictions.

C. The γ -Peptide Family

1. γ -Peptide Foldamers

Like β -peptides, homopolymers of γ -peptides had long been known^{316–319} prior to the search for second-

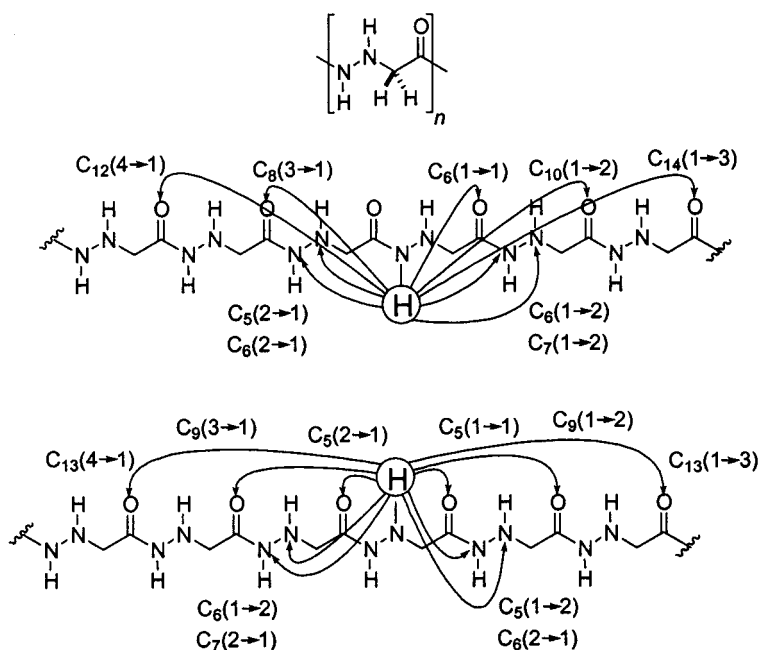


Figure 43. Hydrazino peptide backbones and a diagram showing the many possible intrastrand H-bond interactions in this backbone.

ary structures by systematic studies on discrete oligomers. However, unlike the poly- β -peptides for which helical structures have been clearly established,^{199,202} firm conclusions about the conformational preferences of homopolymers of γ -peptides appear not to have been resolved. From the results of ORD measurements, Rydon suggested a helical structure for the neutral form of poly- γ -D-glutamic acid.³¹⁸ Two left-handed helical models were proposed, both of which invoked three repeats per turn. The models differed as to whether **S(17)** or **S(19)** hydrogen-bonded interactions were involved.³¹⁸ Kajtár and Bruckner synthesized oligo- γ -L-glutamic acids from dimer to heptamer and showed that the ORD signal increases linearly with the chain length, suggesting that the polymer takes on a random conformation.³¹⁶ However, there appears to be no resolution to the question of whether these polymers are helical or conformationally random.^{192,320}

The added torsional degrees of freedom in γ -amino acids^{321,322} might be expected to promote conformationally disordered chains. Yet, just as for β -peptides, this intuitive view does not hold for the γ -peptides either. As stated by Seebach et al., "the surprising difference between the natural α -, and the analogous β - and γ -peptides is that the helix stability increases upon homologation of the residues."²³⁷

The first report demonstrating that chain molecules based on γ -amino acids form regular secondary structure appeared in 1992.³²³ This work targeted the discovery of new classes of protein-like substances with alternative backbones. These oligomers were considered to be vinylogous polypeptides since an (*E*)-ethenyl unit was inserted into each repeat unit to rigidify the backbone. To restrict rotation about the C_{β} - C_{γ} bond and extend the backbone into sheetlike conformations, an α -methyl substituent was initially examined. For this particular substitution pattern, allylic $A^{1,3}$ strain was expected to drive the γ -hydrogen to lie in the plane of the enamide. This conformational preference was borne out in a dipeptide which crystallized into a two-stranded antiparallel sheet; however, longer oligomers failed to form higher order sheetlike structures. Removal of the α -methyl substituent led to vinylogous peptides that organized into long stacks of parallel sheets as revealed by X-ray crystallography. To favor antiparallel alignment, a Pro-Gly dipeptide turn was inserted between a pair of vinylogous amino acids. ¹H NMR data supported the existence of an intramolecular H-bond between the N-H and O=C on the two ends, suggesting the preference of this secondary structure in solution. A peptide sequence which consisted of a vinylogous amino acid, the Pro-Gly turn, and a $\gamma^{2,3}$ -amino acid exhibited a helical conformation that contained 10- and 12-membered H-bond rings.

Two years later, a family of sulfur-containing γ -peptide mimics was reported.^{306,324} This backbone is linked by the sulfonamide group as a replacement for the peptide bond. Being derived from γ -amino- α,β -unsaturated sulfonic acids, these oligomers have come to be known as vinylogous sulfonamidopeptides, closely related to the vinylogous peptides described above. Protein-like side chains added to the γ -carbon gave chiral monomers. The folding patterns of short oligomers ranging from the dimer to the tetramer

have been investigated in solution and the solid state. In chloroform, IR and ¹H NMR studies reveal that the intramolecular H-bond preference is for **S(14)** rings involving the terminal carbamate C=O acceptor. This produces a turn-like motif that is also found in the crystal structures. However, in the solid state a fairly long intramolecular **S(12)** H-bond interaction is formed by utilizing one of the S=O acceptors. Here the carbamate carbonyl is tied up in a much shorter intermolecular H-bond interaction. Although a compact intramolecular H-bond fold is present in solution, the lack of involvement of the S=O bond in all of the oligomers studied calls into question the potential of this backbone to form long-range secondary structures.

In 1998, two reports appeared simultaneously showing that in contrast to this expectation, γ -peptide sequences form remarkably stable helical conformations in solution.^{236,237} The Seebach group described a γ^4 -hexapeptide analogue of the sequence H(-Val-Ala-Leu)₂-OH with L-configuration. Although the CD spectra did not reveal patterns characteristic of secondary structure, conformational analysis by NMR in either pyridine or methanol revealed a right-handed helix with **S(14)** H-bonds from the C=O of residue *i* to the H-N of residue *i*+3 and ca. 2.6 residues per turn. Molecular models of this conformation suggested that the side chains are oriented approximately perpendicular to the helical axis, the H-bonds lie along the helix axis with the dipole moment oriented from the N- to C-terminus, and the C_{α} - C_{β} and C_{β} - C_{γ} bonds adopt (+)-*sc* conformations for this right-handed helix.

Hanessian studied the solution structure of tetra-, hexa-, and octa- γ -peptide analogues of the sequence (-Ala-Val-).²³⁶ All three of these γ^4 -peptides derived from L-amino acids adopted stable right-handed helical conformations in solution. The helical parameters were identical to those found by the Seebach group: 2.6 residues per turn stabilized by **S(14)** H-bonds. Temperature-dependent chemical shifts suggested that these intrastrand interactions are strong. As also noted by Seebach, CD did not reveal a pattern diagnostic of secondary structure. The obvious but important lesson from these reports is that CD cannot be used alone as a means of screening for secondary structure.

Figure 44 compares the 14-helix of the β - and γ -peptides.³²⁵ It is interesting that both backbones prefer H-bond patterns involving 14 atom rings. Obviously these patterns originate differently for the two constitutions. In the case of β -peptides, the **S(14)** H-bond results from the N-H of residue *i*-2 being donated to the carbonyl of residue *i*. In the case of the γ -peptides, the N-H of residue *i* is donated to the carbonyl of residue *i*+3. As a result, with L-amino acids there is a reversal of helix sense, the β -peptide adopting an *M*-helix and the γ -peptide adopting the *P*-helix (as do α -peptides). The direction of the dipole moment is reversed too. Thus, for the β -peptide, the dipole is oriented from the C-terminus to the N-terminus, while for the γ -peptide, it runs from the N-terminus to the C-terminus (as with α -peptides).

Many substituent patterns and stereoisomers are possible for γ -amino acids, but as of yet, these have

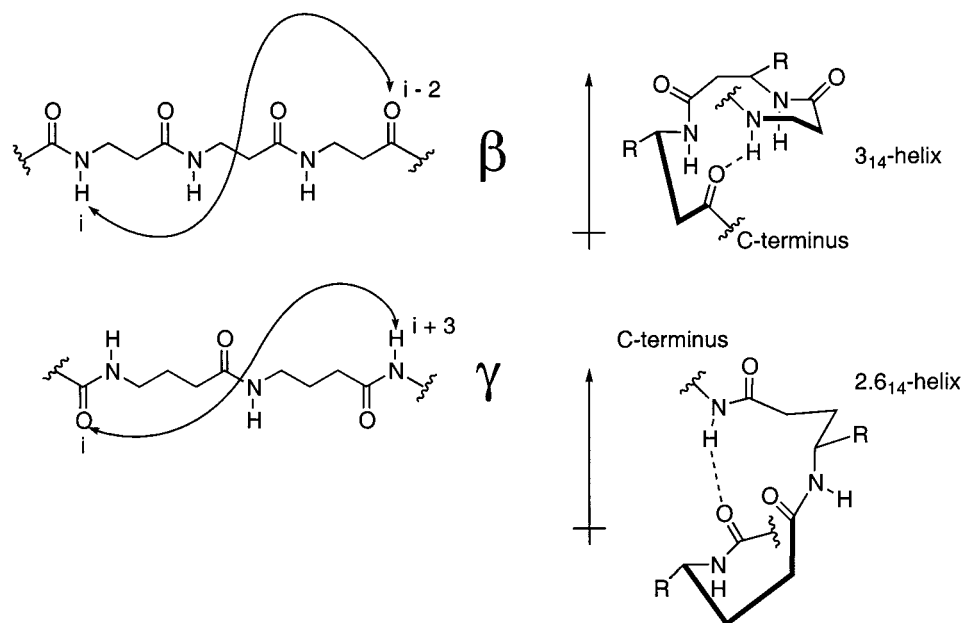


Figure 44. Comparison of helical conformations of β - and γ -peptides.

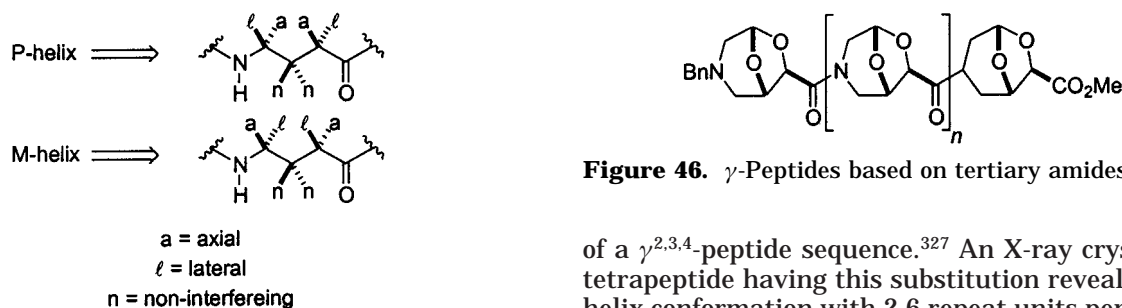


Figure 46. γ -Peptides based on tertiary amides.

Figure 45. Retroanalysis of γ -peptide helices' twist sense.

not been fully characterized. However, Hanessian's initial report²³⁶ included data on $\gamma^{2,4}$ -disubstituted residues. Their observations clearly showed that the addition of an α -substituent can either stabilize or destabilize the helical structure, depending on the relative stereochemistry. Whereas addition of an α -methyl group of *unlike*-configuration stabilized the helical conformation, addition of an α -methyl group having *like*-configuration resulted in the loss of helix formation. They later showed with a different sequence that the $\gamma^{2,4}$ -substitution pattern with L-stereochemistry leads to a reverse turn conformation, stabilized by an **S(14)** H-bond.³²⁶

The Seebach group also investigated substituent effects. On the basis of their helical model, they reasoned that substituents in positions 2 and 4 can occupy either lateral or axial orientations (Figure 45).³²⁵ Axial non-H atoms are projected nearly parallel to the helix axis and severely impinge on the space of the adjacent turn, resulting in helix destabilization. Lateral non-H atoms lie approximately perpendicular to the helix axis and do not experience unfavorable interactions. On position 3, both substituents are tilted with respect to the helix axis and thus oriented in such a way that neither stereochemistry is predicted to interfere with helix formation. These predictions are consistent with Hanessian's observations and are further supported by the study

of a $\gamma^{2,3,4}$ -peptide sequence.³²⁷ An X-ray crystal of a tetrapeptide having this substitution revealed a 14-helix conformation with 2.6 repeat units per turn. A ¹H NMR solution structure in methanol produced a structure nearly superimposed on that obtained by crystallographic analysis. The CD spectrum of this trisubstituted γ -peptide in methanol shows a maximum Cotton effect at 212 nm and zero-point crossing at ca. 196 nm.³²⁵ Other substitution patterns of the γ -peptides have not yet been reported in detail, but preliminary indications suggest that peptide sequences derived from γ^2 - and γ^3 -amino acids do not adopt a preferred secondary structure.³²⁵ However, γ^4 -peptides bearing α - or β -hydroxy groups have been synthesized, and although the structures are still being investigated, CD spectra suggest that these backbones are structured in solution.³²⁵

γ -Peptides that are based on tertiary amides and thus incapable of adopting conformations stabilized by H-bonding interactions have recently been prepared (Figure 46).³²⁸ These oligomers are derived from conformationally rigidified amino acids referred to as BTAA's (bicycles from tartaric acid). As with peptoids,¹⁴⁰ oligomers and polymers of proline,²⁵⁹ and β -peptides based on tertiary amides,^{260,261} complex mixtures of *cis* and *trans* amide rotamers were detected by ¹H NMR spectroscopy and thus hampered solution structure studies. Nonetheless, CD spectra of these oligomers display intense and distinct patterns. On the basis of these data, it was suggested that poly-BTAA's could form secondary structure in solution, although at this time there is no indication of the preferred backbone conformation.

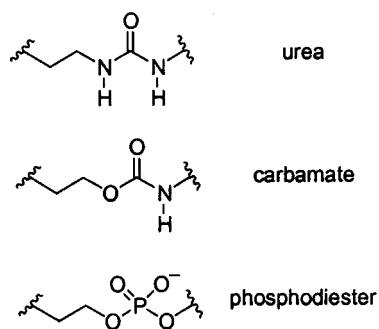


Figure 47. Collection of backbones that can be considered γ -peptide analogues.

2. Other Members of the γ -Peptide Family

Several groups are examining other peptidomimetic backbones, many of which can be classified in the γ -peptide family (Figure 47). Examples include oligoureases,^{329–334} oligocarbamates,^{330,335,336} and phosphodiester.³³⁷ Although at this time the conformational structure of most of these are unknown, it is apparent^{334,338} that they are being considered as foldamer candidates.

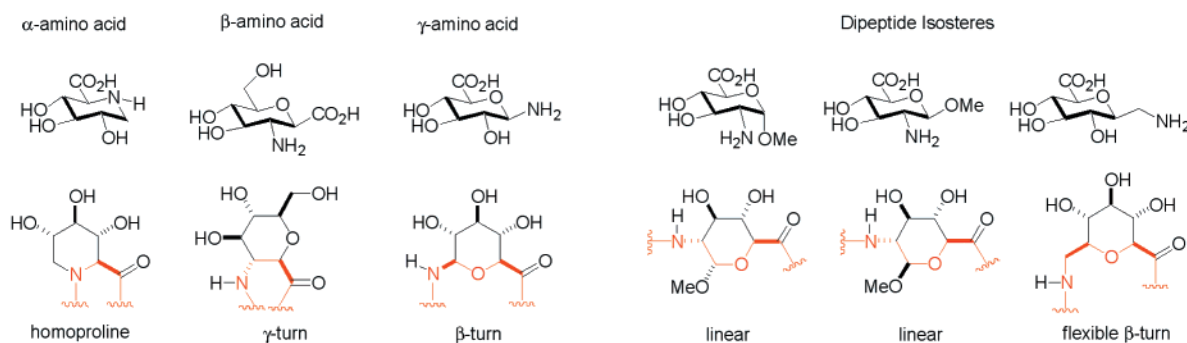


Figure 48. Structures and subunit shapes of sugar amino acids.

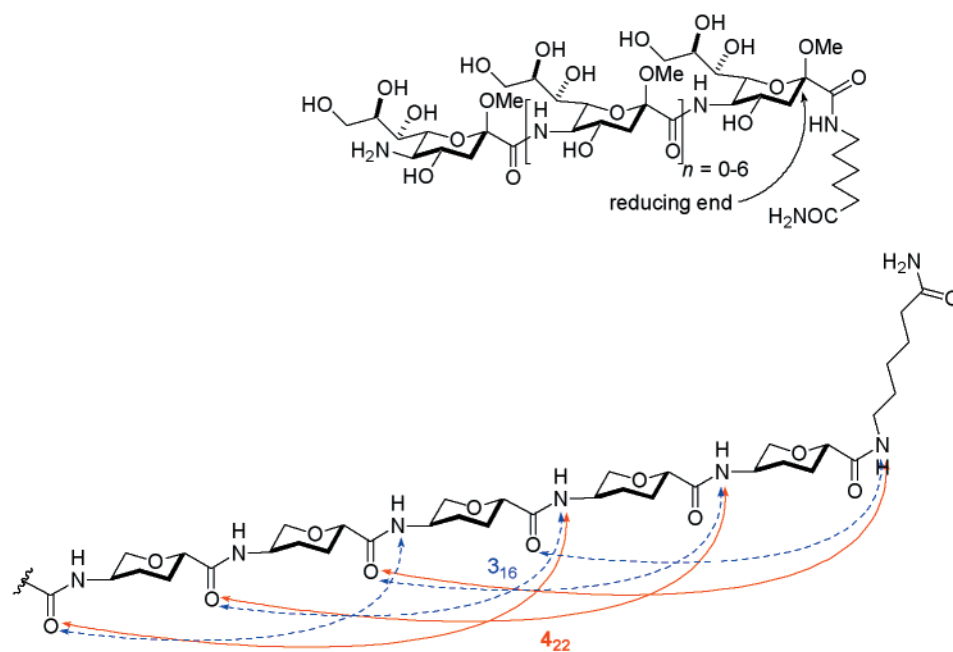


Figure 49. Structures and proposed H-bonding patterns of the 3_{16} and 4_{22} helix for sialooligomers.

D. The δ -Peptide Family

1. Alkene-Based δ -Amino Acids

Members of the δ -peptide family are isosteric replacements of dipeptide units. As such, this is the first member of the peptidomimetics lineage in which a single unit represents two or more α -peptide repeats. The β -turn is a common structural feature of proteins associated with the dipeptide fragment. Thus, it is not surprising that much activity in the δ -peptide family has been aimed at creating β -turn mimics. A long-standing approach has involved δ -amino acids in which the “missing” amide bond is replaced by a *trans*-carbon–carbon double bond.^{339–344} These studies tend to involve the incorporation of a single D-amino acid into a longer α -peptide sequence. Given our focus on peptidomimetic oligomers, the discussion that follows will be on chain sequences based on δ -amino acid repeating units, rather than on β -turn mimetics. Thus far, the chemical literature has mostly involved carbopeptoid backbones.

2. Carbopeptoids

The idea of using carbohydrate amino acids for both³⁴⁵ glyco-^{346–349} and peptidomimetics^{350–352} has

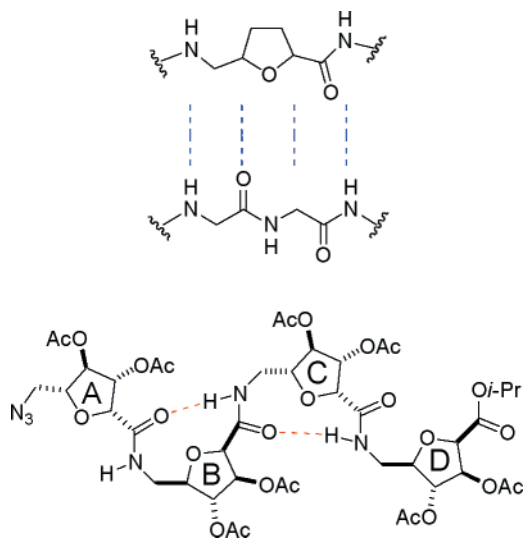


Figure 50. Representation of the solution-phase secondary structure for furanose-based carbopeptoids and a comparison between the α -peptide subunit and the furanose-based subunit as a dipeptide isostere.

gained interest recently. The conformational characteristics of carbohydrate residues incorporated into peptide chains were initially exploited for the rational design of a β -turn mimetic, at which time it was recognized that properly linked sugar amino acids could serve as a dipeptide replacement (Figure 48).³⁵⁰ Carbopeptoids,³⁴⁸ homooligomers of sugar amino acids, have been prepared from both furanose³⁵³ and pyranose³⁵⁴ residues. Additionally, cyclic homooligomers of sugar amino acids have also recently appeared.³⁵⁵

a. Pyranose-Based Carbopeptoid Foldamers.

Motivated by the fact that *O*-glycoside oligomers of sialic acid are helical in solution, Gervay and co-workers reported in 1998 that (1 \rightarrow 5) amide-linked sialooligomers longer than the trimer form ordered secondary structures in water (Figure 49).³⁵⁶ A combination of NMR-determined NH/ND exchange rates (in D₂O/DMSO) and circular dichroism studies (in H₂O) on a series of discrete oligomers showed that a critical length was necessary before evidence of conformational order emerged. However, the conformational features apparently varied with chain length. Thus, while the tetramer, pentamer, and hexamer showed slow exchange of their internal amide protons characteristic of strong intramolecular H-bonds, the heptamer strangely exchanged its protons quickly, suggesting the lack of an ordered structure. The octamer behaved like the pentamer and hexamer. Changes in peak-to-trough intensities as a function of chain length were used to further support the presence of ordered secondary structure in solution.³⁵⁷ In combination with molecular modeling, the hypothesis is that for the shorter oligomers **S(16)** H-bonding interactions stabilize a helix involving three residues per turn while for the octamer **S(22)** hydrogen bonding stabilizes a helix involving four residues per turn.

b. Furanose-Based Carbopeptoid Foldamers.

Shortly after Gervay's report on secondary structure in sialooligomers, Fleet and co-workers announced the observation of secondary structure in furanose

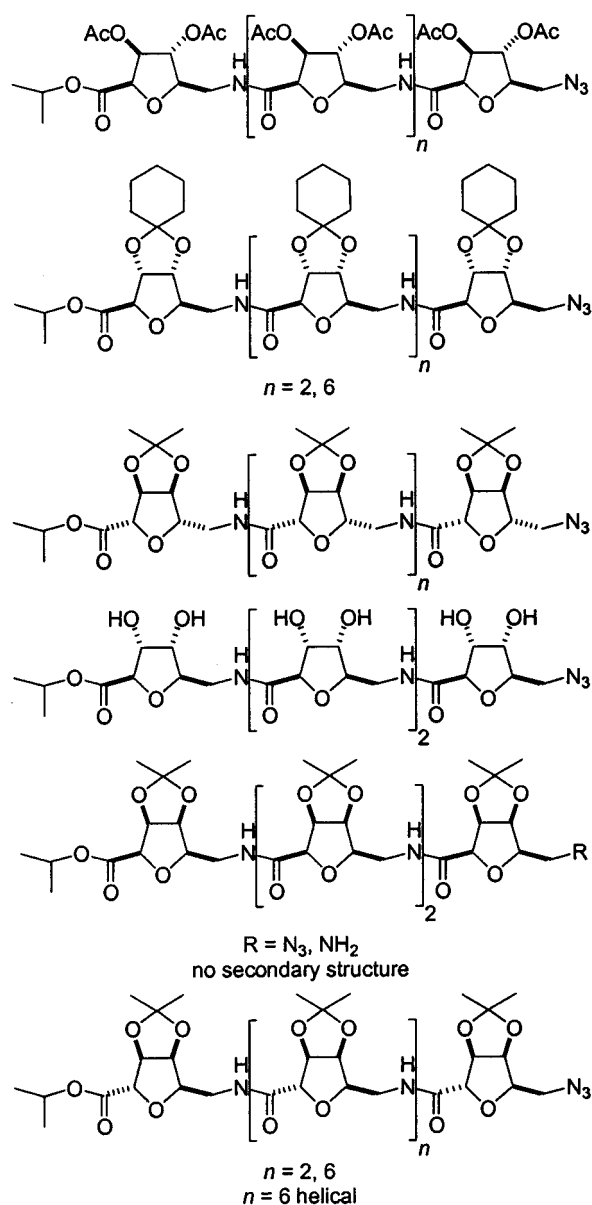


Figure 51. Stereochemical and substituent variations for furanose-based carbopeptoids.

carbopeptoids.³⁵⁸ Their initial finding was based on a β -D-arabino-furanose scaffold, δ -peptides in which each repeat unit can be considered as a dipeptide isostere. On the basis of ¹H NMR NOE data and molecular modeling, a repeating β -turn-type secondary structure was established for the tetramer in CDCl₃ (Figure 50). This structure appears to be stabilized by **S(10)** intramolecular H-bonds between repeat unit *i* and *i-2*.

Subsequent reports by Fleet and co-workers showed that the occurrence and specific type of secondary structure in these furanose-based carbopeptoid foldamers was strongly dependent on both the backbone stereochemistry and the stereochemistry of the ring substituents (Figure 51).³⁵⁹⁻³⁶¹ Various *cis*-linked furanoses mostly exhibit the repeating β -turn-like conformation mentioned above.^{360,361} However, one of the *cis*-linked stereoisomers displayed no indication of secondary structure.³⁵⁹ This surprising result was rationalized in that one methyl group in the isopropylidene unit of the fused ring is positioned in a way

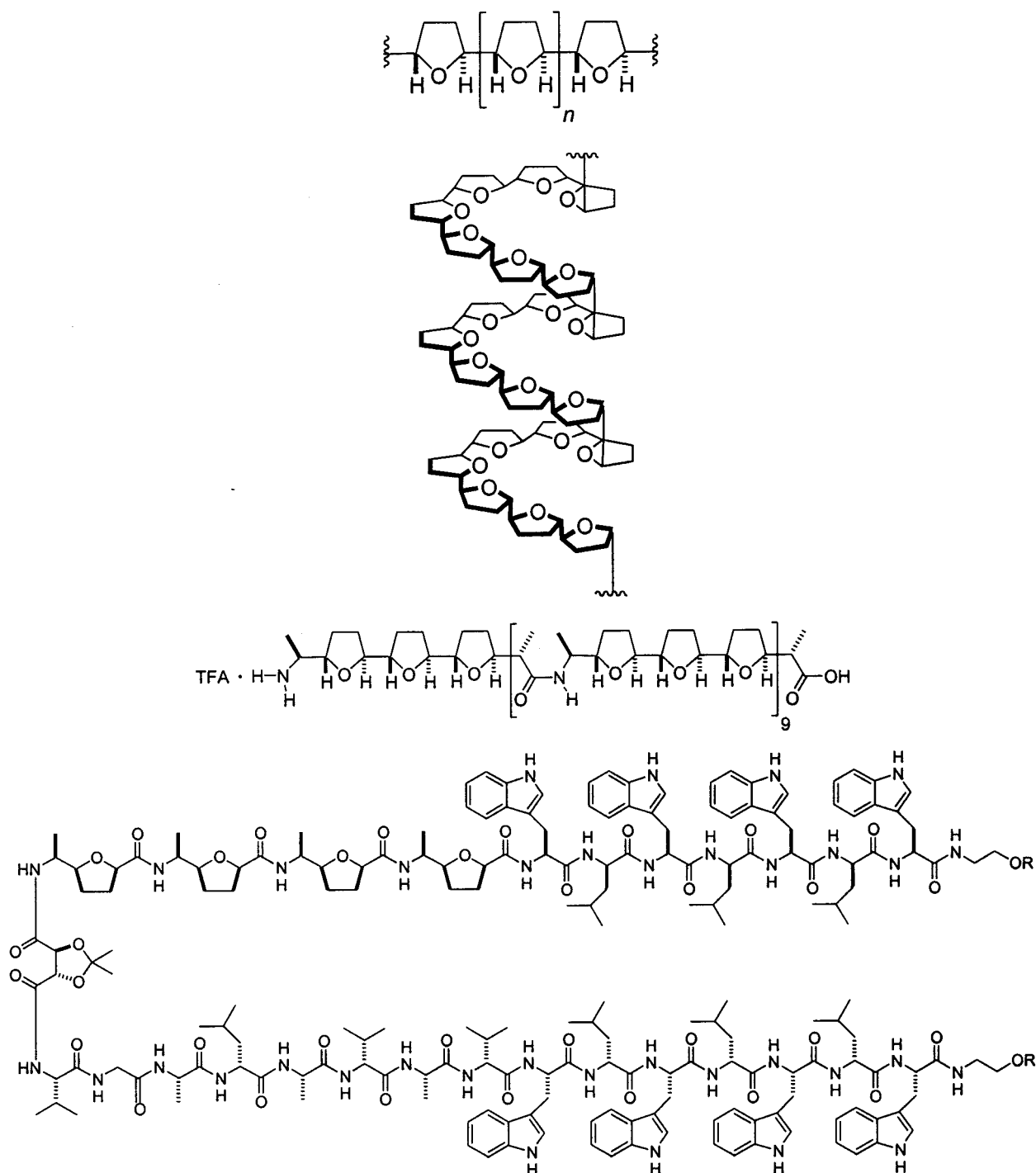


Figure 52. Representative structures of oligotetrahydrofuran amino acid sequences.

that sterically interferes with H-bond formation. In contrast to the β -turns found for the *cis*-linked furanoses, *trans*-linked furanose oligomers give a much different secondary structure. In initial reports that only studied chain lengths up to the tetramer, however, it appeared that no stable secondary structures in the *trans* isomer could be observed.³⁶² ^1H NMR was used to study the solution conformation of a *trans*-linked octamer. At this chain length, it was apparent that a new secondary structure had emerged. In contrast to the backbones derived from *cis*-isomers, long-range NOEs between sugar ring protons were observed. A repeating pattern of NOEs was detected along the backbone, indicating that a regular rela-

tionship exists between adjacent units. Simple modeling suggests a helical structure, stabilized by intrastrand $\text{N}-\text{H}^i \cdots \text{O}=\text{C}^{i-3}$ H-bonds. The conformational preference appeared stronger for octamer than the tetramer since the tetramer has only one stabilizing H-bond. A related octamer in which the protecting groups were removed was studied and found to give a strong Cotton effect at 216 nm in methanol and TFE.³⁶³

Fleet's carbopeptoids are closely related to the oligo tetrahydrofuran amino acid sequence used in the gramicidin-like peptide developed and studied by Koert and co-workers.³⁶⁴ These oligo-THF peptides (Figure 52) were inserted into synthetic lipid bilayer

membranes, and single channel conductance measurements were rationalized by assuming that the oligomers adopt a helical conformation consistent with a cationic channel. Koert's most recent molecular design evolved from his previous studies^{365,366} with 2,5-*trans*-linked THFs as polyether helices. One of his oligomers contained up to 27 furanyl rings and used stereogenic centers bearing methyl groups adjacent to the carbonyl and amino groups to stabilize the helical structure in the region of the peptide bond. The helical conformation was supported on the basis of NMR NOE data and conductance studies of planar lipid bilayers.

V. Single-Stranded Abiotic Foldamers

A. Overview

The peptidomimetic foldamers previously described utilized a top-down design approach; that is, the research involves systematic structural variations of parent chain molecules known to undergo folding reactions. In this section, we describe efforts toward foldamers best classified as employing bottom-up design approaches, involving the identification of novel, abiotic backbones that can fold into secondary structures akin to those found in proteins (helices and sheets). These foldamers often take advantage of rigidity inherent in aromatic units, torsional flexibility of the linkers, and various noncovalent interactions to adopt their discrete folded conformations.³⁶⁷ Since this search has been attempted through a variety of designs, these systems have yet to demonstrate the maturity seen with the peptidomimetics, although a few backbones show great promise and will be described in detail.

While several *polymeric* systems incorporating aromatics into the backbone have been shown to adopt helical conformations, many of these systems will not be described here (although some have previously been included in the literature as foldamers³⁶⁷). In the case of poly(aryl carbonate)s and poly(β -pyrrole)s, solution-phase helical conformations are favorable by atropisomeric bond torsions.^{368,369} Similar bond torsions preset the helical structures of poly(*o*-phenylene)s in the solid state.^{370,371} In contrast, poly(*m*-phenylene)s and poly(ether ketone) PK99, while their conformations are not specified by bond torsion, do not appear to adopt helical structures in solution.^{372,373} Additionally, a poly(*m*-phenylene ethynylene) has been shown to exhibit a reversible hydrogel state in water,³⁷⁴ and sexithiophenes with chiral side chains organize into supramolecular aggregates,^{375,376} but these two examples do not meet the essential criterion of having discrete chain lengths. In general, we have chosen to restrict our treatment of single-stranded foldamers with abiotic backbones according to the definition outlined in the introduction of this article, partitioned by primary folding force and oligomer backbone.

B. Backbones Utilizing Bipyridine Segments

1. Pyridine–Pyrimidines

Polyheterocyclic strands have been used in the spontaneous generation of well-defined secondary

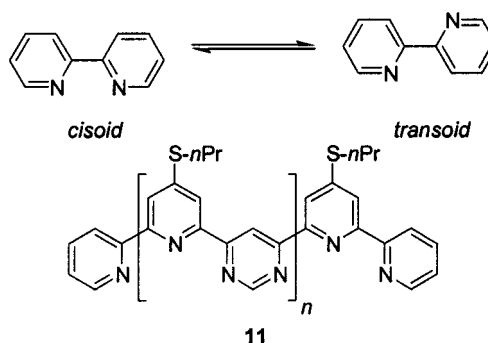


Figure 53. *Cisoid*–*transoid* equilibrium of 2,2'-bipyridine and the structure of oligomer series **11** ($n = 2, 5, 8, 9, 12$).

structures.^{377–380} This system is based on the preference of 2,2'-bipyridine to adopt a *transoid* conformation in solution (Figure 53). The *cisoid* (nonplanar) form of bipyridine has been calculated to be 5.7 kcal·mol⁻¹ less stable than the planar *transoid* conformation. Several other factors are also important for the proper design of a well-defined secondary structure. They include the correct sequence of heterocyclic aromatic rings, the proper linking of the rings at the appropriate positions, and the preference for the *transoid* conformation of the bond which links the aromatic rings. These features were combined in the synthesis and study of several different oligomer lengths **11** ($n = 2, 5, 8, 9, 12$) (Figure 53). The alternating pyridine and pyrimidine rings are connected at the *meta*-position, which provides the proper orientation for the rings to stack into a helical conformation. The helical conformation results from the steric repulsion between the CH groups and the electrostatic interaction stemming from nitrogen atoms on adjacent repeat units.

The sequence-specific, polyheterocyclic oligomers incorporated solubilizing thiopropyl side chains at the C-4 position of the pyridine ring.^{379,380} The characterization of the helical conformation of the oligomers in solution was achieved by a variety of techniques including UV–Vis, fluorescence, and NMR spectroscopy. The shortest oligomer **11** ($n = 2$) gave no indication of a helical conformation regardless of the technique that was employed. Despite the presence of overlapping, terminal pyridine ring, the absence of a helical conformation was attributed to the greater mobility since it can only form one turn. The longer oligomers ($n = 5, 8, 9, 12$) were found to adopt stable, helical conformations in solution (Figure 54). Fluorescence spectroscopy showed that **11** ($n = 5, 8, 9, 12$) in chloroform exhibited an excimer-like emission attributed to intramolecular excited state pyridine dimers. NMR spectroscopy showed that in each case only one folded conformation was observed, indicating the high specificity of the spontaneous helical generation. The assignments of the aromatic signals were made by a combination of COSY and ROESY NMR. In all cases, strong NOE interactions between the expected protons of different aromatic rings were observed in the ROESY NMR. Additional support was offered by a comparison of the chemical shifts of the aromatic protons, which showed progressive upfield shifts with increasing oligomer length,

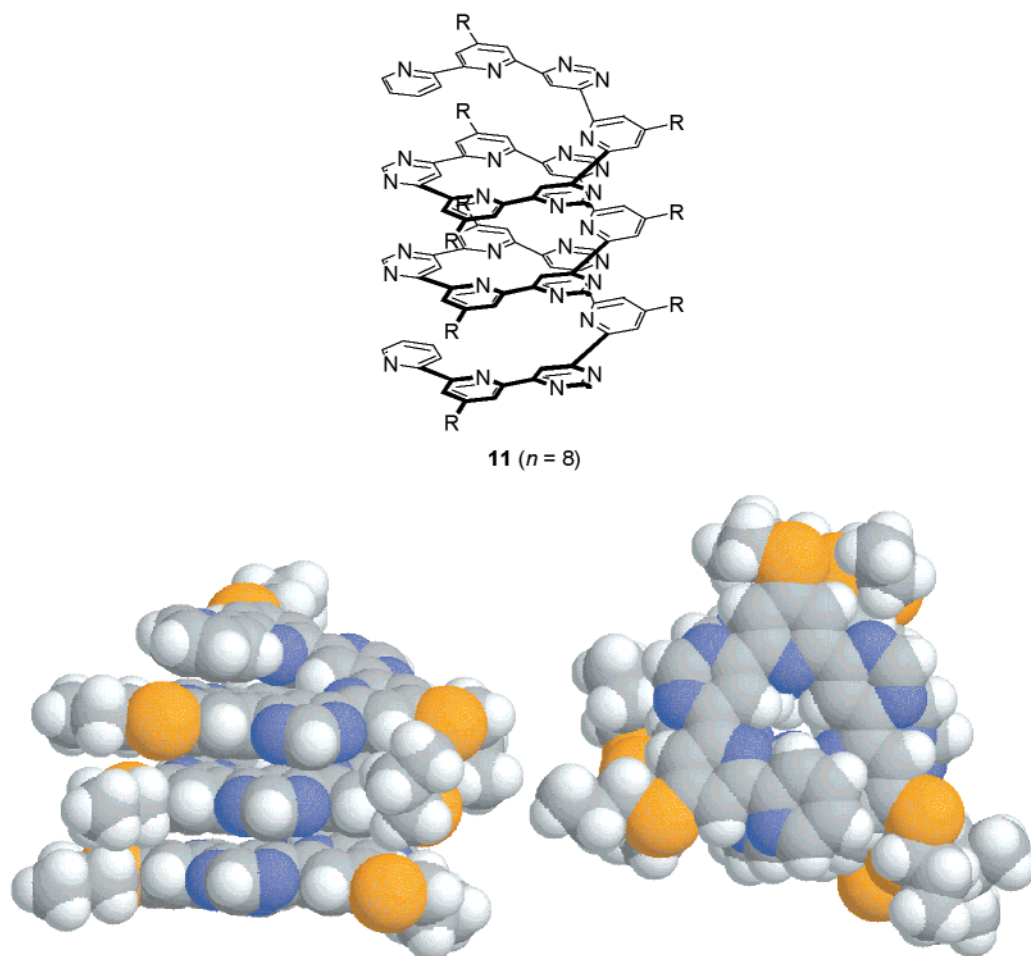


Figure 54. Drawing of the proposed helical conformation of oligomer **11** ($n = 8$), where $R = Sn\text{-}Pr$. Side (bottom left) and top (bottom right) view of the space-filling model of the crystal structure of pyridine–pyrimidine oligomer **11** ($n = 8$) in a helical conformation.

consistent with an increasing number of stacked aromatic rings.

The creation of a chiral, helical structure from polyheterocyclic strands resulted in a racemic mixture of *M* and *P* forms. By using variable temperature NMR and the diastereotopic α -thiomethylene protons, it was possible to determine the barrier to the helical inversion process. A value of $k = 85 \text{ s}^{-1}$ at 251 K and a free energy of activation of $\Delta G^\ddagger = 12.3 \text{ kcal}\cdot\text{mol}^{-1}$ was determined for shorter oligomer **11** ($n = 8$).³⁷⁷ In an analogous fashion, these values were determined for two of the longer oligomers **11** ($n = 5$) ($k = 85 \text{ s}^{-1}$ at 250 K and $\Delta G^\ddagger = 12.4 \text{ kcal}\cdot\text{mol}^{-1}$) and **11** ($n = 12$) ($k = 86 \text{ s}^{-1}$ and $\Delta G^\ddagger = 13.6 \text{ kcal}\cdot\text{mol}^{-1}$).³⁷⁹ The comparable activation free energies led to the proposal that the racemic helical conformation interconverted via a stepwise folding mechanism (Figure 55).³⁷⁹ Interestingly, while this interconversion is certainly dynamic, there is no evidence to indicate that these oligomers undergo the folding reaction (i.e., that they can unfold). The racemization between the *M* and *P* helical conformations was proposed to go through an intermediate, partially unfolded conformation (Figure 55, intermediate B). Furthermore, no spectroscopic evidence was offered to show that the oligomers exist in completely unfolded conformations.

The helical conformation of these oligomers was characterized in the solid state by using X-ray crystallography. Shorter oligomer **11** ($n = 5$) was found to pack in a centrosymmetric cell that contained an enantiomeric pair of oligomers.³⁷⁸ In addition, the helices were found to stack on top of one another creating long channels in the void space of the helix interior. The octamer of **11** was also determined to pack in a helical conformation in the solid-state (Figure 54).³⁷⁹ In this case, a unit cell was found to contain two molecules of only one twist sense, thereby creating a chiral channel from an achiral molecule. Spontaneous chiral resolution occurs concomitantly with crystallization. In both cases a helical pitch of 3.75 Å was determined along with an internal void space from ~ 2.5 to 3 Å. The high degree of solid-state organization led the authors to propose that these systems may have interesting electronic features, when compared to linear molecular wires.

2. Pyridine–Pyrimidines with Hydrazal Linkers

The previous design method has been shown to be highly effective for obtaining well-defined conformations in solution. However, the synthesis of the oligomers described above was challenging. In an attempt to overcome this limitation, Lehn et al. described the synthesis and study of oligomers that

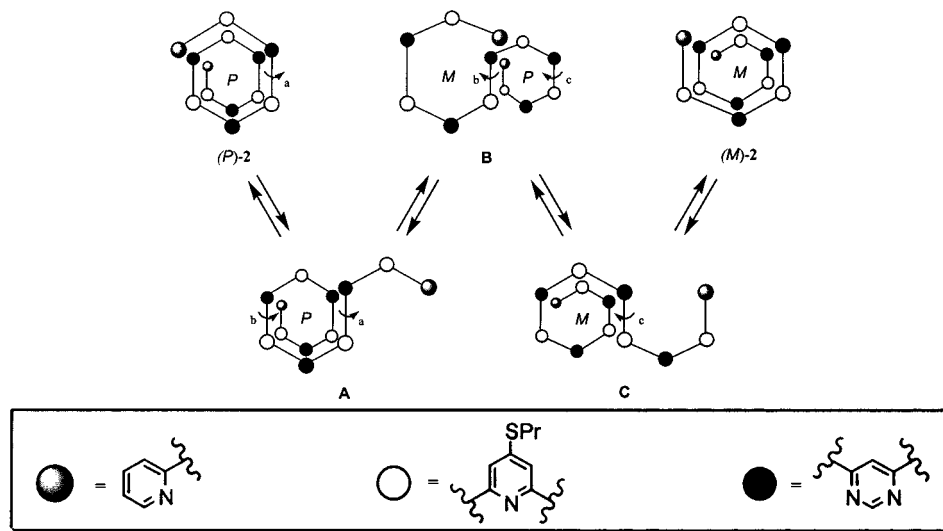


Figure 55. Stepwise mechanism for the helicity inversion of **11** ($n = 5$).

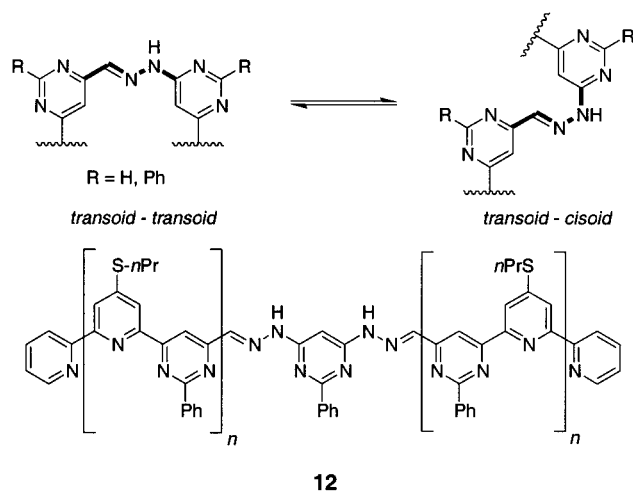


Figure 56. The *transoid*–*transoid* to *transoid*–*cisoid* equilibrium and structure of pyridine–pyrimidine oligomers with hydrazal linkers **12** ($n = 1, 3$).

are more amenable to stepwise synthesis while still taking advantage of selective torsions around adjacent pyridine–pyrimidine bonds.³⁸¹ The system is still based on the preference of 2,2'-bipyridine to adopt a *transoid* conformation in solution (Figure 53). However, the middle portion of the oligomer backbone contains a hydrazal group, which replaces the pyridine fragment of the previously studied oligomers. When α -substituted *N*-heterocycles are used, the *transoid*–*transoid* conformation (Figure 56) is preferred over others (*transoid*–*cisoid* shown for comparison) for several reasons. These include the minimization of secondary steric and electronic interactions, the increased amount of aromatic stacking that occurs when the imine is in the *transoid*–*transoid* conformation, and the conformational rigidity and planarity through conjugation. The synthesis of the desired oligomers **12** ($n = 1, 3$) (Figure 56) remained somewhat difficult but was simplified by having the hydrazal condensation as the final step.

The helical conformation was characterized by NMR spectroscopy and X-ray crystallography. Both oligomers displayed ¹H NMR consistent with a helical conformation as evidenced by the upfield shift of the

aromatic resonances on the terminal pyridine rings. From these data, it was concluded that the shorter oligomer **12** ($n = 1$) adopts a helical conformation of 1.5 turns and the longer oligomer **12** ($n = 3$) adopts a helical conformation containing 2.5 turns. The helical structure of **12** ($n = 1$) was confirmed by X-ray crystallography. The solid-state packing results in an internal cavity of 5.05 Å with the expected aromatic stacking distances of 3.46 Å. These results show that hydrazal condensation is a useful approach for creating longer helical strands and that a pyrimidine–hydrazone subunit is comparable to a pyridine–pyrimidine fragment in polyheterocyclic strands.

3. Pyridine–Pyridazines

Alternative attempts at creating well-defined helical conformations from polyheterocyclic strands have recently been reported by Lehn et al.³⁸² The same design criteria as that used for the previously studied systems was used except that an isomeric pyridine–pyridazine repeat unit was employed (Figure 57). The synthesis of oligomer **13** was accomplished by using a similar procedure to the pyridine–pyrimidine heteronuclear strands.³⁷⁸ It was proposed that **13** would yield a hexagonal, helical structure with 12 rings per turn and a central cavity of ~ 25 Å (determined by molecular modeling). The helical conformation of **13** in solution was characterized by large upfield shifts of the proton resonances for the terminal pyridine rings. The chemical shifts of all aromatic resonances were found to be highly concentration dependent, suggesting that a large amount of intermolecular aggregation was occurring at increased concentrations. Vapor-pressure osmometry measurements showed an apparent molecular weight approximately twice that of the oligomer, indicating a high amount of self-aggregation. Solutions of **13** in dichloromethane and pyridine resulted in gel formation with microstructures that consisted of helical substructures as evidenced by electron microscopy (Figure 58). It was determined that the fibers had an approximate diameter of 80 Å, most likely being composed of two or three bundles of helical stacks. Due to the large size of the cavity, it was proposed that the system

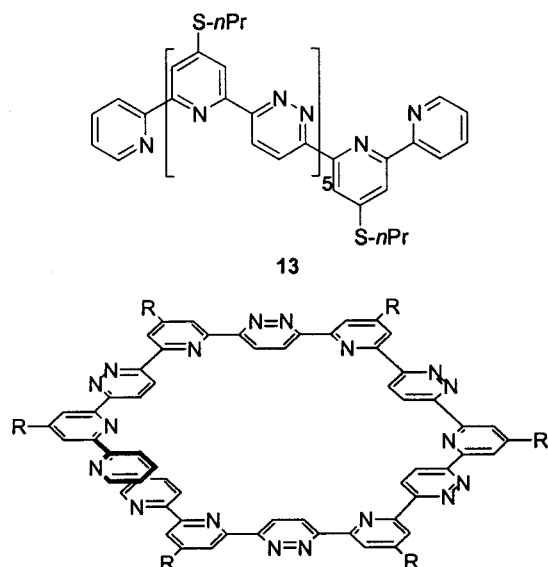


Figure 57. Drawing of the proposed helical conformation of oligomer **13**, where R = Sn-Pr.

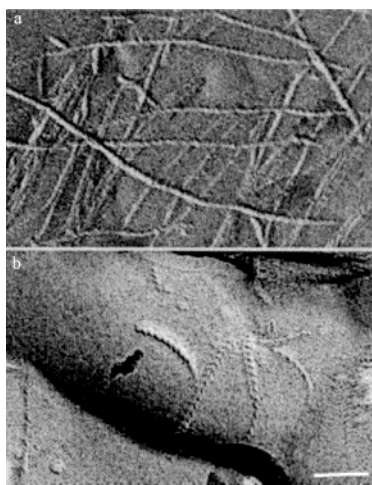


Figure 58. Freeze–fracture electron micrograph of compound **13** in (a) dichloromethane and (b) pyridine showing fiber network formation with helical textures.³⁸² Scale bar represents 100 nm. (Reprinted with permission from ref 382. Copyright 2000 Wiley-VCH.)

self-organized into extended molecular channels with a fairly large opening of ~ 8 Å, potentially useful as functional polymeric materials for ion-active devices requiring internal functionalization with metal coordinating groups. These oligomers and others in their class have yet to show tolerance for groups present on the inside of the helical cavity. The lack of evidence for an unfolded state makes it unclear whether these oligomers exhibit a folding reaction which may be important when dynamic cavity assembly/disassembly is desired.

C. Backbones Utilizing Solvophobic Interactions

1. Qualification

The preceding section of abiotic, single-stranded oligomers employed aromatic stacking to stabilize the folded conformation. The following backbones utilize solvophobic interactions, and in some of these cases, these stacking contacts occur between adjacent mono-

mer units in their folded states. In these cases, the chain conformations might better be described as a collection of independent units rather than as a cooperative group. Therefore, by the nonadjacency criterion in our definition, we cannot strictly classify the following charged, aedamers, and cyclophane backbones as foldamers. At the same time, the water solubility, intercalating properties, and novel scaffolding of these oligomers, respectively, provide insight toward the future development of analogous backbones as foldamers.

2. Guanidines

Oligo(guanidinium) strands form a stacked arrangement by using a combination of aromatic stacking interactions and the preferred conformation of a charged backbone.^{383–387} These systems are based on the conformational preference of a charged *N,N*-diphenylguanidine group in solution (Figure 59).³⁸³ By using a combination of ¹H NMR spectroscopy and X-ray crystallography, it was determined in a *N,N*-diphenyl-*N,N*-dimethylguanidine model system that the *cisoid–cisoid* conformation is predominant over the alternative conformations in water and other polar, aprotic solvents. The guanidium moiety was incorporated into water-soluble, longer length oligomers (**14–17**) containing three and five aromatic rings linked at both the *meta*- and *para*-positions.

The conformation of the oligomers in solution was characterized by NMR spectroscopy and X-ray crystallography. All four oligomers were found to adopt a helical conformation in both solution and the solid-state (Figure 59). X-ray crystallography showed that the dihedral angle between face-to-face phenyl rings was ca. 30° for the *meta*-substituted oligomers (**14** and **15**) and slightly smaller for the *para*-substituted oligomers (**16** and **17**). These findings were somewhat surprising since the parallel structure had been calculated to be less favorable than other conformations. The *meta*-substituted oligomers pack in a chiral conformation in the solid state with both enantiomeric forms present in a 1:1 ratio. NMR spectroscopy showed that the oligomers exist predominantly as layered structures in both organic solvents and water as evidenced by the upfield shifting of the aromatic protons inside the layers when compared to the terminal phenyl rings. These NOE measurements confirmed the existence of stacked, parallel layers. One possible application of this system is as a polyintercalator targeting the minor groove of DNA.³⁸⁶

3. Aedamers

Another system composed primarily of aromatic rings was reported by Iverson and Lokey.³⁸⁸ These structures take advantage of the stacking propensities of the aromatic electron donor–acceptor interactions (*aedamers*) of covalently linked subunits. For the electron-deficient aromatic rings, 1,4,5,8-naphthalenetetracarboxylic diimide rings were employed and 1,5-dialkoxynaphthalene rings were used for the electron-acceptor rings. Crystal structures of model compounds were used to help determine the location for linking the aromatic rings with the correct length of the tethering unit³⁸⁹ between the rings. A series

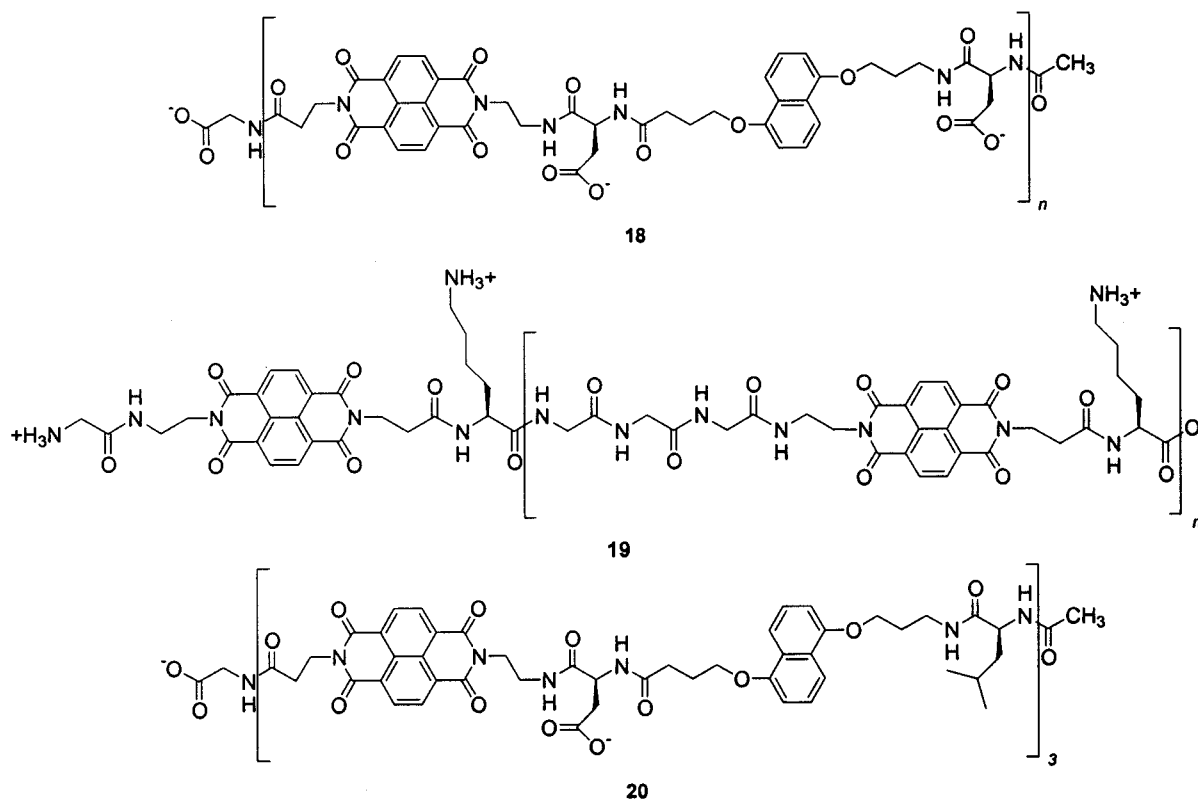


Figure 60. Structures of various aedamers.

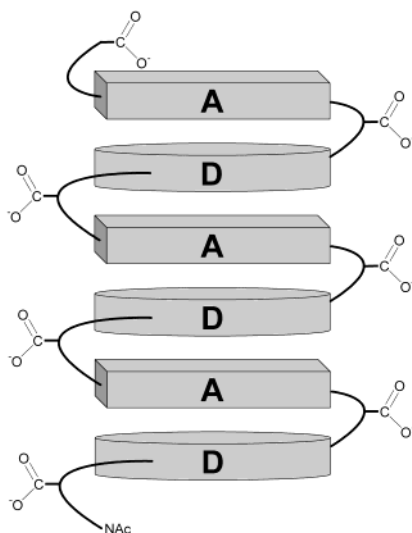


Figure 61. General schematic representation of a secondary structural element based on donor-acceptor interactions.

found that upon heating above 80 °C, 1.5 mM aqueous solutions of **20** undergo an irreversible conformational change (Figure 62). At room temperatures, solutions of **20** are red wine colored. Upon heating, the aedamers begin to unfold and expose the hydrophobic backbones to solution leading to an uncolored, presumably tangled aggregate. It was further found that the transition was induced by the addition of preformed aggregate to solutions of oligomer **20**. This behavior was compared by the authors to the behavior of triple-helix collagen. It was proposed that the color change (red wine to colorless) could therefore be used as a temperature sensor

indicating when a threshold temperature has been reached.

4. Cyclophanes

Differently substituted *N*-benzyl phenylpyridinium cyclophanes have been used as models to probe the solvent effects of face-to-face aromatic stacking (Figure 63).^{392–395} A variety of R groups, both electron-donating and -withdrawing, were explored to measure the aromatic–aromatic stacking interactions. Recently, longer chains with up to five aromatic rings suggest collapsed conformations in aqueous solution, with open conformations in chloroform.³⁹⁶

Investigations into the construction of larger cyclophanes^{397–403} proceeded through the generation of linear oligomers of tetrasubstituted aryl moieties linked through tosylated aminomethyl groups. Through iterative synthesis, chain lengths up to the nonamer⁴⁰¹ were obtained and crystal structures for pentamer **21** revealed stacked, molecular ribbons (Figure 63). Although detailed spectroscopic studies and folding transitions through either solvent or thermal denaturation were not demonstrated, these structures have similar conformations to previously described aedamers. In chloroform, ¹H NMR showed that the S-shaped folded conformation is the preorganized structure before cyclization to the macrocycles.^{398,399} Extensions of this backbone have included the incorporation of *p*-phenylrings,⁴⁰³ pyridines,⁴⁰¹ and biphenyl groups,⁴⁰² as well as the use of thioether linkages.^{397,403}

5. Side Chain–Backbone Interactions

a. Oligo(thiophene)s. Recently, oligothiophenes with chiral *p*-phenyl-oxazoline side chains were

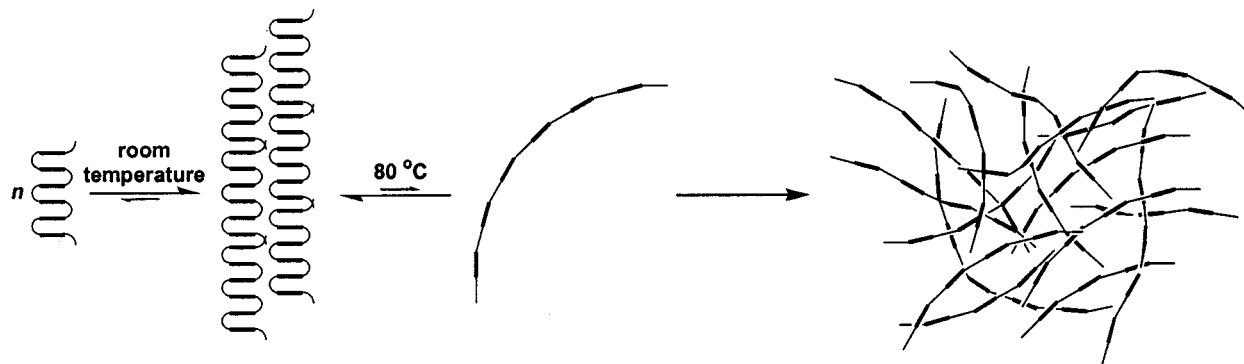


Figure 62. Proposed scheme for the conversion of amphiphilic aedamer **20** to a tangled aggregate state upon heating. (Adapted from ref 391.)

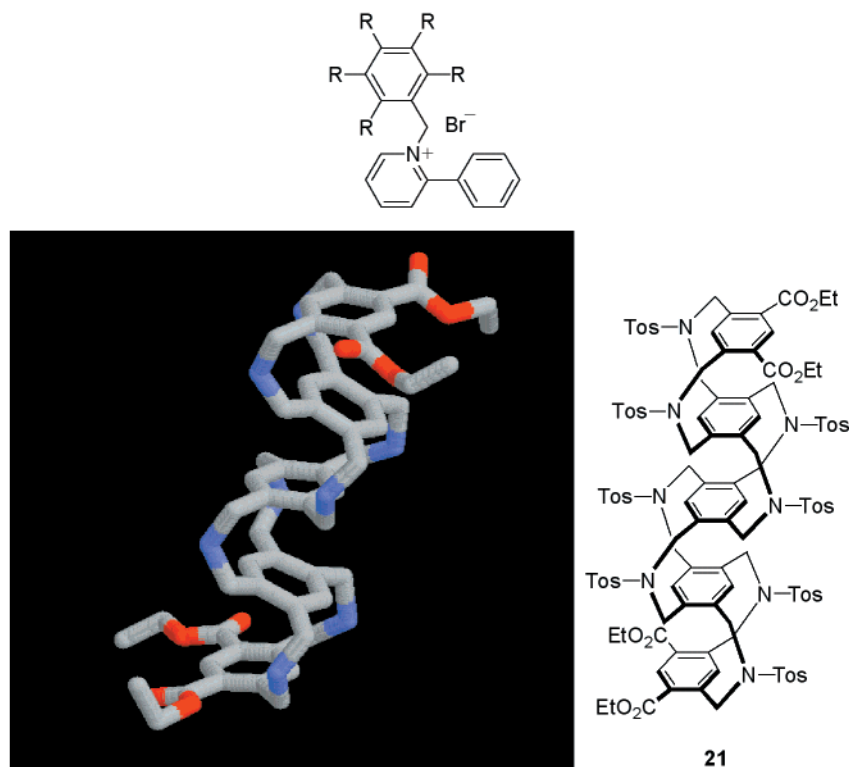


Figure 63. Cyclophanes discussed in the text. (top) Substituted *N*-benzyl phenylpyridinium bromides. (bottom) Part of the crystal structure of the [3.3]*meta*-cyclophane pentamer **21**.³⁹⁹ Side chains have been omitted for clarity.

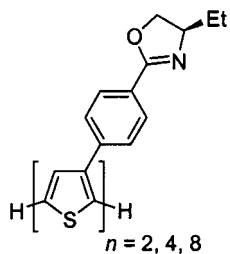


Figure 64. Oligo(thiophene)s bearing chiral *p*-phenyl-oxazoline side chains.

generated by Stille couplings through an iterative divergent/convergent approach (Figure 64).⁴⁰⁴ Though a nonlinear increase in absorptivity was observed in chloroform with increasing chain length, no induced CD was detected. When the octamer was examined in mixtures of chloroform and methanol or acetonitrile, UV red shifts and induced CD signals were seen with increasing amounts of poor solvent; these shifts were not present with the tetramer or hexamer. The

induced CD was independent of the poor solvent used, and the UV and CD showed clear isobestic and isodichroic points, respectively. Both the UV red shifting and the CD signal intensity increased as a function of time, indicating a time dependency for the folding reaction. Although the exact architectural nature of this chain-length-dependent conformational change was not determined, these results are analogous to solvophobic effects seen in the following oligo-(*m*-phenylene ethynylene)s.

b. Oligo(*m*-phenylene ethynylene)s in Solution. A large amount of research has been focused on controlling the secondary structure of nonbiological oligomers through the use of solvophobic interactions. Moore and co-workers synthesized and studied oligomer systems (**22** and **23**) that use nondirectional interactions and local constraints in a covalent backbone to undergo a folding reaction into a helical conformation (Figure 65).⁴⁰⁵ In these systems, the helical preference is controlled by several different

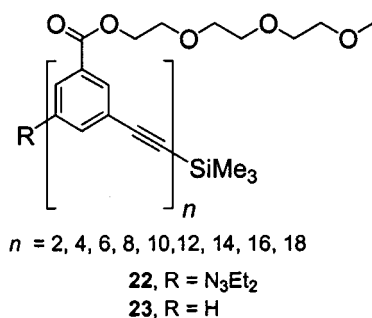


Figure 65. Chemical structures of oligo(*m*-phenylene ethynylene)s.

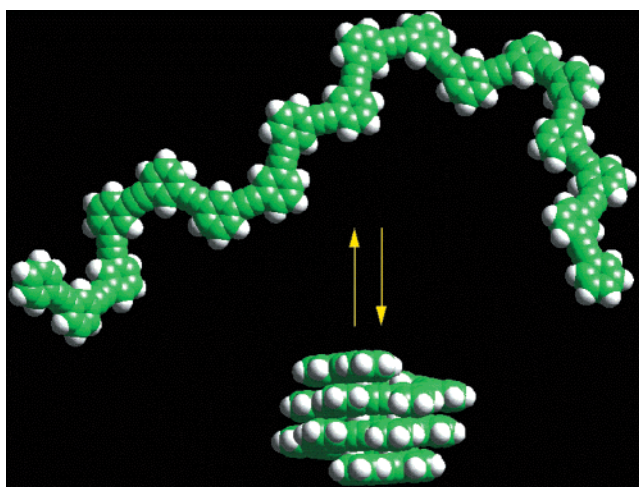


Figure 66. Space-filling model showing the proposed folding reaction for a *m*-phenylene ethynylene oligomer **23** ($n = 18$). Side chains have been omitted for clarity.

factors. These include the *meta*-connectivity of repeat units, which allows the oligomer to fold back upon itself, and the use of polar side chains and a nonpolar backbone. It was postulated that when oligomers of sufficient length are dissolved into a polar solvent, a helical conformation would result since this conformation maximizes the favorable interactions between the polar solvent and polar side chain, maximizes aromatic–aromatic stacking interactions, and minimizes the unfavorable contacts between the hydrocarbon backbone and the polar solvent (Figure 66).

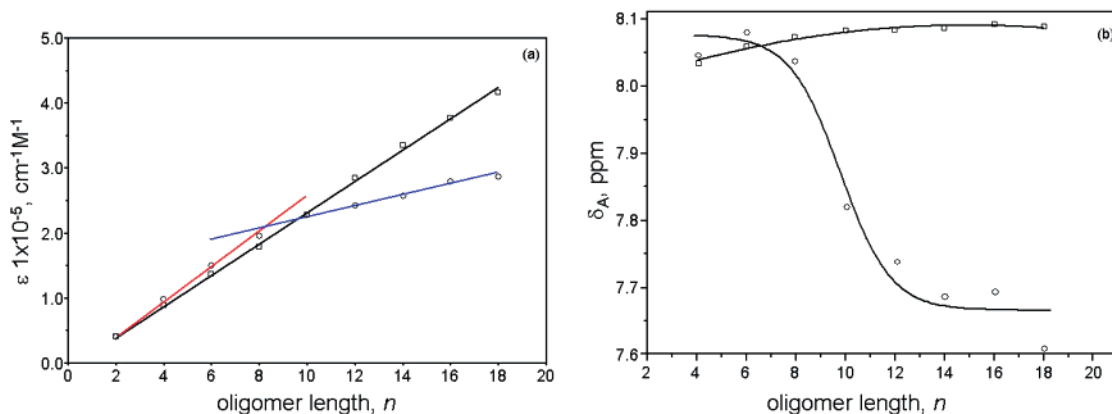


Figure 67. (a) Molar extinction coefficient ϵ (303 nm) versus oligomer length n for oligomer series **22** in chloroform (black, squares) and acetonitrile (red and blue, circles). The lines are linear fits to the data; for acetonitrile, the fits are for $n = 2-8$ (red) and $n = 10-18$ (blue). (b) The average chemical shift δ_A versus chain length n for oligomer series **22** in chloroform (CDCl₃, squares) and acetonitrile (CD₃CN, circles). The curves are drawn only as guides to the eye. All the spectra in chloroform and those of $n = 4, 6, 8$ in acetonitrile did not change upon dilution; the spectra of $n = 10, 12, 14, 16, 18$ in acetonitrile were measured at ca. 10 μM .

The modular nature of phenylene ethynylene oligomers allowed for the synthesis of monodisperse chain lengths and the ability to modify both the pendant groups and backbone in a precise fashion. The syntheses of the oligomers are typically performed using a divergent/convergent growth strategy.^{112,406} The syntheses of the various oligomer series are very similar, differing only by the choice of starting monomer units.

Several different techniques have been used to study the solvophobic driven folding reaction of *m*-phenylene ethynylene oligomers. In the initial studies on oligomer series **22**, a combination of UV–Vis and ¹H NMR spectroscopy was utilized (Figure 67).⁴⁰⁶ Experiments were performed at a concentration where intermolecular interactions are minimized (<10 μM). The lack of aggregation was determined by a combination of vapor-pressure osmometry and dilution experiments. From these studies, it was found that only oligomers with $n > 8$ repeat units were capable of folding into a helical conformation. In a good solvent,⁴⁰⁷ such as chloroform, all oligomers are present in a random conformation since the solvent is able to solvate both the polar side chains and nonpolar backbone. This was confirmed by UV–Vis studies, which indicated a linear dependence of molar absorptivity on oligomer length. ¹H NMR showed little change in the average chemical shift of aromatic resonances indicating no aromatic–aromatic stacking, present in the folded helical conformation. However, in a poor solvent such as acetonitrile, it was observed that oligomers greater than eight units in length exhibit a change in molar absorptivity per repeat unit and an upfield shift of the aromatic resonances. The changes in the UV–Vis spectra were attributed to the increased concentration of a *cisoid* geometry of contiguous aromatic rings typical of the helical confirmation (Figure 68). The changes in the ¹H NMR spectra for the longer oligomer lengths were attributed to the presence of aromatic stacking. In these studies it was also shown that the conformational transition could be controlled by solvent quality and temperature.

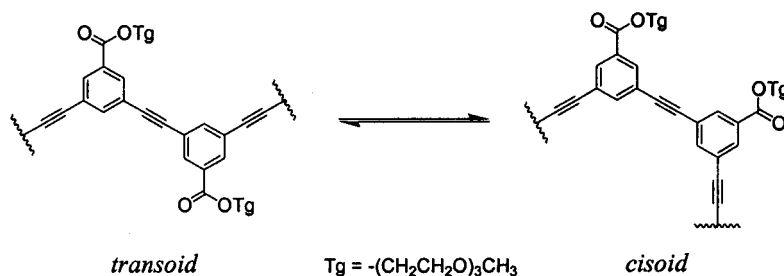


Figure 68. *Transoid*–*cisoid* equilibrium of oligo(*m*-phenylene ethynylene)s.

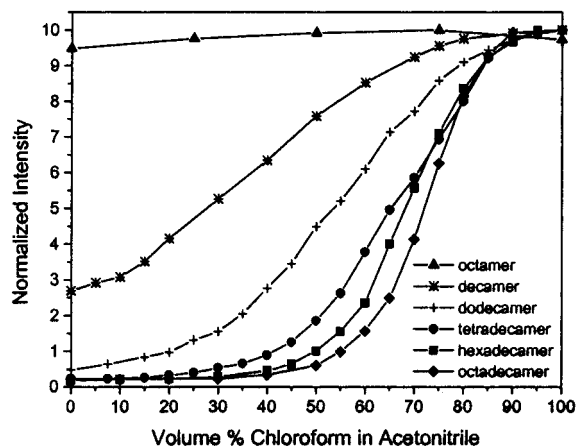


Figure 69. Plot of normalized fluorescence intensity for **23** ($n = 8$) through **23** ($n = 18$) vs the volume percent chloroform in acetonitrile. All spectra were normalized to a constant optical density of 0.1 at 288 nm.

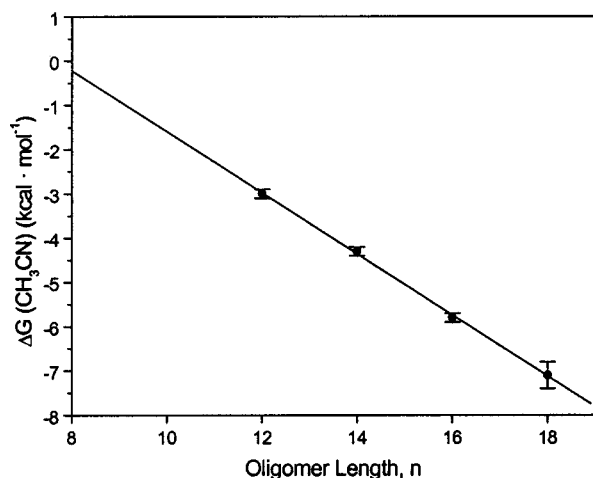


Figure 70. Plot of $\Delta G(\text{CH}_3\text{CN})$ vs oligomer length for **23** ($n = 12$) through **23** ($n = 18$). The linear equation used to fit the data is given by $\Delta G(\text{CH}_3\text{CN}) = 5.1 - 0.68n$ (kcal · mol⁻¹).

Fluorescence spectroscopy also proved to be a valuable tool in characterizing the folding reaction of *m*-phenylene ethynylene oligomers.¹¹² In these studies, oligomer series **23** was used since the hydrogen end group does not quench fluorescence emission. By monitoring the fluorescence signal⁴⁰⁸ as a function of volume percent chloroform (solvophilic) in acetonitrile (solvophobic) (Figure 69), it was possible to estimate the stability of the folded conformation in pure acetonitrile, $\Delta G(\text{CH}_3\text{CN})$ (Figure 70).⁴⁰⁹ For oligomers greater than eight units in length in CH_3CN , a decrease in the 350 nm fluorescence band and the onset of an excimer-like emission band was

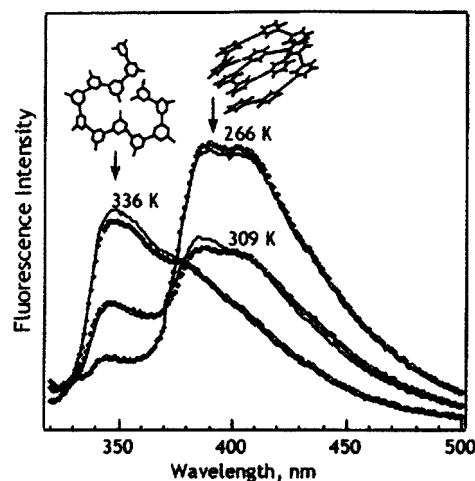


Figure 71. Emission spectra of **23** ($n = 12$) (open diamonds) excited in the broad absorption band peaked at 270–300 nm area diagnostic of its helical content ($\lambda_{\text{ex}} = 288$ nm, 0.5 μM **23** [$n = 12$] in 50:50 v/v THF/methanol.) The folded peak at 400 nm decreases at higher T . A spectral/lattice model prediction (solid line) describes the folding transition and equilibrium constant near-quantitatively. Insets show representative unfolded and folded conformations (side chains omitted for clarity).⁴¹⁰

attributed to the presence of aromatic stacking. This coincided with the chain length (i.e., 10-mer) at which upfield shifting and UV hypochromism was noted in previous studies.⁴⁰⁶ It is evident from Figure 70 that a linear relationship exists between oligomer length and conformational stability. An important conclusion is that the stability of the conformationally ordered state was linearly dependent on chain length. This behavior had previously been predicted on the basis of a molecular modeling study.⁴⁰⁶ Solvent denaturation studies suggested that each additional monomer contributed roughly 0.7 kcal · mol⁻¹ of stability to the folded conformation at 23 °C in acetonitrile. Linear extrapolation yielded a free energy value near zero for the octamer, consistent with the absence of folding seen in Figure 69. The observation that each monomer contributes the same increment of stability to the ordered conformation suggested a regularly repeating conformational structure, such as a helix.

The conformational transition of **23** ($n = 12$) was further quantified by monitoring the fluorescence signal using laser T -jump relaxation measurements (Figure 71).⁴¹⁰ These experiments showed that the oligomer folded to a compact structure on a submicrosecond time scale, which is comparable to short helical peptides. However, it was determined that the folding reaction undergoes a transition to nonexpo-



Figure 72. Equilibrium of *P* and *M* helices for oligo(*m*-phenylene ethynylene)s.

nential kinetics at low temperatures. The fluorescence experiments clearly show that solvophobic interactions can be used to collapse the oligomers to a stable, helical conformation in solution and that this transition occurs in a cooperative fashion.

Several design approaches have been used to control the twist sense bias of *m*-phenylene ethynylene oligomers (Figure 72).^{411–413} One approach involved adding a small, chiral perturbation to the oligomer side chain that resulted in a twist sense preference, without disrupting the conformational stability.⁴¹¹ For these studies, a series of *m*-phenylene ethynylene oligomers with chiral side chains (**24**) was generated (Figure 73). This series was analogous to the previously reported achiral series **23**, except for the introduction of a methyl group at the second carbon of each of the side chains. This placed the

stereochemical information in reasonably close proximity to the aromatic backbone. The chiral unit was derived from *L*-ethyl lactate, which is readily available in high enantiomeric purity, using standard synthetic transformations.⁴¹¹ It was found that, within experimental error, the conformational transitions of chiral oligomers **24** displayed the same chain-length and solvent dependence as their achiral counterparts (**23**) as determined by UV-vis and fluorescence spectroscopy (Figure 74). Therefore, the introduction of a methyl group in the side chain did not destabilize the helical state. In chloroform, chiral oligomers **24** showed no optical activity in the backbone chromophore (250–400 nm), regardless of chain length and temperature studied. This is not surprising since in chloroform the oligomers are expected to be in a random conformation; hence, there is little possibility for transferring chiral information from the side chains to the backbone. In CH₃CN, the ellipticity was found to be chain-length dependent and was zero only for oligomers not long enough to adopt a helical conformation ($n < 10$). These results showed that the transfer of chiral information from the side chains

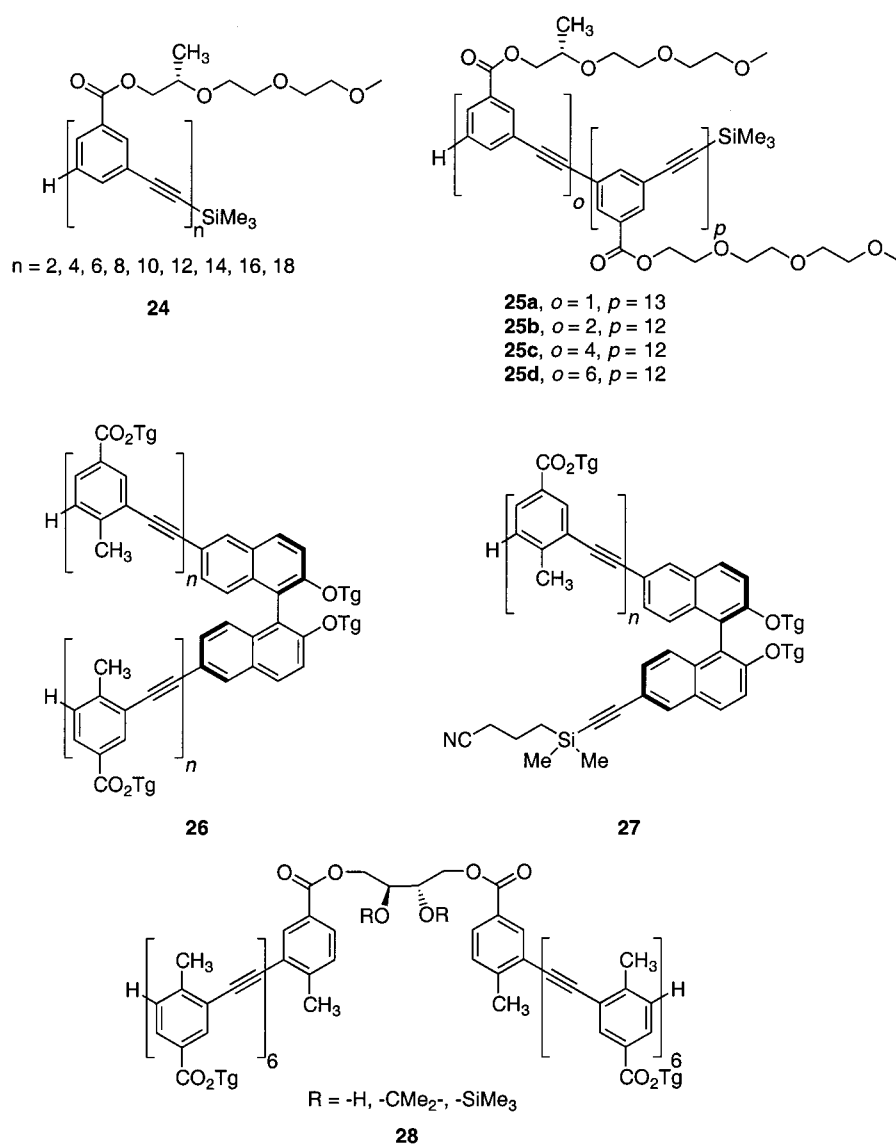


Figure 73. Structures of various oligo(*m*-phenylene ethynylene)s used to bias the twist sense of the helical conformation.

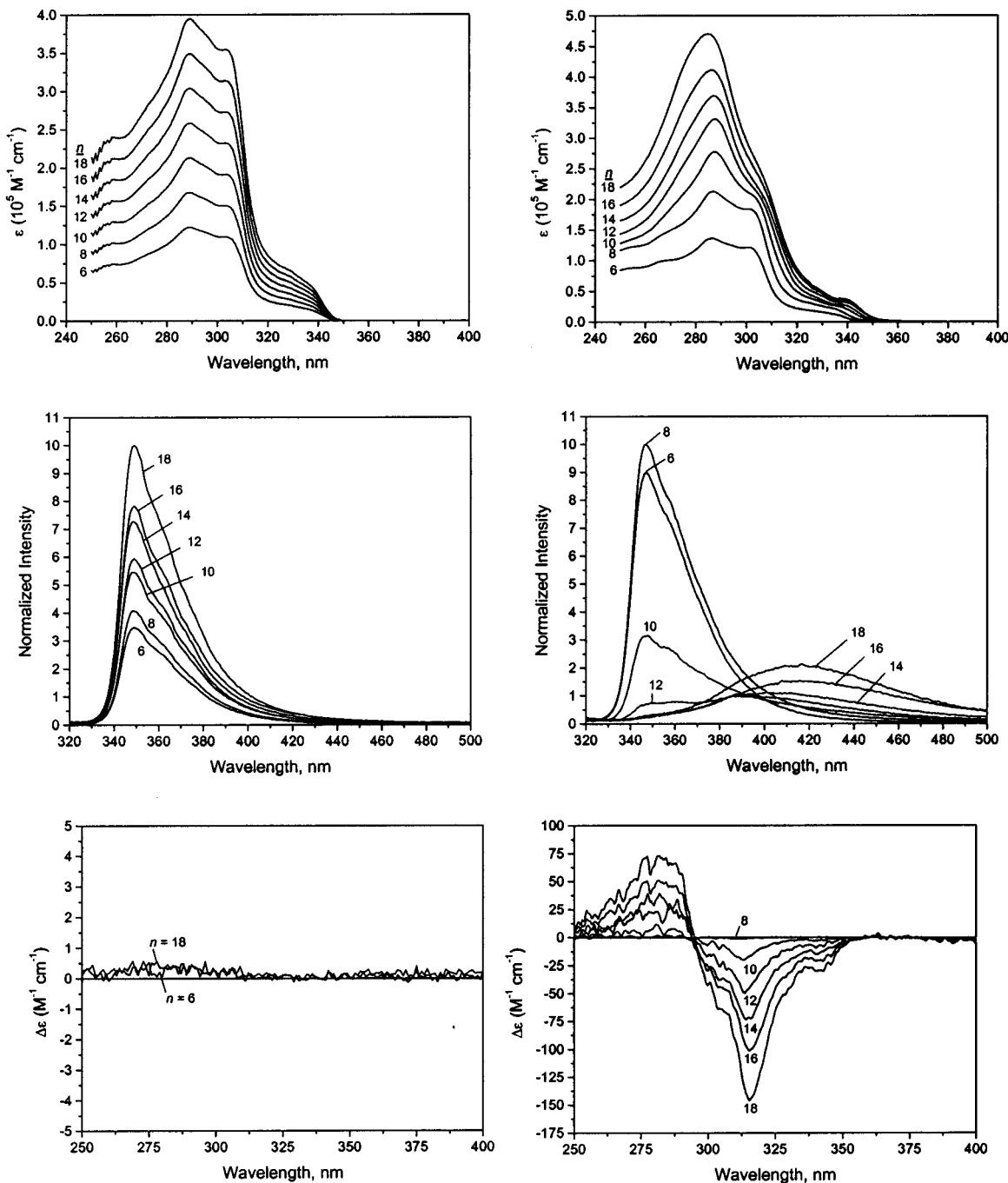


Figure 74. Plots of UV–Vis (top), fluorescence (middle), and circular dichroism spectra (bottom) of oligomers **24** ($n = 6$) through **24** ($n = 18$) in chloroform (left) and acetonitrile (right).

to the main chain could only occur once order is present in the backbone.

By monitoring the CD signal as a function of volume percent chloroform in acetonitrile, it was only at high acetonitrile compositions that a Cotton effect was observed (Figure 75). On the basis of this observation it is plausible that ordering of the solvated side chains, a process that lags behind helix formation, is the mechanism by which chirality is transferred to the backbone. This is analogous to the molten globular state of proteins, a state in which the peptide backbone possesses a native-like conformation while having disordered side chains.^{414,415} An alternative way to explain the observed transition behavior is to consider the dynamics and conforma-

tional uniqueness of the backbone. At high chloroform compositions (but still helical as judged by UV) there are possibly a large number of energetically similar, helical-like backbone conformations that interconvert rapidly. Here, the analogy can also be made to the compact, denatured state of proteins.⁴¹⁶ Regardless of which of these explanations is correct, the transfer of chirality appeared to be a highly cooperative process that required a progression of conformational order beyond the initially formed helical state. These results showed that the side chains played more than just a solubilizing role in these conformationally ordered oligomers.

All members of oligomer series **24** were fully substituted with chiral side chains, not allowing the

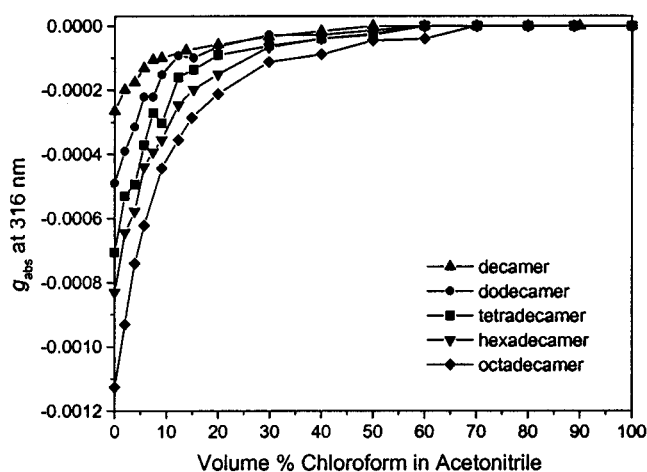


Figure 75. Plot of circular dichroism (g_{abs} at 316 nm, right) for **24** ($n = 10$) through **24** ($n = 18$) vs the volume percent chloroform in acetonitrile.

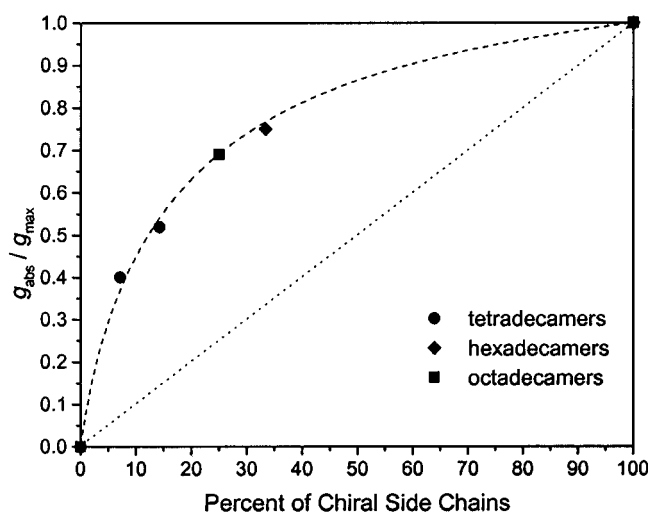


Figure 76. Plot of normalized $g_{\text{abs}}/g_{\text{max}}$ at 315 nm vs percent of chiral side chains for the mixed tetradecamers (**23** ($n = 14$), **25a**, **25b**, and **24** ($n = 14$)), hexadecamers (**23** ($n = 16$), **25c**, and **24** ($n = 16$)), and octadecamers (**23** ($n = 18$), **25d** and **24** ($n = 18$)) in acetonitrile at 20 °C. The dotted lines are meant to guide the eye but do not indicate that an asymptotic value is reached.

cooperativity to be determined. To investigate cooperativity in the folding reaction, oligomers with varying numbers of chiral side chains (**25a–d** in Figure 73) were synthesized and studied.⁴¹⁷ By analogy to the fully chiral (**24**) and achiral (**23**) oligomers, the mixed side-chain oligomers existed in a random conformational state in chloroform and formed a helical conformation in acetonitrile as determined with UV–Vis spectroscopy. Circular dichroism measurements were performed in order to determine the extent of cooperative interactions among the side chains. Shown in Figure 76 is a plot of the normalized Cotton effect ($g_{\text{abs}}/g_{\text{max}}$) vs percent chiral side chains. It can be seen that regardless of overall oligomer length, a positive nonlinear dependence of the optical activity on the percentage of chiral side chain was observed. This positive nonlinear effect strongly supports the cooperative nature of the folding reaction. The results further indicate that the twist sense bias is equally strong for every oligomer length, as

the normalized Cotton effect versus percentage of chiral side chains seems to be independent of chain length.

A CD analysis in aqueous acetonitrile examined the self-assembly of oligomer series **24** into helical columns.⁴¹⁸ The shorter oligomers (**24**, $n = 8, 10, 12$) showed an increase in the stability of the helical conformation with increasing water content. The longer oligomers (**24**, $n = 14, 16, 18$), which have a stable helical conformation in pure acetonitrile, were found to aggregate into multimolecular architectures upon introduction of water. By using the strong intermolecular interactions that exist in aqueous acetonitrile solvent, the intermolecular transfer of chirality was examined for chiral **24** ($n = 18$) and achiral **23** ($n = 18$) octadecamers. In 100% acetonitrile, the CD signal was found to be linearly dependent on the mole percent of chiral octadecamer (Figure 77, top left). These results indicate that if intermolecular aggregation is occurring, there is no transfer of chirality. More importantly, they show that the CD signals observed in 100% acetonitrile can be attributed to a purely intramolecular effect. Examination of solutions in increasing amounts of water showed a positive deviation from linearity; that is, the magnitude of the CD signal was larger than expected for an ideal mixture (Figure 77). Additionally, the observation that the maximum CD signal of certain mixtures of chiral and achiral oligomers was greater than that of the purely chiral octadecamer suggests that more efficient packing is present between achiral molecules than the chiral molecules, since in the former no branching methyl group is present. The transfer of chirality to achiral oligomers appears to be dependent on the presence and intermolecular aggregation of a helical conformation observed for the longer octadecamers. The stacking is promoted by the highly polar aqueous environment, and efficient intermolecular stacking allows for the chirality to be transferred to the achiral helices.

An alternative approach to controlling the twist sense bias involved the use of chiral units in the oligomer backbone (Figure 73).^{412,413} It was determined that a binaphthol unit in the backbone provided a high amount of diastereomeric excess of one twist sense over the other.⁴¹² Circular dichroism spectra of **26** ($n = 2, 4, 6, 12$) in chloroform were independent of chain length, while in acetonitrile a large Cotton effect was observed (Figure 78). The presence of an isodichroic point at 302 nm indicated similar structures of **26** ($n = 2, 4, 6, 12$), and the opposite sign of the signal arising from (*S*)-**26** ($n = 6$) confirmed that the induction of chirality in the backbone was from the binaphthol segment. Furthermore, a continual increase in $\Delta\epsilon$ as the length of the chain increased indicated that the chiral environment persisted along the entire chain length. However, by comparing results on these oligomers to a system containing the binaphthol segment at the chain terminus (**27**), it was determined that the binaphthol in the center causes 3–5 kcal·mol⁻¹ destabilization of the folded, helical conformation.

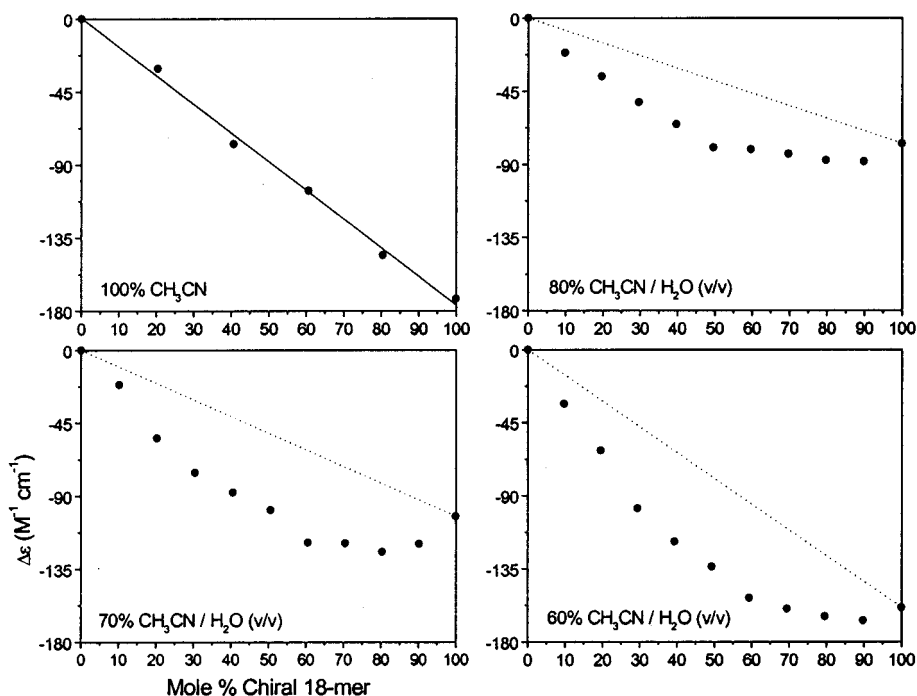


Figure 77. Plot of $\Delta\epsilon_{314}$ vs mole % chiral octadecamer **24** ($n = 18$) for solutions of varying amounts chiral and achiral **23** ($n = 18$) octadecamers in different concentrations of water/acetonitrile (v/v). All spectra were recorded in solutions with a total oligomer concentration of $3.3 \mu\text{M}$. The dotted lines are the expected signals that should arise upon dilution of a sample only containing only chiral octadecamer. The solid line is the least-squares linear fit of the chiral octadecamer dilution data (top left, correlation coefficient = 0.998).

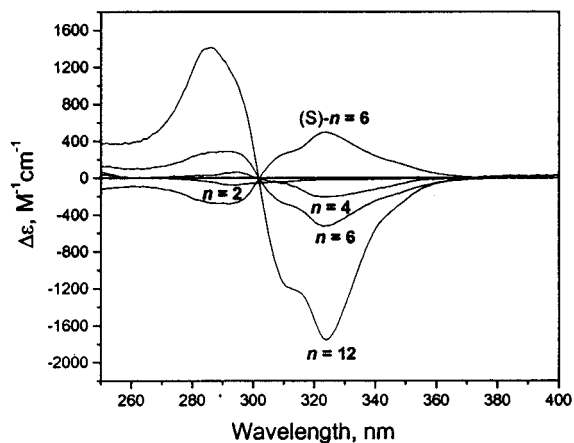


Figure 78. CD spectra of **26** ($n = 2, 4, 6, 12$) in acetonitrile. All samples were prepared with OD ca. 1.0 ($2\text{--}11 \mu\text{M}$ in oligomer), and spectra were recorded at room temperature (23°C).

In another system containing a chiral unit in the backbone, (+)-tartaric acid was used to tether two chains.⁴¹³ It was found that the choice of protecting group on the tartaric acid played an extremely significant role on the magnitude of the twist sense bias **28** ($\text{R} = \text{H}, \text{CMe}_2, \text{SiMe}_3$). The use of a trimethylsilyl ether protecting groups resulted in helices with a very large twist sense bias (Figure 79). Surprisingly, the use of an isopropylidene ketal group or no protecting group was ineffective at helical discrimination and may have possibly inhibited helix formation. At the present time, the exact conformational role of the chiral tether has not been established. Initial molecular modeling experiments indicate that the trimethylsilyl protecting groups may bind within

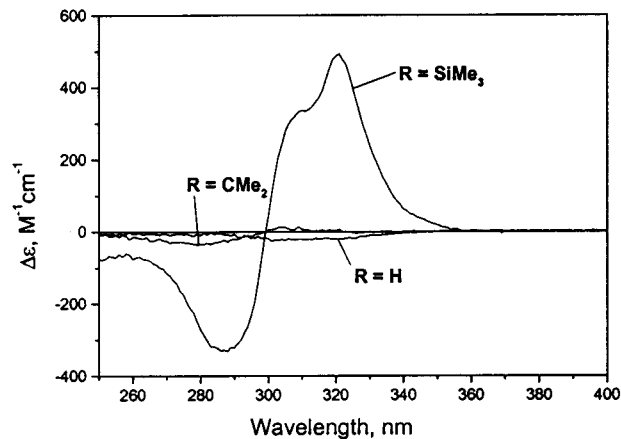


Figure 79. CD spectra of **28** ($\text{R} = \text{H}, \text{CMe}_2, \text{SiMe}_3$) in acetonitrile.

the helical cavity and help in templating helical formation.

Moore and co-workers have also shown that it is possible to control the folding reaction in a nonpolar solvent.⁴¹⁹ For these studies, a series of *m*-phenylene ethynylene oligomers containing nonpolar, (*S*)-3,7-dimethyl-1-octanoxo side chains was synthesized and studied (**29**) (Figure 80). In these oligomers, the addition of apolar side chains rendered the aromatic backbone polar with respect to the side chains. The ability to induce conformational order in such an oligomer was intriguing since both the side chain and backbone are hydrocarbon segments. Structural amphiphilicity in this system is obviously less pronounced, and the promotion of helical order in a lipophilic solvent would bode well for the possibility of forming helical channels in bilayer membranes. UV-Vis and CD measurements indicated that the

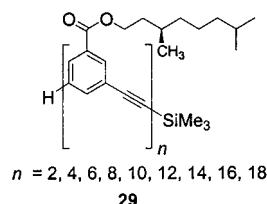


Figure 80. Structure of oligo(*m*-phenylene ethynylene)s **29** with chiral, apolar side chains.

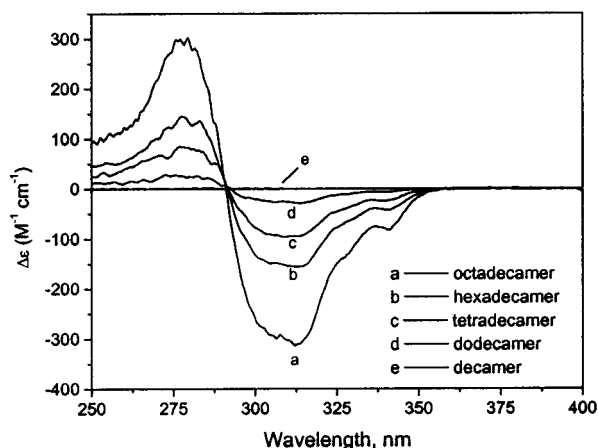


Figure 81. Plots of $\Delta\epsilon$ vs λ for **29** ($n = 10$) through **29** ($n = 18$) in heptane at 20 °C (right). Note the presence of an isodichroic point at 292 nm.

oligomers adopted a random conformation in chloroform as evidenced by a linear dependence of molar absorptivity on chain length and a lack of Cotton effect in the backbone chromophore. In apolar solvents, such as heptane, oligomers of sufficient length ($n > 10$) were found to adopt a helical conformation with a large twist sense bias (Figure 81). In a fashion similar to the chiral polar oligomers **24**, the onset of the twist sense bias occurred abruptly at a solvent composition that was well beyond the conformational transition as monitored by UV spectroscopy. Although the underlying phenomena responsible for this behavior are not well understood, it was apparent that the transfer of chirality was highly coopera-

tive and again required a progression of conformational order beyond the initially formed helical state. It was also noted that for the apolar oligomers **29**, the Cotton effect disappeared at much smaller volume percent chloroform than for the polar, chiral oligomers **24**. This was most likely due to the greater rate at which solvent polarity changes upon addition of chloroform to heptane, in contrast to the smaller change upon addition of chloroform to acetonitrile. It was also shown that the strong twist sense bias was extremely time dependent and could partially be attributed to intermolecular aggregation. These results indicate that nonpolar, solvophobic interactions can be used for controlling the ordering of nonbiological oligomers.

The helical conformation of *m*-phenylene ethynylene oligomers has a tubular cavity, which potentially provides a novel receptor site for catalytic systems. The ordered solution conformation was shown to afford a high-affinity binding site for small molecule guests.⁴²⁰ This was first demonstrated by the diastereoselective complexation of chiral monoterpenes with three different dodecamer length oligomers in polar solvents (Figure 82). The only difference among these oligomers was the addition of methyl groups, which are placed into the tubular cavity upon helical formation, reducing the space available for guest binding. Induced circular dichroism (CD) spectroscopy was used for probing the interaction of small chiral molecules with the achiral oligomers. In the absence of a chiral guest, oligomer **30** exhibited no CD signal as expected for an achiral molecule. However, the addition of enantiomerically pure (–)- α -pinene to a solution of **30** in 40% H₂O/acetonitrile induced a strong Cotton effect in the wavelength range where the oligomer absorbs. The stoichiometry of the complex was strictly 1:1 as determined by the linearity of Benesi–Hildebrand and slope of Hill plots, and the binding affinity constant was found to be ca. 6800 M⁻¹. Molecular models (Figure 83) revealed that the size and shape of α -pinene is complementary to the internal space

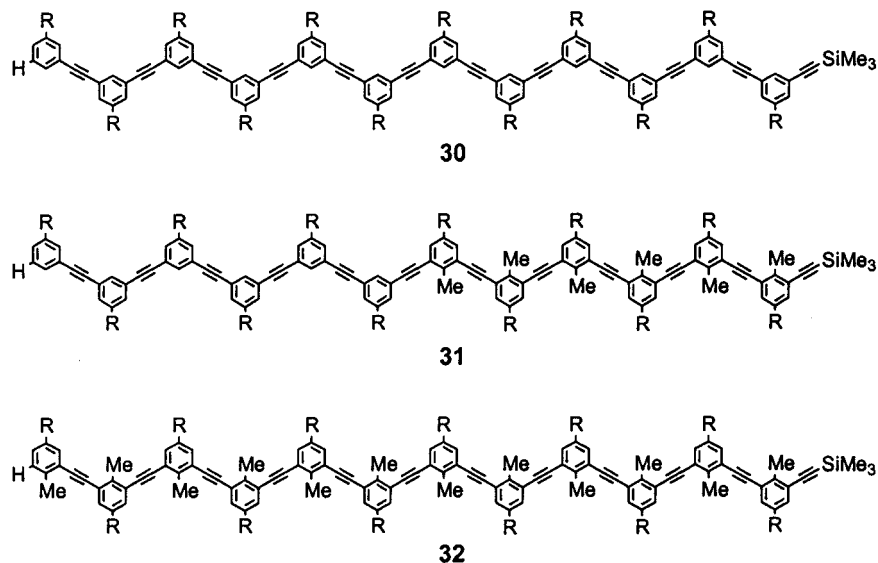


Figure 82. Chemical structures of *m*-phenylene ethynylene oligomeric hosts **30–32** used in binding small molecule guests ($R = -\text{CO}_2(\text{CH}_2\text{CH}_2\text{O})_3\text{CH}_3$).

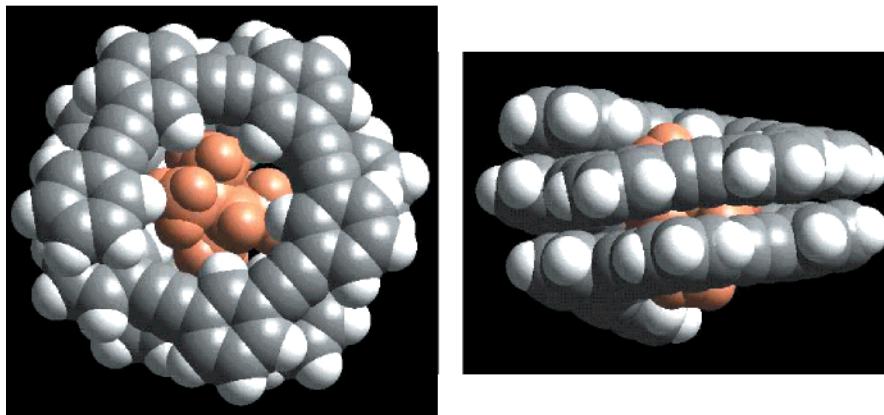


Figure 83. Space-filling model of the 1:1 minimum energy complex of **30** and (-)- α -pinene determined by a Monte Carlo search in which the position and orientation of the helix cavity within the helix cavity was varied. Top and side views are shown.

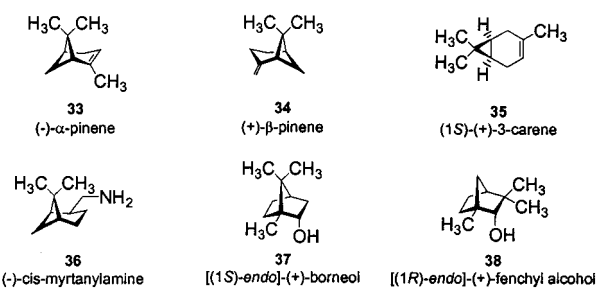


Figure 84. Structures of various terpenes used in the binding study.

Table 6. Association of Oligomer 23 ($n = 12$) with Various Monoterpenes^a

guest	K_{11} (M^{-1})	$-\Delta G^\circ$ ($kcal \cdot mol^{-1}$)	$\Delta \epsilon_\infty$ ($M^{-1} \cdot cm^{-1}$) ^b
33	6830 ^c	5.2	325
34	6000 ^d	5.1	15
35	4450 ^c	5.0	93
36	2970 ^c	4.7	265
37	3920 ^c	4.9	124
38	1790 ^c	4.4	77

^a All measurements were recorded in a mixed solvent of 40% water in acetonitrile (by volume) at 295 K. Abbreviations: K_{11} , association constant; M, molarity; $-\Delta G^\circ$, free energy of complex formation; $\Delta \epsilon_\infty$, saturation value of the CD signal from nonlinear fitting of titration data to a 1:1 binding model. [13 ($n=12$)] = 4.2 μM . ^b CD signal at saturation determined from nonlinear least-squares fitting. ^c Determined from nonlinear least-squares fitting to a 1:1 binding model. ^d Calculated by competition experiments with guest **33**.

of the hydrophobic cavity of the putative helix and interestingly that the molecular volume of α -pinene is roughly 55% of the helix cavity volume, consistent with the criterion suggested by Rebek for molecular encapsulation.⁴²¹ It was also determined that dodecamer **30** forms 1:1 complexes with a variety of monoterpenes **33**–**38** (Figure 84; Table 6). The binding was also found to be a solvophobic driven process, and by extrapolating to pure water, an association constant of 60 000 M^{-1} was estimated.

By performing experiments on modified oligomers (**31** and **32**), it was confirmed that binding was occurring on the interior of the cavity (Figure 85). Each oligomeric host formed a 1:1 complex with (+)- α -pinene, but the association constant dropped by 1 and 2 orders of magnitude for **31** ($K_{11} = 280 M^{-1}$ and $-\Delta G^\circ = 3.3 kcal \cdot mol^{-1}$) and **32** ($K_{11} = 40 M^{-1}$ and

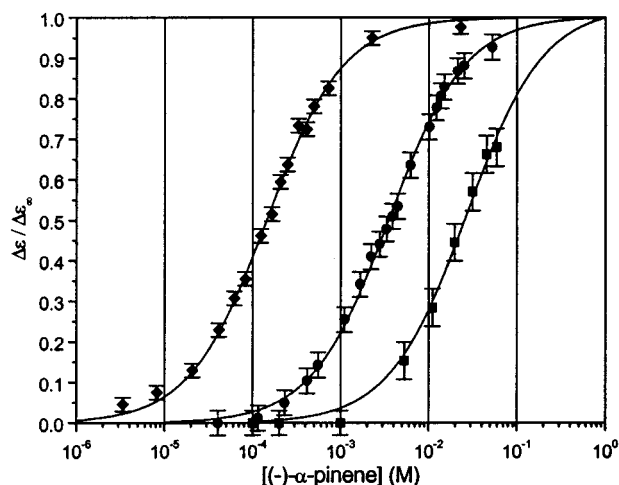


Figure 85. Plot of fractional saturation of the CD signal against (-)- α -pinene concentration for the oligomers: **30** (\blacklozenge); **31** (\bullet); **32** (\blacksquare). The CD signal at saturation, $\Delta \epsilon_\infty$, was obtained from nonlinear least-squares fitting of $\Delta \epsilon$ vs (-)- α -pinene concentration using a 1:1 binding model. The lines are the nonlinear fits of the data to the 1:1 binding model. Error bars are based on the signal-to-noise ratio of the CD spectra. All measurement were recorded in a mixed solvent of 40 volume percent water in acetonitrile (by volume) at 295 K. [oligomer] = 4.2 μM .

$-\Delta G^\circ = 2.1 kcal \cdot mol^{-1}$), respectively. These results indicated that filling the cavity with methyl groups reduced the space for binding. This study shows that conformationally ordered oligomers could serve as a platform for the construction of synthetic receptors. The demonstration that a binding site could be created from a folded chain parallels concepts in biopolymer recognition and suggests a new avenue for supramolecular catalysis. The synthetic modularity of sequence-specific oligomers naturally suggests the use of combinatorial methods in refining the active sites. Molecular adaptation, where binding strength is mediated by conformational changes, is easily imagined from this study.

As an extension of the concept of molecular adaptation, the internal cavity of an oligo(m -phenylene ethynylene) helix was also anticipated to be complementary in shape to rodlike chain molecules of appropriate diameter.⁴²² Molecular interactions of this type, while quite unlike those typical of biomacromolecules, were sought to reveal oligomeric

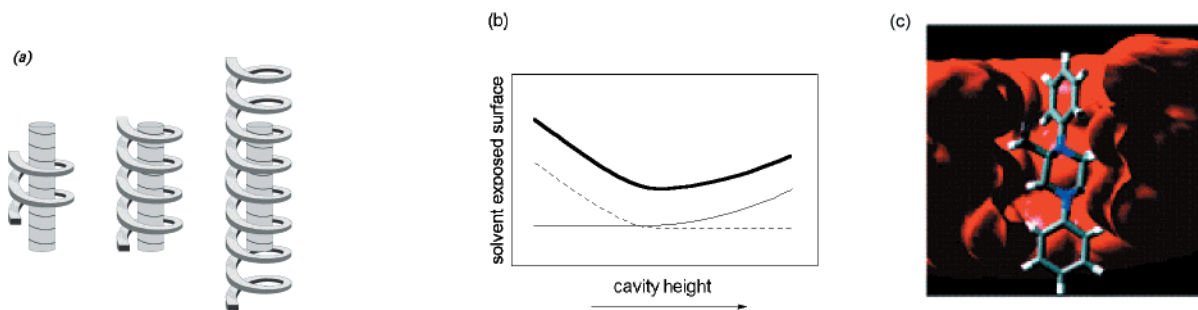


Figure 86. (a) Schematic diagram illustrating the binding of a rodlike guest to helical oligomers of differing lengths. The cavity height is determined by the oligomer length. (b) Solvent-exposed surface of the oligomer cavity (—) and the rodlike guest (---) in a complexed state as a function of cavity height. The total amount of solvent-exposed surface (—) shows a minimum that predicts a cavity length with the highest affinity for the rodlike guest. (c) Minimized structure of **23** ($n = 18$) with **39** determined by a Monte Carlo docking algorithm.

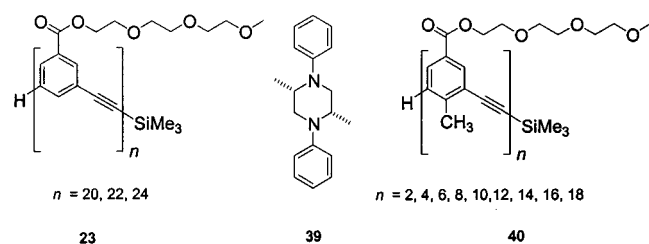


Figure 87. Structures of a rodlike guest and two series of *m*-phenylene ethynylene oligomers.

modularity, both in terms of the helical scaffold and the ligand. Association is based on shape recognition arising from the morphological features of interacting molecular surfaces. These concepts led to the development of rod-shaped chiral guest **39** whose shape is matched to the cylindrical cavity of oligomer series **23** (Figure 86a). The binding affinity of these complexes was postulated to depend on the relative length of the oligomer to its guest, assuming the free energy of binding depends on the area of contact between the interacting molecular surfaces (Figure 86b). Considering the diameter of the cylindrical hydrophobic cavity in helical oligomer series **23**, *cis*-(2*S*,5*S*)-2, 5-dimethyl-*N,N*-diphenylpiperazine **39** was examined as the guest molecule (Figure 87). Compound **39** has a chiral, rodlike structure, and its size and shape are complementary to the cavities of helical **23**, as deduced from molecular modeling studies (Figure 86c).

The binding affinities of **39** with members of oligomer series **23** ($n = 10, 12, 14, 16, 18, 20, 22, 24$) were determined using CD measurements. Induced CD spectra resulting from the interaction of **39** with oligomer series **23** were obtained by subtracting the CD spectrum of **39** from that of the host-guest complex in 40% aqueous acetonitrile. The shape of the induced CD spectra is nearly identical to that obtained when using (–)- α -pinene as the guest molecule.⁴²⁰ CD spectra recorded over a range of guest concentrations showed saturation behavior with an isodichroic point, which is expected for a single stoichiometry relationship between **39** and its oligomeric host. To verify that binding takes place within the helical cavity, solutions of *endo*-methyl-substituted dodecamer **32** with guest **39** as a control were studied. No induced Cotton effect was observed in this case. These results indicate that compound **39** binds to the internal cavity of these oligomers,

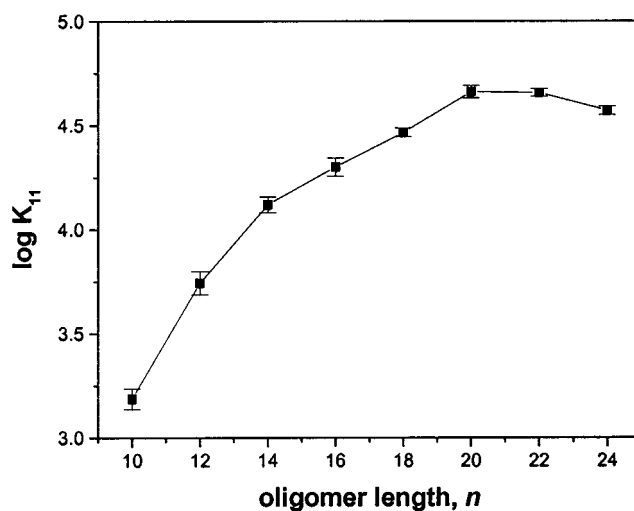


Figure 88. Plot of $\log K_{11}$ versus oligomer length n . The binding affinity of **39** reaches a maximum value with **23** ($n = 20$ and 22). All measurements were recorded in a mixed solvent of 40% H_2O in CH_3CN (by volume) at 294 \pm 1 K. $[\text{39}] = 4.2 \mu\text{M}$.

rather than associating by intercalation. The stoichiometry of the complex of **39** with **23** was determined to be 1:1 by the linearity of Benesi-Hildebrand plots. The association constant (K_{11}), calculated by a nonlinear least-squares fitting method, was found to be $5600 \pm 190 \text{ M}^{-1}$ for the 12-mer of **23**. This value is again similar to that of the complex of (–)- α -pinene and 12-mer of **23**.⁴²⁰ However, a significant dependence of the binding affinities of **39** on the length of the oligomers was observed (Figure 86). In each case, the stoichiometry of the complex was 1:1. The affinity of **39** with the 20-mer and 22-mer of **23** was found to be ca. 30 times larger than that of 10-mer. Interestingly, the K_{11} value of the 24-mer is smaller than that of the 20-mer and 22-mer by an experimentally significant and reproducible margin. The reduction in affinity could be due to destabilization involving a cavity-volume/guest-volume mismatch (Figure 86b).

These results continue to support the hypothesis that all members of oligomer series **23** exist in solution in conformationally well-ordered states with chiral cylindrical cavities capable of binding chiral rodlike guest molecules such as **39**. Co-modularity of host-guest oligomeric pairs such as the system described here raises a number of engaging possibili-

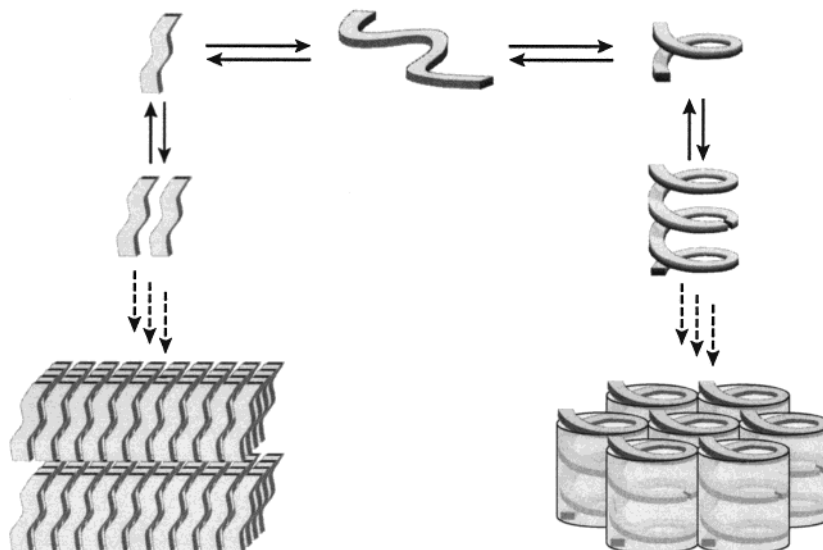


Figure 89. Schematic diagram illustrating the aggregation behavior of *m*-phenylene ethynylene oligomers over a range of concentrations. In dilute solution, the oligomers can exist in a random or helical conformation. At increased concentrations they associate intermolecularly, possibly in an extended lamellar-type fashion or as tubular and hexagonal helical stacks.

ties. It has been presumed that longer rodlike guest molecules will exhibit a maximum affinity to even longer oligomers. For example, the rod lengths of **39** can be easily varied by repeating the aryl–piperazine unit and may possibly be applied to the selective ligation of oligomer fragments to template the growth of chains of a specific length.

c. Oligo(*m*-phenylene ethynylene)s in the Solid State. The solid-state organization of *m*-phenylene ethynylene oligomers has also been investigated.^{423–426} For these studies two different oligomer series were examined (**23** and **40**). Two possible packing models were postulated for the solid-state organization of the oligomers (Figure 89). One possibility is that the oligomers could self-organize into a tubular mesophase.^{427,428} On the other hand, a lamellar organization consisting of extended ribbonlike chains could achieve many of the same local aromatic–aromatic interactions without the costly free volume of the tubular phase. The solid-state conformation was found to be highly dependent on the subtle chemical structure of the backbone.

Oligomer series **23**, which contains a hydrogen-substituted backbone, was found to exhibit a lamellar organization in the solid state. Optical microscopy and differential scanning calorimetry showed that oligomers ($n > 8$) adopt liquid crystalline phases and that they each have a similar mode of solid-state organization. By performing X-ray measurements on samples slowly cooled from the melt⁴²³ or evaporated from solution,⁴²⁵ it was possible to determine that the long-spacing, due to periodic order in the solid state, was directionally proportional to oligomer length (Figure 90). It was also determined that these viscoelastic samples could be mechanically aligned by spreading or rolling the material on flat substrates. This produced macroscopic orientation in the longitudinal direction. It was proposed that the lamellar organization was thermodynamically favored, presumably due to the minimization of free channel void space that would be present in a tubular structure.

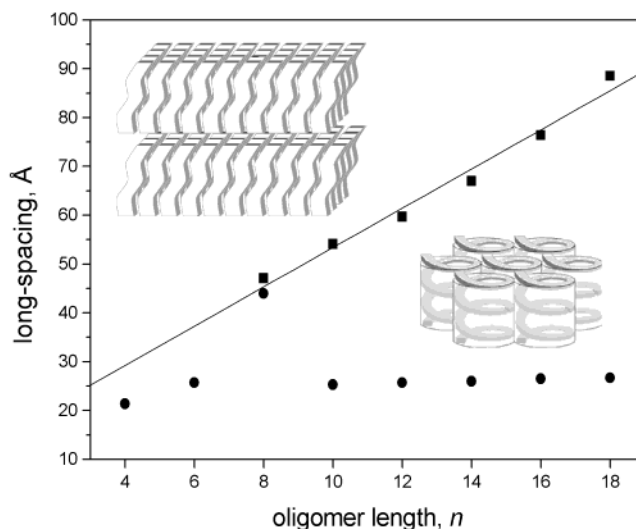


Figure 90. Plot of long-spacings versus oligomer length for two oligo(*m*-phenylene ethynylene) series as observed in SAXD measurements. Series **23** (prepared from the melt) packs in a lamellar arrangement (■, top), and thus, the long-spacings depend linearly on chain length. In contrast, series **40** (prepared from solvent evaporation) exhibits long-spacings that are independent of chain length ($n \geq 10$), suggesting the possibility of helical columns (●, bottom).

Oligomer series **40**, which contains a methyl-substituted backbone, was surprisingly found to adopt a tubular organization in the solid state. Because the melting point of these oligomers exceeds the decomposition point, a new X-ray sample preparation was required. Oligomers were dissolved in a solvent (typically CH_2Cl_2), drawn into a capillary, and left to solidify as evaporation took place. X-ray Bragg spacings were independent of chain length, and each oligomer exhibited a long spacing of 25–26 Å (Figure 90). The small-angle X-ray reflections were indexed to a hexagonal lattice indicating that the oligomers were packing in a tubular arrangement. In addition, it was determined that the oligomers spontaneously acquired a radial macroscopic orientation upon evaporation. These results suggested that the oligomers

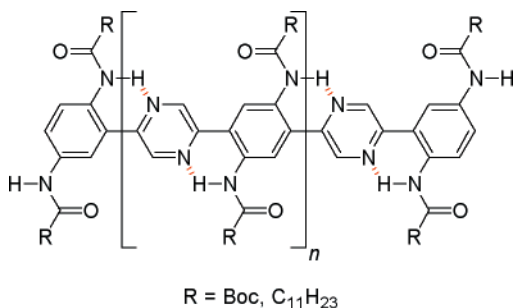


Figure 91. Alternating pyrazine and acylated 1,4-phenylenediamine copolymer that adopts a planarized shape.

that adopt hexagonally packed nanotubes tend to form stable helical conformations in solution (the folded state of oligomer series **40** is more stable than **23** in solution).⁴²⁹ In the case of **40**, the helical stabilization is attributed to the fact that the introduction of methyl groups minimized the costly free space present in series **23**. The tubular structure of this system and others^{377–380,382} could have possible applications as an organic host solid or be used as a template for nano-organization.

D. Backbones Utilizing Hydrogen-Bonding Interactions

1. Aromatic Amide Backbones

Hydrogen bonding is important for creating and stabilizing highly ordered conformations in naturally occurring systems such as α -amino acid peptides and nucleic acids. Recently, H-bonding interactions have been used in combination with the aromatic–aromatic stacking interactions of aromatic rings in oligomer systems. A common motif of this research is the use of aryl amides. It should be mentioned that most of these oligomers make use of interactions between adjacent monomer units only in their H-bonding interactions. Whether these chain conformations behave cooperatively or as a collection of independent units requires experimental verification. Nonetheless, the backbones discussed below are worthy of note in that they each utilize the same repeat unit to achieve various structural ends.

Oligo(acylated 2,2'-bipyridine-3,3'-diamine)s and oligo(2,5-bis[2-aminophenyl]pyrazine)s have shown enhanced planarization and conjugation through intramolecular hydrogen bonding (Figure 91).^{430–432} Dendritic analogues of these oligomers have also been reported.^{433–438}

Hamilton and co-workers reported the generation of a helical conformation based on an oligoanthranilamides (Figure 92).^{439–441} The system is based on the intramolecular H-bonding of two subunits, one being an anthranilamide **41** and the other a 2,6-pyridinedicarboxamide **42**. (Dendritic analogues utilizing anthranilamide and pyridinedicarboxamide subunits have been reported to display solvent-, temperature-, and generation-dependent conformations in solution.^{442–444}) It was proposed that a helical conformation would result from intramolecular H-bonding, the preference of secondary benzamides to adopt a trans conformation in solution, and aromatic–aromatic stacking between the aromatic subunits.

These subunits were combined in the synthesis of several compounds of varying oligomer length (**43**, **44**, **45** R = Me, *n*-Hex).

The helical conformation was characterized by NMR spectroscopy and X-ray crystallography. In chloroform, where H-bonding should be strong, oligomers **43** and **44** exhibited a large downfield shift for the pyridinecarboxamide protons while the terminal NH protons and many of the aromatic protons exhibited a strong upfield shift. These results are indicative of aromatic stacking and H-bonding. The solid-state structure of **43** shows a distinct helical conformation with an aromatic stacking distance of 3.69 Å. The increased bulk of the *N*-oxide unit in **44** resulted in a wider separation of the terminal anthranilamide rings. This resulted in an increased pitch of the helical conformation as evidenced by an increased aromatic stacking distance in the X-ray structure and less significant upfield shifting of the resonances of the terminal aromatic protons.

Intramolecular H-bonding was also used in the creation of systems **45** (R = Me, *n*-Hex) with an extended secondary structure. X-ray crystallography on the less soluble analogue **45** (R = Me) revealed two polymorphs. One contained the desired helical conformation with the expected aromatic stacking distances and two complete turns of the oligomeric backbone. In the solid state, a racemic mixture of right- and left-handed helical conformations is present. Surprisingly, another polymorph contained a left-handed helix for the first portion of the oligomer that reversed to a right-handed helical conformation at the phenylenediamine unit in the center of the strand. The solution conformation showed the expected downfield shifting of H-bonded amide protons and upfield shifting of aromatic resonances due to aromatic stacking. However, the lack of any NOE signals prevented the complete characterization of the solution conformation. Therefore, it was not possible to determine if alternative structures existed. Nonetheless, these results demonstrate that the combination of aromatic stacking interactions and intramolecular H-bonding can be used for the generation of secondary structures in solution. Given the combination of adjacent and nonadjacent noncovalent interactions that contribute to conformational stability, these oligomers do qualify as foldamers.

Additionally, predisposed intramolecular H-bonding has been used for the helical formation of oligo(amide)s (Figure 93).^{445–447} Using a structure akin to one published by Nowick,^{154,155} these systems involve *meta*-connected diaryl amide oligomers (**46**) and the presence of a three-center intramolecular H-bond, which leads to a rigidification of the backbone. Ab initio molecular calculations show a strong preference (>11 kcal·mol⁻¹) for the three-center H-bond over possible alternative conformations. These units were incorporated into oligomer **47** containing six aromatic rings. Upon placing the oligomers in a chloroform solution, an almost complete circle was formed, which represents the first turn of a helical conformation. ¹H NMR NOESY experiments revealed the expected 10 cross-peaks between the amide protons and the protons of the alkoxy α -methylene and methoxy

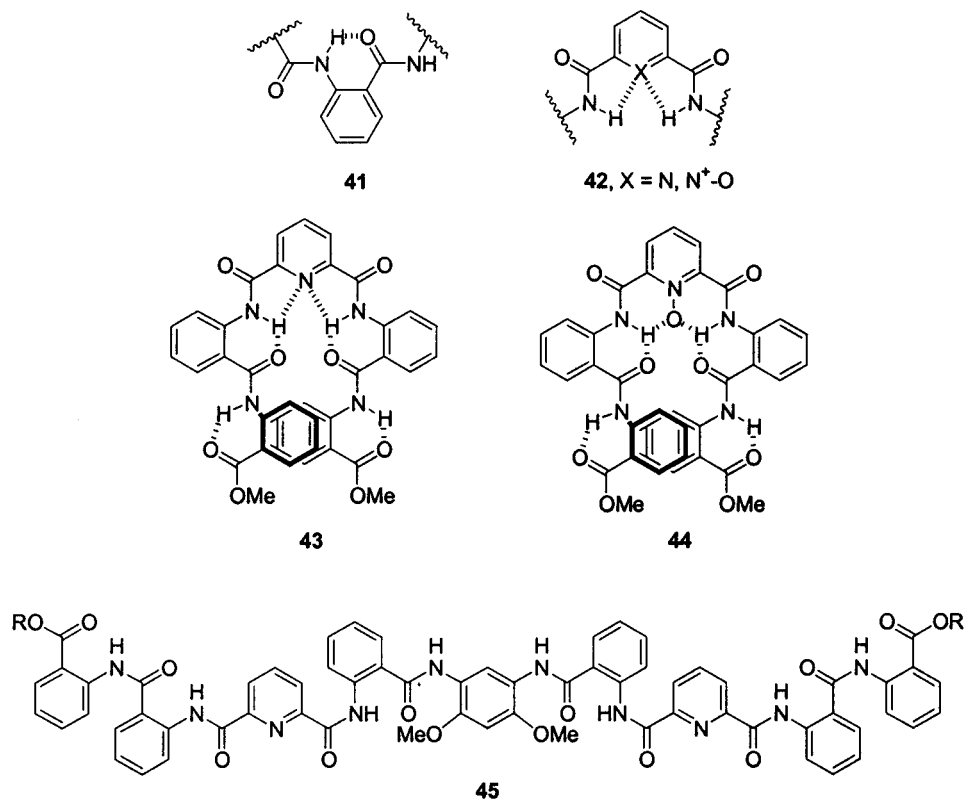


Figure 92. Anthranilamide motifs and derivative oligomers.

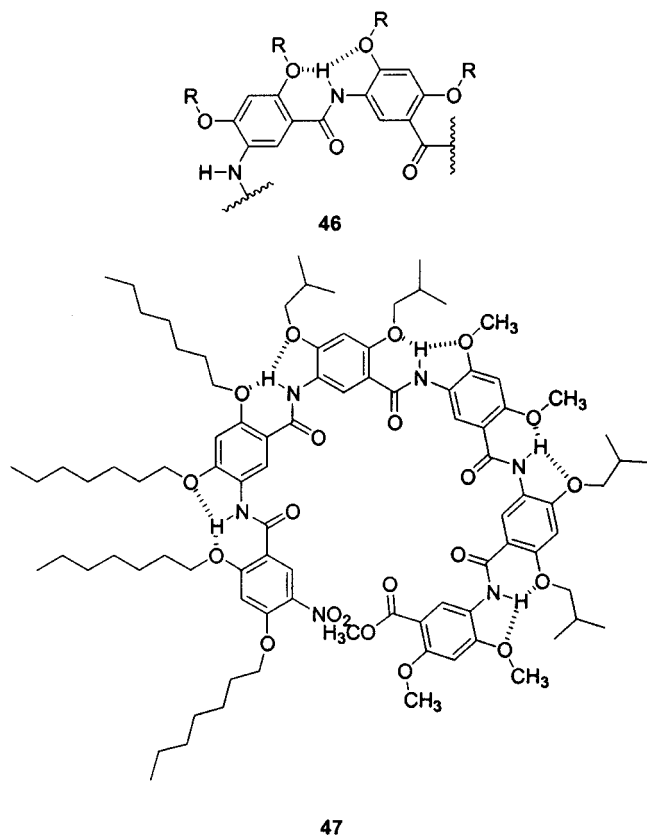


Figure 93. Chemical structure of an oligo(amide) motif and a crescent oligo(amide).

groups, supporting the formation of a curved conformation. On the basis of molecular modeling, this conformation has a ~ 10 Å hydrophobic cavity. At the present time, no oligomers longer than six units have

been synthesized, so it is therefore not known if longer strands would result in a helical conformation. However, if this does occur, it would create a large internal cavity that could possibly be used for the binding of small molecules.

2. Receptor Motif Backbones

a. Diaminopyridine Backbones Templated by Cyanurate.

Molecular recognition mediated by H-bonding between a host diaminopyridine and a guest cyanurate unit (**48**) has also been used for the generation of well-defined foldamers (Figure 94).⁴⁴⁸ An oligomer strand **49** containing four diaminopyridine subunits was synthesized and studied. It was proposed that the interaction of oligomer **49** with 2 equiv of a monosubstituted cyanurate **50** would result in helical conformation **52** (through conformation **51**) stabilized by H-bonding and aromatic stacking interactions. ¹H NMR spectroscopy was used to characterize the interaction of oligomeric host **49** with cyanurate guest **50**. In chloroform and polar, hydrogen bond-competing solvents such as methanol, the spectrum of **49** is broad and poorly resolved, indicating a variety of nonspecific intermolecular interactions. Upon the addition of 2 equiv of cyanurate guest **50**, a sharpening of the signals is observed along with the downfield shift of the amide hydrogens resonances. These results indicated the formation of a well-defined, H-bonding complex whose 2:1 stoichiometry was confirmed by a Job's plot analysis.^{449,450} The binding was determined to be a cooperative process where the binding constant of the second guest was twice that of the first guest. This could be attributed to the preorganization of the strand for the binding of the second guest molecule

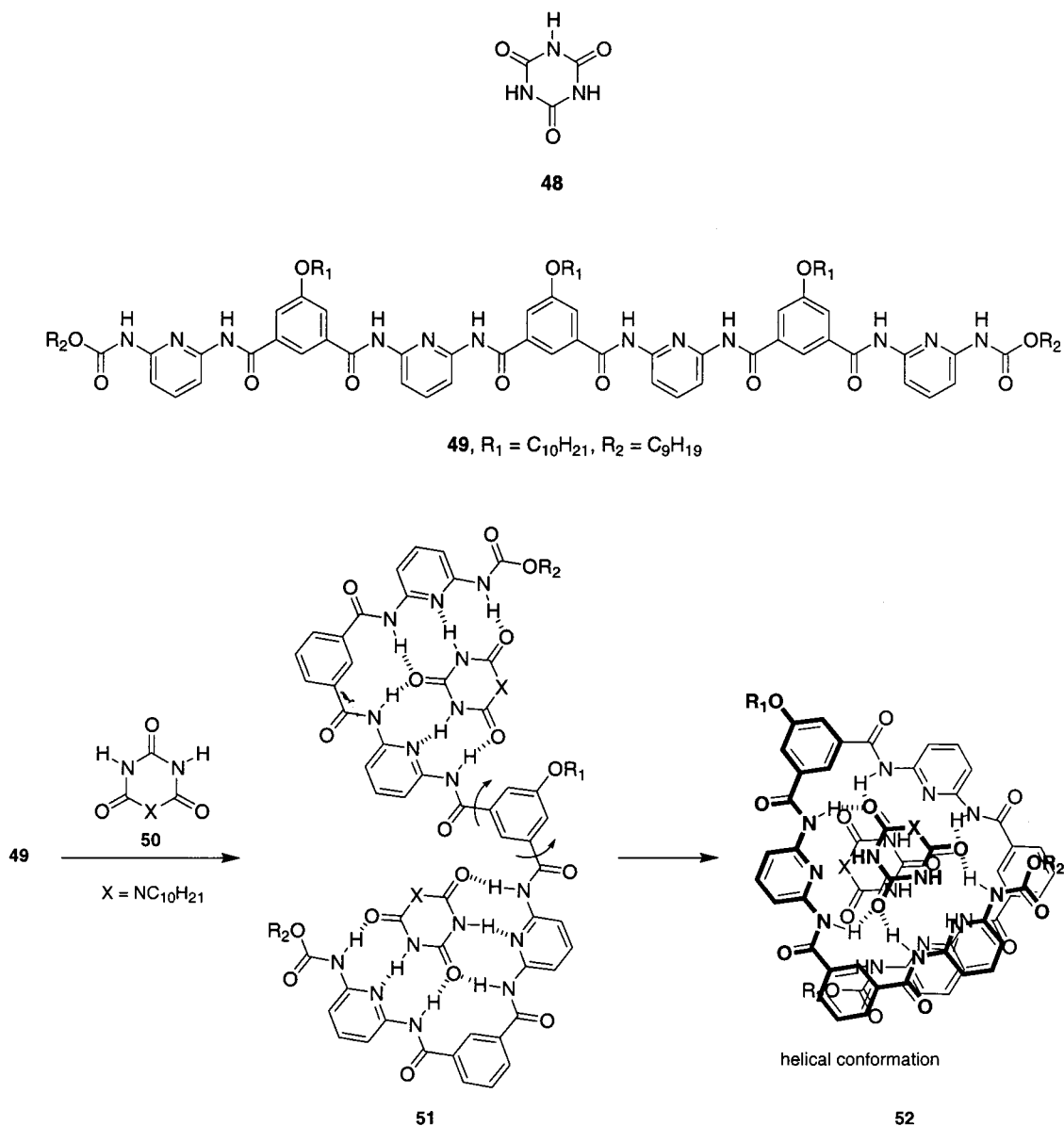


Figure 94. Motifs, oligomers, and helical structure of cyanurate-binding oligo(diaminopyridine)s.⁴⁴⁸

upon binding of the first molecule. An examination of concentrated solutions in hydrocarbon solvents by optical and electron microscopy revealed the presence of entangled fibers. This behavior was attributed to the intermolecular aggregation of the helical conformation **52**, similar to previously described systems.³⁸² These results show that the proper use of intermolecular interactions between a host and guest molecule can template helical conformations and higher ordered structures in solution.

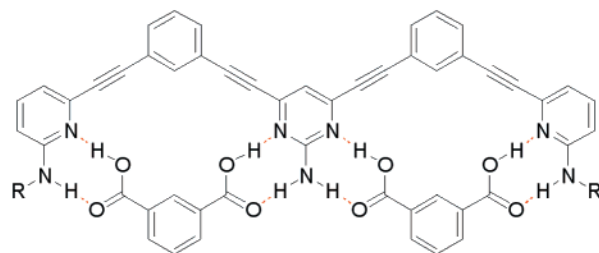
b. Phenylene–Pyridine–Pyrimidine Ethynylene Backbones Templated by Isophthalic Acid. Moore and co-workers reported a phenylene ethynylene-based isophthalic acid receptor that can be extended to a dual-site complex.⁴⁵¹ While this system does not utilize aromatic stacking to adopt a planar conformation, it does employ the rigidity of a phenylacetylene backbone to properly bind its guest via H-bonding. Cocrystallization of the precursor trimer and isophthalic acid gives single crystals of a complex suitable for X-ray structure determination. The resulting complex clearly displays four H-bonds and

packs in 2D sheets. Job's method confirmed the 1:1 stoichiometry of the complex in solution.^{449,450} Pentamer **53**, which can bind 2 equiv of isophthalic acid in solution (stoichiometry determined by Job's method^{449,450}), was also examined by X-ray structural studies. Eight H-bonds were revealed corresponding to the planar configuration of the complex (Figure 95). Overall, these results show that the binding of a guest can modulate the conformation of its respective host and that extending the host backbone can result in multisite foldamer receptors.⁴⁵²

E. Backbones Utilizing Metal Coordination

1. Overview

Up to this point in the review, foldamer structures primarily stabilized by hydrogen bonding and aromatic–aromatic stacking have been considered. At the same time, a significant amount of work has been conducted on chains that fold upon binding ionic species, especially coordination of metal ions, termed *helicates*.⁴⁵³ The folding reaction of these backbones



53

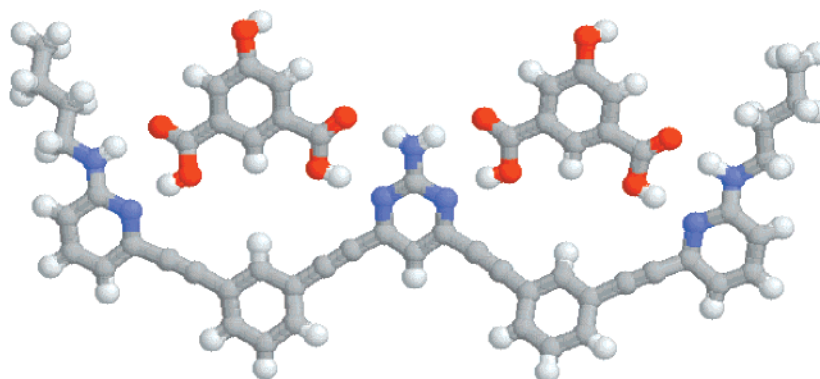


Figure 95. Crystal structure of a trimeric receptor with two molecules of bound isophthalic acid.

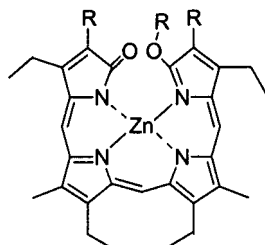


Figure 96. Helical zinc–bilinone complex.

is coupled to the assembly–disassembly process of metal coordination. We are unaware of any reference to helicate structures as foldamers in the literature, although they fulfill the foldamer criteria outlined in this review. Herein, we only consider examples that are chain molecules (at least two repeat units in the backbone) with the stipulation that they must demonstrate an ability to be extended to longer chain lengths. Furthermore, we will not consider infinite helical complexes since they are by their nature polymeric. Thus, the purpose of this section is not an exhaustive review of the helicate literature^{454–457} but an exploration of chain molecules that fold through metal coordination.

2. Metal-Binding Backbones

a. Zinc Bilinones. Acyclic porphyrin derivatives known as bilinones incorporate functionalized pyrroles into a tetrameric backbone such that binding of Zn(II) induces single-stranded helical conformations (Figure 96). Studies aimed at shifting the helical twist sense have involved covalent attachment of chiral moieties to the chain terminus^{458,459} or as tethers⁴⁶⁰ in addition to binding of chiral guests such as amino acids.^{461,462} Using chiral end group modified

bilinones, a recent solvent study demonstrated that solvents of lower polarizability were more efficient at this helical induction since intramolecular van der Waals contacts responsible for the diastereomeric discrimination are more favorable in these solvents.⁴⁵⁹ Although these tetrameric chains adopt folded conformations, it is difficult to envision a homomorphic extension of the chain to longer lengths with retention of these foldamer characteristics. Because of this, discussions of bilinones as foldamers does not seem promising and will not be considered further.

b. Oligopyridines. Although a variety of heteronuclear ligands employing pyridines, imines, and other Lewis basic functionalities have been incorporated into single-stranded helicates, we will focus here primarily on oligopyridines since they are the most common metal-coordinating ligands and have been incorporated into many complex structures.⁴⁵⁶ Oligopyridines are a family of chain molecules that have been thoroughly studied for their ability to bind a variety of metal ions in different stoichiometries and with predictable geometries due to their substitution patterns along the aromatic rings. As the oligomer length increases, *cisoid* and *transoid* conformational states are possible at each interannular torsion along the chain. Quaterpyridines (qtpy) exist as all-*transoid* conformations in the solid-state, with interannular twisting observed in solution,⁴⁶³ while adopting all-*cisoid* planar conformations when complexed (Figure 97) to a variety of transition-metal ions (examples include Co(II),⁴⁶⁴ Co(III),⁴⁶⁵ Cu(II),⁴⁶⁴ Ni(II),⁴⁶³ Pd(II),⁴⁶⁶ Cr(III),⁴⁶⁷ and Y(III)).⁴⁶⁸ Qtpy oligomers are the longest chains of this family that consistently adopt planar conformations within a single-stranded complex. Longer oligopyridine chains,



Figure 97. All-*transoid* solution conformation of qtpy, and the all-*cisoid* coordinated form.

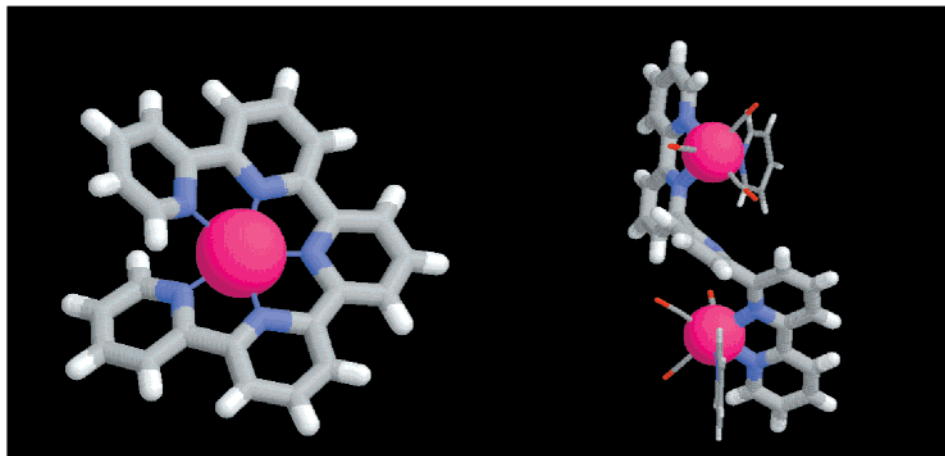
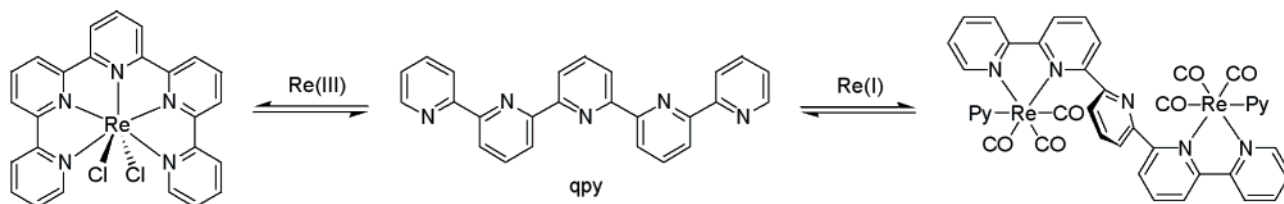


Figure 98. Two different single-stranded qpy helicites in two different Re oxidation states. Crystal structures are shown for each.

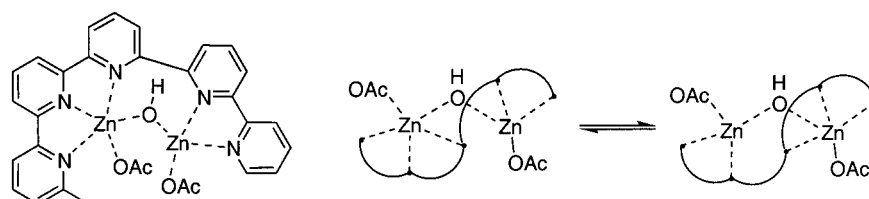


Figure 99. Solution equilibrium of a dinuclear qpy Zn(II) helicate containing a bridging hydroxide.

however, adopt helical conformations upon metal coordination and demonstrate various folded architectures, although becoming increasingly insoluble with longer lengths. Recent approaches that incorporate 4-*tert*-butyl phenyl⁴⁶⁹ and *n*-propylthio side chains⁴⁷⁰ greatly aid in solubilizing these oligomers.

The ability of metal ions to optimize their coordination sphere while minimizing their geometric constraints results in the ability to selectively coordinate to preferred segments within a chain molecule. This is a powerful supramolecular construct for foldamers whose level of architectural control has not been fully exploited. For instance, with Re(III), quinquepyridine (qpy) ($n = 5$) adopts a mononuclear, all-*cisoid* helical complex (also observed in a [Ag(qpy)]-[PF₆]₃ complex⁴⁷¹) (Figure 98). With Re(I), one of two isolated crystals was determined to be the dinuclear helicate where the metal ions partition the oligomer into two bipy segments, leaving the central pyridine uncoordinated.⁴⁷² With Re(III), the helical conformation occurs by interannular twists in the backbone to assuage steric interactions between the termini.

In the Re(I) helicate, the dinuclear coordination mode in the S-shaped conformation is adopted in order to alleviate steric hindrance in alternative complexations (as well as to accommodate the geometric preferences of the CO ligands) with the dihedral angles between the central ring and the bipy fragments opening up to 110° and 112°. ¹H NMR confirmed that the solid-state conformations of both complexes were retained in solution. Similarly, a single-stranded 6,6''-dimethyl-qpy chain binds two Zn(II) ions (bridged by a hydroxyl group) and two acetate species. In the solid state, bipy and tpy oligomer segments bind separately in order to ideally match steric constraints and satisfy the coordination spheres of the Zn(II) ions (Figure 99).⁴⁷³ In solution, the central pyridine coordinates to either of the Zn(II) ions in a dynamic equilibrium as evidenced by ¹H NMR. With sexipyridines (spy), Eu(III) forms a monohelical, 10-coordinate complex through torsional adjustments in the backbone to minimize chain end interactions,⁴⁷⁴ while with Pd(II), spy coordinates to

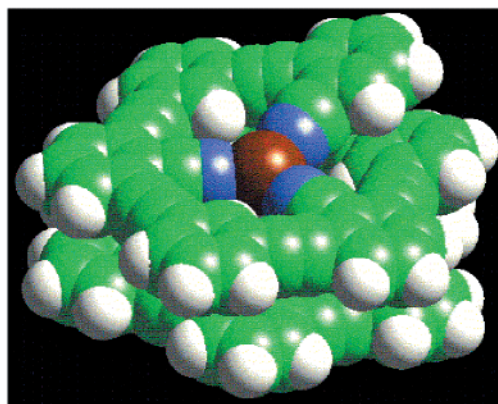
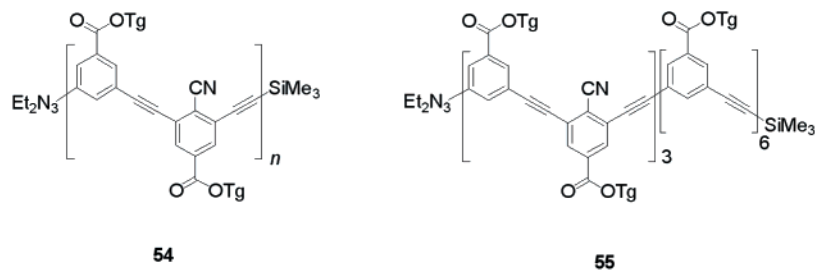


Figure 100. Structures of cyano-substituted oligo(*m*-phenylene ethynylene)s and a space-filling model of **54** coordinated to two Ag^+ ions. Side chains have been omitted for clarity.

two metal ions through two tpy fragments in the chain.⁴⁷⁵

c. Oligo(*m*-phenylene ethynylene)s. A modification of the tubular cavity of oligo(*m*-phenylene ethynylene)s led to the first example of a nonbiological oligomer whose secondary structure could be controlled by both nonspecific (solvophobic) and specific (metal-coordination) interactions.⁴⁷⁶ These features were present in dodecamer **54**, consisting of 12 nonpolar phenylacetylene backbone units, each attached to a polar triethyleneglycol monomethyl ether side chain (Figure 100). Six metal-coordinating cyano groups are located on every other aromatic ring, between the acetylenic linkages. In the helical conformation, this sequence places the six cyano groups into the interior of the tubular cavity creating two approximately trigonal planar coordination sites. Molecular models revealed that each nitrogen atom lies about 2.1 Å from the helical axis, a distance consistent with that needed for metal–nitrile ligation (Figure 100). Both UV–vis and ^1H NMR measurements showed that a helical conformation could be produced by the use of solvophobic interactions alone, indicating that the cyano groups on the interior of the helical cavity did not inhibit the formation of helical structures. All metal-binding experiments were performed in tetrahydrofuran since this solvent does not solvophobically induce helical conformations. Silver triflate (AgO_3SCF_3) was used as the metal source, since it favors a trigonal planar coordination environment. By using a combination of UV–Vis, ^1H NMR, electrospray MS, and isothermal titrational microcalorimetry, it was determined that dodecamer **54** cooperatively bound two moles of AgO_3SCF_3 resulting in a stable, folded conformation. Control experiments on oligomers that did not contain cyano groups (oligomer series **23**) clearly indicated that the

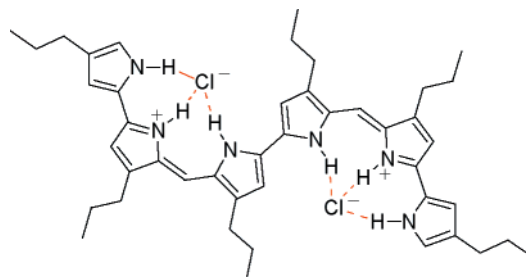


Figure 101. Structure of a hexapyrrin bound to two chloride anions.

conformational changes were a direct result of the interactions between the silver ions and the cyano groups. By performing experiments on a modified oligomer (**55**), it was also possible to determine that solvophobic interactions were playing an important role in the formation and stability of the metal-induced helical formation. The studies showed that oligomer series **22** could be modified to tightly and selectively bind metal ions within the internal cavity of a helical structure. Furthermore, the strength of metal ion binding appeared to be derived from a combination of solvophobic interactions that favored the helical structure along with the more usual metal–ligand interactions.

3. Anionic-Binding Backbones—Hexapyrrins

Compared to their cation-binding analogues, anion-binding foldamers are far less common, purportedly due to the lack of discrete denticity in anion coordination chemistry. However, 5,15,25-tris-nor-hexapyrrins, similar in structure to the bilinones, display a discrete “S”-shaped conformation in solution and in the solid state (Figure 101).⁴⁷⁷ Bilin-derived and respective linear tetrapyrrolic analogues have long been studied as supramolecular building blocks due

to their role as precursors in the generation of natural products such as macrocyclic porphyrins. Sessler and co-workers synthesized fully conjugated hexapyrrin with four *n*-propyl side chains. Crystallization of the dihydrochloric acid salt of this foldamer showed the chain to lie in a completely planar conformation, where one chloride ion rests in each of the two clefts generated in the “S” shape. This configuration allows each of the anions to engage in three hydrogen bonds, where one is ionic in character. The dihydrochloric acid salt was the only analogue generated that packed in this way. Data gained from NOE spectroscopy confirmed that the prevalent solution-phase conformation was also planar. Yet, the presence of an overlapped helix could not be ruled out given that no new cross-peaks could be observed by this method for such a conformation.

VI. Nucleotidomimetic Foldamers

A. Overview

Although the oligomer systems described thus far have involved only single chain folding reactions, the field of foldamers is not limited to this definition. In fact, the scope of foldamers extends to multistrand assemblies where oligomer chains associate and fold through noncovalent *intermolecular interactions between strands*. Within this field, nucleotidomimetics aim at improving the understanding of natural oligonucleotides,⁴⁷⁸ seeking insight on the origins of life,^{479–481} and on the development of antisense (targeting mRNA) and antigene (targeting the major groove of double-stranded DNA) agents.^{482–486} These approaches involve correlating structural modification of the backbone and the nucleobases with conformational changes in the chain and the stability of the generated duplexes. Conformational changes are measured directly by NMR and other structurally determinant techniques or indirectly by thermal denaturation using classic UV melting curves.

To our knowledge, the literature has not completely connected these structures with foldamers since the motivation for research in this area derives primarily from generating stable supramolecular complexes. Because of this, studies of nucleotidomimetic foldamers can best be summarized as “research on foldamers” where the folding reaction is implied but not the central focus as it has been with peptidomimetic and single-stranded abiotic foldamers. From the perspective of the foldamer field, nucleotidomimetics aim to ascertain the interdependence between sugar–backbone conformations and the *strength* of interstrand interactions. That is, given the variety of sequence-dependent pairing motifs and complex-induced conformations possible in natural oligonucleotides, it is of interest to determine how variation of the backbone affects the mode and selectivity of strand association. Examples described herein can afford an expanded conceptualization for the construction of novel foldamer complexes while at the same time approach the field from the point of view of chain folding *and* association. Just as with peptidomimetic foldamers, nucleotidomimetics are approached through a top-down design, and therefore, the success of structural modification is often ascertained by direct comparison to their biological counterparts.

In general, DNA strands adopt unique conformations upon association through interstrand contacts. On the other hand, not only does RNA form duplex structures, but also single chains also commonly fold through intrastrand interactions into complex secondary structures such as hairpins and loops.⁴⁸⁷ Prior to duplex formation, single-stranded oligonucleotides show significant conformational preorganization. This preorganization is a result of phosphates in the backbone linearly extending the oligonucleotide chain through electrostatic repulsion (similar to polyanionic polymer backbones³¹) and base-stacking interactions that align the backbone into an expanded state.⁴⁸⁸ Upon duplex formation, realignment of the oligonucleotide backbone proceeds at an entropic cost in order to maximize the enthalpic gain from intra- and interstrand base interactions within the double helix, thus refining the overall conformation through base pairing. The recognition selectivity is primarily a function of the interstrand base-pairing interactions shown in Figure 102. Exhaustive conformational analysis of the furanose ring in oligonucleotide backbones has revealed several preferred puckered states due to the flexibility of the five-membered ring; these ring conformations are seen in DNA and RNA sequences (Figure 103).^{487,489} In double-stranded (ds) complexes, RNA backbones primarily adopt the 3'-*endo* A-type conformation whereas DNA (d) backbones adopt both the A- and 2'-*endo* B-type conformations (Figure 104). These conformations influence the tilting of the nucleobases; the B-type conformation orients the bases perpendicular to the helical axis, while the bases of the A-type conformation are inclined ca. 14–20° to the axis.⁴⁹⁰ The resulting duplex architectures are stabilized through Watson–Crick (*WC*) base-pairing and have information-rich surfaces both in the major groove, where oligonucleotides can bind through Hoogsteen (*H*) pairing to form triple-helical assemblies, and the minor groove, which contains sites for small molecule interactions.⁴⁸⁷

The successful design of an *oligonucleotide foldamer* will be evaluated in two ways: first, the ability of the foldamer to adopt backbone conformations that promote base interactions, both pairing and stacking, by their intra- or intermolecular stability and, second, the demonstration of attributes such as cooperativity and base selectivity that provide insight into the folding reaction. This survey will primarily focus on backbone modifications of the carbohydrate, linkage, and nucleobases (for reviews, see refs 486 and 491), and to a lesser extent foldamers that bind in the minor groove of oligonucleotide duplexes. On the whole, nucleotidomimetic foldamers are robust. This behavior is perhaps a fundamental property of repeating, polyelectrolyte chain molecules. They can tolerate a variety of modifications within the backbone while retaining their duplex stability primarily due to a well balanced set of supramolecular interactions that, most importantly, includes electrostatic repulsion. It is worth mentioning that thermal denaturation data provided in this discussion is system specific, and therefore, comparisons can only be made to isostructural systems studied under identical conditions.

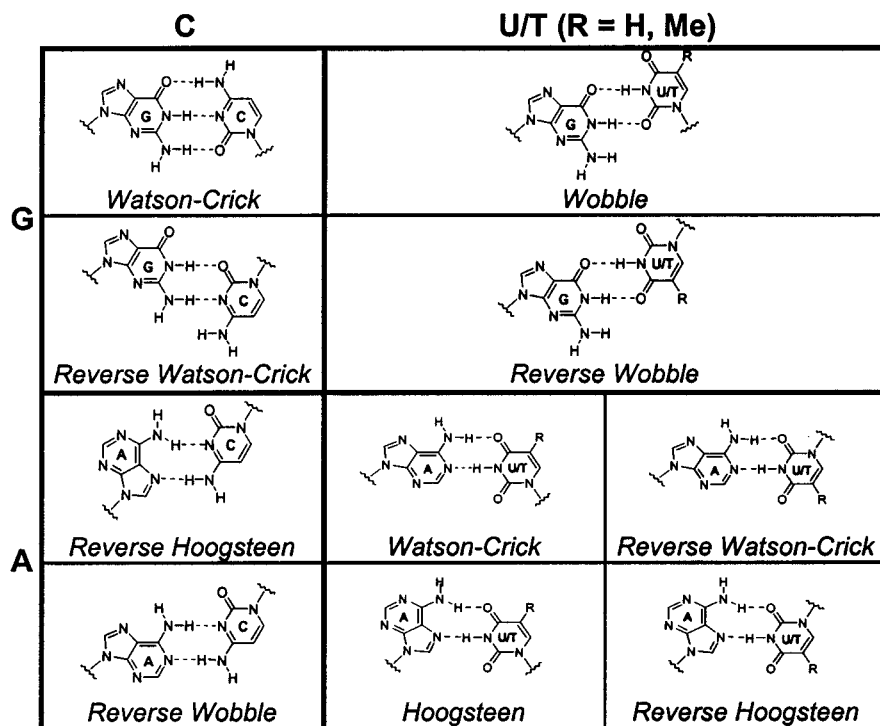


Figure 102. Common nucleotide base-pairing motifs and acronyms used throughout this section.

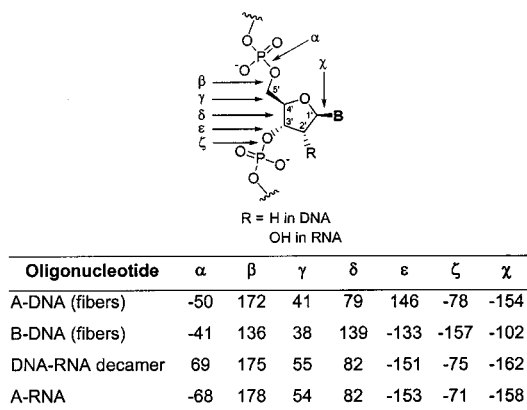


Figure 103. Average torsional angles (in degrees) for the furanose ring in several oligonucleotides from crystal structures.⁴⁸⁹

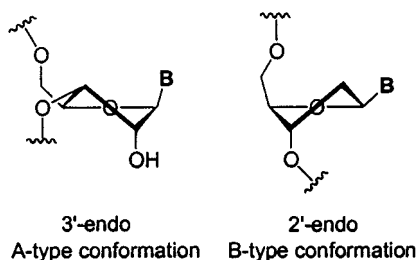


Figure 104. Puckered ring conformations found in the backbones of RNA (A only) and DNA (A and B) duplexes.

B. Isomeric Oligonucleotides

1. Iso-RNA and Iso-DNA

The most straightforward modifications of natural oligonucleotide backbones are constitutional changes involving the 5'→3' phosphodiester linkage. Since 5'→2' oligonucleotides are biologically known but not

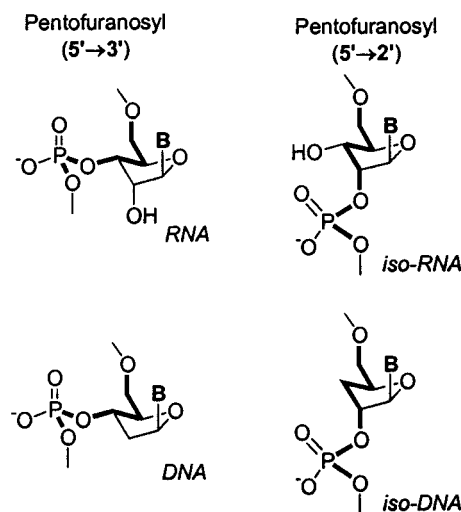


Figure 105. Natural and isomeric furanosyl backbones. **Bold** indicates backbone bonds.

demonstrated to be involved in information transfer,⁴⁹² these isomeric forms of natural RNA and DNA were clear starting points for investigations into alternative backbones (Figure 105). Detailed research on 5'→2' isomeric RNA and DNA (iso-RNA and iso-DNA) duplex formation was reported in three papers in 1992.⁴⁹³⁻⁴⁹⁵ NMR studies on self-complementary iso-RNA⁴⁹⁵ and iso-DNA-CGGCGCCG⁴⁹⁶ indicated antiparallel strand orientation within the *WC* right-handed duplex analogous to the natural duplexes. UV melting studies were conducted on these duplexes where T_m values indicate the temperature at 50% duplex dissociation. The complementary duplex iso-DNA-A₁₂/iso-DNA-U₁₂ was shown to be less stable ($\Delta T_m = 18^\circ\text{C}$) than the corresponding natural DNA duplex, while the self-complementary iso-DNA-(AU)₆ had a higher denaturation temperature ($\Delta T_m = 9.4$

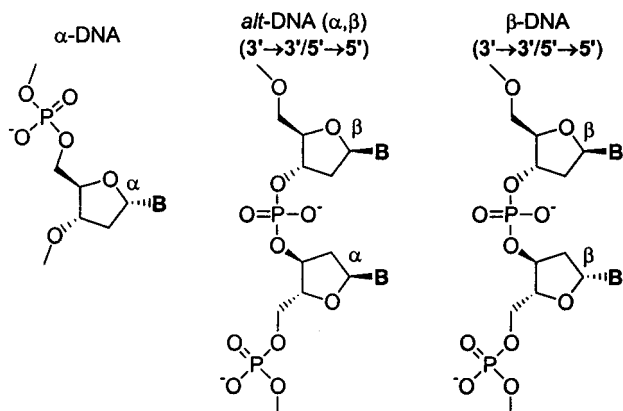


Figure 106. α -, *alt*-, and β -DNA backbones.

$^{\circ}\text{C}$) but was less cooperative than $\text{d}(\text{AT})_6$.⁴⁹⁴ Iso-DNA-G/C duplexes have one-half the thermodynamic stability as DNA⁴⁹⁷ and have been characterized by ESI-MS.⁴⁹⁸ With heteromeric 16-mers (containing one or two 5'→2' iso-DNA A/T monomers within the 5'→3' backbone), self-complementary strands associate with significantly lower stability than their DNA counterparts.⁴⁹³ Furthermore, iso-RNA-C/U oligomers formed a duplex with its RNA G/A complement but not with DNA⁴⁹⁹ as was found for iso-DNA/RNA duplexes.^{500,501} The order of thermal stability of homo- and heterostranded duplexes for iso-RNA was determined to be as follows: RNA:RNA > DNA:DNA ~ RNA:DNA > RNA:iso-RNA > iso-RNA:iso-RNA ≫ DNA:iso-RNA indicating lower association efficiency for isomeric oligonucleotides.^{502,503} A mixture of iso-DNA-A₁₆ and iso-DNA-T₁₆, which was not able to form complementary duplexes,⁴⁹³ associated into triplexes with reduced thermodynamic stability versus 5'→3' triplex structures,⁵⁰⁴ while iso-RNA-A₇/T₇ and -A₁₀/T₁₀ formed both duplexes and triplexes depending on the oligomer ratio and salt concentration.⁵⁰⁵ Iso-RNA segments linked to DNA hairpins are capable of templating the oligomerization of 2-Me-ImpG (a mononucleotide successfully coupled with DNA templates⁵⁰⁶) although with lower activity than RNA segments.⁵⁰⁷ The research on iso-oligonucleotides highlights the important principle in this field that even subtle backbone modifications can have pronounced effects on interstrand association, reflecting the subtle balance of noncovalent forces at play in oligonucleotide complexes.

2. α -DNA, *alt*-DNA, and L-DNA

Another isomeric modification of deoxyribonucleotides involved the change in the anomeric configuration from the natural β -position to an α -linkage (α -DNA) (Figure 106). NMR studies of α -hexamers duplexed with the natural β -DNA complements established C3'-*endo* and C2'-*endo* furanose conformations for α -T and α -C nucleotides, respectively.⁵⁰⁸ Additionally, α -DNA strands showed enhanced base stacking,⁵⁰⁹ WC antiparallel orientations in ds- α -DNA,⁵⁰⁹ and parallel orientations in α, β -DNA hybrid duplexes in B-type conformations⁵¹⁰ with higher binding to RNA than DNA.⁵¹¹ Initial studies on α, β -T₂₈, a heteromeric sequence of alternating α - and β -deoxynucleotides connected through 3'→3' and

5'→5' linkages (*alt*-DNA), induced less stable hybrid duplexes with both β -d-A₂₈ and poly r-A than either homomeric α - or β -T₂₈ strands.⁵¹² Through the alternating connectivities in α, β -strands, bases are equidistantly aligned since the "flipping" of the nucleotide by the alternating linkages is corrected by the configuration at the base-sugar position. Alternating 3'→3'/5'→5' linkages in β -T₂₈ produced a more significant degree of destabilization than α, β -T₂₈ due to the nonequidistant base arrangement. α, β -DNAs incorporating canonical bases (A, T, C, and G) showed backbone-dependent duplex stabilities and mismatch discrimination with natural DNA and RNA strands.^{513,514} In general, *alt*-DNA has a higher affinity for DNA strands than RNA, adopting B- and A-type conformations, respectively. Although these results are promising for α -DNA as a nucleotidomimetic, some inconsistencies in thermal transitions do exist in that both increased⁵¹⁵ and decreased⁵¹⁶ stabilities are observed, suggesting that certain sequences can lead to conflicting theories about the overall stability induction of the α -backbone. These irregularities in stability trends were also observed in L-DNA A-strands, the enantiomeric form of the natural DNA, where triplexes with poly(U) were stable⁵¹⁷ while L-DNAs with mixed bases did not bind to either RNA or DNA.⁵¹⁸ Other isomeric forms of DNA that have been studied include xylose-DNA,⁵¹⁹ where homostranded duplexes show higher thermal stabilities through multistate transitions, and arabinose-DNA,⁵²⁰ forming stable duplexes with arabinose-A oligomers and poly-U and -T.

C. Carbohydrate Modifications

Modifications of the sugar backbone primarily aim at answering a specific question: why nature chose ribofuranosyl nucleotides rather than some other backbone as the molecular basis for the genetic system of life?^{71,479–481,521,522} The work of Eschenmoser in this area has focused on the search for a chemical etiology of oligonucleotides, approached in a similar vein as peptidomimetic foldamer research, that is, the systematic modification of the backbone to determine relationships between structure and stability. Structural modifications that explore various (CH₂O)_{*n*} aldose-based (*n* = 4, 5, or 6) backbones are depicted in Figure 107.⁵²² Although strides to investigate the constitutional isomers of the furanose nucleotides have been made, the question of how this sugar arose as the "backbone of life" remains a mystery. Due to the extensive work conducted on pyranosyl-RNAs (p-RNAs), they will be explored here in detail as the closest examples to date of foldamer research on nucleotidomimetics.

1. Backbones with C1'-Base Connectivities

a. The Tetrofuranosyl Family. Through the removal of the C5 in the ribopentanosyl backbone, (3'→2')- α -threofuranosyl oligonucleotides (TNA) (Figure 107) were investigated to determine if furanosyl backbones with a "five-bonds-per-backbone" motif (as opposed to six in natural systems) could participate in self- and cross-duplexing with RNA and DNA.⁵²³ In TNAs, WC base-pairing between antiparallel

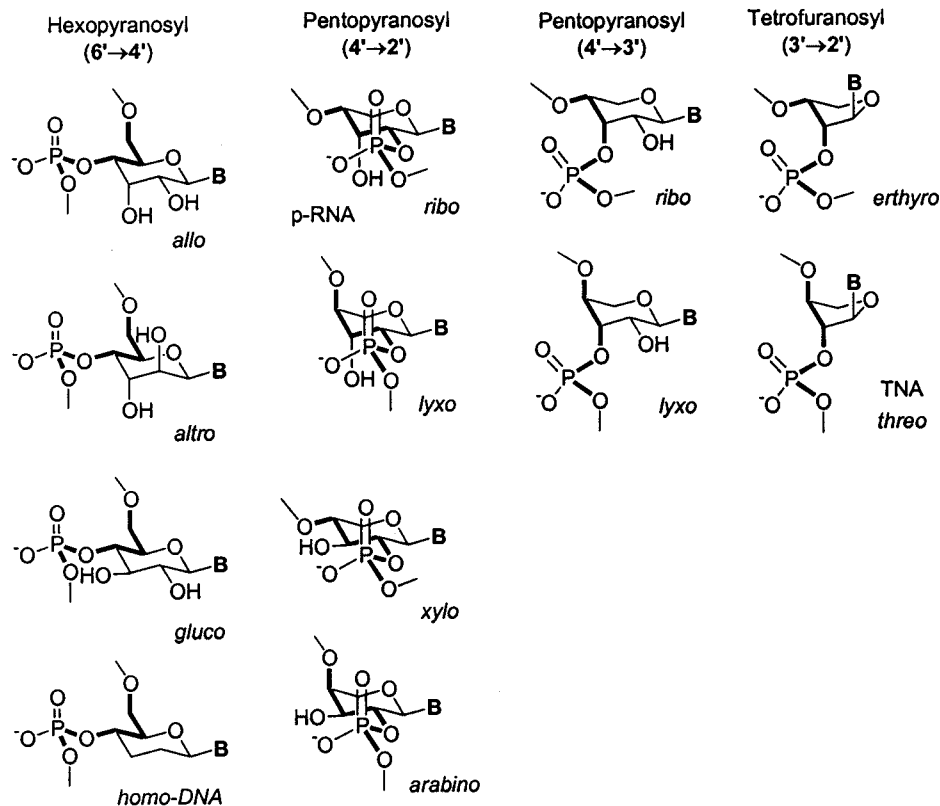


Figure 107. Alternative oligonucleotide backbones investigated with aldohexoses (CH_2O)_n ($n = 4, 5, \text{ or } 6$). **Bold** indicates backbone bonds.

strands is the preferred interaction within the duplex. TNA duplexes show stabilities that are comparable to RNA and DNA duplexes (of the same sequence), are capable of forming hairpins, and form stable cross-paired systems with complementary natural backbones. In particular, much more stable hexadecamer duplexes are formed when the natural backbone is an all-pyrimidine (T) sequence and the TNA is an all-purine (A) sequence, with a T_m decrease of 48 °C for RNA and 32 °C for DNA observed when the base complementarity is switched. By comparing these constitutional analogues to natural oligonucleotides, promising backbones such as TNAs have provided chemical clues about the fitness of DNA and RNA for information storage and transfer.⁵²⁴

b. The Pentopyranosyl Family. *i. p-RNAs.* One of the most thoroughly investigated alternative nucleotide backbones is the 4'→2' *ribopyranosyl* isomer of RNA (p-RNA) with the phosphodiester linkage extending from the C4' to the C2' positions of the hexose (Figure 107). The idealized oligomer conformation reveals an overall linear extension of the chain such that stabilization of the ladder-like duplex formation should occur by *WC* pairing between antiparallel strands with further stabilization provided by *interstrand* base stacking (as opposed to the *intrastrand* stacking known in natural backbones).

Through a variety of 1D- and 2D-NMR methods in D_2O , a self-pairing p-CGAATTCG duplex was determined to exist as a *quasi*-linear conformation with a weak left-handed helical twist in solution,⁵²⁵ which was not predicted from initial modeling (Figure 108). Specifically, two dihedral angles of the ribopyranosyl

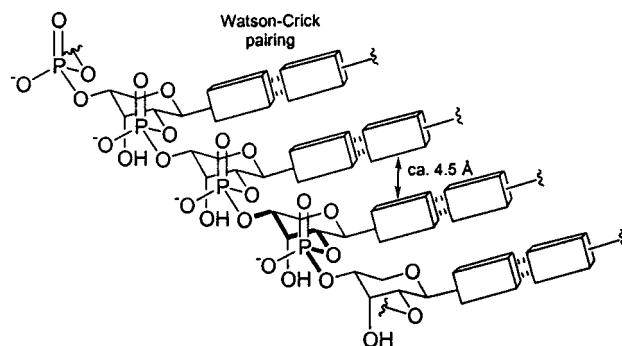
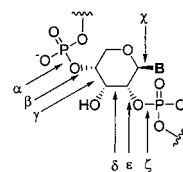


Figure 108. Idealized conformation of a p-RNA duplex (second strand backbone omitted for clarity).



p-RNA	α	β	γ	δ	ϵ	ζ
Idealized	60	180	180	180	-60	180
p-CGAATTCG	70	145	-180	-180	-85	-170

Figure 109. Six dihedral angles of the p-RNA backbone predicted for a linear conformation (actual values determined by NMR and molecular dynamics techniques for the left-handed helix).

backbone were resolved to $\beta = +145 \pm 6^\circ$ and $\epsilon = -85 \pm 5^\circ$, deviating significantly from the idealized angles of $\beta = 180^\circ$ and $\epsilon = -60^\circ$ (Figure 109). The dihedrals γ and δ were estimated to be close to the predicted value of 180° , resulting in an adjustment (calculated from simulations) of α from 60° to ca. 70°

and ζ from 180° to -170° to preserve the proper chair conformation of the ring for pairing interactions (confirmed from UV melting curves of duplexes). This is believed to be a result of minimized steric interactions between the phosphate linkage, the equatorial hydrogens on ribopyranose (distances increase about 1 Å), and increased interstrand stacking through decreased base distances (from over 4 to ca. 3.5 Å). These results suggest that the backbone realignment is a consequence of the intermolecular association. Observed χ values ranged from -120° to -135° within the sequence, while the terminal G residue had a much lower χ value indicating higher conformational lability at this position. Proton exchange experiments and molecular-dynamics simulations supported *WC* pairing throughout the duplex and a rapid opening and closing of the terminal base pairs. Interstrand NOEs confirmed an antiparallel orientation resulting in the inclination of the base pair from the backbone by an angle of 35° and 45° , suggesting that interstrand base interactions should be favorable for purine–purine and purine–pyrimidine stacking but not between two pyrimidines. In addition, an inter-pyranose distance between 3.6 and 4.0 Å was calculated, producing a translational step of 6.5–6.9 Å along the backbone and a pitch of ca. 110 Å, incorporating 18–19 monomers per turn.

Through oligomerization of β -D-ribose phosphoramidite derivatives^{526,527} by automated synthesis and purification by HPLC, adenine (A) and uracil (U) containing p-RNA octamers were initially synthesized and characterized to ascertain the stability of the duplexes formed.⁵²⁸ Although self-pairing A₈ duplexes have formed in other alternative oligonucleotides,⁵²⁹ p-A₈ remains as a single strand under these conditions, indicating that alternative pairing interactions are disfavored due to the topological backbone constraints in this pairing mode, thus enhancing the oligomer's pairing selectivity. The *WC* paired duplex formed from a 1:1 mixture of p-A₈ and p-U₈ revealed concentration-dependent and reversible UV melting curves, temperature-dependent CD spectra, and composition-dependent UV absorptions with a minimum at a 1:1 stoichiometry. The self-complementary octamers, p-A₄U₄, p-U₄A₄, p-(AU)₄, and p-(UA)₄, show duplex formation by self-pairing in an antiparallel orientation.⁵³⁰ Additionally, the higher melting temperature of the p-A₄U₄ duplex in comparison to the natural RNA oligomer indicates an increased stability through stronger base-pairing interactions. This is attributed to the smaller entropic cost of organization necessary to form the p-RNA duplex since the *quasi*-linear rigid chain is preorganized for the proper *WC* pairing orientation. Other nucleobases incorporated into p-RNAs for duplex formation studies include guanine (G), cytosine (C), isoguanine (isoG), 2,6-diaminopurine (Dp), and thymine (T).⁵³¹ In a chain-length study, UV and CD spectra confirmed that p-G_{*n*} (*n* = 6, 8, and 10) exist as single strands at ambient temperature (as do the p-isoG₈ and p-Dp₈ strands). In equimolar mixtures of oligo-p-G_{*n*} and oligo-p-isoG_{*n*} (*n* = 6 and 8), duplex formation proceeds through purine–purine *WC* pairing showing higher thermal stability than DNA sequence analogues.

Duplexes of p-RNA having strands of opposite chirality form through alternative base-pairing modes such as reverse Watson–Crick (*RWC*) pairing.⁵³² The noncanonical bases, isoguanine (isoG) and 5-methylisocytosine (5-Me-isoC), that have the potential to participate in *RWC* pairing with homo-G and -C strands were incorporated into L- and D-p-RNA strands. Both homochiral (D/D) and heterochiral (L/D) duplexes of homomeric strands were compared, in terms of melting curves, to determine the degree of specificity dictated by the backbone stereochemistry. Strands of D-p-isoG_{*n*} and D-p-C_{*n*} (*n* = 6 and 8) did not show any self-pairing or duplex formation under the given conditions, while duplex formation was accomplished using the L-p-isoG_{*n*} with D-p-C_{*n*} (*n* = 6 and 8). The isoG bases promote *RWC* pairing with C in this duplex, allowing for proper co-linear orientation of the strands. Other p-RNA mixtures were shown to form L/D but not D/D duplexes most likely through the *RWC* pairing mode, though pairing assignments in the case of D- and L-p-isoG_{*n*} remain uncertain since mixing curves showed aggregate formation. The p-RNA chains of opposite chirality pair inefficiently as evidenced by the lower melting temperatures of duplexes formed from mixing homochiral D-p-RNAs with complementary L-p-RNAs. This enantioselectivity, as well as the observed pairing selectivity (*WC* only), is believed to be due to the more conformationally restrained p-RNA backbone. It has only four flexible bonds (as opposed to six in DNA) due to the three large substituents occupying equatorial positions. Furthermore, the more constrained phosphodiester linkages connect to secondary carbons on the ring, whereas DNA linkages attach to a primary carbon (5') allowing for greater flexibility. Finally, the alignment of the nucleobases as a consequence of the backbone conformation promotes antiparallel interstrand interactions through *WC* base-pairing only, since *H* and reverse-Hoogsteen (*RH*) pairing disfavor the preferred co-linear chain orientation. This study demonstrates the ability of p-RNAs to form duplexes with the same or opposite sense of chirality backbones, depending on the specific nucleobases used.

In order to mimic RNA architectures and their conformational diversity, a necessary secondary structure is the hairpin turn, a sequence-dependent structure promoted by intramolecular base pairing over interstrand interactions. Investigations of hairpin formation in a series of self-complementary p-RNA base sequences studied at low concentrations (3 μM) with a central p-T₂ segment resulted only in duplex formation while with three T bases competitive duplex formation was observed in melting curves at higher concentrations.⁵³³ Only at the critical length of four T bases did the oligonucleotide show a similar *T_m* at both concentrations, indicating a stabilized hairpin. Furthermore, hairpin p-RNAs synthesized with a noncomplementary base (A or C) at either the 2'- or 4'-end supported the expectation, from modeling of p-RNA duplexes,⁵²⁵ that a dangling base at the 2'-end would stabilize the structure through interstrand stacking of the two terminal bases with purine–purine contacts leading to greater stability than

Table 7. UV Melting Curves for Four Pyranosyl Oligonucleotides

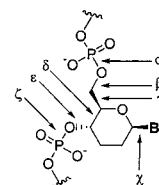
sequence (4'→2')	T_m [°C] ^a					ΔG°_{298} (kcal·mol ⁻¹)				
	pr	pl	px	pa	RNA	pr	pl	px	pa	RNA
A ₈ + T ₈	40.0	47.0	35.4	71.1	16.3 ^b	10.5	-12.3	-8.2	-15.7	-7.3
A ₁₂ + T ₁₂ ^c	60.8	68.0	63.0	95.0	34.9 ^b	-15.4	-19.8	-17.0		-66.3
A ₄ T ₄	27.0	38.2	16.3	61.2	11 ^b	-7.3	-9.4	-6.1	-13.5	-5.6
T ₄ A ₄	40.0	47.0	40.3	69.4	10.8 ^b	-9.8	-11.4	-8.7	-14.5	-5.2
(AT) ₄	38.0	38.3	28.6	60.0		-9.2	-9.5	-6.2		
(TA) ₄	40.0	37.9	33.8	60.8		-9.3	-9.4	-7.6		

^a 0.15 M NaCl. ^b 1.0 M NaCl. ^c Data from ref 535.

pyrimidine–purine stacking. Only dangling bases at the 2'-end led to an increased stability of the p-RNA pairing complex.

ii. α -Lyxo, β -Xylo, and α -Arabinopyranosyls. From the findings on p-RNAs, the question arises, can the properties of p-RNAs be extended to the constitutional isomers of (4'→2') ribopyranosyl: α -lyxo, β -xylo, and α -arabino? A recent study investigated the duplex stability of foldamers with these alternative backbones for comparison to the D- β -ribopyranosyl oligonucleotides.⁵³⁴ Table 7 shows T_m and ΔG values for the complementary and self-complementary AT sequences. Although the β -xylo duplexes are somewhat weaker than D- β -ribo complex, the D- α -arabinopyranosyl duplex has a much higher stability than RNAs or p-RNAs. The stability of the arabinopyranosyls is a consequence of the increased steric constraint induced by the equatorial 3'-hydroxyl in concurrence with the highly constrained pyranose chair from the 4'-axial phosphodiester linkage. Though these backbones show higher stabilities due to stronger base pairing, the tolerance for mismatches is evident from self-pairing of the A₈ and T₈ single strands of the α -lyxo (A and T) and the α -arabino-T₈ backbones. Furthermore, by mixing complementary strands of the four different pyranosyl backbones, duplexes formed with comparable stabilities to homobackbone duplexes, indicating the ability of all four members to adopt similar *WC quasi-linear* conformations as seen in p-RNAs.⁵³⁵ A thorough chain-length and sequence investigation on the (4'→2')- α -L-lyxopyranosyl backbone has recently been reported exploring the self-pairing, complementary pairing, and hairpin formation in this system.⁵³⁶ These results show that with the natural RNA backbone, maximization of base-pairing strength is not realized. In addition, the ability of the pyranosyl family to form stronger duplexes through enhanced base pairing comes at the cost of lower base-matching fidelity.

Extension of the studies on the pyranosyl family involved modification of the phosphodiester linkage from (4'→2') to (4'→3') in the α -ribo and α -lyxo backbones leading to a shortened backbone involving only five instead of the usual six torsions.⁵³⁷ Although the (4'→3') α -ribopyranosyl backbones showed no duplex formation with self-complementary strands, the corresponding α -lyxopyranosyl duplexes showed slightly weaker stabilities from their (4'→2') counterparts. Additionally, this system had the capacity to form intersystem duplexes and triplexes with a complementary strand of either RNA or DNA, believed to be due to the smaller backbone inclination



dd-A ₅ T ₅	α	β	γ	δ	ϵ	ζ	χ (A)	χ (T)
Idealized A	-60	180	60	60	180	-60	-120	-120
Idealized B	180	180	180	60	180	-60	-120	-120
Model A	-56	155	64	49	-137	-68	-75	-101
	to	to	to	to	to	to	to	to
	-72	172	86	67	-178	-80	-91	-139
Model B	165	173	160	50	-154	-59	-108	-78
	to	to	to	to	to	to	to	to
	-167	-136	-174	61	-180	-105	-119	-113

Figure 110. Six hexose dihedral angles of the homo-DNA backbone and the base–hexose torsion as predicted for a linear conformation (actual values determined by NMR and molecular dynamics techniques). For models A and B, values indicate the lower and upper limits of the dihedral angles observed.

and the diaxial phosphodiester orientation of the backbone. These results, as well as the observations with TNAs, suggested that six torsions per repeat unit are not necessary to form stable complexes with natural complements, further revealing the tolerance for structural variation in these polyelectrolyte backbones.

c. The Hexopyranosyl Family. *i. Homo-DNAs.* Further studies aimed at exploring alternative backbones focused on the introduction of a methylene unit between the C1'- and C2'-positions of furanosyl units of oligonucleotides to generate hexopyranosyl backbones (homo-DNA). Investigations include comparative conformational analysis between natural oligonucleotides and homo-DNA (dd),^{538,539} synthesis and characterization of these oligonucleotides,⁵²⁶ the conformational characterization of a homo-DNA duplex in solution,⁵⁴⁰ and the self-pairing and complementary pairing in the duplex formation.^{529,530,541} Homo-DNA maintains the six-bonds-per-repeat-unit motif of natural systems, having the same configurational orientation of the phosphodiester linkage as in DNA. Idealized models predicted similar conformations to those seen in p-RNAs, where a linear extension of the chain would result in *WC* pairing of bases in an antiparallel fashion with bases adopting anti conformations.⁵³⁸ Dihedral angles for homo-DNA were determined through 1D- and 2D-NMR techniques and molecular dynamics simulations to ascertain the solution structure of a self-complementary dd-A₅T₅ duplex (Figure 110).⁵⁴⁰ The two *quasi-linear* backbone conformations, A and B, are in dynamic equilibrium related by two 120° rotations with all three constitu-

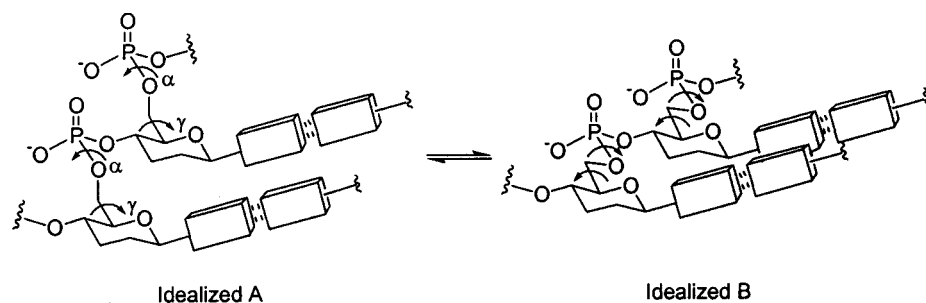


Figure 111. Two idealized conformations of the homo-DNA backbone. Conversion from A to B occurs through a 120° rotation about α and γ of the phosphodiester linkage.

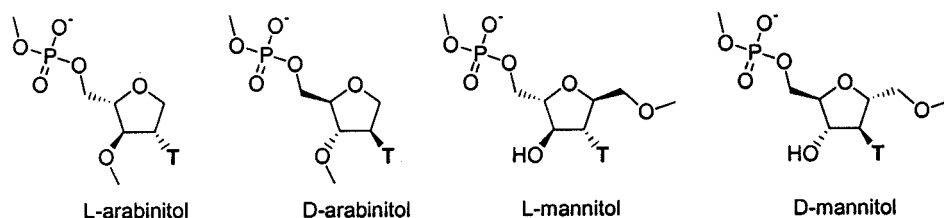


Figure 112. Structures of isonucleosides.

ents of the hexose chair conformation in equatorial positions (Figure 111). A much looser orientation of base pairs was observed through a range of adopted χ torsions in addition to extensive fluctuations in base-pair distances, deviation from coplanarity, and a base-stacking distance of ca. 4.5 Å.

In general, homo-DNA duplexes demonstrate a pairing priority of G–C > A–A ~ G–G > A–T where G–C and A–T pair through the *WC* motif while *RH* pairing occurs in A–A and G–G dd-sequences.⁵²⁹ Through a chain-length study on dd- A_n ($n = 3–6$), self-paired duplexes showed increasing UV melting temperatures with increasing chain length (for $n = 3$, no T_m ; $n = 4$, $T_m < 12$ °C; $n = 5$, $T_m = 32$ °C; $n = 6$, $T_m = 43$ °C) and increasing concentrations (from 4.9 to 92 μ M, $\Delta T_m = 15$ °C), sigmoidal hypochromicity curves (dependent on [NaCl]; where [NaCl] = 15 mM to 1.5 M, $\Delta T_m = 9$ °C), and temperature-dependent CD spectra. Self-complementary dd-(AT) $_n$ ($n = 3–6$) duplexes showed high stability with melting curves ca. 30–40 °C higher than in the corresponding DNA duplexes. Though the self-paired duplex (dd- A_6) $_2$ persisted when mixed with the complementary dd- T_6 , the self-pairing dd- G_6 could be disrupted with dd- C_6 to form the heterostranded complex. Further investigations into the pairing properties of dd-purine sequences revealed *WC* pairing between dd-(G) $_n$ /dd-(isoG) $_n$ and dd-(Dp) $_n$ /dd-(xanthines) $_n$ (X) while dd-(isoG) $_n$ and dd-(Dp) $_n$ oligomers self-pair through *RH* motifs.⁵⁴¹ Overall, sequence discrimination is lower in homo-DNA than DNA due to the linear orientation of the strands, inefficient base-stacking, and the conformational rigidity of the hexose ring which leads to a preorganization of the single strand and decreases the conformational entropic cost of duplex formation.

ii. Other Hexoses. In homo-DNA as in DNA, hydroxyl groups are not present as they are in RNA and the pyranosyl backbones described thus far. Further investigations into hexopyranosyl (6'→4') backbones incorporated 2'- and 3'-hydroxyl groups in β -allo (2'-eq, 3'-ax), β -altro (2'-ax, 3'-ax), and β -gluco

(2'-eq, 3'-eq) (Figure 107).⁵²¹ The presence of these hydroxyls causes intrastrand steric repulsion in the duplex conformation that disrupts *WC* base pairing, encourages purine–purine *RH* self-pairing in allo and altro backbones, and leads to sequence-dependent and lower T_m values than for RNA. For the self-complementary sequence CGCGAARRCGCG (R = U in allo and altro backbones, T in DNA and homo-DNA), no duplex formation was observed for allo and altro backbones at room temperature (though T_m values increased at lower pH) in great contrast to both DNA and homo-DNA. The inclusion of hydroxyls in the hexopyranosyl backbones must induce the backbone to adopt conformations that disfavor the folded state necessary for ideal base pairing in the duplex.

Other variants of hexoses include 2,4- and 3,4-dideoxyhexopyranosyl backbones^{542,543} and have similar connectivities to iso-DNAs but incorporate methylene groups into the ring between the C1–C2 and C2–C3 connections. With one to four multiple-T substitutions of either modified monomer into DNA 13-mers, the 3,4-backbone destabilized the duplex with complementary d- A_{13} to a higher extent than the 2,4-modification, although these heteromeric duplexes retain cooperative transitions. The effect on the duplex with the 3,4-connectivity is similar to the results obtained with homo-DNA. Homomeric 2,4- T_{13} oligomers were unable to form duplexes with the complementary DNA.

2. Backbones with C2'-Base Connectivities

a. Isonucleosides. Another modification of deoxynucleotides involved the repositioning of the base-sugar connection from the C1- to the C2-position to afford 1,4-anhydro-2-deoxy-D- and -L-arabinitol,⁵⁴⁴ dubbed isonucleosides (Figure 112). In 14-mer strands with homo-T bases, D-arabinitol formed slightly less stable duplexes with d- A_{14} ($\Delta T_m = -5.9$ °C) than with d- T_{14} , while L-arabinitol was unable to complex with this complement.⁵⁴⁵ Addition of a methylhydroxyl moiety to the C1'-position of the D-arabinitol gener-

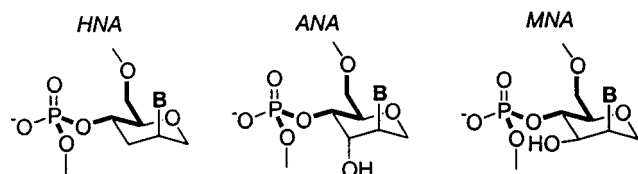


Figure 113. HNA, ANA, and MNA backbones.

ates the D-mannitol monomer, and 14-mers of both D-⁵⁴⁶ and L-mannitol⁵⁴⁵ complexed with d-A₁₄ showed that the methylhydroxyl promotes stability by $\Delta T_m = +1.2$ °C.

b. HNAs. Analogous to investigations into homo-DNA, synthetic insertion of an additional methylene group between the O4' and C1' positions of a furanose generates 1,5-anhydro-D-arabino-hexitol nucleic acids (HNAs),^{547,548} maintaining the natural conformations of the phosphodiester linkage, the axial orientation of C1'-base configuration for intramolecular base-stacking with natural systems, and promoting the 3'-endo, A-type sugar conformation (Figure 113). Initial studies on A and T HNA (h-) 13-mers showed aqueous solubility, self-pairing in the T strand,⁵⁴⁹ stronger WC-paired duplexes than the corresponding DNA duplex ($\Delta T_m = +42.3$ °C), and sequence-dependent stabilities in HNA:DNA duplexes (d-A₁₃:h-T₁₃ $\Delta T_m = +11.4$ °C and h-A₁₃:d-T₁₃ $\Delta T_m = -13.0$ °C).⁵⁴⁹⁻⁵⁵¹ Nucleobases successfully incorporated into HNAs include A, T, C, G, U, D, and Me-C, retaining WC pairing with corresponding complements.⁵⁵² Four different solutions of salts and buffers were explored in order to optimize duplexing and eliminate self-pairing (as indicated by a linear vs sigmoidal increase in absorption with increasing concentration). Furthermore, through a series of HNA mixed sequences complexed with RNA and DNA complements, the higher stability of HNA:RNA over HNA:DNA was demonstrated, as well as a mismatch discrimination in HNA:DNA dodecamer duplexes. ΔT_m changed from -9.0 to -20.3 °C for a single mismatch, indicating a strong sensitivity in base selectivity. CD studies revealed that the HNA:RNA and RNA:RNA duplex have very similar spectra, supporting A-type HNA conformations. Furthermore, NMR studies of an HNA:RNA duplex revealed the HNA strand to have similar conformations as RNA but with a more rigid backbone.⁵⁵³ HNAs containing pyrimidine bases form less stable duplexes than those with purines, and duplex stability in this system follows the stability order of HNA:RNA > RNA:RNA > DNA:RNA. Molecular dynamics simulations revealed that solvation of the minor groove is a critical factor to the higher stability of the HNA:RNA complex over HNA:DNA since the presence of the additional hydrophobic methylene is compensated for by the hydrophilic 2'-OH of RNA.^{554,555} An HNA-GCGCTTTTGCGC strand can form a self-complementary duplex where the T segments form T-T wobble (W) motifs through this pairing mismatch.⁵⁵⁶ Finally, gel electrophoresis studies showed that HNA strands are able to displace an RNA strand of similar length from its homostranded duplex. Overall, the HNA nucleotidomimetic demonstrates the ability of foldamers analogous to natural systems to mimic and even enhance their pairing and selectivity properties through subtle modifications,

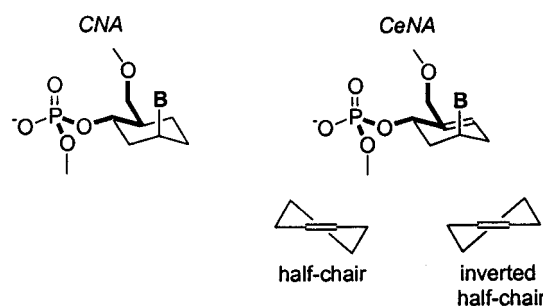


Figure 114. CNA and CeNA backbones with puckered states of CeNAs.

underlying the complexity of parameters responsible for the stability of nucleic acids structures.

c. ANAs. Following the successful design of HNAs, a structural analogue incorporating a C3'-(S)-hydroxyl was synthesized⁵⁵⁷ and has been called ANA (for 1,5-anhydro-D-altritol nucleic acids) (Figure 113). Similar to HNAs, ANAs form A-type WC duplexes stronger with RNA than DNA, but with higher thermal stabilities for homo- and heterostranded duplexes such that the hybrid stability order is ANA:RNA > HNA:RNA > ANA:DNA > HNA:DNA > DNA:RNA.⁵⁵⁸ ANA strands discriminate mismatches to the same degree as DNA and HNA, favoring antiparallel over parallel orientations. The ANA 3'-OH stabilizes hybrid complexes primarily through improved solvation by increasing the polarity of the solvent-accessible surface of the minor groove, as confirmed by molecular dynamics simulations.⁵⁵⁵

d. MNAs. Another member of this series involves inversion of the C3'-OH configuration from (S) in ANAs to (R) in 1,5-anhydro-D-mannitol nucleic acids (MNAs)⁵⁵⁹ (Figure 113). Although NMR studies showed that the MNA monomers preferred the axial base orientation, two AG mixed hexamers did not form duplexes with complementary RNA or DNA at low salt concentrations and formed weak duplexes with HNA. At 1 M NaCl, weak hybridization was observed with RNA. Melting curves of these complexes were very broad indicating multiple transitions over this temperature range. Molecular modeling revealed a more conformationally restrained backbone, through formation of an intramolecular hydrogen bond between the 3'-OH and the 6'-O of the phosphate linkage. This interaction thermodynamically disfavors complexation with RNA.⁵⁵⁵ Hence, even in cases of subtle structural modification, the oligonucleotide backbones can become "too preorganized", illustrating the critical balance between rigidity and flexibility in foldamers.

e. CNAs. With the successful design of HNAs, structural analogues were pursued to determine if hybridization was still operative if the conformationally determinant O of the hexose was replaced by a methylene, resulting in a more flexible carbocyclic ring (Figure 114). These carbohexanyl nucleic acids (CNAs) prefer equatorial base orientations as monomers and therefore were speculated to form quasi-linear chain conformations akin to homo-DNA.⁵⁶⁰ However, CNA oligomers of D-configuration form stable WC antiparallel complexes with both RNA and DNA, while corresponding L-CNA strands do not.⁵⁶¹

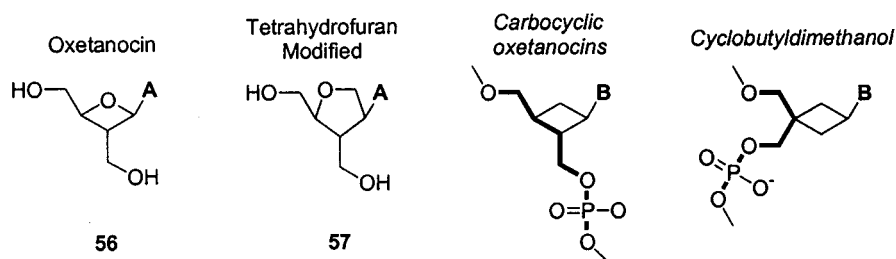


Figure 115. Representative examples of modifications to the sugar backbone.

It is believed that the CNA backbone undergoes a chair inversion to adopt axial base orientations within the duplex to promote base pairing. Homochiral CNA complexes (D/D or L/L) of A₁₃ or T₁₃ are more stable than ds-DNA but show multiple transitions in the melting curve, while heterochiral CNA duplexes (D/L) are much less stable with mixed AT sequences forming only as homochiral complexes. No self-pairing of CNA strands was observed. This study demonstrates that conformational intuition of monomer structures does not easily translate to backbone conformations that favor duplex formation. Thus, CNAs are examples of nucleotidomimetics where a unique backbone conformation is only adopted through the optimization of nonadjacent contacts.

f. CeNAs. The carbocyclic cyclohexene nucleotides (CeNAs) extend CNA research by introducing a 5'-6' alkene within the analogous ring, thereby increasing the flexibility of the backbone such that the energy difference between chair conformations is approximately 0.4 kcal·mol⁻¹ (Figure 114).⁵⁶² When one to three CeNA-A monomers were incorporated into either an RNA or DNA strand and complexed with complementary DNA or RNA, respectively, the thermal stability of the DNA:RNA hybrid was increased up to 5.2 °C with CeNA-DNA and decreased -1.5 °C with CeNA-RNA.⁵⁶³ NMR studies showed that the incorporated CeNAs had little effect on the global structure of the DNA backbone. Although CeNA-A₁₃ associate with complementary DNA and RNA oligomers with comparable and higher stabilities than DNA, triplex formation was also observed. On the basis of CD studies, CeNAs adopt the half-chair conformation in the A-type RNA and the inverted half-chair in the B-type DNA.⁵⁶⁴

g. Other Ring Systems. The discovery of the antibiotic oxetanocin A,⁵⁶⁵ an isomer of deoxyadenosine isolated from *Bacillus megaterium* and containing an oxetanose instead of a furanose ring, led to the incorporation of moiety **56** and a second isomer, involving a C2'-base connectivity **57**, into self-complementary DNA dodecamers. Resulting complexes showed slightly lower *T_m* values (Figure 115).⁵⁶⁶ Extension of this structure to carbocyclic oxetanocin strands led only to triplex formation with RNA hybridization that was stronger than DNA.^{567,568} Similarly, 3,3-bis(hydroxymethyl)cyclobutyl A and T oligomers generated homostranded complexes as well as heterostranded complexes with DNA.^{569,570} Although these nucleic acid variants have not been fully explored as oligomers (a large body of work exists on the properties of similar nucleosides^{571,572}), they demonstrate the tolerance of RNA/DNA pairing motifs toward a variety of structurally related backbones.

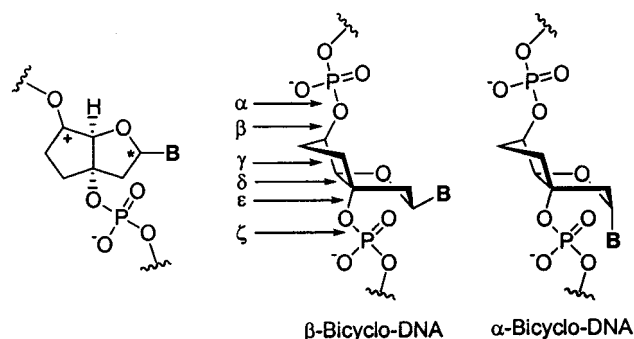


Figure 116. Representative structures of bicyclonucleotides.

3. Torsionally Restricted Oligonucleotides

The incorporation of hexoses into oligonucleotides led to, in certain cases, increased duplex stability through preorganization from the more conformationally restricted six-membered rings versus natural ribose backbones with flexible torsions. This approach has been taken a step further through the use of constrained backbones in which bridging linkages of fused-pyranosyl nucleotides limit the conformational flexibility of the ring.⁵⁷³ This preorganization of the strand then minimizes the entropic cost of organization in duplex formation, and the success of such an approach is often measured by melting temperatures of the heterostranded duplex incorporating the natural, complementary oligonucleotide. Although a variety of fused-oligonucleotides have been investigated, two backbones will be discussed here, dubbed *bicyclic-oligonucleotides* and *locked nucleic acids (LNAs)*, as representative examples of this class of modified ribopyranosyls.

a. Bicyclic-Oligonucleotides. Bicyclicodeoxynucleotides (bicyclo-DNA or bcd) involve an ethylene bridge between the C3' and C5' positions, which constrains the furanose ring into the C2'-endo conformation seen in B-type DNA duplexes through the rotational restriction of the γ and δ torsions (Figure 116).⁵⁷⁴ Adenine decamers of β -bicyclo-DNA form stronger duplexes with RNA and DNA, while bcd-T₁₀ pairs more weakly with comparable base-pairing selectivity, shows increased triplex stability (also demonstrated with bcd-G₆),⁵⁷⁵ and exhibits a higher sensitivity to salt concentration.^{576,577} Through sequential synthesis of various oligomers containing the canonical bases and by determining their pairing properties with complementary bcd, RNA and DNA strands, bicyclo-DNA pairs preferably form through *H* over *WC* motifs and, as a consequence, form parallel (*H* mode) and antiparallel (*RH* mode) orientations due to the torsion angle γ (set to +100°

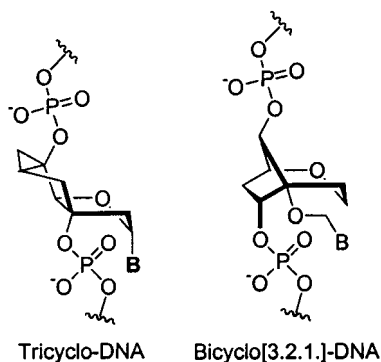


Figure 117. Structures of tricyclo- and bicyclo[3.2.1]-DNA.

relative to DNA).^{578,579} In the *WC* mode, bicyclo-DNA prefers antiparallel orientations as in DNA. The stability of bcd duplexes is dependent on the number of G–C pairs since A–T pairs appeared to be energetically impartial. Furthermore, the rigid bicyclic backbone decreases the entropic cost of intermolecular association while destabilizing the duplex by lowering the enthalpic contribution of complexation. Unexpectedly, hairpin structures were reported⁵⁷⁹ from bcd-CGCGAATTCGCG, a potentially self-complementary sequence. The -AATT- segment forms the hairpin turn, since the A–T pairing does not contribute enthalpically and duplex formation comes at an entropic cost. Overall, the bridging moiety in bicyclo-DNA imparts a number of organizational changes in complex formation, both inter- and intramolecularly, through constraints in the furanose ring that differ considerably from both homo-DNA and p-RNA backbones.

Extensions on the bicyclo-DNA theme have been pursued to explore how similar structural modifications with constrained-ribose backbones affect base-pairing modes and strand orientations. Switching of the base–furanose bond from the β - to the α -position (α -bicyclo-DNA) causes a rearrangement of the pairing properties relative to β -bicyclo-DNA such that parallel hybrid duplexes are favored in AT sequences with comparable stabilities to RNA and DNA.⁵⁷⁵ Reversal of the 5'-OH from (*R*) to (*S*), named 5'-epibicyclo-DNA,^{580,581} eliminates pairing altogether in a decamer T block with complementary RNA, DNA, or bicyclo-DNA. Tricyclo-DNAs extend these examples of covalently constrained rings by incorporating a cyclopropyl ring into the 5'/6'-positions of the carbocyclic ring in bicyclo-DNAs (Figure 117).^{582–584} In duplex studies with itself and DNA, tricyclo-DNA showed enhanced stabilities with the homostranded tricyclo-DNA duplexes having ΔT_m as high as 48 °C over the natural DNA duplex. Again, *H* and *RH* pairing are preferred as in bicyclo-DNA. They have also been shown to stabilize hairpin loops and form triplexes with DNA duplexes. Finally, moieties inducing torsional constraints far removed from the bases have been demonstrated with bicyclo[3.2.1]-DNA in which the base linkage is extended by an oxygen tether (Figure 117).^{585,586} Pyrimidine-based bicyclo[3.2.1]-DNAs are capable of forming *WC* antiparallel duplexes of A-type conformations with complementary DNA. They have slightly lower T_m values, indicating that increased degrees of freedom

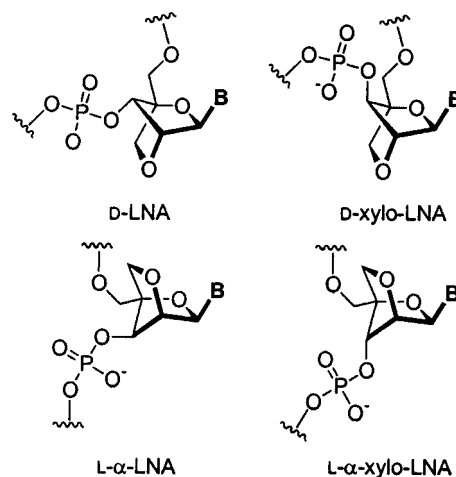


Figure 118. Four of the eight stereoisomers of locked nucleic acids (LNAs).

in the base–backbone linkage can be compensated by more rigid backbones, even modifications far removed than in ribose backbones.

b. LNAs. The pentofuranose backbone can also be restricted to the 3'-*endo* conformation by installing a 2'-*O*,4'-*C*-methylene bridge^{587,588} to generate a class of structures known as locked nucleic acids (LNAs) (Figure 118).^{573,589} When incorporating various nucleobases (A, C, G, T, 5-Me-C, and U) into oligonucleotides or as homooligomeric sequences, LNAs significantly increase T_m values of heterostranded duplexes with RNA (4–8 °C) and DNA (3–5 °C) complements^{588,590,591} without disrupting backbone conformations.⁵⁹² Improved sequence selectivity, aqueous solubility, formation of duplexes only (no triplexes), preorganization of neighboring natural nucleotides, and high binding affinities are traits demonstrated by this system. Stopped-flow kinetics of LNAs revealed that LNA–DNA duplex formation involves a rate-determining association with a subsequent rapid sealing step and that the higher duplex stability with LNAs results from a slower dissociation of the duplexes.⁵⁹³ From the LNA skeleton, eight stereoisomers incorporating T^{594–596} and A⁵⁹⁷ have been generated where β -D/L-ribo-, α -D/L-ribo-, and β -D/L-xylo-LNAs show increased duplex stability with RNA, while no association was observed for α -D/L-xylo-LNAs and RNA.^{594–597} Homooligomeric LNAs, through *WC* antiparallel duplexes with RNA and DNA, adopt the A-type furanose conformation and induce flanking of natural nucleotides into similar conformations, thereby arranging the strand for more efficient base interactions as evidenced by NMR^{598,599} (and consistent with an X-ray analysis⁶⁰⁰). Furthermore, removal of the nucleobase in an incorporated LNA monomer within a DNA strand causes duplex destabilization, confirming that preorganization alone cannot promote stability but instead induces favorable alignment for base stacking.^{601,602} These results indicate LNAs as promising antisense agents in therapeutic applications.⁶⁰³

Bridged nucleic acids, or 2,4'-BNAs, are structurally the same as D-LNA, but research on BNAs has focused on triplex formation with ds-DNA.^{587,588} As observed with D-LNA, 2'-4'-BNA-C and -T incorpo-

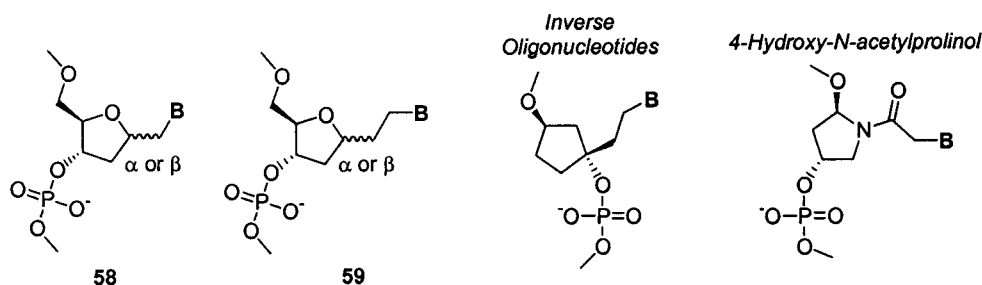


Figure 119. Structures of base–sugar extended oligo(nucleotide)s.

rated in DNA strands promote hybridization of BNA-modified-DNA from 1 to 5 °C and DNA–RNA from 4–6 °C.⁶⁰⁴ Single 2',4'-BNA substitution into DNA strands showed enhanced triplex stabilization and sequence selectivity of ds-DNA at neutral pH. BNA-T incorporation enhances the triplex T_m by 10 °C over DNA-T, while BNA-C increases triplex T_m by 7 °C over DNA-C.⁶⁰⁵ Although these data demonstrate 2',4'-BNA monomers to be potent triplex stabilizers through *H* pairing, homo-BNA strands were not able to form triplexes with ds-DNA presumably due to their rigidity.⁶⁰⁶ Additionally, a 2',4'-BNA incorporating an oxazole nucleobase recognized a C–G pair better than d-T, as evidenced by a triplex T_m increase of 3 °C.⁶⁰⁷ Studies on an isomeric modification of BNA involving bridge attachment from the O3 to C4 (3',4'-BNAs), thereby connecting through 2',5'-linkages,^{608,609} demonstrated that 3',4'-BNA enhanced binding selectivity for RNA over DNA in duplex formation⁶¹⁰ with more stable modified-DNA:RNA duplexes than analogous iso-RNA duplexes.^{499,502}

4. Torsionally Flexible Oligonucleotides

a. Base–Sugar Extensions. An approach to increase the affinity of *alt*-DNA for RNA involved the extension of the base–sugar connection through the insertion of methylene^{611,612} **58** and ethylene⁶¹³ **59** groups into both α - and β -deoxynucleotides (Figure 119). Modeling studies suggested improved base alignment with A-type backbones using these nucleotides since additional conformers are accessible. Single-point 3'→5' substitutions of β -**58** with the canonical bases into DNA strands destabilized a DNA duplex by 9–10 °C,^{612,614} indicating unfavorable steric interactions, while homooligomers of β -**58** were unable to form duplexes with DNA complements. Of the modifications investigated, only the 3'→3' incorporation of α -**58**-T into a DNA strand improved affinity for the complementary RNA strand over DNA.⁶¹⁴ In a similar approach with a carbocyclic ring, single substitutions of *inverse nucleotides*, with ethylene base–sugar connectivities, in d-A₁₃ or d-T₁₃ resulted in a decreased duplex T_m of 4.3 and 11 °C, respectively.⁶¹⁵ Finally, 4-hydroxy-*N*-acetylprolinol nucleotides incorporate amide base–backbone connectivities and T 13-mers duplex with complementary RNA with comparable stability to the natural system.⁶¹⁶

b. Acyclic Backbones. Thus far, the nucleotidomimetics described have focused on modifications of the sugar backbone to investigate intermolecular association through covalent constraint of torsions. In another approach, acyclic glycerol derivatives

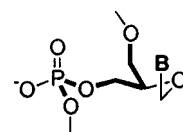


Figure 120. Structure of nucleotides incorporating a glycerol unit in place of the sugar.

incorporating phosphodiester linkages and nucleobases were explored to determine whether increased flexibility promotes duplex formation.⁶¹⁷ Glycerol nucleotides are an isosteric form of the ribose backbone with the C2 removed leading to a more flexible branched chain (Figure 120). One to two glycerol nucleotides were incorporated into central positions in DNA strands and complexed to complementary all-ribose DNA strands. Overall, the melting temperatures of the resulting duplexes were lowered 9–15 °C per glycerol nucleotide due to the increased entropic cost of backbone organization for ideal complexation. This was further confirmed by the absence of duplex formation (<0 °C) when an 11-mer glycerol nucleotide with 5'-d-C and 3'-d-G was mixed with a complementary d-CA₁₁G strand (the natural duplex has a T_m of 55 °C). This system demonstrates that, even with the six bond repeat unit, glycerol nucleotides eliminate the torsional constraints present in natural oligonucleotides that preorganize the strand for ideal association (as seen in another acyclic system, 1,2-*seco*-DNA⁶¹⁸). Similar investigations into acyclic nucleotides incorporated into natural backbones^{619–622} showed, in general, somewhat lower melting temperatures for the resulting duplexes relative to natural systems as well as sequence-dependent heterostrand duplex formation from fully acyclic oligomers with their natural complements.

D. Modifications of the Nucleotide Linkage

The earliest approach to enhancing oligonucleotide duplex stability involved the modification of the phosphodiester linkage, being synthetically accessible and presumed to have minimal deleterious impacts on the puckering states of the furanose ring since they are the most remote functionalities from base interactions. By maintaining the same number of torsions found with phosphodiester backbones with alternative linkages can explore conformational impacts and duplex stability of these structural changes. Even subtle modifications, such as an O→S conversion in phosphorothioates, have been thoroughly explored since their complexation with complemen-

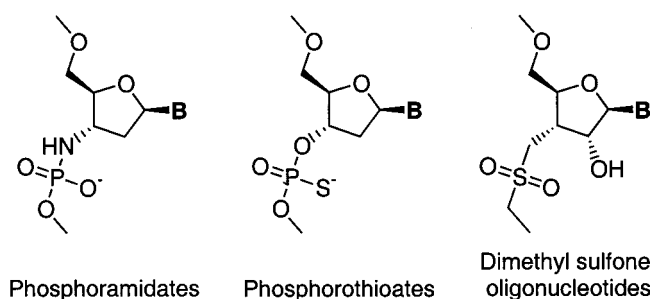


Figure 121. Representative modifications of the phosphate linkage.

tary oligonucleotides^{623–625} and with natural systems has initiated their use as antisense agents.^{626–628} Other linkages that have been used toward these ends include methylphosphonates,^{629,630} amides,^{631–633} sulfonates,⁶³⁴ sulfonamides,⁶³⁵ methyl sulfides,⁶³⁶ methyl sulfoxides,⁶³⁶ phosphorodithioates,⁶³⁷ acetals,⁶³⁸ formacetals,^{639,640} and thioacetals.^{641,642} Though numerous alternative linkages have been investigated to enhance oligonucleotide duplex stability,⁶⁴³ a survey of variants with more foldamer-like research approaches will be discussed herein.

Considerable progress has been accomplished with oligonucleotides where linkages are N3'→P5' phosphoramidates (np-DNA) through substitution of the deoxyribonucleotide O3' to N3' (Figure 121).^{644,645} Initial studies found that this modest modification enhanced *WC* duplex stability of a mixed C/T/A np-DNA 11-mer with complementary DNA by $\Delta T_m = +11.7$ °C and to a much greater extent with RNA ($\Delta T_m = +22.9$ °C).⁶⁴⁴ In addition, self-complementary np-DNAs showed duplex thermal stabilities much higher than ds-DNA or ds-RNA ($\Delta T_m = +26.0$ and $+17.6$ °C, respectively).⁶⁴⁶ Phosphoramidate oligomers also show good water solubility, mismatch discrimination, and enhanced duplex stabilities that were, by and large, found to be base and sequence independent. CD and NMR experiments of duplexes from self-complementary np-DNA strands showed uniform C3'-endo, A-type backbone conformations,^{647,648} while crystal structures revealed that the hydration of the minor groove stabilizes this conformation.⁶⁴⁹ Distamycin, a ds-DNA minor groove binder, was unable to bind with double-stranded np-DNA, supporting the A-type backbone conformations within the duplex.⁶⁴⁶ Triplex formation^{644,646} of 11-mers to a ds-DNA 23-mer was much more stable for np-DNA ($T_m = 45$ °C) than isosequential RNA ($T_m = 26$ °C) or DNA ($T_m < 10$ °C).⁶⁵⁰ Similar results have been obtained with np-RNAs.^{651,652} Finally, recent experiments demonstrated np-DNAs' ability to act as sequence-specific antisense agents through inhibition of protein expression^{653–655} as well as affinity to major groove binding α -helical peptides to the same degree as RNAs.⁶⁵⁶ Interestingly, when the N substitution was made at the O5' rather than the O3', 5'-np-DNA strands were unable to form duplexes with complementary DNA (conversion to the *N*-methyl amidate also disrupted complexation).⁶⁴⁶ Molecular dynamics simulations showed that although the single-stranded 3'- and 5'-amidate-modified DNA strands are solvated to the same degree, the N5' groups are buried in the A-type 5'-np-DNA:RNA duplex while the N3'

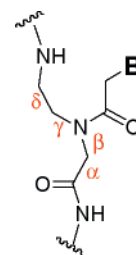


Figure 122. Structure of peptide nucleic acids (PNAs) labeled with dihedral angles.

remains solvent exposed.⁶⁵⁷ The solvent-accessible surface area of the N5' was estimated to be 10 times less than the N3', sufficiently disabling duplex formation altogether.

In an attempt to promote duplex stability through the elimination of interstrand electrostatic repulsion, the neutral, isosteric, and isoelectronic dimethyl sulfone linkage^{658,659} was investigated in RNA backbones. The crystal structure of a GC duplex suggested similar conformations to a *WC* antiparallel ds-RNA,⁶⁶⁰ whereas a UC dimer formed non-*WC* parallel duplexes in *d*-chloroform by NMR.⁶⁶¹ Self-complementary (for antiparallel orientations) dimethyl sulfone linked oligonucleotides showed stronger unimolecular self-pairing than duplexation with RNA or DNA complements.⁶⁵⁹ Furthermore, each oligosulfone has its unique set of properties (solubility, foldability, reactivity), which strongly depend on sequence, varying widely and unpredictably. Chimeric oligomers incorporating one sulfone linkage induced significant decreases in duplex strength when functionalized in the middle of DNA strands.⁶³⁶ In summary, these nonpolar chains behave more like proteins than nucleic acids⁶⁵⁹ in that proteins have variable structure types whereas nucleic acids generally have one universal structure type. Polyanion (repeating charge) seems to be the key to nucleic acid recognition, by modulating the strength of the interaction through electrostatic repulsion. These studies highlight the importance of ionic functionalities in DNA backbones to maintain extended, noncollapsed structures.

1. PNAs

Peptide nucleic acids (PNAs) and structural analogues are the most thoroughly investigated nucleotidomimetic systems studied to date with a number of reviews recently appearing on the subject.^{662–666} PNAs are neutral, δ -peptide backbones with nucleobase extensions from a methylenecarbonyl linker at the β -position (Figure 122). Although progress to date on PNAs has been very promising, the poor water solubility of these oligomers remains a considerable limitation.

Through the successful incorporation of canonical bases to the PNA backbone,^{667–669} PNA oligomers were capable of forming *WC* duplexes with both DNA and RNA in antiparallel and parallel orientations (with the antiparallel orientation defined as the amino terminus of PNA and the 3'-end of the oligonucleotide at the same end). The antiparallel PNA:DNA and PNA:RNA duplexes have T_m s $+13.4$ and $+21.1$ °C, respectively, higher than the parallel form.

Formation proceeds through strand displacement in the oligonucleotide duplex. Kinetic CD studies revealed that PNA complexes form through a rapid base-pairing step, followed by a slow reorganization in the backbone in order to adopt the most thermodynamically stable helical conformation.⁶⁷⁰ Furthermore, ds-PNA duplexes showed increased thermal stabilities⁶⁷⁰ with the duplex stability following the order PNA:PNA > PNA:RNA > PNA:DNA > DNA:DNA.^{668,671} This enhanced stability arises from hydrophobic effects and the absence of interstrand electrostatic repulsion, evidenced by the similarity of PNA:DNA and ds-DNA T_m values in solutions of high ionic strength, where polyanionic backbones are screened by counterions.^{671,672} Chain-length studies on 44 PNA–DNA duplexes revealed an average base-pair binding contribution of 1.6 kcal·mol⁻¹ in lengths from 6- to 20-mers.⁶⁷³ Elucidation of binding sequence-specificity in single-mismatched 9- and 12-mer strands in PNA–DNA duplexes primarily revealed destabilization dependent on the particular base-pair mismatch, its location on the PNA or DNA strand, and its nearest-neighbor environment.⁶⁷³ Single-stranded PNAs terminated with L-lysine (which can induce a helical twist sense of the strand) showed minimal CD intensities indicating the lack of preorganized, helical base stacking⁶⁷⁰ while, within ds-PNA, the CD signal was very intense and resembled ds-DNA.

A crystal structure of a PNA–PNA duplex revealed a widened P-helix relative to DNA–DNA and a large pitch of approximately 18 base pairs, resulting in a deep major groove and a shallow minor one.⁶⁷⁴ Additionally, the polyamide backbone demonstrates “constrained flexibility” in solution such that the PNA strand accommodates the complexed conformation more easily than ribose backbones through greater torsional relaxation. In fact, NMR studies revealed multiple resonances for the uncomplexed PNA backbone, indicating random-coil conformations,⁶⁷⁵ which converge to a singular resonance in an A-type PNA–RNA helix⁶⁷⁶ and a PNA–DNA helix.^{677,678} Although molecular modeling suggested that intrastrand α -helical-type H-bonding in the PNA backbone would result in higher conformational order,^{679–681} NMR studies revealed that this stabilization was not observable in these systems, although this is under debate.⁶⁸² Though PNA folding proceeds via intermolecular complexation, these chain molecules adopt unique conformations through intrastrand *cis*–*trans*-amide isomerization and interstrand noncovalent complementary base pairing, even showing the capacity to form hairpins.⁶⁸³ Though the A-type PNA:RNA duplex shows conformational similarity to ds-RNA, recent molecular dynamics simulations revealed that PNA:DNA duplexes have conformational characteristics of both the A- and B-type as well as a much more flexible PNA backbone than natural oligonucleotides, while retaining torsional preferences.⁶⁸⁴ Crucial to the proper directional sequence selectivity, mixed backbone PNA/DNA chimeras complexed to both RNA and DNA formed exclusively antiparallel duplexes over the parallel orientation.^{665,685}

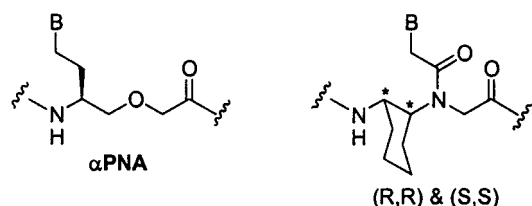


Figure 123. Representative examples of PNA structural modifications.

The potential for PNAs to act as transcription inhibitors has been demonstrated through investigations into effective DNA strand displacement (forming D-loops in PNA–DNA duplexes,^{686,687} PD-loops with bis-PNAs⁶⁸⁸ in (PNA)₂DNA triplexes,⁶⁸⁹ and other architectures^{690,691} including double duplex strand invasion⁶⁹²) such that both DNA strands form duplexes with the pseudocomplementary PNAs. Triplex PNAs^{663,664} have elucidated a right-handed PNA–PNA–DNA^{668,689,693–696} where a third PNA *H*-pairs to the *WC* PNA strand,⁶⁹⁵ while a chain-length study showed a T_m stabilization of 10 °C per monomer unit⁶⁶⁸ as well as a PNA–PNA–PNA triplex.⁶⁹⁰

Along with inhibitory binding, PNAs can participate in fundamental genetic processes. PNAs facilitate the oligomerization of complementary RNA and vice versa, demonstrating a pathway for information transfer along with providing possible insight into the origin of the RNA world.^{697,698} Furthermore, PNAs can act as primers for DNA polymerases.⁶⁹⁹ Finally, promising antisense and antigene properties⁷⁰⁰ as well as key issues such as improved solubility, stability at physiological conditions, nuclease resistance, and improving cellular uptake of PNA-conjugates are being pursued in efforts to treat disease with PNAs through inhibition of gene expression.^{685,701}

Since a variety of PNA-like oligomers have been synthesized for nucleotide recognition, representative examples of strand modification, both backbone and base linking, are worth mentioning in terms of folding properties (Figure 123). Cyclohexyl-derived PNAs with a more rigid backbone formed stable duplexes with (*S,S*) configurations, while duplexes incorporating the (*R,R*) isomers resulted in decreased stabilities in the right-handed duplex.⁷⁰² Bis-PNAs rapidly form triplex structures due to reduced entropic costs by converting triplex formation into a bimolecular process.^{703,704} PNA chimeras⁶⁶⁵ have been synthesized to form PNA hybrids with DNA⁶⁶⁵ and enhance binding affinities and sequence selection. They also form complexes with peptides⁷⁰⁵ to form conjugates that retain the biological functions of both. A different peptide–PNA conjugate, dubbed α -helical PNAs (α PNAs), incorporates three amino acids into the monomeric backbone unit. α PNAs demonstrate stronger binding to DNA strands (in an all-or-none-type complexation) compared to traditional PNAs, and they have greater water solubility.⁷⁰⁶ A representative PNA–PNA duplex and a PNA₂–DNA triplex are shown in Figure 124. To summarize, the PNA family of nucleotidomimetic foldamers are novel backbones that successfully complex to oligonucleotides even though they are neutral and acyclic. Clearly, the structural rules for ideal complexation of oligonucleotides and neutral, acyclic nucleotido-

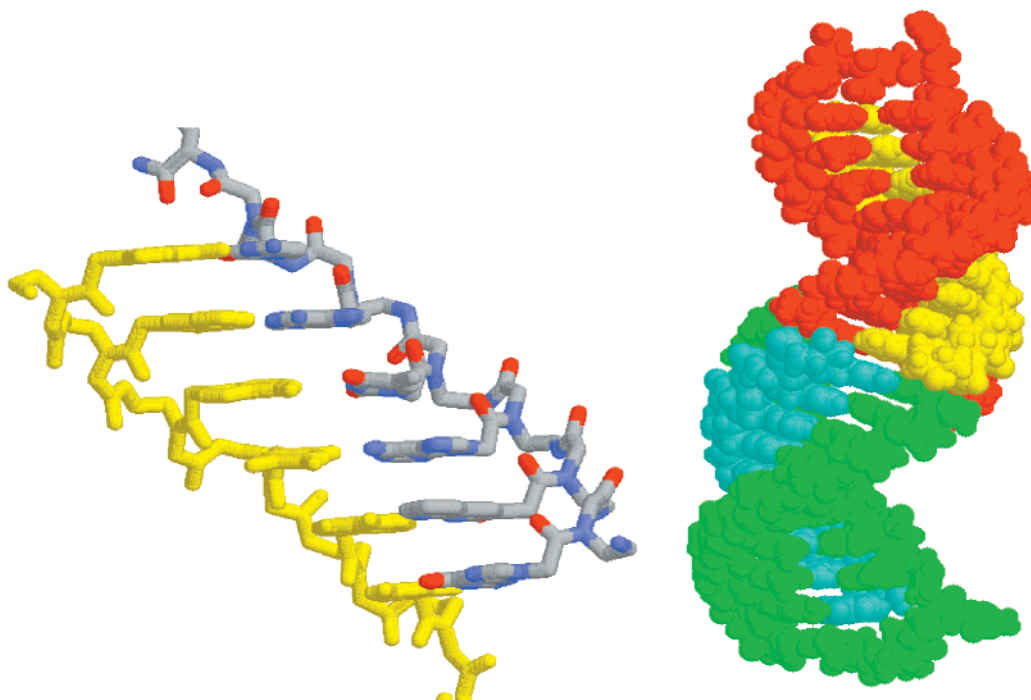


Figure 124. Crystal structure of a peptide nucleic acid duplex (left).⁹⁰¹ For clarity, one strand is colored yellow and the other uses conventional atom colors: PNA₂-DNA triplex (right).⁷¹⁰ Four chains are shown. The DNA chains are colored yellow and blue. The DNA sequence is 5'-(GAAGAAGAG)-3'. The PNA chains are colored red and green. The PNA sequence is H₂N-(CTCTTCTTC-His-Gly-Ser-Ser-Gly-His-CTTCTTCTC)-CO₂H.

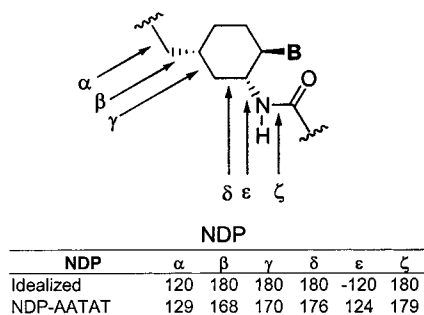


Figure 125. NDPs and their torsion angles.

mimetic chains molecules have yet to be fully determined.

2. NDPs

Nucleo- δ -peptides (NDP) incorporate cyclohexyls linked by carbamoylmethyl groups such that the oligomer is preorganized into an ideal linear conformation analogous to p-RNAs.^{707,708} NDPs map onto α -peptide backbones with three predefined torsions (γ , δ , and ζ) due to the conformation restriction of the cyclohexyl moieties. NMR studies on an NDP-AATAT sequence revealed an antiparallel WC self-paired duplex stabilized by interstrand base stacking. Torsional angles of the backbone are shown in Figure 125, where the dangling A-ends further stabilize the duplex. The global conformation was further refined using molecular dynamics and determined to be a right-handed double helix with a twist of ca. $10 \pm 2^\circ$ and a unit height of $7.5 \pm 0.1 \text{ \AA}$.

3. Fused Sugar-Base Backbones

A recent series of investigations was undertaken to determine if a fusion between the sugar and the

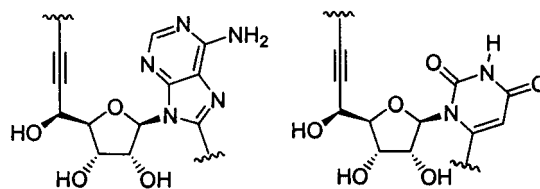


Figure 126. Fused sugar-backbone structures.

nucleobase would provide conformational accessibility to intermolecular complexation. Through the convergent Sonogashira coupling of an iodo-nucleobase to an acetylenic linker, dimers and tetramers of A and U fused bases were generated to explore these chain molecules (Figure 126).⁷⁰⁹⁻⁷¹² UV studies on these single strands did not show any evidence of base interactions, indicating that intrastrand base stacking had been disrupted through this backbone modification. In a related system, phosphodiester-fused A and U bases were single-site incorporated into 14-mer DNA strands and led to duplex formation destabilized by an amount on the order of only one mismatch pair.^{713,714} These examples clearly demonstrate that the double-helix architecture has a strong preference for comblike structures where the backbone adopts conformations that project nucleobases in orthogonal orientations to the helical axis.

4. Cationic Linkages

Oligonucleotide complex stability has also been enhanced with cationic deoxynucleic and ribonucleic guanidine backbones (DNG and RNG) (Figure 127), which are electrostatically attracted to the anionic phosphodiester backbone of natural chains within a complex (substituted guanidinium linkages have also been investigated⁷¹⁵). Through both solution-⁷¹⁶⁻⁷¹⁸ and solid-phase synthesis,⁷¹⁹⁻⁷²² pentameric DNG T

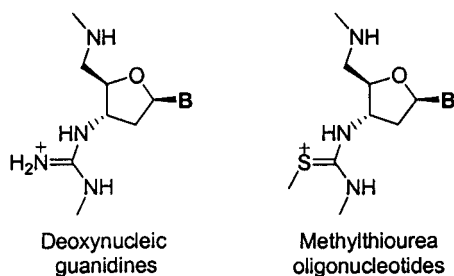


Figure 127. Cationic backbone modifications DNG and DNmt.

strands were generated and formed very stable duplexes and triplexes with poly(rA) and duplexes with poly(dA), remaining intact even near boiling temperatures, while the DNG₂:poly(dA) triplex has a T_m of 85 °C. DNG-T₅ did not bind to poly-(dG), -(dC), and -(dT), showing sequence discrimination.^{718,723} With DNA oligomers, single-point C mismatches lower duplex T_m DNG-T by 4–5 °C at terminal and 15 °C at internal sites.⁷²¹ A thermodynamic and kinetic study of DNG complexation with DNA strands containing G mismatches showed that the electrostatic attraction between the strands overrides base-pairing selectivity in certain cases.^{724,725} Decreased duplex stability is observed at higher ionic strength since the interstrand electrostatic attraction is diminished as a consequence of screening. The major groove width of the DNG:RNA A-type duplex increases while the minor groove width tightens relative to ds-RNA due to the electrostatic contraction of the complex as revealed by molecular modeling⁷²³ and dynamics simulations.⁷²⁶ Similar results were demonstrated in RNG backbones.^{727–729} Hybrid DNG–PNA strands,^{730,731} as well as chimeric DNG–methylthiourea oligonucleotides,⁷³² allow for attenuation of the degree of positive charge embedded in these neutral backbones, enhancement of water solubility of neutral backbones, and minimization of deleterious effects of electrostatic attraction. To increase the hydrophobicity of cationic oligonucleotides, *S*-methylthiourea backbones (DNmt) were generated by solution-^{733,734} and solid-phase synthesis.⁷³⁵ DNmt backbones function similarly to DNG with weaker complex stabilities observed.^{736–738} Overall, these cationic backbones show remarkable stability with their complementary natural oligonucleotides through utilization of electrostatic attraction as a supra-molecular construct, thereby incorporating another stabilizing noncovalent interaction.

E. Alternative Nucleobases

The use of nonbiological nucleobases to enhance oligonucleotide duplex stability is widespread, and an exhaustive exploration of this field is beyond the scope of this review. At the same time, recent studies exist that go beyond this goal with the aim of understanding the function of base interactions in duplex stability and the impact of unusual nucleobases on both conformation and assembly. Herein, we focus on a few of these examples as representatives of the field and to highlight how modifications at nucleobase sites that are “remote” from the backbone can have profound architectural effects on

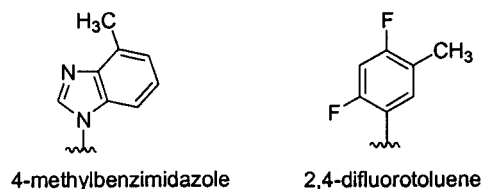


Figure 128. Hydrophobic nucleotide bases.

oligonucleotide complexes. This field has recently been reviewed.⁷³⁹

The role of face-to-face aromatic interactions within duplex DNA and RNA is less evident than base pairing since H-bonding in duplexes can be rationalized through predictable acceptor–donor motifs while the nature and rules of aromatic stacking are less understood. Aromatic–aromatic interactions have been attributed to electrostatics, hydrophobicity, and dispersion forces. To elucidate the factors in nucleobase stacking, the use of nucleotides with alternative nucleobases⁷⁴⁰ at the 5'-termini of DNA strands (dangling ends) to study duplex stabilization was undertaken. Initial studies revealed the overall order of stacking ability to be pyrene > methylindole > phenanthroline ~ naphthalene ≥ difluorotoluene > A > benzene > T, where less polar aromatics of similar size stack stronger than more polar ones.⁷⁴¹ Further investigations with the canonical bases showed the stacking ability to be A > G ≥ T ~ C.⁷⁴² Overall, the best correlation between stacking ability and various properties of the nucleobases was found with the surface area of the aromatic moiety; bases with small overlap, such as pyrrole, stack with the weakest strength and pyrene stacks the strongest. Thus, solvophobic effects were concluded to be the most significant force in the base stacking interactions of this series.

Although the common base-pairing motifs formed through H-bonding interactions in duplexes are well understood, it is unknown whether oligonucleotide complexation can proceed through non-H-bonded pairing. Considerable work has been conducted on alternative H-bonded pairings through isomeric forms of nucleobases, such as iso-C and iso-G,^{743–746} as well as isomorphous nucleobases,^{747–750} aimed at the expansion of the genetic alphabet⁷⁵¹ through enzymatic incorporation. A problem with alternative acceptor–donor systems is the susceptibility of the nucleobases to undergo deleterious tautomeric isomerization.^{745,752,753} To elucidate the necessity of H-bonded pairing in duplex stabilization, single-site substitution in ds-DNA 12-mers with the “complementary” pair of pyrene and hydrogen (an abasic site) nucleotides destabilized the duplex to a smaller extent than expected ($\Delta T_m = 1.6–2.2$ °C relative to an A–T pair) while pyrene oppositely paired to canonical bases reduced the stability to a greater extent ($\Delta T_m = 2.3–4.6$ °C).⁷⁵⁴ Surprisingly, a pyrene–pyrene pair generates a duplex with comparable stability to the unmodified natural duplex. Another non-H-bonded pairing motif, 4-methylbenzimidazole:2,4-difluorotoluene,⁷⁵⁵ destabilized the ds-DNA ($\Delta T_m = 12.1$ °C relative to a central T–A pair) but retained the B-type conformation of the backbone according to NMR and molecular dynamics simulations⁷⁵⁶ (Figure 128). Destabilization in this system is primarily due to cost of solvation of these more hydro-

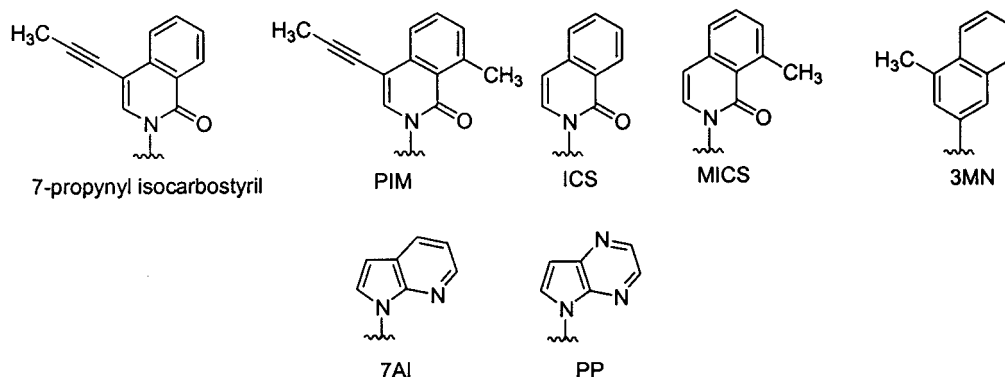


Figure 129. Examples of alternative nucleobases.

phobic bases.⁷³⁹ In similar studies, various aromatic nucleobases have been incorporated into DNA strands for duplex stability as a segue to alternative nucleobase pairing motifs that may be incorporated into DNA strands by polymerases. Of the variety of non-H-bonding aromatic nucleobases investigated,⁷³⁹ promising results for unnatural DNA pairing modes in terms of duplex stability, mismatch discrimination, and incorporation during template-directed polymerase syntheses^{757–759} (see Kool⁷⁶⁰ for a recent review) include 7-propynyl isocarbostyryl:7-propynyl isocarbostyryl,⁷⁵¹ 7AI:ICS,⁷⁶¹ PP:MICS,⁷⁶² PIM:PIM,⁷⁶³ and 3MN:3MN⁷⁶⁴ (Figure 129). Recently, the 7AI:7AI self-pair was not only efficiently incorporated into a growing DNA strand, but also allowed primer extension using mammalian polymerase β , which was not seen using the Klenow fragment of *Escherichia coli* polymerase I.⁷⁶⁵ These nonbiological base-pairing motifs demonstrate the acceptance of the oligonucleotide duplex architecture for non-H-bonding interactions, stressing the importance of base stacking for stability and the potential dispensability of H-bonding interactions at select sites.

Although it is clear that cationic, inorganic species (such as Mg^{2+}) are essential to the structures and stability of the oligonucleotide backbone,⁴⁸⁷ metal–ligand coordination in oligonucleotides has gained increasing attention. Recent studies have utilized the coordination strength of transition metals to incorporate alternative nucleobases into DNA strands as an unconventional interstrand base-pairing motif. After single-site incorporation of pyridine and 2,6-pyridinedicarboxylic methyl diester nucleotides into complementary DNA 15-mers followed by hydrolysis of the methyl diesters, equimolar mixtures of the two strands showed no duplex formation and remained dissociated even at low temperatures (14 °C) (Figure 130).⁷⁶⁶ Upon addition of Cu^{2+} (1, 2, and 5 equiv), duplex formation not only proceeds but comparable thermal stabilities were obtained to the natural ds-DNA ($\Delta T_m = 2.6, 1.7,$ and 1.1 °C lower relative to an A–T pair, respectively). A variety of other transition metals were tested ($Ce^{3+}, Mn^{2+}, Fe^{2+}, Co^{2+}, Ni^{2+}, Zn^{2+}, Pd^{2+},$ and Pt^{2+}) but did not lead to duplex stabilization. Ligand–nucleobase mismatch discrimination was demonstrated with canonical bases where duplexes with mispairs were typically destabilized by ≥ 10 °C. In a related system, 2,2'-bipyridines were attached through a C1'-methylene to the furanose ring (dubbed *ligandosides*) and incorporated at single sites into self-complementary DNA 11-mers.⁷⁶⁷ Upon

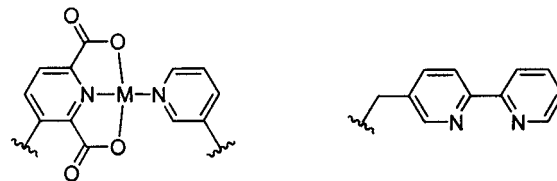


Figure 130. Metal-binding nucleobases.

addition of 1.0 equiv of Cu^{2+} , the T_m of the duplex increased from 56.6 to 64 °C and showed a more cooperative melting transition. Dimeric oligonucleosides have been generated with Cu^{2+} and Ag^+ .⁷⁶⁸ Significantly, these metal-coordinating nucleotides have two potential structural advantages over helicates. First, the ligands are remote from the backbone whereas in helicates the metal-coordinating portions are part of the backbone. Second, the phosphodiester linkages can stabilize the cationic metal center, decreasing any deleterious effects counterions may have in helicates. A recent study has shown that bipyridine ligands can also stabilize DNA duplexes through interstrand base stacking in the *absence* of metal ions.⁷⁶⁹ Efforts toward developing other metal-binding nucleosides include phenylenediamine: $Pd(II)$,⁷⁷⁰ catechol-borates,⁷⁷¹ and 2-aminophenols.⁷⁷² Overall, these systems show great promise for the development of novel nucleotidomimetics incorporating metal coordination as a supramolecular construct in the design of foldamer structures.

VII. Multistranded Abiotic Foldamers

Just as single-stranded abiotic foldamers mimic the secondary structures of proteins through a bottom-up approach, multistranded abiotic foldamers mimic DNA architectures through the assembly and folding of two or more chains through nonadjacent contacts. The following is a survey of the backbones, some very similar to previously described chains in the single-stranded abiotic section, that utilize various non-covalent interactions in adopting their unique conformations.

A. Hydrogen-Bonding-Stabilized Foldamer Multiplexes

Foldamer multiplexes¹¹⁸ incorporating H-bonding motifs have been investigated to generate novel structures that associate through similar motifs as

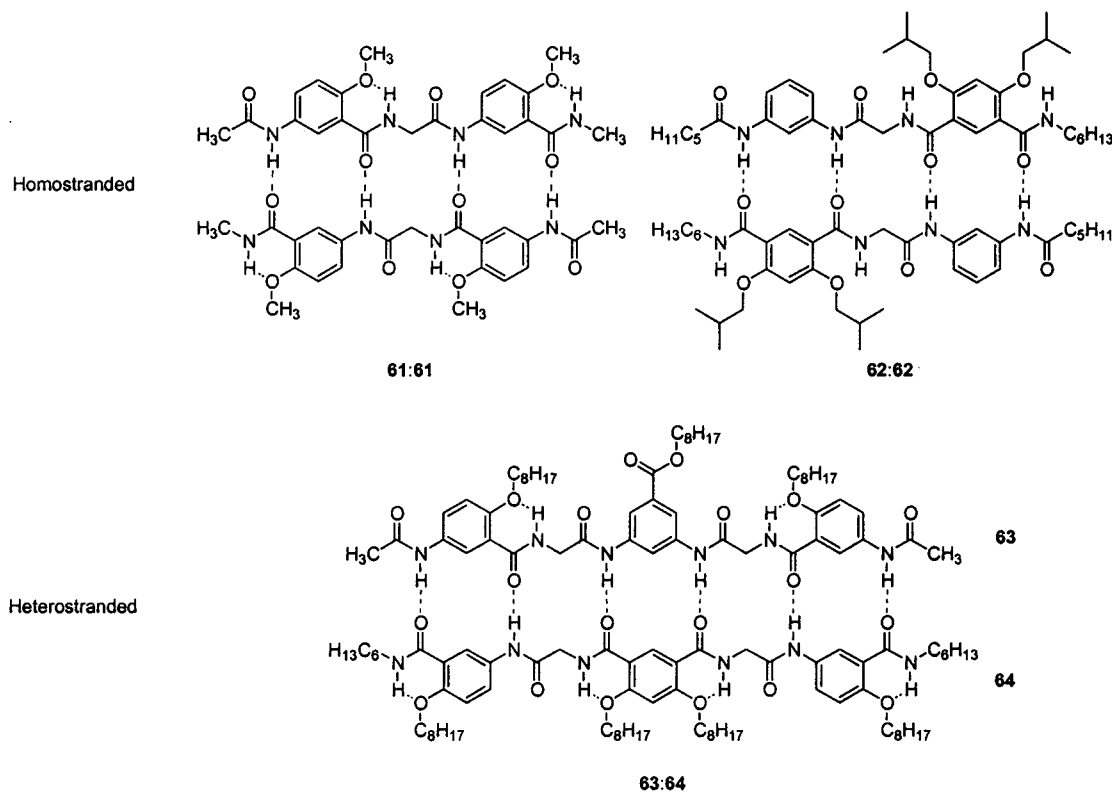


Figure 132. Oligo(arylamide)s complexed through self-complementary ADAD and AADD duplexes and a complementary ADAADA/DADDAD strand.

addition of 10% MeOH. An artificial sheet was constructed in which the Hao unit was attached to one end of Nowick's previously described molecular scaffold while to the other end an α -tripeptide was connected. This structure resulted in an artificial β -sheet that dimerized in solution via the H-bond donors and acceptors on the top edge.⁷⁷³

Arylamide oligomers with various D/A sequences have been recently investigated by Gong et al.^{445,446} Quadruply H-bonded complexes, **61:61** and **62:62**, with D/A sequences DADA and DDAA, respectively, were shown by ¹H NMR and X-ray studies to dimerize through self-complementarity from two dimeric strands (Figure 132). The association constant of **62:62** was determined to be marginally more stable than **61:61** ($6 \times 10^4 \text{ M}^{-1}$ vs $4 \times 10^4 \text{ M}^{-1}$) even though more favorable electrostatic interactions exist with **62**. Although some torsional flexibility exists in both foldamers, these H-bonded duplexes form readily through both intra- and intermolecular H-bonds to adopt planar, β -sheetlike structures. Extension of these preliminary studies to trimeric oligomer lengths enabled the formation of self-complementary planar duplexes stabilized by six H-bonding interactions.⁴⁴⁶ The two symmetric heterotrimers, **63** and **64**, have two and four intramolecular H-bonding interactions and D/A sequences of DADDAD and ADAADA, respectively. Preorganization through intramolecular H-bonding interactions predispose these oligomers to planar, extended conformations, exposing sequence sites for intermolecular association. NOESY experiments under complexing conditions (i.e., CDCl₃) confirmed the close interstrand proximity of the methylene groups. Slight downfield shifting of a NH signal in **64** upon dilution (100 to 10 μm) was

speculated to be a result of decreasing intermolecular stacking interactions. Self-association of both **63** and **64** could produce dimers stabilized by four H-bonding interactions. The self-complexation association constant for **64** was determined to be approximately $4 \times 10^4 \text{ M}^{-1}$ compared to the lower limit **63:64** association constant of $9 \times 10^7 \text{ M}^{-1}$. Recent studies showed that mismatches in the AD sequence lead to a conformational rearrangement of the backbone driven by steric interactions that resulted in >40 times lower duplex stability as evidenced by isothermal titration calorimetry.⁷⁷⁹

A system capable of two-state conformational switching has been produced from two complementary naphthyridinyl urea oligomers (Figure 133).⁷⁸⁰ Both linear molecules **65** and **66** form associated structures through intramolecular H-bonding by rotation about the arylamide bonds. In frame-shifted (relative to **66**) monoaromatic **65**, the folded conformation is observed to intermolecularly associate to produce oligomeric species (of unknown *n*) through noncooperative association at all concentrations. At low concentrations, the bent form of **66** associates to form dimer **67**, while at higher concentrations the extended conformation of **66** dimerizes to **68**. Upon mixing of **66** and **65**, a complementary complex **69** self-assembles with the extended, planar conformations of both molecules at all concentrations. This occurs since the association constant for the formation of **69** is greater than either of the duplexing modes.

Bis-2-ureido-4[1*H*]-pyrimidinones are capable of self-associating into a duplex structure stabilized by eight H-bonding interactions with **70** that are adaptive through a *keto-enol* tautomerization (Figure

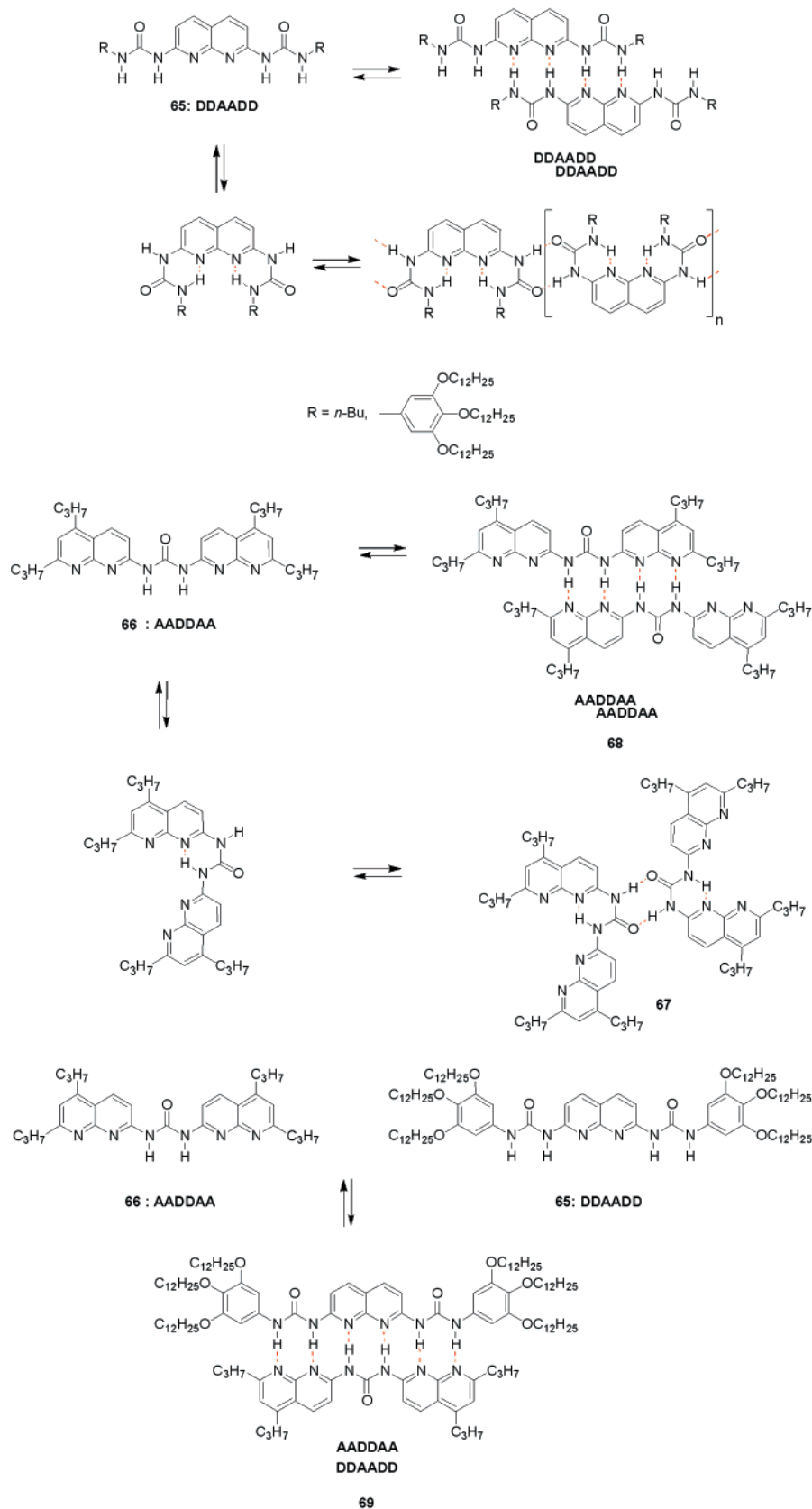


Figure 133. Intra- and intermolecular pairing modes for DDAADD and AADDAA strands.

134).⁷⁸¹ In **70**, two D/A sequences, the *keto* DDAA and the *enol* ADAD, are possible through proton transfer and a switch in the intramolecular H-bonding by a N–C rotation in the urea moiety. X-ray analysis of crystals revealed pyrimidinone aromatic–aromatic

stacking and intermolecular H-bonding where crystals obtained from DMF revealed two possible syn coplanar orientations in the solid-state while crystals grown from CHCl3 showed anti or helical orientations. NOE and 2D-ROESY experiments revealed

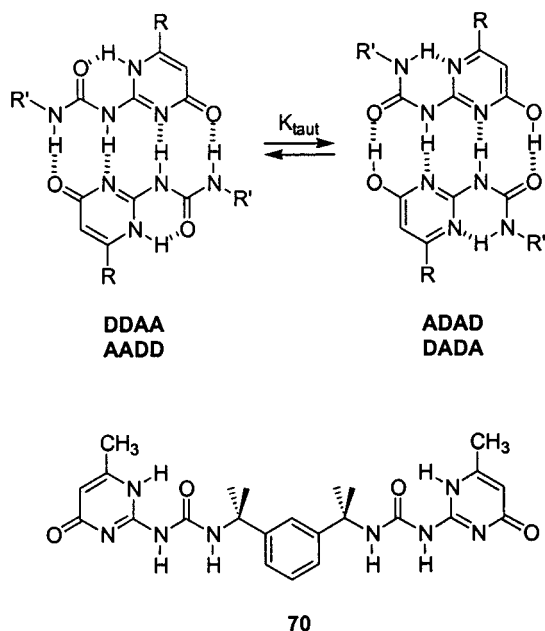


Figure 134. Keto-enol tautomerism in an A/D strand.

cooperative formation and equilibration between the two conformations as well as slow conversion to a third isomer, identified as a *keto-enol* asymmetric duplex with one interstrand pyrimidinone complex and one enolized pyrimidinol pair. At equilibrium, the syn/anti ratio to *keto-enol* duplexes exist in an approximately 3:1 ratio.

Recently, an oligomer backbone incorporating aminotriazene repeat units tethered together by methylene groups effectively forms hydrogen-bonded duplexes.⁷⁸² Complexation of the dimeric strands is much stronger in the amine-linked backbone ($X = \text{NH}$) where intrastrand H-bonding preorganizes the dimer for duplexation, whereas the ether-linked backbone ($X = \text{O}$) shows significantly lower association constants (Figure 135).⁴⁵²

B. Duplexes Stabilized by Hydrogen-Bonding and Aromatic-Aromatic Interactions

1. Zipper Duplexes

Hydrogen bonding and aromatic aromatic-aromatic stacking interactions have also been used in the intermolecular organization of complementary

oligomeric strands (Figure 136).⁷⁸³⁻⁷⁸⁸ The system is based on intramolecular H-bonding between an amide carbonyl group and an amide nitrogen. In addition, two aromatic edge to face interactions between an isophthalic acid moiety and a 1,1-bis(4-amino-3,5-dimethylphenyl)cyclohexane group are also important for stabilization. The dimer conformation **72** resulting from the intermolecular H-bonding of two strands of **71** was confirmed by ¹H NMR spectroscopy, which revealed a downfield shift of all amide protons and an upfield shift of the aromatic protons on the isophthaloyl group. These results indicate the presence of H-bonding and aromatic-aromatic stacking interactions.

The symmetry of the initial complexes **72** prevented a definitive confirmation of the structure. To overcome this difficulty, different yet complementary systems were developed (Figure 137). Monomers **73** and **74** are self-complementary and form stable homodimers in solution as homocomplexes as determined by ¹H NMR spectroscopy. However, it was found that the heterocomplex **75** was an order of magnitude more stable than either of the self-complementary strands. NOE experiments revealed several interstrand interactions and indicated contact along the entire length of the complex. Experiments were performed to help probe the possibility of cooperative binding in the recognition process.⁷⁸⁴ The association constants of several heterocomplexes of increasing length were determined by ¹H NMR spectroscopy, showing that as the length of the oligomers increased, the stability of the corresponding complexes increased in a nonlinear fashion indicative of a cooperative binding process. Additionally, significant intermolecular interaction was observed along the entire length of the chain.

2. Pyridylamide Oligomers

Intramolecular H-bonding has been used to create a system that can adopt a single- or double-stranded helical conformation in solution.^{113,789,790} The system is based on 2'-pyridyl-2-pyridinecarboxamide units which are predisposed to form intramolecular H-bonds (Figure 138). H-bonding present in oligomeric strands **76-78** is expected to generate a helical conformation. Dilute solutions of **76** in CDCl₃ (0.5

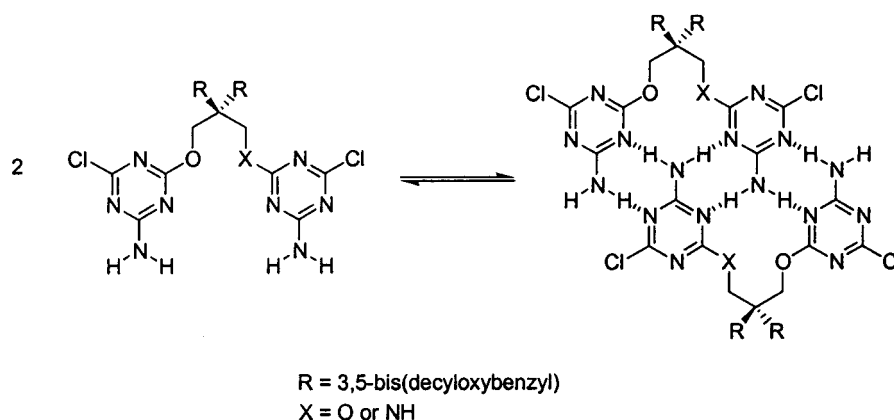


Figure 135. Methylene-bridged triazene dimers and their hydrogen-bonding duplexation.

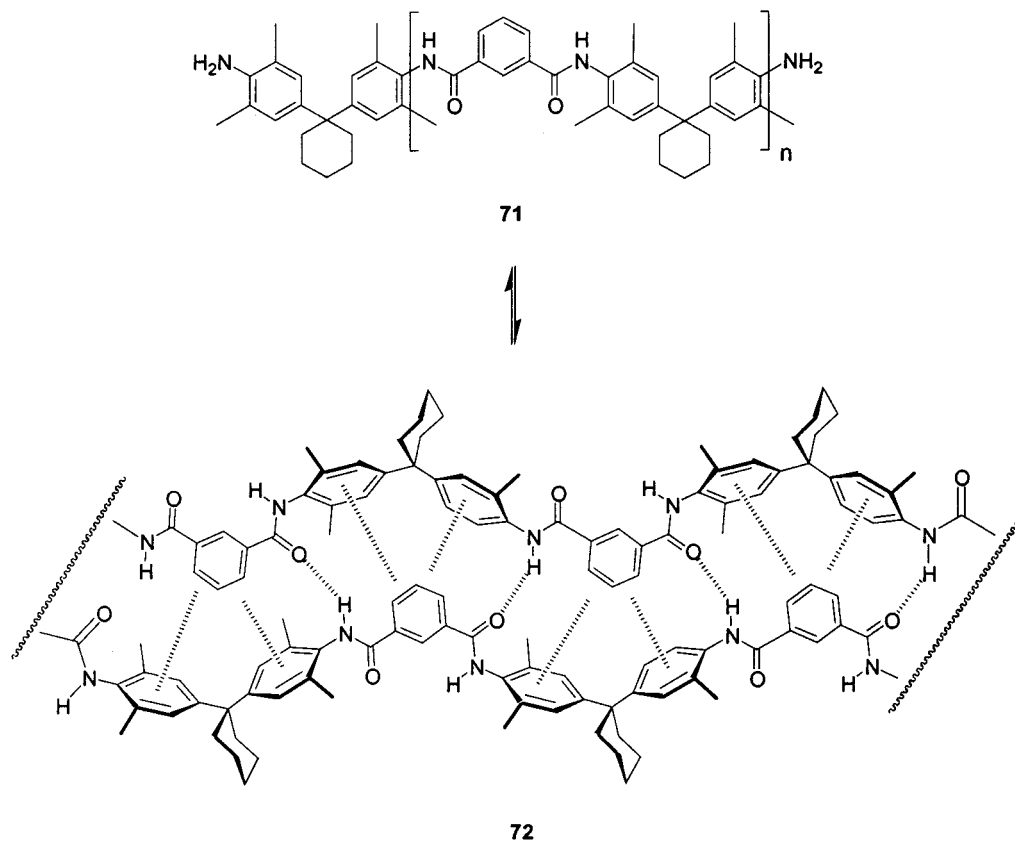


Figure 136. Self-complementary oligomer in a zipper structure. Dotted lines indicate edge–face aromatic–aromatic interactions.

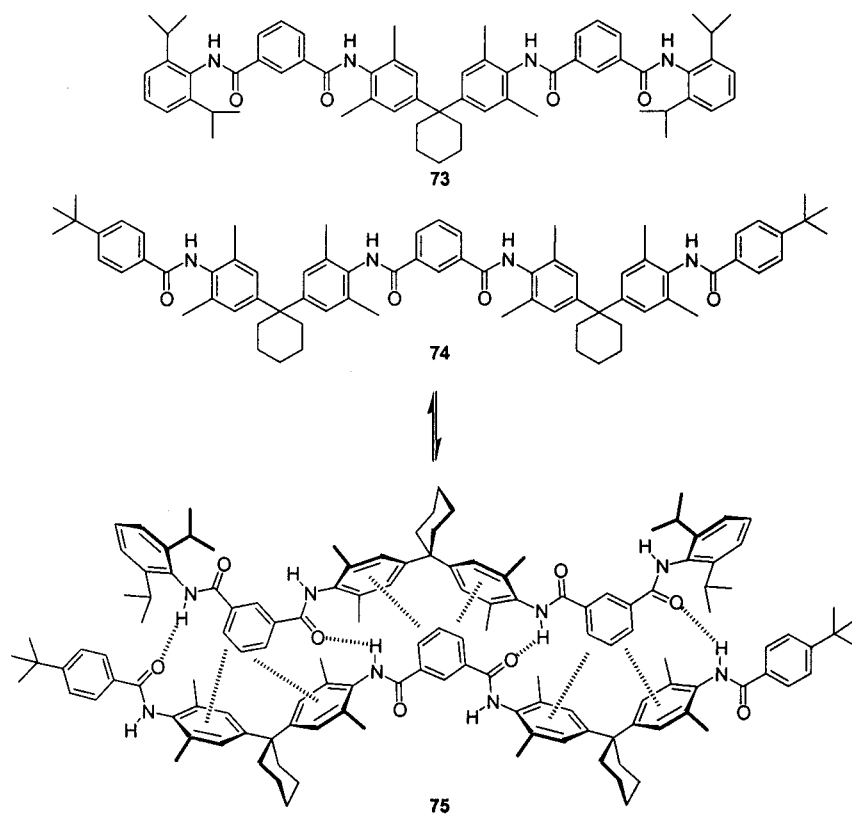


Figure 137. Complementary oligomers in zipper structures.

mM) indicate the presence of a single species as evidenced by a single set of sharp ^1H NMR signals. Aromatic stacking as demonstrated by the upfield

shifting of several of the aromatic signals and an X-ray crystal structure from DMSO/ CH_3CN showed the expected helical conformation.

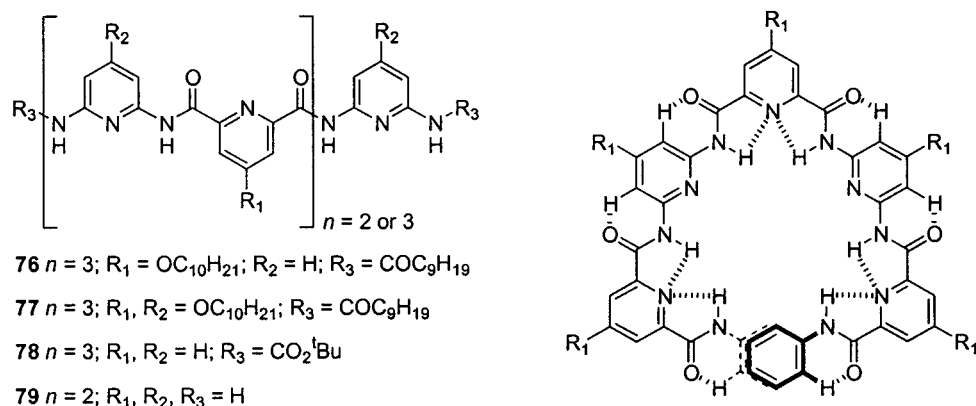


Figure 138. Series of oligo(pyridylamide)s capable of forming single- and double-stranded helices.

Concentration of samples of **76** in chloroform resulted in the generation of a second set of signals proposed to be a double-helical conformation.⁷⁹⁰ An exchange rate between monomer and dimer species was determined to be 8.7 s^{-1} at $25 \text{ }^\circ\text{C}$, and an association constant (K_{dim}) was measured by NMR spectroscopy to be $25\text{--}30 \text{ M}^{-1}$. A crystal structure of less soluble analogue **78** from nitrobenzene/heptane confirmed a double-helical conformation with an average aromatic–aromatic stacking distance of 3.5 \AA . From the X-ray crystal structure, it was concluded that the aromatic stacking between individual strands was responsible for stabilizing the dimer formation since most of the H-bonds were within the same strand and primarily stabilized the helical conformation of the individual chains. This is in contrast to ds-DNA, where aromatic stacking is responsible for intramolecular stabilization and H-bonding is responsible for intrastrand organization. This system was studied in various chlorohydrocarbon solvents, but no correlation existed between solvent polarity and double-helical stability. It was determined that the deleterious presence of water in these solvents competed with intermolecular H-bonding causing destabilization of the complex. The dimerization constant was determined to be $6.5 \times 10^4 \text{ M}^{-1}$. Molecular dynamics simulations revealed a possible folding pathway that involved rearrangement of a loose complex into the double-stranded conformation as well as the stability of the duplex on the time span of the simulation.

C. Helicates: Metal-Coordinating Foldamer Duplexes

1. Oligopyridines

As mentioned earlier in this review, oligopyridines have been thoroughly investigated for their ability to adopt helical conformations upon metal coordination (for reviews on this field, see refs 456, 457, 791, and 792). Thus far, only single-stranded helices from oligopyridines have been described. Yet, the same oligomers may adopt double-stranded helical conformations depending on the coordination metal ion employed. Although quaterpyridine (qtpy) oligomers adopt single-stranded helical conformations with a variety of metal ions, they complex with Cu(I) and Ag(I) in double-helical conformations.⁷⁹³ Double-

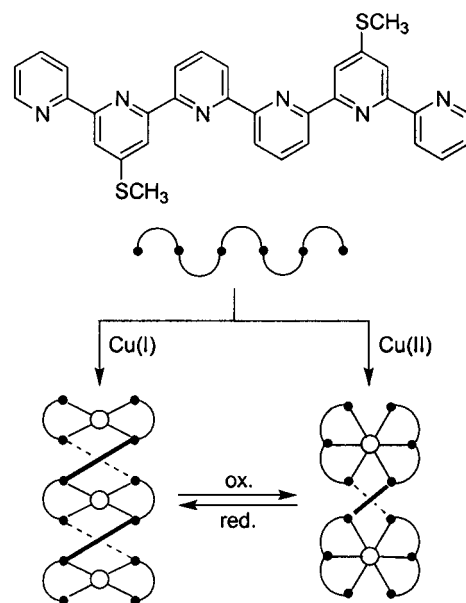


Figure 139. Formation of di- and trinuclear double-stranded helicates from a substituted sexipyridine ligand through supramolecular and electrochemical pathways.

stranded complexation is also possible with quinquepyridines (qpy) when complexed to Pd(II), whereas the shorter qpty associates with two Pd(II) ions in planar, single-stranded conformations.⁴⁶⁶ Crystal structures of sexipyridine complexes revealed a binuclear double-helix with Cd(II)⁴⁶⁶ but a trinuclear double helicate with Cu(II).^{466,475}

A systematic chain-length study of oligopyridines was undertaken using tpy,⁷⁹⁴ qtpy,⁷⁹⁵ qpy,^{795,796} sexipyridines (spy),⁷⁹⁶ septipyridines (septipy),⁴⁷⁰ and oligomers up to the decipyridine ($n = 10$). Alkanethiol side chains on oligomers promote solubility of the longer chains.⁷⁹⁷ Investigations on spy strands and their di- and trinuclear helical complexes were investigated with the goal of forming different metal coordination spheres both synthetically and electrochemically (Figure 139). Both the Cu(I) and Cu(II) helicates were synthesized discretely and converted from one to another by CV as evidenced by spectroelectrochemical analysis.⁷⁹⁶ In these longer oligopyridines, double-helical conformations are a result of the system maximizing coordination bonds and aromatic–aromatic stacking while minimizing the number of components in the assembly. When septipyridine oligomers are complexed to either Co(II) or Cu(II),

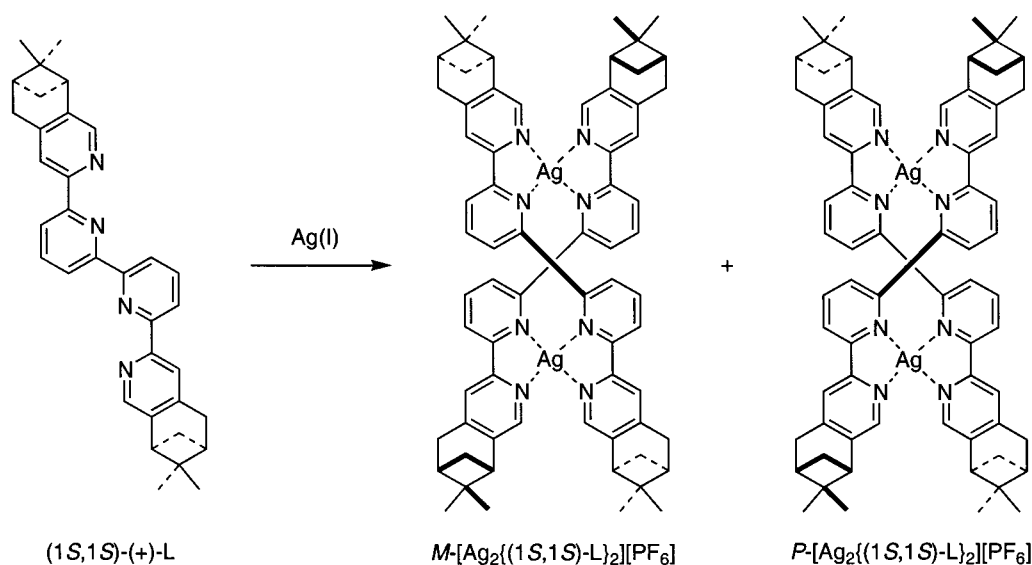


Figure 140. *M* and *P* helical conformations of double helicates from a dimer with a chiral ligand.

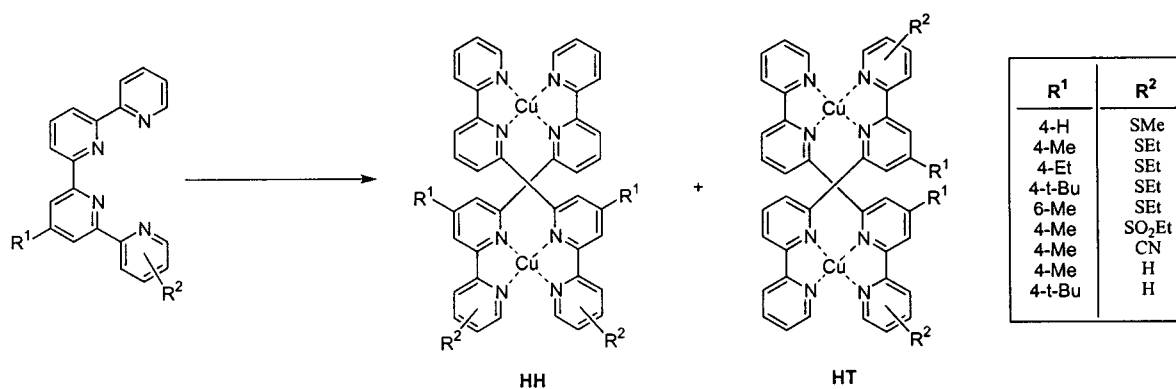


Figure 141. Head-to-head and head-to-tail conformations of double helicates from substituted qtpy ligands.

octahedral coordinations incorporate only six of the seven pyridines in the backbone, leading to strand slipping in solution.⁴⁷⁰ To design out this molecular motion, 1,3-phenylene monomers incapable of coordinating to the metal ions have been used to replace the central positions in qpy,⁷⁹⁸ spy,⁷⁹⁹ and septipy⁸⁰⁰ strands, thereby dividing the chain into localized coordinating segments. Alkynyl linkages have also been incorporated into oligopyridine backbones promoting helicate formation by maintaining the rigidity of the backbone while decreasing interstrand steric interactions.^{801,802}

Helicate duplexes incorporating symmetric oligomers do not possess strand directionality, unlike (3'→5') oligonucleotide duplexes. To enhance architectural control of these assemblies, the covalent attachment of chiral end groups, either through the incorporation of fused moieties or attachment through single bonds to terminal chain ends, has been explored. Qpty strands incorporating fused chiral (1*S*)-(-)- α -pinene end groups formed *M* and *P* helical complexes with Ag(I) (Figure 140).^{803–805} Diastereomeric excess in these complexes can shed light on the effect of interstrand steric interactions on the thermodynamics of helicate formation. It was found in CH₃CN that a 0.024:1.0 ratio (95.3% de) of complexes formed. Upon crystallization, only the major isomer was isolated which was identified as the *P* helix. The

(1*R*,1*R*)-(+)- α -pinene-terminated strand was also synthesized and proved to form the *M* helicate after crystallization. The origin of selectivity arose from interactions of the pinene end groups with the pyridine ligands in the backbone. Additionally, the Cu(I) helicates from this ligand formed in solution with 98.7% de, and after crystallization, again only the *P* helix was isolated. Qpty strands with thioethyl side chains and a methyl end group at the 4'-position were reacted with Cu(I) to produce a 3:2 mixture of the head-to-head (HH) and head-to-tail (HT) configurations, as evidenced by ¹H NMR (Figure 141).⁸⁰⁶ Variation of the side chain and the end group by systematically incorporating bulkier groups at these positions revealed no increased selectivity when groups such as ethyl or *tert*-butyl were employed as the end group while the thioethyl side chain remained.^{807,808} In the absence of a side chain, the *tert*-butyl-terminated quaterpyridine helicate formed the parallel HH configuration exclusively. All other cases resulted in a mixture of HH and HT with the HH configuration preferred. It was speculated that this preference was dependent on the electronic character of the side chain and the resulting helical pitch due to steric interactions between intrastrand substitutions at either the side chain or end group. Constable and co-workers^{809–811} utilized a terpyridine ligand coupled to (1*S*)-(-)-borneol at one terminus to impart

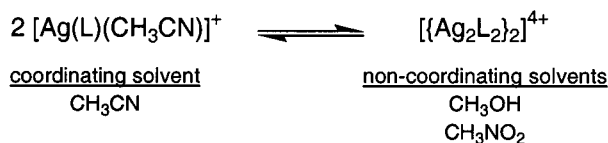
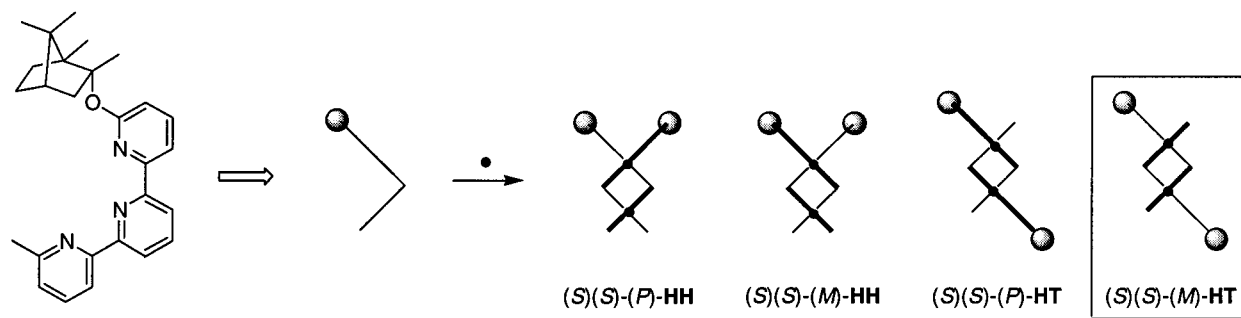


Figure 142. Solvent effects on the formation of helicate structures from a terpy strand. Head-to-tail double-stranded helicates obtained from borneol-terminated terpy ligands.

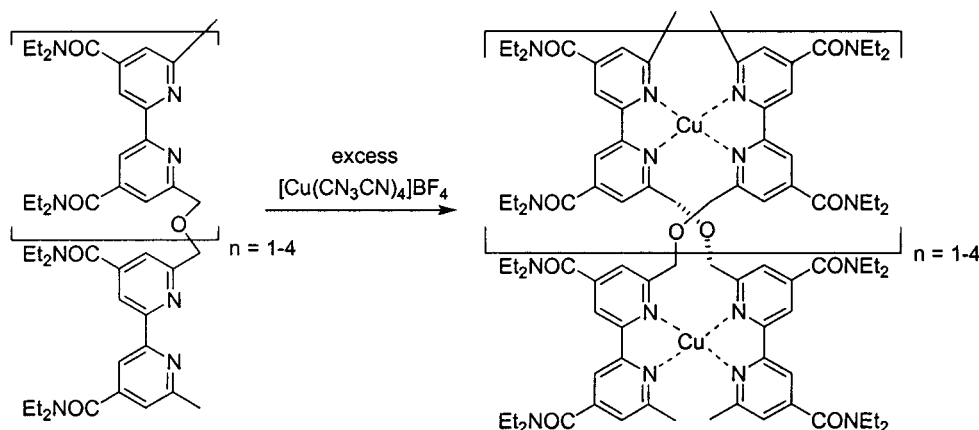


Figure 143. Formation of double-stranded helicates from bipyridine oligomers.

asymmetry in the helicate complex (Figure 142).⁸⁰⁹ Since this strand lacks a C_2 -symmetric axis, four possible helicate isomers may be realized. Molecular modeling studies revealed that the HH isomers are much higher in energy due to steric repulsion of the borneol units. Reaction of the ligands with $[\text{Cu}(\text{MeCN})_4][\text{PF}_6]$ formed a 6.5:1 ratio of two unidentified components in CH_3CN by ^1H NMR, presumably the two diastereomers of the HT configurations. Crystallization of this mixture produced only the major isomer, which was shown to be the $(S)(S)-(M)-\text{HT}$ by X-ray analysis. It is unclear why the M helix was favored over the P helix. With $\text{Ag}(\text{I})$, the equilibrium between the mononuclear complex and the dinuclear helicate could be shifted by the choice of solvent.⁸¹⁰ Acetonitrile solutions favored the mononuclear complex through competitive solvent coordination, while less coordinating solvents such as methanol and nitromethane favored the helical duplex, as confirmed by both ^1H NMR and CD.

2. Linked Oligopyridines

a. Ether-Linked Oligopyridines. The incorporation of flexible linkages within the backbone provides

oligopyridine-based chains that can adopt ideal, less constrained coordination geometries within helicate assemblies. One of the most thoroughly investigated systems involves the incorporation of methyl(methoxy) ether linkages between bipy or terpy segments. Initial chain-length studies showed these modified oligomers of varying length ($n = 3-5$) form homostranded helicates with $\text{Cu}(\text{I})$ ⁸¹² (Figure 143) and $\text{Ag}(\text{I})$ ⁸¹³ in CH_3CN .⁸¹⁴ To investigate self-recognition selectivity, a mixture of 2 equiv of the dimer, 1 equiv of the tetramer, and 3 equiv of $\text{Cu}(\text{I})$ produced only the homostranded complexes, demonstrating the preference for homostranded complexation.⁸¹⁵ Furthermore, a mixture of all four oligomers, upon addition of $\text{Cu}(\text{I})$, also formed only the homostranded double-helical structures after reaching equilibrium. Given the lack of heterostranded complexes, this system demonstrates length dependence and multinuclearity matching in the self-recognition process. This example further reveals the sensitivity of the association to alignment mismatches. Self-organization in the assembly of these strands has been shown to be cooperative.^{816,817} The attachment of thymine-nucleoside side chains to these oligopyridine strands produced a double helicate with nucleosides extend-

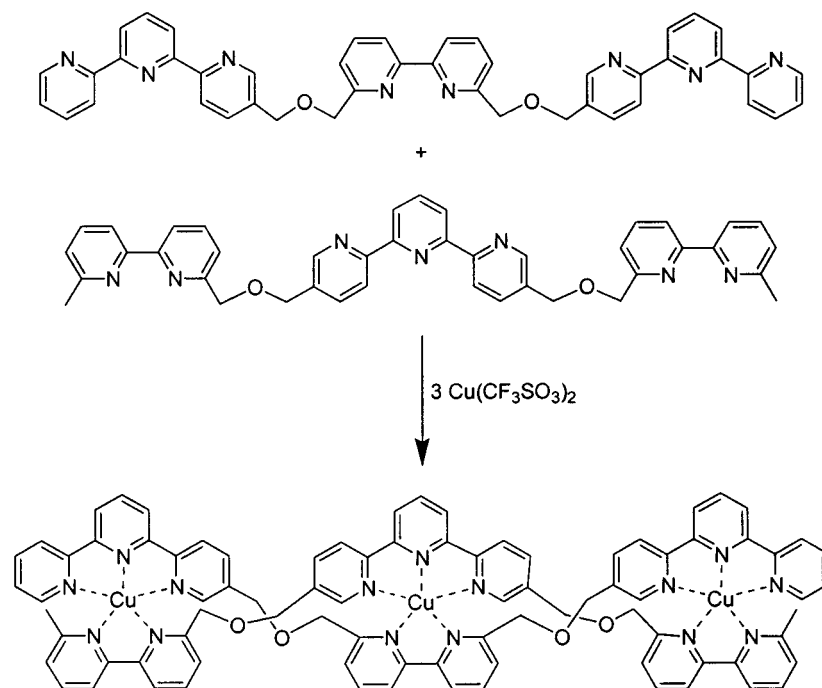


Figure 144. Heterostrand heterotopic double-stranded helicates from tpy-bipy-tpy and bipy-tpy-bipy trimers.

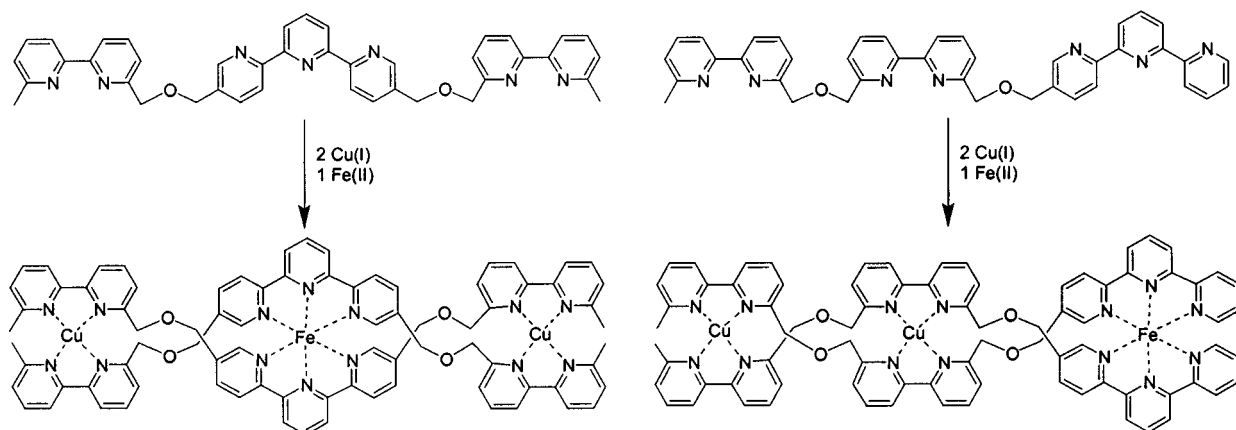


Figure 145. Heteronuclear double-stranded helicates from trimers incorporating bipy and tpy ligands.

ing out from the ionic interior,^{818,819} an architecture similar to one once proposed as the structure of DNA.⁸²⁰

A variety of heteromeric oligopyridine-based strands have been synthesized and complexed into helicates to assess the impact of non-bipy ligands on self-assembly. Two trimeric oligomer strands incorporating a bipy-tpy-bipy and a tpy-bipy-tpy oligomer were generated and complexed with pentacoordinate-preferring Cu(II) ions (Figure 144).⁸²¹ Only the heterotopic, heterostrand helicate was obtained after crystallization. These structures are reminiscent of DNA base matching in that the two separate strands encoded with complementary ligands form into a single complex through segment matching. Upon addition of 2 equiv of Cu(I) and 1 equiv of Fe(II), both bipy-tpy-bipy and bipy-bipy-tpy oligomers formed homostrand, heteronuclear helicates (Figure 145). Phen segments, having similar structure and denticity to bipy but lacking torsional flexibility, have also been incorporated into these oligomers, and double-stranded helicates were formed from Cu(I), Ag(I), and Zn(II) (Figure 146).⁸²² A more

systematic look at bipy/phen mixed trimers involved the synthesis of bipy₃, bipy-phen-bipy, phen-bipy-phen, and phen₃ trimers complexed with Cu(I) and Ag(I) (Figure 147).⁸²³ The homooligomeric phen sequence formed a double-stranded helicate with Cu(I), although a mixture of helicate complexes resulted upon addition of Ag(I). An excess of Ag(I) shifted the equilibrium toward the double-helical complex completely. The heterotopic strand of phen-bipy-phen formed double-stranded helicates with both Cu(I) and Ag(I), indicating that the central unit in the ligand may influence the stability of the helicate through steric interactions.

To probe heterostrand helicate formation, mixtures of these four ligands under helicate-forming conditions were tested (Figure 148). It was found that whether the ligands were mixed prior to ion addition or helicate solutions were mixed together, the heterostrand helicates were thermodynamically favored providing statistical (1:2:1) helicate distributions. Further investigation into the role of the central unit in double-stranded helicates from trimers allowed determination of binding affinity by cyclic voltam-

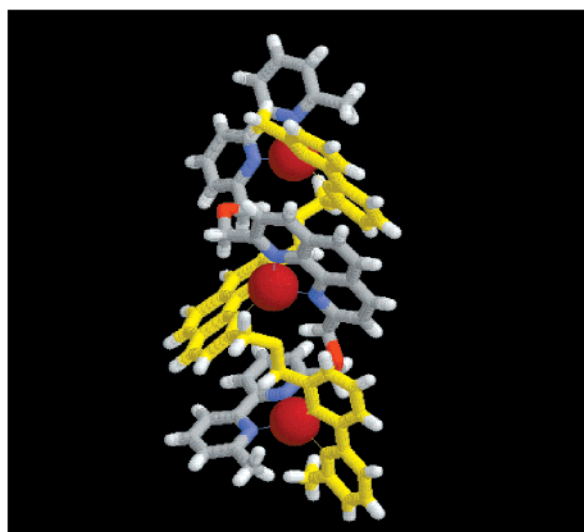
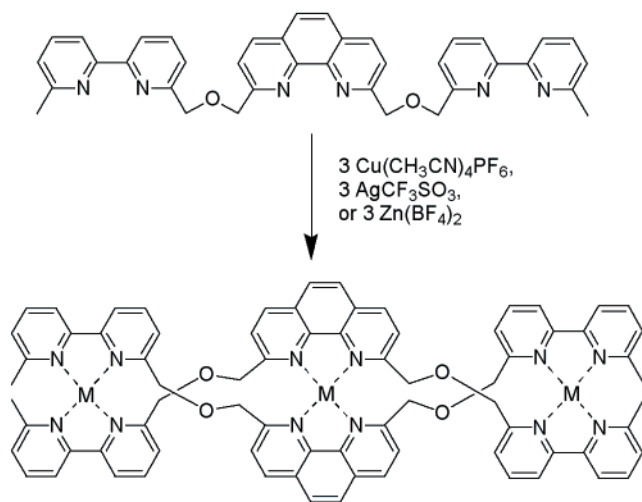


Figure 146. Homotopic helicates from a bipy-phen-bipy trimer. The crystal structure of the Cu(I) complex is shown.⁸²²

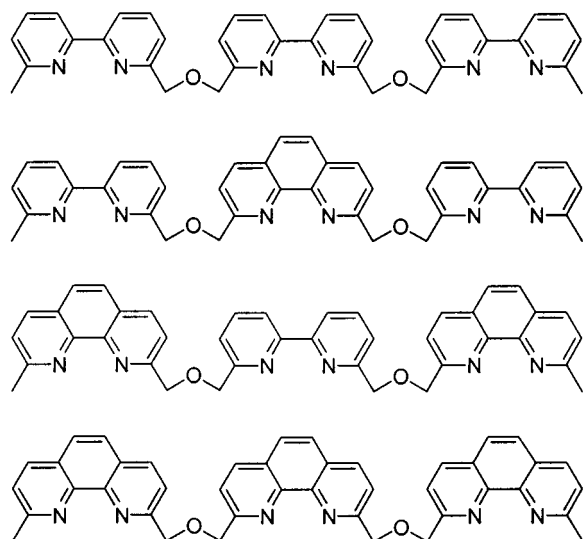


Figure 147. Four trimers consisting of bipy and phen segments.

metry for a series of four different ligands.⁸²⁴ It was found that the central phenanthroline unit in a trimeric ligand binds to Cu(I) 10 times more strongly than a bipy unit and 10^6 times more strongly than a

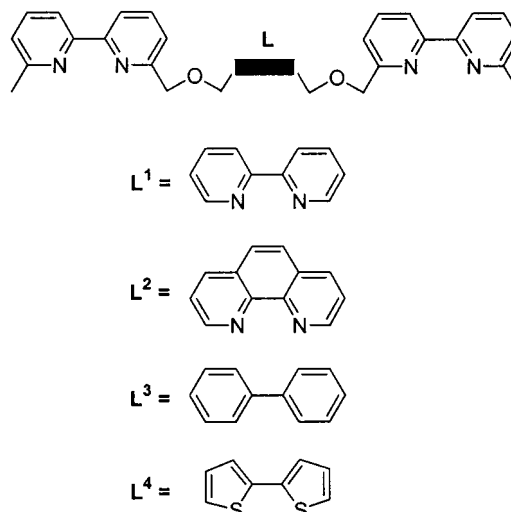


Figure 148. Four trimers consisting of bipy-L-bipy segments.

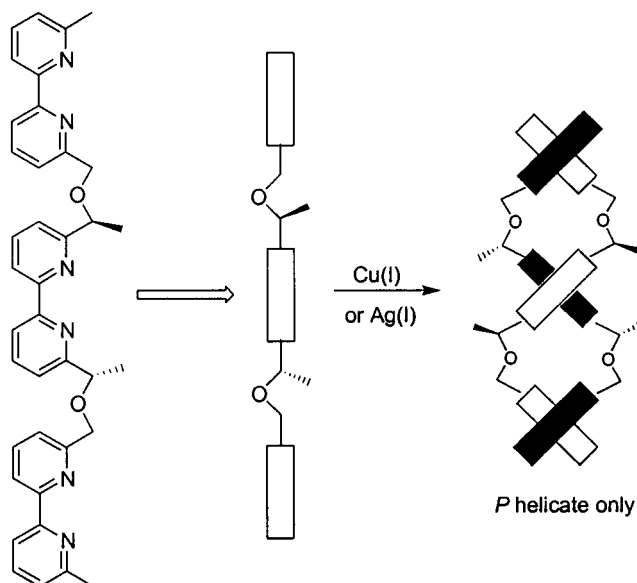


Figure 149. *P* double-stranded helicate from a bipy trimer incorporating stereogenic centers within the linkers.

bithiophene unit. Self-recognition in these ligands was demonstrated by mixing the bipy with either bithiophene- or phen-containing oligomers, where only the homostanded helicates were obtained. However, a mixture of the phen- and the bipy-containing oligomers produced homo- and heterostanded helicates in a statistical 1:2:1 distribution. These results suggest that the Cu(I) ion preferentially binds to two weaker chain segments (bithio) rather than one strong and one weak one. From these investigations, sequence matching in heterotopic helicate formation emerges as an approach to encoding helicates with structural information in recognition processes.

The linked oligopyridine-based foldamers described thus far lack any asymmetric functionalities able to shift the *P* and *M* helical equilibrium. The first report attempting to bias the twist sense of a helicate involved chiral ether linkages to a bipy₃ strand (Figure 149).⁸²⁵ When these oligomers were complexed with 3 equiv of either Cu(I) or Ag(I), only the *P* helicate was obtained. In this conformation, the

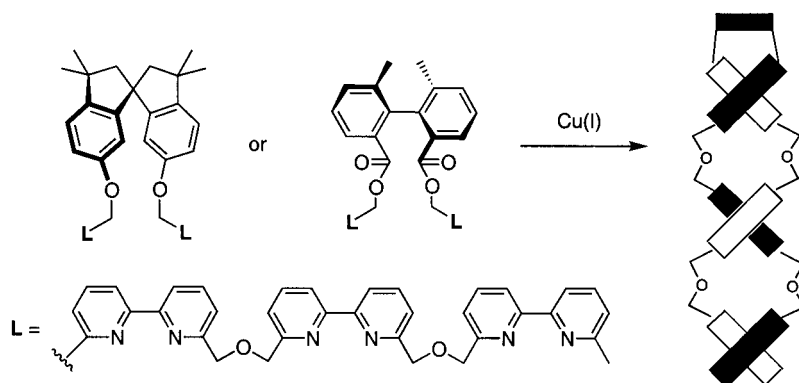


Figure 150. Bipy trimers tethered by chiral bridges.

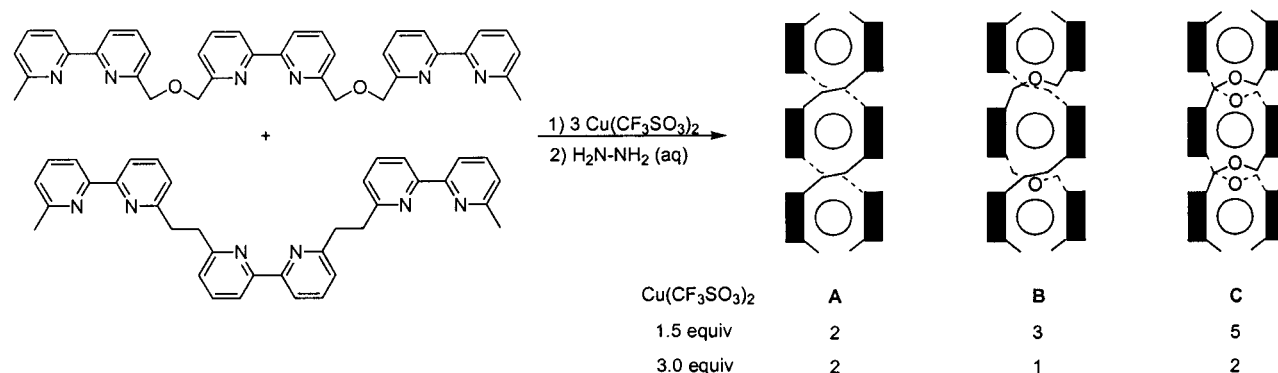


Figure 151. Homo- and heterostranded helicates from two different bipy strands.

methyl groups extend outward to minimize steric repulsions. Rigid, chiral bridges such as spirobisindanol or dimethylbiphenic acid, tethering two bipy₃ oligomers, can effectively bias the twist sense of a Cu(I) helicate by dictating the absolute configuration of the strands through more rigid constraints (Figure 150).^{826,827}

b. Alkyl-Linked Oligopyridines. With the success of the ether-linked bipy helicates, other linkages involving ethyl- and ethylene-linked bipy trimers were explored.⁸²⁸ Oligomers incorporating the alkene spacer did not produce a discrete double-stranded helicate with Cu(I) as evidenced by ¹H NMR, due to the lack of flexibility in the backbone. On the other hand, the ethyl-linked strands were effectively incorporated into the complex. An imine linker has also been utilized to form double-stranded helicates with Cu(I) and Ag(I).⁸²⁹ When the alkyl- and ether-linked oligomers were mixed under helicate-forming conditions to test for recognition, a mixture of homo- and heterostranded complexes was formed in a ratio of 2:2:1 (Figure 151). At equilibrium, the homostranded helicate is favored over the heterostranded helicate, deviating from the statistical distribution, presumably due to the electrostatic attraction between the oxygen and Cu(I) ions and the lower flexibility of the ethyl linker. Furthermore, ethyl-linked bipy₃ strands formed triple-helical complexes with Ni(II),⁸³⁰ while ethyl-linked tpy₃ complexed with Fe(II) produced double-stranded helicates,⁸³¹ where both complexes formed through octahedral coordination geometries. To test the self- vs nonself-recognition selectivity between the ether and alkyl bipy strands, Cu(I) and Ni(II) were added to a mixture of these two oligomers (Figure 152).⁸¹⁵ These trimers self-assembled

into two discrete homostranded helicates: a double-stranded, tetrahedral Cu(I) complex with the ether-linked strand and a triple-stranded, octahedral Ni(II) complex incorporating the alkyl-linked strand. No heterostranded species were observed by ¹H NMR or ESI-MS. Here, the end groups of the strands, as well as the nature and length of the linker group between the ligands endow the oligomer with structural information that directs the self-assembly process. The power of self-recognition processes in the formation of highly organized structures is clear in this case: 11 chemical components of four types (two organic oligomers and two transition-metal ions) combine to form two discrete supramolecular species. At the same time, the ether-linked bipy₃ and the ethyl-linked tpy₃ oligomers formed a heterostranded helicate which was able to form through complexation with Cu(II) (Figure 153).⁸³² Although the Cu(II) ion prefers a pentacoordinate geometry, trigonal bipyramidal and square pyramidal coordination are both possible. In this case, the central copper coordination adopted a trigonal bipyramidal geometry while the terminal ends of the strands coordinate to the terminal copper through square pyramidal orientations as evidenced by X-ray analysis. This occurs since the steric demands at the termini are not as stringent as the central segments.

When the ethyl-linked bipy₃ oligomer was combined with an equimolar quantity of FeCl₂ in ethylene glycol at 170 °C, a pentameric circular helicate was exclusively produced (Figure 154).⁸³³ This complex is believed to form from templation by the Cl⁻ counterion. Further investigations into this system with a variety of counterions revealed a second

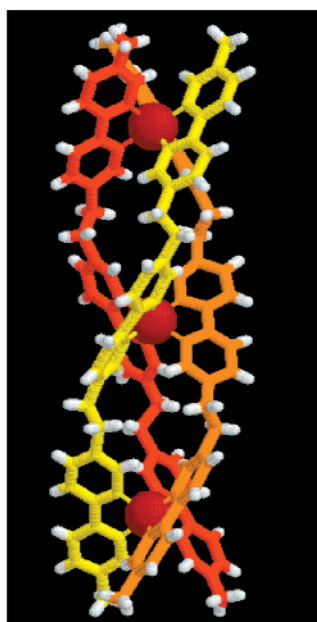
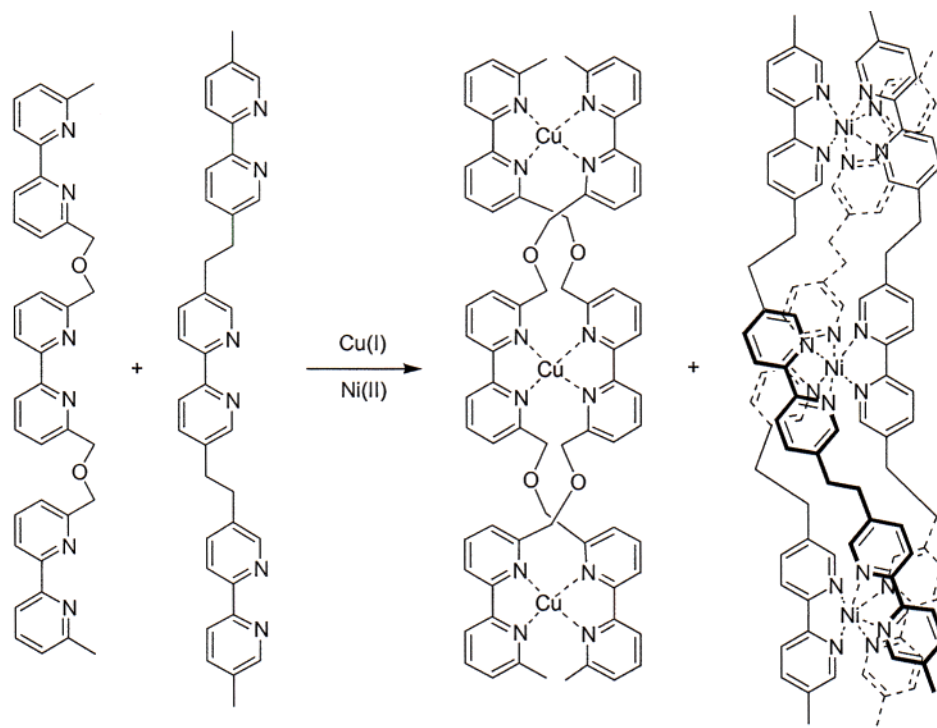


Figure 152. Formation of only homostranded helicates from a mixture of two different bipyridine trimers. Crystal structure of the Ni(II) triple-stranded helicate with the alkyl-linked trimers is shown.⁸⁷⁸

circular helicate, the hexameric complex, in which the counterion is believed to also bind in the central cavity.^{834,835} When a hexanuclear circular helicate prepared using FeSO_4 was heated in the presence of Cl^- , ^1H NMR and ES-MS analysis revealed the shift to the pentameric circular helicate exclusively. This indicates that the Cl^- ion can selectively template the pentameric assembly from the equilibrating mixture of complexes. Investigations into the mechanism of this circular helicate formation revealed that the kinetic product of this reaction is the linear triple-stranded helicate, which over the course of 24 h reassembles into the thermodynamic product, the pentameric circular helicate.⁸³⁶ Similar results were obtained with the use of NiCl_2 under conditions that

accelerated the dissociation of the metal complexes. In this case, a 2:1 ratio of the circular vs the linear Ni(II) species was obtained after a period of 4 days, at which point strand decomposition became a factor. Hence, the additional flexibility of the alkyl linkage within the backbone provides the torsional freedom in the chain necessary to adopt a variety of conformations within the various helicate complexes.

3. Pyridine Analogues

A variety of helicates incorporating pyridine-based analogues have been described in the literature including methylene-linked benzimidazoles⁸³⁷ and their derivatives,^{838–840} bis(phenyloxazoliny)pyridines,^{841,842} bis(pinene-bpy) ligands,⁸⁴³ and bis-imino-

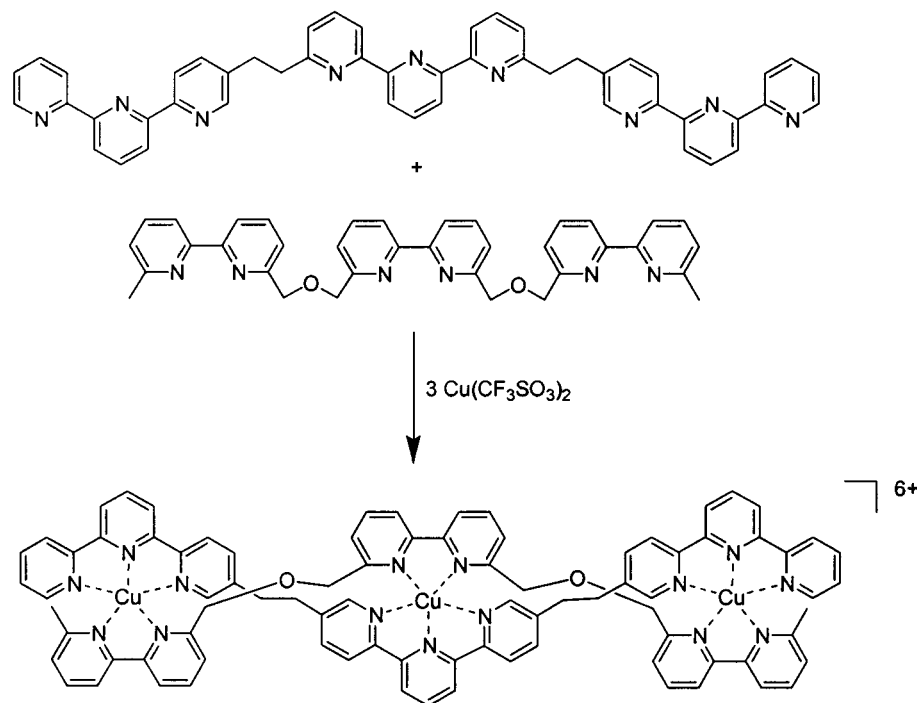


Figure 153. Formation of heterostranded helicates from a bipy trimer and terpy trimer.

quinolines.^{844,845} While these ligands effectively form helicates with a variety of metal ions, we do not consider them as foldamers since it is difficult to envision how their chain lengths may be easily extended, a similar criteria that was used for ruling out many of the receptor systems. Since they do not satisfy our criteria for foldamers, we will not discuss them further (some of these systems have been discussed in recent reviews⁴⁵⁷). However, dipyrromethene oligomers, structurally isomorphous to the phytychromobilins,⁸⁴⁶ have been recently shown to form double-stranded helicates with Zn(II) and Co(II), where a hexameric strand complexes to Zn(II) in a 3:2 ratio (Figure 155).⁸⁴⁷ The oligomers have also been extended to incorporate alkyl spacers of varying length.^{848,849}

4. Catecholates

Catecholates also have the ability to form helicates when complexed to gallium and titanium metal ions.^{455,457} Investigations into the effect of spacer length (and the distance between the metal ions) on self-recognition were conducted with catecholamide ligands.⁸⁵⁰ Ditopic ligands with three different aromatic spacers were synthesized and complexed with Ga(III) to form triple-helical structures (Figure 156). A 1:1:1 mixture of the three ligands with Ga(III) provided only the homostranded helicates as evidenced by ¹H NMR and ESI-MS. The authors argue that the self-recognition process is a combination of effects whereby the helicate structure is favored over polymeric structures due to an entropic driving force disfavoring the polymeric structure, the rigid spacers disfavoring heterostranded helicate formation, and the presence of an energetic drive to fully saturate the coordination sphere of Ga(III). In this mixture, the lack of flexibility in the spacer promotes formation of only the homostranded helicates, since spatial

mismatching could only be compensated by higher order strand incorporation. Variable temperature ¹H NMR studies revealed a dynamic rearrangement involving a twist sense reversal within these triple helicates wherein one or more strands pass through a *meso* state in which the strands adopt a parallel, fully extended conformation.^{851,852} Related dimeric catecholamides form triple-helical complexes with either Ti(III) or Ga(III). Yet, upon the addition of Me₄N⁺, these complexes are interconverted to a tetrahedral cluster in order to provide the necessary cavity space to accommodate the cationic guest (Figure 157).^{853,854}

Self-recognition processes have also been demonstrated to coincide with template-driven helicate formation.⁸⁵⁵ Dimeric catechol-derived strands, previously shown to bind Li⁺^{856,857} or Na⁺⁸⁵⁸ within triple-stranded helicates, were synthesized with methylene and ethylene spacers, and the mixtures were coordinated to “Ti(IV)” in the presence of different carbonate bases to form triple-stranded helicates. When the helicate was prepared using Na₂CO₃, only the homostranded species were observed. Upon addition of Li₂CO₃, both homostranded species were observed along with a heterostranded species (2 methylene + 1 ethylene strand). When K₂CO₃ was used, the ethylene strands formed dinuclear helicates while the methylene bridged ligands formed indistinguishable higher oligomeric species. Interestingly, when 1:1 mixtures of the bases were utilized, only the homostranded helicates formed. It is worth mentioning that a nonaromatic backbone has also been incorporated into a double-stranded helicate.⁸⁵⁹

D. Multistranded Receptors

Foldamer duplex receptors that assemble through multimodal interactions have been developed in order to generate supramolecular host assemblies for

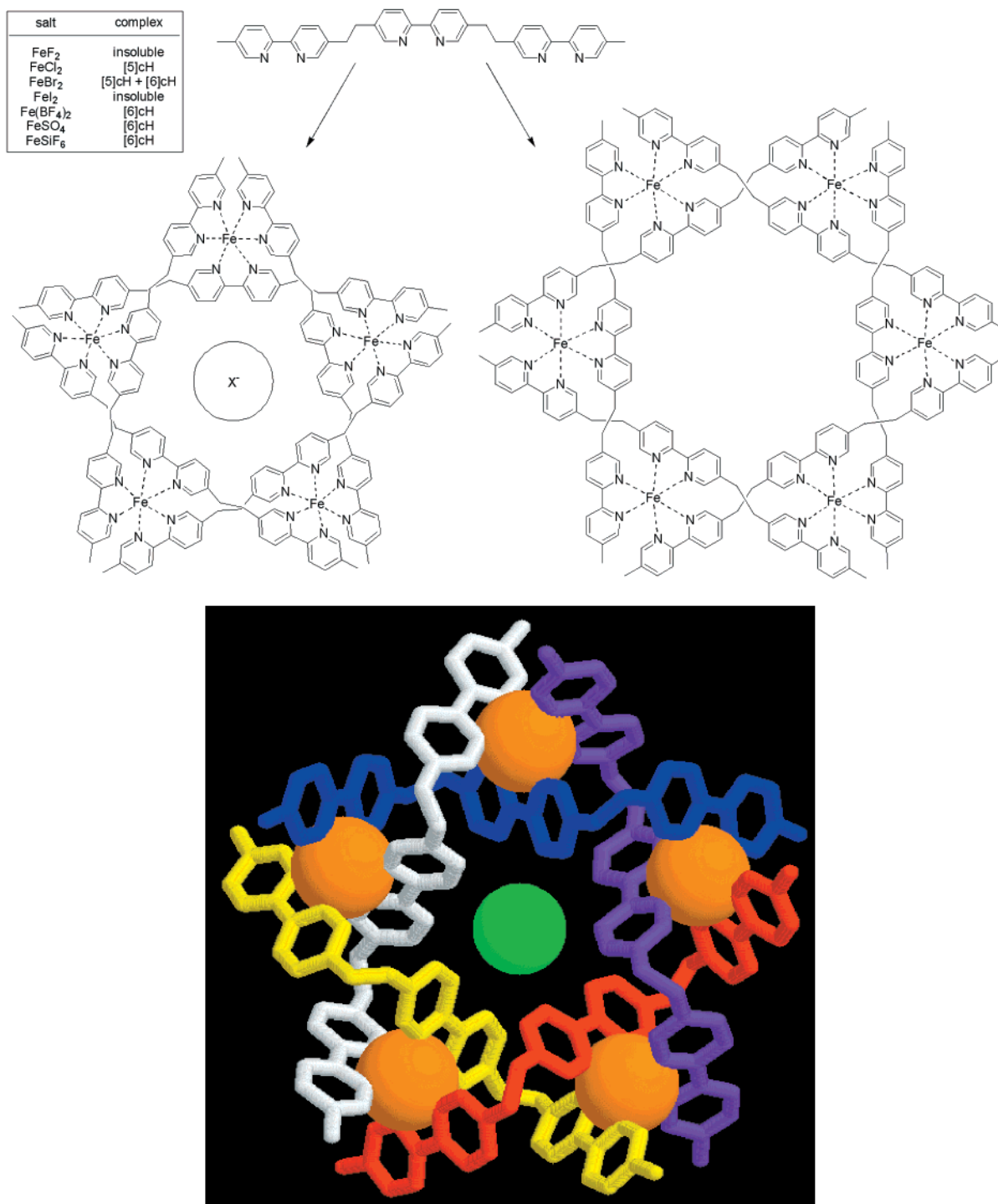


Figure 154. Penta- and hexameric cyclic helicates formed through host–guest templation. The crystal structure of the pentameric complex is shown.

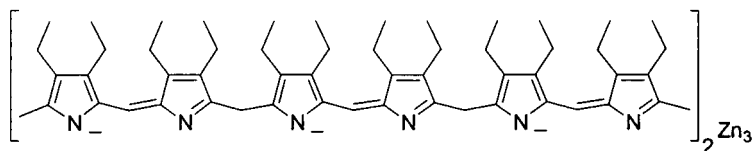


Figure 155. Dipyrromethene double helicates.

molecular recognition of small organic guests.^{114,860} This has been accomplished through the use of heterotopic strands with metal-coordinating ligands and D/A segments such that self-assembly occurs through multiple, noncovalent interactions between

two oligomer chains, a metal ion, and an organic guest. In this way, the metal-coordinating segments are conformationally restricted in the complex while the D/A segments have the torsional flexibility to potentially accommodate structurally diverse guests.

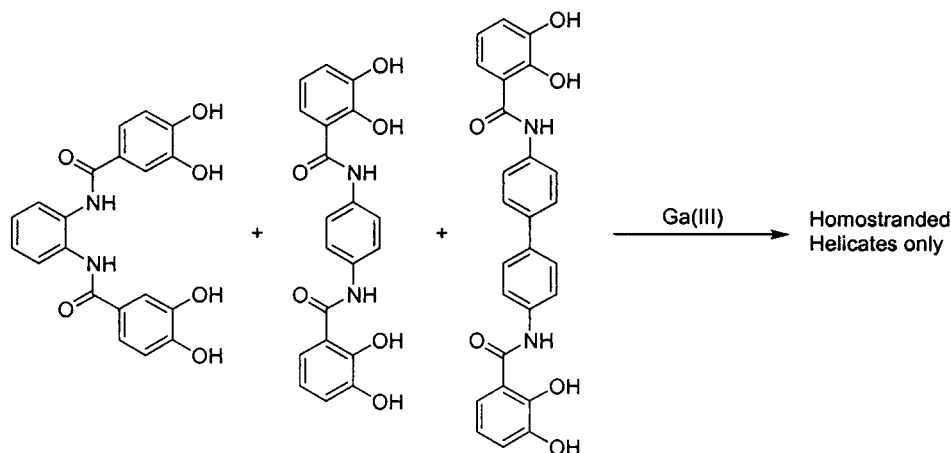


Figure 156. Homostranded helicates from catecholate strands with three different spacers.

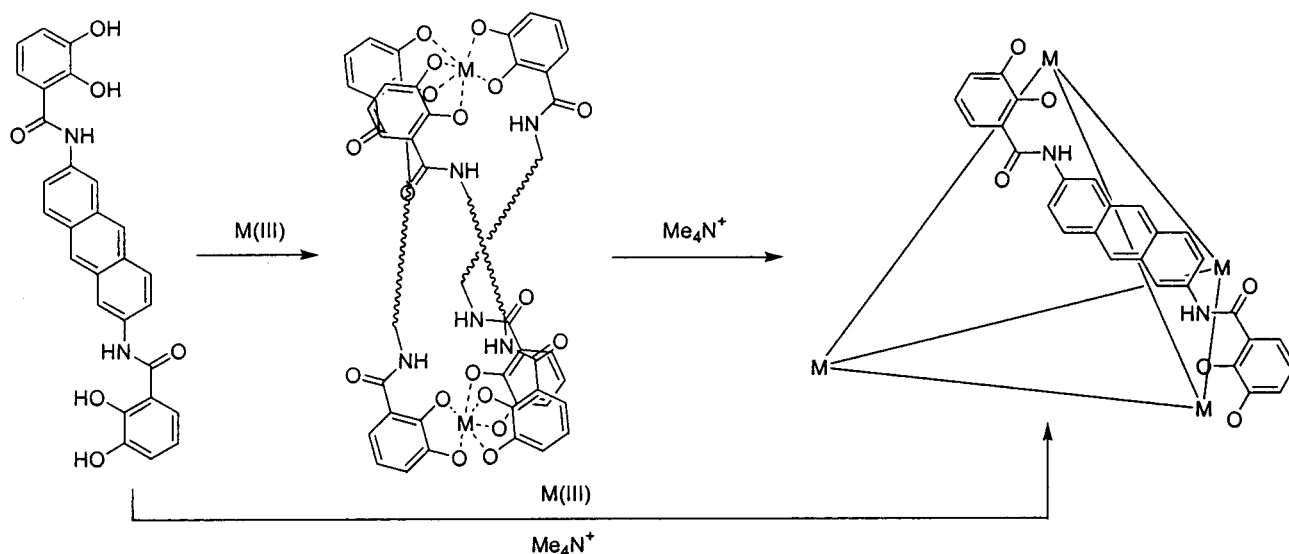


Figure 157. Formation of a triple-stranded helicate and a tetrahedral cluster from catecholate dimers.

These architectures are more commonly referred to as artificial receptors while at the same time fitting under the categorization of foldamer duplexes since they adopt their unique conformations through these noncovalent interactions and form similar architectures as described in the previous two sections on multistranded abiotic foldamers.

In a series of experiments aimed at guest-induced equilibrium shifting of metal-coordinated assemblies, bis(carboxamidobipyridine) ligands with ^tBu **80** (R = Me or H) and with DAD H-bonding caproylpyridyl **81** (R = Me or H) peripheral groups were complexed with Cu(I) and Pd(II) ions to form double-stranded, tetracoordinate complexes (Figure 158).⁸⁶¹ Through the addition of complementary (ADA) guests with varying degrees of flexibility (**82–86**) in the presence of **80** and **81** (both R = Me), a shift in the equilibrium from the **80:80** to the **81:81** complex was promoted through H-bonding in the guest assembly. Guests **82** and **84** are rigid, while **83**, **85**, and **86** have various numbers of single bonds, which increases their torsional flexibility. With 0.5 equiv of Cu(I), **80** (1 equiv) and **81** (1 equiv) formed distorted tetrahedral complexes in chloroform, and by ¹H NMR, the degree of uncomplexed ligand was determined to be 27% of **80** and 73% of **81**. Upon addition of **82**, **83**,

84, or **85**, no shift in the equilibrium was observed though shifts in the NMR indicated H-bonding interactions between **80** and the guests. However, with the addition of **86**, the proportions of the free ligands were shifted to 48% of **80** and 52% of **81** through simultaneous H-bonding between two strands and this bridging guest. When similar Pd(II) complexes formed with **80** and **81** (where R = H) in 5% DMSO in CHCl₃, a square-planar coordination geometry arranges the strands in a coplanar orientation, thereby suggesting a planar, rigid guest could possibly shift the equilibrium toward the host–guest assembly. Binding of the guest shows the ability of each guest to enhance the formation of complexes, as indicated by the proportions of ligands involved in complexes determined by ¹H NMR. Guest **82** is capable of concurrently H-bonding to each strand and stabilizing the **81:81**:Pd(II) complex (even enhancing the shift at lower temperatures).

E. Foldamer–Oligomer Interactions

As the final section of this review, we wish to present more advanced examples of foldamer architectures that lay the foundation for the development of backbones capable of homo- or heterostranded foldamer–foldamer interactions seen with natural

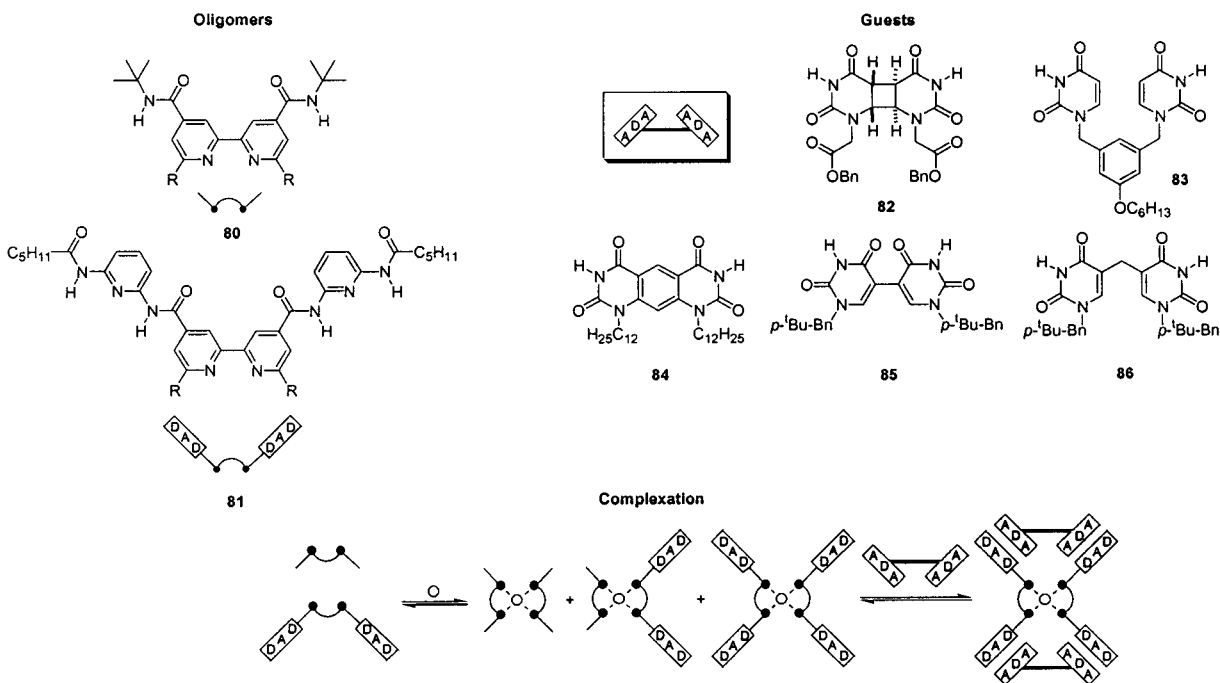


Figure 158. Multistranded receptor formation through H-bonding and metal coordination.

systems (i.e., protein–protein or protein–DNA interactions). This requires two structurally different backbones to associate through recognition processes embedded in the surfaces of their folded conformations. To date, natural systems that adopt secondary structures and *template* the association and folding of small oligomers (or segments of homomorphous backbones) have only been accomplished. These are best described as foldamer–oligomer interactions and provide insight into this next step within the foldamer field.

1. Minor Groove Binding Oligomers

Major groove binding of oligonucleotide variants through triplex formation has been discussed in terms of stability and sequence selectivity. The folding reaction considered here is one in which complexation induces conformational order in an unstructured oligomer. Yet, no nonnucleotidomimetic foldamers have been demonstrated to target the major groove,⁸⁶² suggesting the potential of this unexplored area. However, the minor groove of DNA duplexes offers crucial sites for noncovalent supramolecular recognition, as demonstrated by recent X-ray crystal structures of DNA polymerase:ds-DNA complexes.^{863–865} Although studies aimed at elucidating protein–oligonucleotide interactions are currently being investigated with nucleotidomimetics,^{866–868} we limit our discussion here to members of the lexitropsin and duocarmycin antibiotics, which have shown considerable progress in adapting these systems for more complex sequence recognition.

a. Lexitropsins. The lexitropsin class of natural oligo(*N*-methylpyrrolicarboxamide)s, isolated from *streptomyces* strains,⁸⁶⁹ binds in the minor groove of duplexed DNA through a combination of van der Waals' contacts, H-bonding, hydrophobic, and electrostatic interactions. Distamycin-A is a crescent-shaped, amide-linked *N*-methylpyrrole oligomers with

guanidinium and formyl termini that shows preferential binding to AT-rich sequences in 1:1 and 2:1 stoichiometries with ds-DNA (in antiparallel orientations) (Figure 159). NMR studies have determined that in a distamycin-A:d(CGCGAATTCGCG)₂ complex, two of the pyrroles (Py) remain planar while the third ring rotates to conform to the minor groove twist.⁸⁷⁰ The first chain-length studies ($n = 1–6$) on modified distamycins effectively demonstrated the ability to extend the minor groove sequence recognition of small oligomeric molecules.^{871,872} Through incorporation of imidazoles (Im)⁸⁷³ and hydroxypyrrroles (Hp)⁸⁷⁴ into lexitropsin oligomers, pairing rules for minor groove binding have been ascertained: Py/Im targets C–G, Py/Hp targets A–T, Hp/Py targets T–A, and Im/Py targets G–C.⁸⁷⁵ Since lexitropsin backbones cannot effectively coil around oligonucleotide duplexes at chain lengths higher than five, incorporated β -alanine units add flexibility to the oligomer and also enhance sequence recognition.⁸⁷⁶ Linking of lexitropsin oligomers by γ -butyric acid tethers allow the 2:1 binding mode to become a unimolecular process, thereby enhancing affinity by ca. 100.⁸⁷⁷ A single substitution of imidazole for pyrrole in a lexitropsin hairpin structure showed a decrease in affinity of 2 orders of magnitude, demonstrating the efficient mismatch discrimination in these oligomers.⁸⁷⁸ This field has expanded exponentially, primarily due to the work of the Dervan group, since the development of solid-phase synthetic methodologies.⁸⁷⁹ Since this field has been thoroughly reviewed elsewhere,^{875,880–883} here we only mention the lexitropsins to draw their connection to the field of foldamers; that is, they adopt their unique conformations by undergoing a folding reaction through complexation with the ds-DNA minor groove. Hence, conformational stability is derived by intermolecular noncovalent interactions.

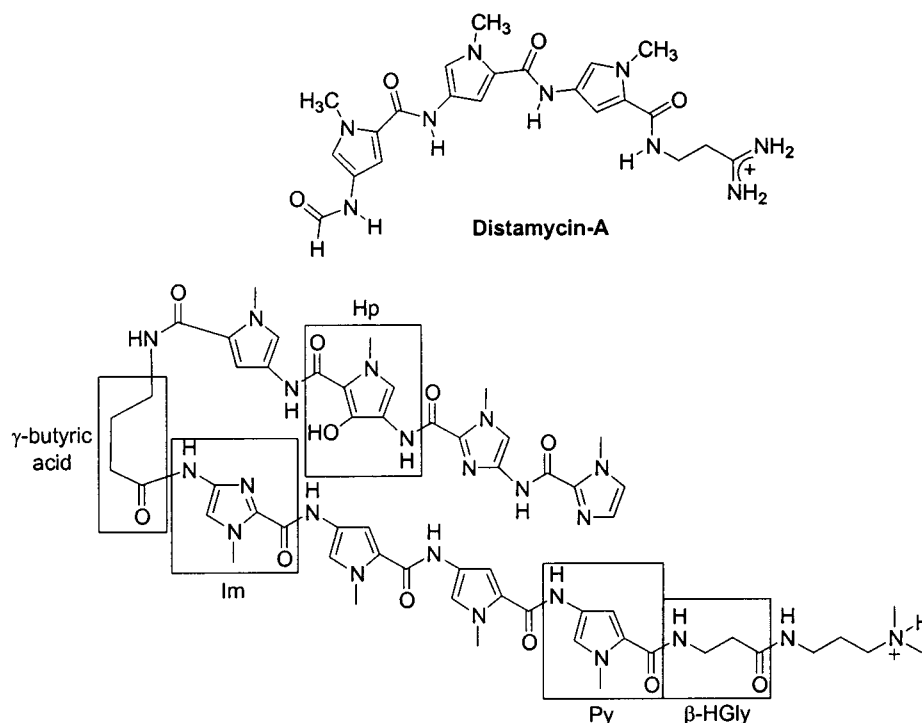


Figure 159. Chemical structure of distamycin-A and an oligomeric analogue.⁸⁷⁵

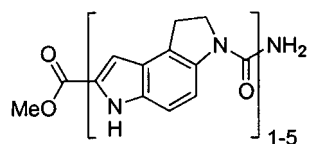


Figure 160. Series of homooligomeric (+)-CC-1065 analogues used to probe the minor groove binding of duocarmycin.

b. Duocarmycins. (+)-CC-1065, isolated from *Streptomyces zelensis*,^{884,885} and the related duocarmycins are a thoroughly investigated class of potent antitumor antibiotics.^{886–889} Their cytotoxic activity occurs from an alkylation of adenine via an adenine-N3 ring-opening S_N2 attack on the cyclopropapyrroloindole (DSA) when bound in the AT-rich nucleotide stretches of the B-DNA minor groove.^{886,887,889} These agents are concave, relatively planar molecules⁸⁹⁰ capable of penetrating the deep and narrow minor groove of an AT-rich complex for alkylation by adopting a conformation that extends along the 5'→3' DNA backbone.^{891,892} Duocarmycin analogues aimed at elucidating the structural origin of the sequence-selectivity and noncovalent binding focused on the generation of homooligomers ($n = 1–5$) to mimic the properties of (+)-CC-1065 (Figure 160).^{893,894} Thermal incubation and denaturation studies of an oligomer series with poly(dA):poly(dT) under approximate physiological conditions revealed increased binding affinity at higher chain lengths, though the kinetic accessibility decreased with increasing length due to the higher entropic costs of organizing longer chains. Initial complexation of the tetramer with ds-DNA associated through a dimeric segment, followed by a much slower rearrangement to the fully complexed conformation, consistent with high-energy rotational barriers predicted by molecular modeling. The most optimal agent for minor groove complexation was the

five base-pair spanning trimer, effectively combining favorable kinetic and thermodynamic properties. This complex is stabilized through hydrophobic and van der Waals interactions, allowing deep penetration into the narrow groove of an AT-rich sequence.

A thorough examination of numerous structural studies aimed at probing the relationship between (+)-CC-1065 minor groove binding and catalytic adenine alkylation revealed a binding-induced conformational change that effectively activates the ligand for nucleophilic attack.⁸⁹⁵ In order for the ligand to bind deep in the AT-rich minor groove to maximize hydrophobic and van der Waals interactions, the ligand is forced to adopt to the intrinsic helical twist of ds-DNA. This is possible only through a torsional rotation between the nitrogen and the carbonyl of the amide, which subsequently destabilizes the ligand ground state by diminishing the vinylogous amide conjugation. Thus, through the noncovalent interactions that promote this unique, folded conformation of (+)-CC-1065 within the complex, the reactivity of the ligand is enhanced.

2. Peptide–Oligomer Complexes

In biological systems, protein–ligand interactions are crucial to molecular recognition and are dominated by noncovalent interactions and conformational matching. Chain molecules capable of interacting with peptides or proteins have targeted their macromolecular surfaces for binding, since active sites of receptors are typically shallow and therefore the extension to longer chains is not possible. Additionally, these exterior surfaces do not typically have repeating functionalities of the same type such that a chain could make regular noncovalent contacts over a long range. These systems have similarity to DNA minor groove binding oligomers where the folding of an oligomer is templated by the folded

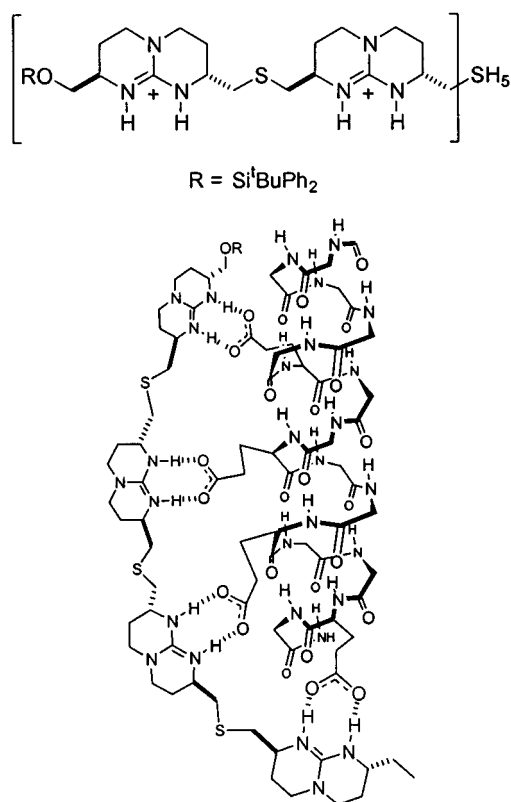


Figure 161. Tetraguanidinium chain bound to aspartate side chains of an α -helical peptide. Charges have been omitted for clarity.

conformation of a completely different backbone. This type of complex hints at foldamer–foldamer interactions that have yet to be demonstrated with two different backbones.

Cationic guanidinium oligomers capable of forming duplexes with peptides containing carboxylate side chains have been developed to interact with the α -helical surface through electrostatic and hydrogen-bonding interactions.^{896–898} When dimeric or tetrameric guanidinium oligomers were mixed with a hexadecameric peptide containing aspartate and asparagine side chains in every third position in 10% H₂O in MeOH, an increase in the CD intensity associated with increased α -helicity was observed. NMR experiments confirmed interstrand interactions as well as the induced α -helical conformation of the peptide (Figure 161).⁸⁹⁶ Further studies revealed that the tetraguanidinium oligomer interacts specifically with the anionic carboxylates extending from the helical peptide.⁸⁹⁷ Increased length of the peptidic side chains from aspartates to glutamates led to lower binding strengths, indicating the importance of a more rigid surface for proper alignment within the guanidinium–peptide complex.⁸⁹⁸

VIII. Conclusion

This review has surveyed the field of foldamers—the study of conformational control in synthetic chain molecules. The products of this field are new oligomeric backbones that adopt a particular type of secondary structure through noncovalent interactions. In this review, we have provided examples of

the secondary structure types schematically represented in Figure 1. When one looks deeper into the chemical details making up these secondary structures, what emerges to date is that only a relatively small number of “good folders” have as of yet been identified. Clearly, there is a long road to travel before “masterpiece sequences” of tyligomers are routinely produced. Yet, even with the limited examples of good folders that are known, one can also conclude that nature is now not alone; at least in terms of structure, we can now point to synthetic chains that begin to approach the order seen in nature’s conformationally structured molecules.

When contemplating new foldamers, it will be instructive to remember the qualities that are common to the good folders. One aspect is the proper balance of flexibility and rigidity within the backbone, defined by the number of torsional degrees of freedom per repeat unit and the torsional potential energy surfaces. Another aspect is the type, strength, location, and number of attractive and repulsive noncovalent interactions that stabilize the desired conformation while destabilizing the energetically accessible but unwanted conformations. In short, the crux of foldamer design and the accompanying folding reaction hinges on the tradeoff between entropy and enthalpy.

Hydrogen bonds and metal coordination bonds have been the mainstay of the supramolecular chemist when it comes to the intentional manipulation of noncovalent interactions. However, nature’s examples teach us the power of using weak, non-directional interactions to stabilize the folded state and deepen the folding funnel. Thus, van der Waals and solvophobic interactions are crucial to foldamer design, although they have been scarcely utilized in synthetic systems. In the simplest sense, such input is realized by incorporating amphiphilic character into the chain.

The long-term future—function through tyligomers—is easy to envision, but plotting a course of action is fraught with difficulty. While oligomeric-sized molecules are relatively easy to generate, the preparation of high molecular weight heteropolymers of a specific sequence represents one of today’s greatest unsolved synthetic challenges. Until this barrier can be overcome, there are certainly valuable properties to be found and fundamental discoveries to be made in the foldamers themselves. At least for today, the oligomer—the chemist’s middle child—comes to the fore.

IX. Acknowledgments

The authors thank members of the Moore group for suggestions and comments as well as J. Gray, D. Loudermilk, and N. Nathan and for their artistic contributions. Work from the authors’ laboratory was supported by grants from the National Science Foundation (NSF CHE 00-91931) and the Department of Energy (DEFG02-91ER45439).

X. References

- (1) Kepler, J. *Mysterium Cosmographicum*; Tuebingen, 1596.
- (2) Bernal, J. D.; Crowfoot, D. *Nature* **1934**, *153*, 794–795.

- (3) The word was coined by Gellman and first published in ref 32.
- (4) Gellman, S. H. *Acc. Chem. Res.* **1998**, *31*, 173–180.
- (5) Deshayes, K.; Broene, R. D.; Chao, I.; Knobler, C. B.; Diederich, F. *J. Org. Chem.* **1991**, *56*, 6787–6795.
- (6) Paruch, K.; Katz, T. J.; Incarvito, C.; Lam, K.-C.; Rhatigan, B.; Rheingold, A. L. *J. Org. Chem.* **2000**, *65*, 7602–7608 and references therein.
- (7) Green, M. M.; Park, J. W.; Sato, T.; Teramoto, A.; Lifson, S.; Selinger, R. L. B.; Selinger, J. V. *Angew. Chem., Int. Ed. Engl.* **1999**, *38*, 3138–3154.
- (8) Lin, L. N.; Brandts, J. F. *Biochemistry* **1980**, *19*, 3055–3059.
- (9) Noe, C. R.; Miculka, C.; Bats, J. W. *Angew. Chem., Int. Ed. Engl.* **1994**, *33*, 1476–1478.
- (10) Nakano, T.; Okamoto, Y.; Hatada, K. *J. Am. Chem. Soc.* **1992**, *114*, 1318–1329.
- (11) Mattice, W. L.; Suter, U. W. *Conformational Theory of Large Molecules*; John Wiley & Sons: New York, 1994.
- (12) Gange, D.; Magnus, P.; Bass, L.; Arnold, E. V.; Clardy, J. *J. Am. Chem. Soc.* **1980**, *102*, 2134–2135.
- (13) Kiupel, B.; Niederalt, C.; Nieger, M.; Grimme, S.; Vögtle, F. *Angew. Chem., Int. Ed. Engl.* **1998**, *37*, 3031–3034.
- (14) Fujii, K.; Furuta, T.; Tanaka, K. *Org. Lett.* **2001**, *3*, 169–171.
- (15) Chan, H. S.; Bromberg, S.; Dill, K. A. *Philos. Trans. R. Soc. London, Ser. B* **1995**, *348*, 61–70.
- (16) Lehn, J.-M. *Supramolecular Chemistry: Concepts and Perspectives*; VCH: Weinheim, Germany, 1995.
- (17) Quinkert, G.; Egert, E.; Griesinger, C. *Aspects of Organic Chemistry*; VCH: Basel, 1996.
- (18) Lightner, D. A.; McDonagh, A. F.; Wijekoon, W. M. D.; Reisinger, M. *Tetrahedron Lett.* **1988**, *29*, 3507–3510.
- (19) Blauer, G. *Isr. J. Chem.* **1983**, *23*, 201–209.
- (20) Chen, Q. Q.; Huggins, M. T.; Lightner, D. A.; Norona, W.; McDonagh, A. F. *J. Am. Chem. Soc.* **1999**, *121*, 9253–9264.
- (21) Kar, A. K.; Tipton, A. K.; Lightner, D. A. *Monatsh. Chem.* **1999**, *130*, 833–843.
- (22) Boiadjev, S. E.; Lightner, D. A. *J. Heterocycl. Chem.* **1999**, *36*, 969–977.
- (23) Boiadjev, S. E.; Lightner, D. A. *Tetrahedron: Asymmetry* **1999**, *10*, 2535–2550.
- (24) Tipton, A. K.; Lightner, D. A.; McDonagh, A. F. *J. Org. Chem.* **2001**, *66*, 1832–1838.
- (25) Tucci, F. C.; Rudkevich, D. M.; Rebek, J., Jr. *Chem. Eur. J.* **2000**, *6*, 1007–1016.
- (26) Schmuck, C. *J. Org. Chem.* **2000**, *65*, 2432–2437.
- (27) Galow, T. H.; Ilhan, F.; Cooke, G.; Rotello, V. M. *J. Am. Chem. Soc.* **2000**, *122*, 3595–3598.
- (28) Mena-Osteritz, E.; Meyer, A.; Langeveld-Voss, B. M. W.; Janssen, R. A. J.; Meijer, E. W.; Bauerle, P. *Angew. Chem., Int. Ed.* **2000**, *39*, 2679–2684.
- (29) Crisma, M.; Moretto, A.; Toniolo, C.; Kaczmarek, K.; Zabrocki, J. *Macromolecules* **2001**, *34*, 5048–5052.
- (30) Mirsky, A. E.; Pauling, L. *Proc. Natl. Acad. Sci. U.S.A.* **1936**, *22*, 439–447.
- (31) Flory, P. J. *Principles of Polymer Chemistry*; Cornell University Press: Ithaca, NY, 1953.
- (32) Appella, D. H.; Christianson, L. A.; Karle, I. L.; Powell, D. R.; Gellman, S. H. *J. Am. Chem. Soc.* **1996**, *118*, 13071–13072.
- (33) Moore, J. S. *Curr. Opin. Colloid Interface Sci.* **1999**, *4*, 108–116.
- (34) Baldwin, R. L. *Nat. Struct. Biol.* **1999**, *6*, 814–817.
- (35) Anfinsen, C. B. *Science* **1973**, *181*, 223–230.
- (36) Osguthorpe, D. J. *Curr. Opin. Struct. Biol.* **2000**, *10*, 146–152.
- (37) Shortle, D. *Curr. Biol.* **1999**, *9*, R205–R209.
- (38) Dinner, A. R.; Sali, A.; Smith, L. J.; Dobson, C. M.; Karplus, M. *Trends Biol. Sci.* **2000**, *25*, 331–339.
- (39) Bryngelson, J. D.; Onuchic, J. N.; Socci, N. D.; Wolynes, P. G. *Proteins: Struct., Funct., Genet.* **1995**, *21*, 167–195.
- (40) Kauzmann, W. *Adv. Protein Chem.* **1959**, *14*, 1–63.
- (41) Dill, K. A. *Biochemistry* **1990**, *29*, 7133–7155.
- (42) Eaton, W. A.; Muñoz, V.; Hagen, S. J.; Jas, G. S.; Lapidus, L. J.; Henry, E. R.; Hofrichter, J. *Annu. Rev. Biophys. Biomol. Struct.* **2000**, *29*, 327–359.
- (43) Brawer, S. A. *Relaxation in Viscous Liquids and Glasses*; American Ceramic Society: New York, 1983.
- (44) Jackle, J. *Rep. Prog. Phys.* **1986**, *49*, 171–232.
- (45) Go, N. *Annu. Rev. Biophys. Eng.* **1983**, *12*, 183–210.
- (46) Dill, K. A.; Bromberg, S.; Yue, K.; Fiebig, K. M.; Yee, D. P.; Thomas, P. D.; Chan, H. S. *Protein Sci.* **1995**, *4*, 561–602.
- (47) Jackson, S. E. *Folding Des.* **1998**, *3*, R81–R91.
- (48) Sali, A.; Shakhnovich, E.; Karplus, M. *Nature* **1994**, *369*, 248–251.
- (49) Levinthal, C. *Mossbauer Spectroscopy in Biological Systems*; 1969, pp 22–24.
- (50) Fisher, M. E. *J. Chem. Phys.* **1966**, *44*, 616–622.
- (51) Guttman, A. J. *J. Phys. A* **1987**, *20*, 1839–1854.
- (52) Fisher, M. E.; Hiley, B. J. *J. Chem. Phys.* **1961**, *34*, 1253–1267.
- (53) Camacho, C. J.; Thirumalai, D. *Phys. Rev. Lett.* **1993**, *71*, 2505–2508.
- (54) Jones, C. M.; Henry, E. R.; Hu, Y.; Chan, C. K.; Luck, S. D.; Bhuyan, A.; Roder, H.; Hofrichter, J.; Eaton, W. A. *Proc. Natl. Acad. Sci. U.S.A.* **1993**, *90*, 11860–11864.
- (55) Mattice, W. L. *Annu. Rev. Biophys. Biophys. Chem.* **1989**, *18*, 93–111.
- (56) Muñoz, V.; Henry, E. R.; Hofrichter, J.; Eaton, W. A. *Proc. Natl. Acad. Sci. U.S.A.* **1998**, *95*, 5872–5879.
- (57) Zimm, B. H.; Bragg, J. K. *J. Chem. Phys.* **1959**, *31*, 526–535.
- (58) Poland, D.; Scheraga, H. *Theory of Helix-Coil Transitions in Biopolymers*; Academic Press: New York, 1970.
- (59) Clarke, D. T.; Doig, A. J.; Stapley, B. J.; Gareth, R. J. *Proc. Natl. Acad. Sci. U.S.A.* **1999**, *96*, 7232–7237.
- (60) Eaton, W. A.; Munoz, V.; Thompson, P. A.; Henry, E. R.; Hofrichter, J. *Acc. Chem. Res.* **1998**, *31*, 745–753.
- (61) Elmer, S.; Pande, V. S. *J. Phys. Chem. B* **2001**, *105*, 482–485.
- (62) Yang, W. Y.; Prince, R. B.; Sabelko, J.; Moore, J. S.; Gruebele, M. *J. Am. Chem. Soc.* **2000**, *122*, 3248–3249.
- (63) Daura, X.; van Gunsteren, W. F.; Mark, A. E. *Proteins: Struct., Funct., Genet.* **1999**, *34*, 269–280.
- (64) Riddle, N. S.; Santiago, J. V.; Bray, S. T.; Doshi, N.; Grant-charova, V.; Yi, Q.; Baker, D. *Nat. Struct. Biol.* **1997**, *4*, 805–809.
- (65) Wolynes, P. G. *Nat. Struct. Biol.* **1997**, *4*, 871–874.
- (66) Chan, H. S.; Dill, K. A. *J. Chem. Phys.* **1991**, *95*, 3775–3767.
- (67) White, S. H.; Jacobs, R. E. *J. Mol. Evol.* **1993**, *36*, 79–95.
- (68) Rao, S. P.; Carlstrom, D. E.; Miller, W. G. *Biochemistry* **1974**, *13*, 943–952.
- (69) Chan, H. S.; Dill, K. A. *Macromolecules* **1989**, *22*, 4559–4573.
- (70) Shakhnovich, E.; Farztdinov, G.; Gutin, A. M.; Karplus, M. *Phys. Rev. Lett.* **1991**, *67*, 1665–1668.
- (71) Shakhnovich, E.; Gutin, A. M. *Proc. Natl. Acad. Sci. U.S.A.* **1993**, *90*, 7195–7199.
- (72) Sali, A.; Shakhnovich, E.; Karplus, M. *J. Mol. Biol.* **1994**, *235*, 1614–1636.
- (73) Bryngelson, J. D.; Wolynes, P. G. *Proc. Natl. Acad. Sci. U.S.A.* **1987**, *84*, 7524–7528.
- (74) Derrida, B. *Phys. Rev. B* **1981**, *24*, 2613–2626.
- (75) Bryngelson, J. D.; Onuchic, J. N.; Socci, N. D.; Wolynes, P. G. *Proteins: Struct., Funct., Genet.* **1995**, *21*, 167–195.
- (76) Onuchic, J. N.; Luthey-Schulten, Z.; Wolynes, P. G. *Annu. Rev. Phys. Chem.* **1997**, *48*, 545–600.
- (77) Dinner, A. R.; Sali, A.; Karplus, M.; Shakhnovich, E. *J. Chem. Phys.* **1994**, *101*, 1444–1451.
- (78) Chan, H. S.; Dill, K. A. *J. Chem. Phys.* **1993**, *99*, 2116–2127.
- (79) Gutin, A. M.; Abkevich, V. I.; Shakhnovich, E. I. *Biochemistry* **1995**, *34*, 3066–3076.
- (80) Onuchic, J. N.; Luthey-Schulten, Z.; Wolynes, P. G. *Annu. Rev. Phys. Chem.* **1997**, *48*, 545–600.
- (81) Echt, O.; Sattler, K.; Recknagel, E. *Phys. Rev. Lett.* **1981**, *47*, 1121–1124.
- (82) Berman, A. L.; Kolker, E.; Trifonov, E. N. *Proc. Natl. Acad. Sci. U.S.A.* **1994**, *91*, 4044–4047.
- (83) Lindgård, P. A.; Bohr, H. *Phys. Rev. Lett.* **1996**, *77*, 779–782.
- (84) Wales, D. *Chem. Phys. Lett.* **1998**, *285*, 330–336.
- (85) Kellman, M. E. *J. Chem. Phys.* **1996**, *105*, 2500–2508.
- (86) Yue, K.; Dill, K. A. *Proc. Natl. Acad. Sci. U.S.A.* **1995**, *92*, 146–150.
- (87) Wolynes, P. G. *Simplicity and Complexity in Proteins and Nucleic Acids*; Dahlem University Press: 1999.
- (88) Myers, J. K.; Oas, T. G. *Nat. Struct. Biol.* **2001**, *8*, 552–558.
- (89) Gilis, D.; Rooman, M. *Proteins: Struct., Funct., Genet.* **2001**, *42*, 164–176.
- (90) See ref 86.
- (91) DeGrado, W. F.; Summa, C. M.; Pavone, V.; Nastro, F.; Lombardi, A. *Annu. Rev. Biochem.* **1999**, *68*, 779–819.
- (92) Go, N.; Taketomi, H. *Proc. Natl. Acad. Sci. U.S.A.* **1978**, *75*, 559–563.
- (93) Unger, R.; Moulton, J. *J. Mol. Biol.* **1996**, *259*, 988–994.
- (94) Abkevich, V. I.; Gutin, A. M.; Shakhnovich, E. I. *J. Mol. Biol.* **1995**, *252*, 460–471.
- (95) Fersht, A. R.; Shakhnovich, E. I. *Curr. Biol.* **1998**, *8*, R478–R479.
- (96) Otzen, D. E.; Kristensen, O.; Proctor, M.; Oliveberg, M. *Biochemistry* **1999**, *38*, 6499–6511.
- (97) Chan, H. S.; Dill, K. A. *Proteins: Struct., Funct., Genet.* **1998**, *30*, 2–33.
- (98) Abkevich, V. I.; Gutin, A. M.; Shakhnovich, E. I. *J. Chem. Phys.* **1994**, *101*, 6052–6062.
- (99) Socci, N. D.; Onuchic, J. N. *J. Chem. Phys.* **1994**, *101*, 1519–1528.
- (100) Eastwood, M.; Wolynes, P. *J. Chem. Phys.* **2001**, *114*, 4702–4716.
- (101) Socci, N. D.; Onuchic, J. N. *J. Chem. Phys.* **1995**, *103*, 4732–4744.
- (102) Li, H.; Helling, R.; Tang, C.; Wingreen, N. *Science* **1996**, *273*, 666–669.
- (103) Lipman, D. J.; Wilbur, W. J. *Proc. R. Soc. London, Ser. B* **1991**, *245*, 7–11.

- (104) Govindarajan, S.; Goldstein, R. A. *Biopolymers* **1995**, *36*, 43–51.
- (105) Wang, T.; Miller, J.; Wingreen, N. S.; Tang, C.; Dill, K. A. *J. Chem. Phys.* **2000**, *113*, 8329–8336.
- (106) Martin, R. E.; Diederich, F. *Angew. Chem., Int. Ed.* **1999**, *38*, 1350–1377.
- (107) Tour, J. M. *Chem. Rev.* **1996**, *96*, 537–554.
- (108) Nelson, J. C.; Young, J. K.; Moore, J. S. *J. Org. Chem.* **1996**, *61*, 8160–8168.
- (109) Nelson, J. C. Ph.D. Thesis, University of Illinois, Urbana, IL, 1997.
- (110) Prince, R. B.; Okada, T.; Moore, J. S. *Angew. Chem., Int. Ed.* **1999**, *38*, 233–236.
- (111) Moore, J. S.; Hill, D. J.; Mio, M. J. In *Solid-Phase Synthesis*; Burgess, K., Ed.; Wiley-Interscience: New York, 2000.
- (112) Prince, R. B.; Saven, J. G.; Wolynes, P. G.; Moore, J. S. *J. Am. Chem. Soc.* **1999**, *121*, 3114–3121.
- (113) Berl, V.; Huc, I.; Khoury, R. G.; Krische, M. J.; Lehn, J.-M. *Nature* **2000**, *407*, 720–723.
- (114) Linton, B.; Hamilton, A. *CHEMTECH* **1997**, 34–40.
- (115) Schmidtschen, F. P.; Berger, M. *Chem. Rev.* **1997**, *97*, 1609–1646.
- (116) Davis, A. P.; Wareham, R. S. *Angew. Chem., Int. Ed.* **1999**, *38*, 2978–2996.
- (117) Mazik, M.; Sicking, W. *Chem. Eur. J.* **2001**, *7*, 664–670.
- (118) Archer, E. A.; Gong, H.; Krische, M. J. *Tetrahedron* **2001**, *57*, 1139–1159.
- (119) Beer, P. D.; Gale, P. A. *Angew. Chem., Int. Ed.* **2001**, *40*, 486–516.
- (120) Czarnik, A. W. *Acc. Chem. Res.* **1994**, *27*, 302–308.
- (121) Desilva, A. P.; Gunaratne, H. Q. N.; Gunnlaugsson, T.; Huxley, A. J. M.; McCoy, C. P.; Rademacher, J. T.; Rice, T. E. *Chem. Rev.* **1997**, *97*, 1515–1566.
- (122) Metzger, A.; Anslyn, E. V. *Angew. Chem., Int. Ed. Engl.* **1998**, *37*, 649–652 and references therein.
- (123) Robertson, A.; Shinkai, S. *Coord. Chem. Rev.* **2000**, *205*, 167–199.
- (124) Leininger, S.; Olenyuk, B.; Stang, P. J. *Chem. Rev.* **2000**, *100*, 853–908.
- (125) Baxter, P. N. W.; Lehn, J.-M.; Baum, G.; Fenske, D. *Chem. Eur. J.* **2000**, *6*, 4510–4517.
- (126) Zimmerman, N.; Moore, J. S.; Zimmerman, S. C. *Chem. Ind. (London)* **1998**, 604–610.
- (127) Bosman, A. W.; Janssen, H. M.; Meijer, E. W. *Chem. Rev.* **1999**, *99*, 1665–1688.
- (128) Hirschmann, R. *Angew. Chem., Int. Ed. Engl.* **1991**, *30*, 1278–1301.
- (129) Giannis, A.; Kolter, T. *Angew. Chem., Int. Ed. Engl.* **1993**, *32*, 1244–1267.
- (130) Gante, J. *Angew. Chem., Int. Ed. Engl.* **1994**, *33*, 1699–1720.
- (131) Hruby, V. J.; Li, G.; Haskell-Luevano, C.; Shenderovich, M. *Biopolymers* **1997**, *43*, 219–266.
- (132) Hanessian, S.; McNaughton-Smith, G.; Lombart, H. G.; Lubell, W. D. *Tetrahedron* **1997**, *53*, 12789–12854.
- (133) Ripka, A. S.; Rich, D. H. *Curr. Opin. Chem. Biol.* **1998**, *2*, 441–452.
- (134) Rizo, J.; Gierasch, L. M. *Annu. Rev. Biochem.* **1992**, *61*, 387–418.
- (135) Schneider, J. P.; Kelly, J. W. *Chem. Rev.* **1995**, *95*, 2169–2187.
- (136) Nowick, J. S.; Smith, E. M.; Pairish, M. *Chem. Soc. Rev.* **1996**, *25*, 401–415.
- (137) Soth, M. J.; Nowick, J. S. *Curr. Opin. Chem. Biol.* **1997**, *1*, 120–129.
- (138) Simon, R. J.; Kania, R. S.; Zuckermann, R. N.; Huebner, V. D.; Jewell, D. A.; Banville, S.; Ng, S.; Wang, L.; Rosenberg, S.; Marlowe, C. K.; Spellmeyer, D. C.; Tan, R.; Frankel, A. D.; Santi, D. V.; Cohen, F. E.; Bartlett, P. A. *Proc. Natl. Acad. Sci. U.S.A.* **1992**, *89*, 9367–9371.
- (139) Möhle, K.; Hofmann, H.-J. *Biopolymers* **1996**, *38*, 781–790.
- (140) Kirshenbaum, K.; Barron, A. E.; Goldsmith, R. A.; Armand, P.; Bradley, E. K.; Truong, K. T. V.; Dill, K. A.; Cohen, F. E.; Zuckermann, R. N. *Proc. Natl. Acad. Sci. U.S.A.* **1998**, *95*, 4303–4308.
- (141) Armand, P.; Kirshenbaum, K.; Falicov, A.; Dunbrack, R. L.; Dill, K. A.; Zuckermann, R. N.; Cohen, F. E. *Folding Des.* **1997**, *2*, 369–375.
- (142) Wu, C. W.; Sanborn, T. J.; Zuckermann, R. N.; Barron, A. E. *J. Am. Chem. Soc.* **2001**, *123*, 2958–2963.
- (143) Armand, P.; Kirshenbaum, K.; Goldsmith, R. A.; Farr-Jones, S.; Barron, A. E.; Truong, K. T. V.; Dill, K. A.; Mierke, D. F.; Cohen, F. E.; Zuckermann, R. N.; Bradley, E. K. *Proc. Natl. Acad. Sci. U.S.A.* **1998**, *95*, 4309–4314.
- (144) Wu, C. W.; Sanborn, T. J.; Huang, K.; Zuckermann, R. N.; Barron, A. E. *J. Am. Chem. Soc.* **2001**, *123*, 6778–6784.
- (145) Miller, S. M.; Simon, R. J.; Ng, S.; Zuckermann, R. N.; Kerr, J. M.; Moos, W. H. *Bioorg. Med. Chem. Lett.* **1994**, *4*, 2657–2662.
- (146) Zuckermann, R. N.; Kerr, J. M.; Kent, S. B. H.; Moos, W. H. *J. Am. Chem. Soc.* **1997**, *119*, 10646–10647.
- (147) Murphy, J. E.; Uno, T.; Hamer, J. D.; Cohen, F. E.; Dwarki, V.; Zuckermann, R. N. *Proc. Natl. Acad. Sci. U.S.A.* **1998**, *95*, 1517–1522.
- (148) Nowick, J. S.; Powell, N. A.; Nguyen, T. M.; Noronha, G. *J. Org. Chem.* **1992**, *57*, 3763–3765.
- (149) Etter, M. C. *Acc. Chem. Res.* **1990**, *23*, 120–126.
- (150) Etter, M. C.; MacDonald, J. C.; Bernstein, J. *Acta Crystallogr.* **1990**, *B46*, 256–262.
- (151) Jeffrey, G. A. *An Introduction to Hydrogen Bonding*; Oxford: New York, 1997.
- (152) Nowick, J. S.; Abdi, M.; Bellamo, K. A.; Love, J. A.; Martinez, E. J.; Noronha, G.; Smith, E. M.; Ziller, J. W. *J. Am. Chem. Soc.* **1995**, *117*, 89–99.
- (153) Nowick, J. S.; Mahrus, S.; Smith, E. M.; Ziller, J. W. *J. Am. Chem. Soc.* **1996**, *118*, 1066–1072.
- (154) Nowick, J. S.; Holmes, D. L.; Mackin, G.; Noronha, G.; Shaka, A. J.; Smith, E. M. *J. Am. Chem. Soc.* **1996**, *118*, 2764–2765.
- (155) Nowick, J. S.; Pairish, M.; Lee, I. Q.; Holmes, D. L.; Ziller, J. W. *J. Am. Chem. Soc.* **1997**, *119*, 5413–5424.
- (156) Nowick, J. S. *Acc. Chem. Res.* **1999**, *32*, 287–296.
- (157) Nowick, J. S.; Chung, D. M.; Maitra, K.; Maitra, S.; Stigers, K. D.; Sun, Y. *J. Am. Chem. Soc.* **2000**, *122*, 7654–7661.
- (158) Smith, A. B. I.; Keenan, T. P.; Holcomb, R. C.; Sprengeler, P. A.; Guzman, M. C.; Wood, J. L.; Carroll, P. J.; Hirschmann, R. *J. Am. Chem. Soc.* **1992**, *114*, 10672–10674.
- (159) Smith, A. B. I.; Guzman, M. C.; Sprengeler, P. A.; Keenan, T. P.; Holcomb, R. C.; Wood, J. L.; Carroll, P. J.; Hirschmann, R. *J. Am. Chem. Soc.* **1994**, *116*, 9947–9962.
- (160) Smith, A. B. I.; Favor, D. A.; Sprengeler, P. A.; Guzman, M. C.; Carroll, P. J.; Furst, G. T.; Hirschmann, R. *Bioorg. Med. Chem.* **1999**, *7*, 9–22.
- (161) Smith, A. B. I.; Akaishi, R.; Jones, D. R.; Keenan, T. P.; Guzman, M. C.; Holcomb, R. C.; Sprengeler, P. A.; Wood, J. L.; Hirschmann, R.; Holloway, M. K. *Biopolymers* **1995**, *37*, 29–53.
- (162) Smith, A. B. I.; Benowitz, A. B.; Favor, D. A.; Sprengeler, P. A.; Hirschmann, R. *Tetrahedron Lett.* **1997**, *38*, 3809–3812.
- (163) Meyers, A. I.; Reine, A. H.; Gault, R. *J. Org. Chem.* **1969**, *34*, 698–705.
- (164) Huisgen, R.; Brade, H. *Chem. Ber.* **1957**, *90*, 1432–1436.
- (165) Smith, A. B. I.; Hirschmann, R.; Pasternak, A.; Guzman, M. C.; Yokoyama, A.; Sprengeler, P. A.; Darke, P. L.; Emini, E. A.; Schleif, W. A. *J. Am. Chem. Soc.* **1995**, *117*, 11113–11123.
- (166) Lee, K. H.; Olson, G. L.; Bolin, D. R.; Benowitz, A. B.; Sprengeler, P. A.; Smith, A. B. I.; Hirschmann, R. F.; Wiley, D. C. *J. Am. Chem. Soc.* **2000**, *122*, 8370–8375.
- (167) Lucarini, S.; Tomasini, C. *J. Org. Chem.* **2001**, *66*, 727–732.
- (168) Gante, J. *Synthesis* **1989**, 405–413.
- (169) Han, H.; Janda, K. D. *J. Am. Chem. Soc.* **1996**, *118*, 2539–2544.
- (170) Gante, J.; Krug, M.; Lauterbach, G.; Weitzel, R.; Hiller, W. *J. Pept. Sci.* **1995**, *2*, 201–206.
- (171) Reynolds, C. H.; Hormann, R. E. *J. Am. Chem. Soc.* **1996**, *118*, 9395–9401.
- (172) Perona, J. J.; Craik, C. S. *Protein Sci.* **1995**, *4*, 337–360.
- (173) André, F.; Boussard, D.; Bayeul, D.; Didierjean, C.; Aubry, A.; Marraud, M. *J. Pept. Res.* **1997**, *49*, 556–562.
- (174) Thormann, M.; Hofmann, H.-J. *J. Mol. Struct.* **1999**, *469*, 63–76.
- (175) Ramachandran, G. N.; Sasisekharan, V. In *Advances in Protein Chemistry*; Anfinsen, C. B. J., Anson, M. L., Edsall, J. T., Richards, F. M., Eds.; Academic Press: New York, 1968; Vol. 23.
- (176) Schulz, G. E.; Schirmer, R. H. *Principles of Protein Structure*; Springer-Verlag: New York, 1979.
- (177) Richardson, J. S. In *Advances in Protein Chemistry*; Anfinsen, C. B., Edsall, J. T., Richards, F. M., Eds.; Academic Press: New York, 1981; Vol. 34.
- (178) Branden, C.; Tooze, J. *Introduction to Protein Structure*, 2nd ed.; Garland: New York, 1999.
- (179) Glickson, J. D.; Applequist, J. *J. Am. Chem. Soc.* **1971**, *93*, 3276–3281.
- (180) Narita, M.; Doi, M.; Kudo, K.; Terauchi, Y. *Bull. Chem. Soc. Jpn.* **1986**, *59*, 3553–3557.
- (181) Drey, C. N. C. In *Chemistry and Biochemistry of the Amino Acids*; Barrett, G. C., Ed.; Chapman and Hall: London, 1985.
- (182) Cole, D. C. *Tetrahedron* **1994**, *50*, 9517–9582.
- (183) Möhle, K.; Günther, R.; Thormann, M.; Sewald, N.; Hofmann, H.-J. *Biopolymers* **1999**, *50*, 167–184.
- (184) Wu, Y.-D.; Wang, D.-P. *J. Am. Chem. Soc.* **1998**, *120*, 13485–13493.
- (185) Wu, Y.-D.; Wang, D.-P. *J. Am. Chem. Soc.* **1999**, *121*, 9352–9362.
- (186) Günther, R.; Hofmann, H.-J.; Kuczera, K. *J. Phys. Chem. B* **2001**, *105*, 5559–5567.
- (187) Graf, R.; Lohaus, G.; Börner, K.; Schmidt, E.; Bestian, H. *Angew. Chem., Int. Ed. Engl.* **1962**, *1*, 481–489.
- (188) Kovacs, J.; Ballina, R.; Rodin, R. L.; Balasubramanian, D.; Applequist, J. *J. Am. Chem. Soc.* **1965**, *87*, 119–120.
- (189) Bestian, H. *Angew. Chem., Int. Ed. Engl.* **1968**, *7*, 278–285.
- (190) Schmidt, V. E. *Angew. Makromol. Chem.* **1970**, *14*, 185–202.

- (191) Saudek, V.; Stokrova, S.; Schmidt, P. *Biopolymers* **1982**, *21*, 2195–2203.
- (192) Hardy, P. M.; Haylock, J. C.; Rydon, H. N. *J. Chem. Soc., Perkin Trans. 1* **1972**, 605–611.
- (193) Glickson, J. D.; Applequist, J. *Macromolecules* **1971**, *2*, 628–634.
- (194) Chen, F.; Lepore, G.; Goodman, M. *Macromolecules* **1974**, *7*, 779–783.
- (195) Yuki, H.; Taketani, Y. *Polym. Lett.* **1972**, *10*, 373–378.
- (196) Yuki, H.; Okamoto, Y.; Taketani, Y.; Tsubota, T.; Marubayashi, Y. *J. Polym. Sci., Polym. Chem. Ed.* **1978**, *16*, 2237–2251.
- (197) Kajtár, M.; Hollósi, M.; Riedl, Z. *Acta Chim. Acad. Sci. Hung.* **1976**, *88*, 301–308.
- (198) Yuki, H.; Okamoto, Y.; Doi, Y. *J. Polym. Sci., Polym. Chem. Ed.* **1979**, *17*, 1911–1921.
- (199) Fernández-Santín, J. M.; Aymamí, J.; Rodríguez-Galán, A.; Muñoz-Guerra, S.; Subirana, J. A. *Nature* **1984**, *311*, 53–54.
- (200) Krauthäuser, S.; Christianson, L. A.; Powell, D. R.; Gellman, S. H. *J. Am. Chem. Soc.* **1997**, *119*, 11719–11720.
- (201) Seebach, D.; Abele, S.; Gademann, K.; Jaun, B. *Angew. Chem., Int. Ed.* **1999**, *38*, 1595–1597.
- (202) Fernández-Santín, J. M.; Muñoz-Guerra, S.; Rodríguez-Galán, A.; Aymamí, J.; Lloveras, J.; Subirana, J. A. *Macromolecules* **1987**, *20*, 62–68.
- (203) Doty, P.; Wada, A.; Yang, J. T.; Blout, E. R. *J. Polym. Sci.* **1957**, *23*, 851–861.
- (204) López-Carrasquero, F.; Alemán, C.; Muñoz-Guerra, S. *Biopolymers* **1995**, *36*, 263–271.
- (205) Alemán, C.; Bella, J.; Perez, J. J. *Polymer* **1994**, *1994*, 2596–2599.
- (206) Alemán, C.; Navas, J. J.; Muñoz-Guerra, S. *Biopolymers* **1997**, *41*, 721–729.
- (207) Bella, J.; Alemán, C.; Fernández-Santín, J. M.; Alegre, C.; Subirana, J. A. *Macromolecules* **1992**, *25*, 5225–5230.
- (208) Bode, K. A.; Applequist, J. *Macromolecules* **1997**, *30*, 2144–2150.
- (209) López-Carrasquero, F.; García-Alvarez, M.; Navas, J. J.; Alemán, C.; Muñoz-Guerra, S. *Macromolecules* **1996**, *29*, 8449–8459.
- (210) Martínez de Iarduya, A.; Alemán, C.; García-Alvarez, M.; López-Carrasquero, F.; Muñoz-Guerra, S. *Macromolecules* **1999**, *32*, 3257–3263.
- (211) Cheng, J.; Deming, T. J. *Macromolecules* **2001**, *34*, 5169–5174.
- (212) Fasman, G. D. In *Poly- α -Amino Acids*; Fasman, G. D., Ed.; Marcel Dekker: New York, 1967.
- (213) Karle, I. L. In *The Peptides*; Gross, E., Meienhofer, J., Eds.; Academic Press: New York, 1981; Vol. 4.
- (214) Pavone, V.; Lombardi, A.; Yang, X.; Pedone, C.; Di Blasio, B. *Biopolymers* **1990**, *30*, 189–196.
- (215) Di Blasio, B.; Lombardi, A.; Yang, X.; Pedone, C.; Pavone, V. *Biopolymers* **1991**, *31*, 1181–1188.
- (216) Di Blasio, B.; Lombardi, A.; D'Auria, G.; Saviano, M.; Isernia, C.; Maglio, O.; Paolillo, L.; Pedone, C.; Pavone, V. *Biopolymers* **1993**, *33*, 621–631.
- (217) Pavone, V.; Lombardi, A.; Saviano, M.; Natri, F.; Fattorusso, R.; Maglio, O.; Isernia, C.; Paolillo, L.; Pedone, C. *Biopolymers* **1994**, *34*, 1517–1526.
- (218) Pavone, V.; Lombardi, A.; Saviano, M.; Di Blasio, B.; Natri, F.; Fattorusso, R.; Maglio, O.; Isernia, C. *Biopolymers* **1994**, *34*, 1505–1515.
- (219) For references concerning this hydrogen-bond annotation, see Etter, M. C. *Acc. Chem. Res.* **1990**, *23*, 120–126. Etter, M. C.; MacDonald, J. C.; Bernstein, J. *Acta Crystallogr.* **1990**, *B46*, 256–262.
- (220) Morita, H.; Nagashima, S.; Takeya, K.; Itokawa, H.; Iitaka, Y. *Tetrahedron* **1995**, *51*, 1121–1132.
- (221) Matthews, J. L.; Overhand, M.; Kuhnle, F. N. M.; Ciceri, P. E.; Seebach, D. *Liebigs Ann.* **1997**, 1371–1379.
- (222) Seebach, D.; Matthews, J. L.; Meden, A.; Wessels, T.; Baerlocher, C.; McCusker, L. B. *Helv. Chim. Acta* **1997**, *80*, 173–182.
- (223) Seebach, D.; Overhand, M.; Kuhnle, F. N. M.; Martinoni, B.; Oberer, L.; Hommel, U.; Widmer, H. *Helv. Chim. Acta* **1996**, *79*, 913–941.
- (224) Pavone, V.; Di Blasio, B.; Lombardi, A.; Isernia, C.; Pedone, C.; Benedetti, E.; Valle, G.; Crisma, M.; Toniolo, C.; Kishore, R. *J. Chem. Soc., Perkin Trans. 2* **1992**, 1233–1237.
- (225) Dado, G. P.; Gellman, S. H. *J. Am. Chem. Soc.* **1994**, *116*, 1054–1062.
- (226) Abele, S.; Seiler, P.; Seebach, D. *Helv. Chim. Acta* **1999**, *82*, 1559–1571.
- (227) Quinkert, G.; Egert, E.; Griesinger, C. In *Peptides: Synthesis, Structure, and Applications*; Gutte, B., Ed.; Academic Press: San Diego, 1995.
- (228) Seebach, D.; Matthews, J. L. *Chem. Commun.* **1997**, 2015–2022.
- (229) Seebach, D.; Albert, M.; Arvidsson, P. I.; Rueping, M.; Schreiber, J. V. *Chimia* **2001**, *55*, 345–353.
- (230) Yokouchi, M.; Chatani, Y.; Tadokoro, H.; Teranishi, K.; Tani, H. *Polymer* **1974**, *14*, 267–273.
- (231) Müller, H.-M.; Seebach, D. *Angew. Chem., Int. Ed. Engl.* **1993**, *32*, 477–502.
- (232) Landschulz, W. H.; Johnson, P. F.; McKnight, S. L. *Science* **1988**, *240*, 1759–1764.
- (233) Karle, I. L.; Flippen-Anderson, J. L.; Uma, K.; Sukumar, M.; Balaram, P. *J. Am. Chem. Soc.* **1990**, *112*, 9350–9356.
- (234) Matthews, J. L.; Gademann, K.; Jaun, B.; Seebach, D. *J. Chem. Soc., Perkin Trans. 1* **1998**, 3331–3340.
- (235) Tromp, R. A.; van der Hoeven, M.; Amore, A.; Brussee, J.; Overhand, M.; van der Marel, G. A.; van der Gen, A. *Tetrahedron: Asymmetry* **2001**, *12*, 1109–1112.
- (236) Hanessian, S.; Luo, X.; Schaum, R.; Michnick, S. *J. Am. Chem. Soc.* **1998**, *120*, 8569–8570.
- (237) Hintermann, T.; Gademann, K.; Jaun, B.; Seebach, D. *Helv. Chim. Acta* **1998**, *81*, 983–1002.
- (238) Appella, D. H.; Christianson, L. A.; Klein, D. A.; Powell, D. R.; Huang, X.; Barchi, J. J., Jr.; Gellman, S. H. *Nature* **1997**, *387*, 381–384.
- (239) Appella, D. H.; Christianson, L. A.; Karle, I. L.; Powell, D. R.; Gellman, S. H. *J. Am. Chem. Soc.* **1999**, *121*, 6206–6212.
- (240) Barchi, J. J., Jr.; Huang, X.; Appella, D. H.; Christianson, L. A.; Durrell, S. R.; Gellman, S. H. *J. Am. Chem. Soc.* **2000**, *122*, 2711–2718.
- (241) Appella, D. H.; Christianson, L. A.; Klein, D. A.; Richards, M. A.; Powell, D. R.; Gellman, S. H. *J. Am. Chem. Soc.* **1999**, *121*, 7574–7581.
- (242) Applequist, J.; Bode, K. A.; Appella, D. H.; Christianson, L. A.; Gellman, S. H. *J. Am. Chem. Soc.* **1998**, *120*, 4891–4892.
- (243) Kilpatrick, J. E.; Pitzer, K. S.; Spitzer, R. *J. Am. Chem. Soc.* **1947**, *69*, 2483–2488.
- (244) Schweizer, W. B. In *Structure Correlation*; Bürgi, H.-B., Dunitz, J. D., Eds.; VCH: Weinheim, 1994; Vol. 1.
- (245) Benedetti, E.; Corradini, P.; Pedone, C. *J. Phys. Chem.* **1972**, *76*, 790–797.
- (246) Lifson, S.; Warshel, A. *J. Chem. Phys.* **1968**, *49*, 5116–5129.
- (247) Claridge, T. D. W.; Goodman, J. M.; Moreno, A.; Angus, D.; Barker, S. F.; Taillefumier, C.; Watterson, M. P.; Fleet, G. W. J. *Tetrahedron Lett.* **2001**, *42*, 4251–4255.
- (248) Seebach, D.; Gademann, K.; Schreiber, J. V.; Matthews, J. L.; Hintermann, T.; Jaun, B.; Oberer, L.; Hommel, U.; Widmer, H. *Helv. Chim. Acta* **1997**, *80*, 2033–2038.
- (249) Seebach, D.; Abele, S.; Gademann, K.; Guichard, G.; Hintermann, T.; Jaun, B.; Matthews, J. L.; Schreiber, J. V. *Helv. Chim. Acta* **1998**, *81*, 932–982.
- (250) Watterson, M. P.; Pickering, L.; Smith, M. D.; Hudson, S. J.; Marsh, P. R.; Mordaunt, J. E.; Watkin, D. J.; Newman, C. J.; Fleet, G. W. J. *Tetrahedron: Asymmetry* **1999**, *10*, 1855–1859.
- (251) Suhara, Y.; Hildreth, J. E. K.; Ichikawa, Y. *Tetrahedron Lett.* **1996**, *37*, 1575–1578.
- (252) Seebach, D.; Ciceri, P. E.; Overhand, M.; Jaun, B.; Rigo, D. *Helv. Chim. Acta* **1996**, *79*, 2043–2066.
- (253) Guichard, G.; Abele, S.; Seebach, D. *Helv. Chim. Acta* **1998**, *81*, 187–206.
- (254) Seebach, D.; Sifferlen, T.; Mathieu, P. A.; Häne, A. M.; Krell, C. M.; Bierbaum, D. J.; Abele, S. *Helv. Chim. Acta* **2000**, *83*, 2849–2864.
- (255) Jacobi, A.; Seebach, D. *Helv. Chim. Acta* **1999**, *82*, 1150–1172.
- (256) Rueping, M.; Jaun, B.; Seebach, D. *Chem. Commun.* **2000**, 2267–2268.
- (257) Sifferlen, T.; Rueping, M.; Gademann, K.; Jaun, B.; Seebach, D. *Helv. Chim. Acta* **1999**, *82*, 2067–2093.
- (258) Wu, Y.-D.; Zhao, Y.-L. *J. Am. Chem. Soc.* **2001**, *123*, 5313–5319.
- (259) Rabanal, R.; Ludevid, M. D.; Pons, M.; Giralt, E. *Biopolymers* **1993**, *33*, 1019–1028.
- (260) Huck, B. R.; Langenhan, J. M.; Gellman, S. H. *Org. Lett.* **1999**, *1*, 1717–1720.
- (261) Abele, S.; Vögli, K.; Seebach, D. *Helv. Chim. Acta* **1999**, *82*, 1539–1558.
- (262) Hintermann, T.; Seebach, D. *Synlett* **1997**, 437–438.
- (263) Gung, B. W.; Zhu, Z. *J. Org. Chem.* **1997**, *62*, 6100–6101.
- (264) DeGrado, W. F.; Schneider, J. P.; Hamuro, Y. *J. Pept. Res.* **1999**, *54*, 206–217.
- (265) Schellman, J. A. *Compt. Rend. Trav. Lab. Carlsberg, Ser. Chim.* **1955**, *29*, 230–259.
- (266) Qian, H.; Schellman, J. A. *J. Phys. Chem.* **1992**, *96*, 3987–3994.
- (267) See ref 57.
- (268) Goodman, M.; Verdini, A. S.; Toniolo, C.; Phillips, W. D.; Bovey, F. A. *Proc. Natl. Acad. Sci. U.S.A.* **1969**, *64*, 444–450.
- (269) Kemp, D. S.; Oslick, S. L.; Allen, T. J. *J. Am. Chem. Soc.* **1996**, *118*, 4249–4255.
- (270) Baldwin, R. L.; Rose, G. D. *Trends Biochem. Sci.* **1999**, *24*, 26–33.
- (271) Baldwin, R. L.; Rose, G. D. *Trends Biochem. Sci.* **1999**, *24*, 77–83.
- (272) Wallimann, P.; Kennedy, R. J.; Kemp, D. S. *Angew. Chem., Int. Ed.* **1999**, *38*, 1290–1292.
- (273) Seebach, D.; Schreiber, J. V.; Abele, S.; Daura, X.; van Gunsteren, W. F. *Helv. Chim. Acta* **2000**, *83*, 34–57.
- (274) Gademann, K.; Jaun, B.; Seebach, D.; Perozzo, R.; Scapozza, L.; Folkers, G. *Helv. Chim. Acta* **1999**, *82*, 1–11.

- (275) Daura, X.; van Gunsteren, W. F.; Mark, A. E. *Proteins: Struct., Funct., Genet.* **1999**, *34*, 269–280.
- (276) Daura, X.; Gademann, K.; Jaun, B.; Seebach, D.; van Gunsteren, W. F.; Mark, A. E. *Angew. Chem., Int. Ed.* **1999**, *38*, 236–240.
- (277) Seebach, D.; Abele, S.; Sifferlen, T.; Hänggi, M.; Gruner, S.; Seiler, P. *Helv. Chim. Acta* **1998**, *81*, 2218–2243.
- (278) Spatola, A. F. In *Chemistry and Biochemistry of Amino Acids, Peptides, and Proteins*; Weinstein, B., Ed.; Marcel Dekker: New York, 1983; Vol. 7.
- (279) Griffith, O. W. In *Annual Review of Biochemistry*; Richardson, C. C., Boyer, P. D., Dawid, I. B., Meister, A., Eds.; Annual Reviews, Inc.: Palo Alto, CA, 1986; Vol. 55.
- (280) Abele, S.; Guichard, G.; Seebach, D. *Helv. Chim. Acta* **1998**, *81*, 2141–2156.
- (281) Gung, B. W.; Zou, D.; Stalcup, A. M.; Cottrell, C. E. *J. Org. Chem.* **1999**, *64*, 2176–2177.
- (282) Appella, D. H.; Barchi, J. J., Jr.; Durell, S. R.; Gellman, S. H. *J. Am. Chem. Soc.* **1999**, *121*, 2309–2310.
- (283) Appella, D. H.; LePlae, P. R.; Raguse, T. L.; Gellman, S. H. *J. Org. Chem.* **2000**, *65*, 4766–4769.
- (284) Wang, X.; Espinosa, J. F.; Gellman, S. H. *J. Am. Chem. Soc.* **2000**, *122*, 4821–4822.
- (285) Lee, H.-S.; Syud, F. A.; Wang, X.; Gellman, S. H. *J. Am. Chem. Soc.* **2001**, *123*, 7721–7722.
- (286) Seebach, D.; Jacobi, A.; Rueping, M.; Gademann, K.; Ernst, M.; Jaun, B. *Helv. Chim. Acta* **2000**, *83*, 2115–2140.
- (287) Arvidsson, P. I.; Rueping, M.; Seebach, D. *Chem. Commun.* **2001**, 649–650.
- (288) Cheng, R. P.; DeGrado, W. F. *J. Am. Chem. Soc.* **2001**, *123*, 5162–5163.
- (289) Hintermann, T.; Seebach, D. *Chimia* **1997**, *51*, 244–247.
- (290) Frackenpohl, J.; Arvidsson, P. I.; Schreiber, J. V.; Seebach, D. *ChemBioChem* **2001**, *2*, 445–455.
- (291) Gademann, K.; Ernst, M.; Hoyer, D.; Seebach, D. *Angew. Chem., Int. Ed.* **1999**, *38*, 1223–1226.
- (292) Werder, M.; Hauser, H.; Abele, S.; Seebach, D. *Helv. Chim. Acta* **1999**, *82*, 1774–1783.
- (293) Hamuro, Y.; Schneider, J. P.; DeGrado, W. F. *J. Am. Chem. Soc.* **1999**, *121*, 12200–12201.
- (294) Liu, D.; DeGrado, W. F. *J. Am. Chem. Soc.* **2001**, *123*, 7553–7559.
- (295) Porter, E. A.; Wang, X.; Lee, H.-S.; Weisblum, B.; Gellman, S. H. *Nature* **2000**, *404*, 565.
- (296) Gellman, S. H. *Curr. Opin. Chem. Biol.* **1998**, *2*, 717–725.
- (297) Haque, T. S.; Little, J. C.; Gellman, S. H. *J. Am. Chem. Soc.* **1996**, *118*, 6975–6985.
- (298) Chung, Y. J.; Christianson, L. A.; Stanger, H. E.; Powell, D. R.; Gellman, S. H. *J. Am. Chem. Soc.* **1998**, *120*, 10555–10556.
- (299) Chung, Y. J.; Huck, B. R.; Christianson, L. A.; Stanger, H. E.; Krauthäuser, S.; Powell, D. R.; Gellman, S. H. *J. Am. Chem. Soc.* **2000**, *122*, 3995–4004.
- (300) Huck, B. R.; Fisk, J. D.; Gellman, S. H. *Org. Lett.* **2000**, *2*, 2607–2610.
- (301) Hanessian, S.; Yang, H. *Tetrahedron Lett.* **1997**, *38*, 3155–3158.
- (302) Motorina, I. A.; Huel, C.; Quiniou, E.; Mispelter, J.; Adjadj, E.; Grierson, D. S. *J. Am. Chem. Soc.* **2001**, *123*, 8–17.
- (303) Yang, D.; Ng, F.-F.; Li, Z.-J. *J. Am. Chem. Soc.* **1996**, *118*, 9794–9795.
- (304) Yang, D.; Qu, J.; Li, B.; Ng, F.-F.; Wang, X.-C.; Cheung, K. K.; Wang, D.-P.; Wu, Y.-D. *J. Am. Chem. Soc.* **1999**, *121*, 589–590.
- (305) Wu, Y.-D.; Wang, D.-P.; Chan, K. W. K.; Yang, D. *J. Am. Chem. Soc.* **1999**, *121*, 11189–11196.
- (306) Gennari, C.; Salom, B.; Potenza, D.; Williams, A. *Angew. Chem., Int. Ed. Engl.* **1994**, *33*, 2067–2069.
- (307) Moree, W. J.; van der Marel, G. A.; Liskamp, R. J. *J. Org. Chem.* **1995**, *60*, 5157–5169.
- (308) Gude, M.; Piarilli, U.; Potenza, D.; Salom, B.; Gennari, C. *Tetrahedron Lett.* **1996**, *37*, 8589–8592.
- (309) Monnee, M. C. F.; Marjine, M. F.; Brouwer, A. J.; Liskamp, R. M. J. *Tetrahedron Lett.* **2000**, *41*, 7991–7995.
- (310) Bolm, C.; Moll, G.; Kahmann, J. D. *Chem. Eur. J.* **2001**, *7*, 1118–1128.
- (311) Bindal, R. D.; Golab, J. T.; Katzenellenbogen, J. A. *J. Am. Chem. Soc.* **1990**, *112*, 7861–7868.
- (312) Radkiewicz, J. L.; McAllister, M. A.; Goldstein, E.; Houk, K. N. *J. Org. Chem.* **1998**, *63*, 1419–1428.
- (313) Gennari, C.; Gude, M.; Potenza, D.; Piarulli, U. *Chem. Eur. J.* **1998**, *4*, 1924–1931.
- (314) Langenhan, J. M.; Fisk, J. D.; Gellman, S. H. *Org. Lett.* **2001**, *3*, 2559–2562.
- (315) Günther, R.; Hofmann, H.-J. *J. Am. Chem. Soc.* **2001**, *123*, 247–255.
- (316) Kajtár, M.; Bruckner, V. *Tetrahedron Lett.* **1966**, *7*, 4813–4818.
- (317) Kajtár, M.; Hollósi, M. *Acta Chim. Acad. Sci. Hung.* **1970**, *65*, 403–432.
- (318) Rydon, H. N. *J. Chem. Soc.* **1964**, 1328–1333.
- (319) Watanabe, T.; Ina, T.; Ogawa, K.; Matsumoto, T.; Sawa, S.; Ono, S. *Bull. Chem. Soc. Jpn.* **1970**, *43*, 3939–3940.
- (320) Kajtár, M.; Hollósi, M.; Snatzke, G. *Tetrahedron* **1971**, *27*, 5659–5671.
- (321) Hoffmann, R. W.; Lazaro, M. A.; Caturla, F.; Framery, E. *Tetrahedron Lett.* **1999**, *40*, 5983–5986.
- (322) Hoffmann, M.; Caturla, F.; Lazaro, M. A.; Framery, E.; Bernabeu, M. C.; Valancogne, I.; Montalbetti, C. A. G. N. *New J. Chem.* **2000**, *24*, 187–194.
- (323) Hagihara, M.; Anthony, N. J.; Stout, T. J.; Clardy, J.; Schreiber, S. L. *J. Am. Chem. Soc.* **1992**, *114*, 6568–6570.
- (324) Gennari, C.; Salom, B.; Potenza, D.; Longari, C.; Fioravanzo, E.; Carugo, O.; Sardone, N. *Chem. Eur. J.* **1996**, *2*, 644–655.
- (325) Brenner, M.; Seebach, D. *Helv. Chim. Acta* **2001**, *84*, 1181–1189.
- (326) Hanessian, S.; Luo, X.; Schaum, R. *Tetrahedron Lett.* **1999**, *40*, 4925–4929.
- (327) Seebach, D.; Brenner, M.; Rueping, M.; Schweizer, W. B.; Jaun, B. *Chem. Commun.* **2001**, 207–208.
- (328) Machetti, F.; Ferrali, A.; Menchi, G.; Occhiato, E. G.; Guarna, A. *Org. Lett.* **2000**, *2*, 3987–3990.
- (329) Burgess, K.; Linthicum, D. S.; Shin, H. *Angew. Chem., Int. Ed. Engl.* **1995**, *34*, 907–909.
- (330) Moran, E. J.; Wilson, T. E.; Cho, C. Y.; Cherry, S. R.; Stephans, J. C.; Fodor, S. P. A.; Adams, C. L.; Sundaram, A.; Jacobs, J. W.; Schultz, P. G. *Biopolymers* **1995**, *37*, 213–219.
- (331) Kim, J.-M.; Wilson, T. E.; Norman, T. C.; Schultz, P. G. *Tetrahedron Lett.* **1996**, *37*, 5309–5312.
- (332) Kim, J.-M.; Paikoff, S. J.; Schultz, P. G. *Tetrahedron Lett.* **1996**, *37*, 5305–5308.
- (333) Kruijtzter, J. A. W.; Lefeber, D. J.; Liskamp, R. M. J. *Tetrahedron Lett.* **1997**, *38*, 5335–5338.
- (334) Wilson, M. E.; Nowick, J. S. *Tetrahedron Lett.* **1998**, *39*, 6613–6616.
- (335) Cho, C. Y.; Moran, E. J.; Cherry, S. R.; Stephans, J. C.; Fodor, S. P. A.; Adams, C. L.; Sundaram, A.; Jacobs, J. W.; Schultz, P. G. *Science* **1993**, *261*, 1303–1305.
- (336) Cho, C. Y.; Youngquist, R. S.; Paikoff, S. J.; Beresini, M. H.; Herbert, A. R.; Berleau, L. T.; Liu, C. W.; Wemmer, D. E.; Keough, T.; Schultz, P. G. *J. Am. Chem. Soc.* **1998**, *120*, 7706–7718.
- (337) Lin, P.; Ganesan, A. *Bioorg. Med. Chem. Lett.* **1998**, *8*, 511–514.
- (338) Stigers, K. D.; Soth, M. J.; Nowick, J. S. *Curr. Opin. Chem. Biol.* **1999**, *3*, 714–723.
- (339) Hann, M. M.; Sannes, P. G.; Kennedwell, P. D.; Taylor, J. B. *J. Chem. Soc., Chem. Commun.* **1980**, 234–235.
- (340) Cox, M. T.; Heaton, D. W.; Horbury, J. *J. Chem. Soc., Chem. Commun.* **1980**, 799–800.
- (341) Gardner, R. R.; Liang, G.-B.; Gellman, S. H. *J. Am. Chem. Soc.* **1995**, *117*, 3280–3281.
- (342) Gardner, R. R.; Liang, G.-B.; Gellman, S. H. *J. Am. Chem. Soc.* **1999**, *121*, 1806–1816.
- (343) Wipf, P.; Fritch, P. C. *J. Org. Chem.* **1994**, *59*, 4875–4886.
- (344) Wipf, P.; Henninger, T. C.; Geib, S. J. *J. Org. Chem.* **1998**, *63*, 6088–6089.
- (345) Suhara, Y.; Izumi, M.; Ichikawa, M.; Penno, M. B.; Ichikawa, Y. *Tetrahedron Lett.* **1997**, *38*, 7167–7170.
- (346) Fuchs, E.-F.; Lehmann, J. *Carbohydr. Res.* **1976**, *49*, 267–273.
- (347) Wessel, H. P.; Mitchell, C. M.; Lobato, C. M.; Schmid, G. *Angew. Chem., Int. Ed. Engl.* **1995**, *34*, 2712–2713.
- (348) Nicolaou, K. C.; Flörke, H.; Egan, M. G.; Barth, T.; Estevez, V. A. *Tetrahedron Lett.* **1995**, *36*, 1775–1778.
- (349) Suhara, Y.; Ichikawa, M.; Hildreth, J. E. K.; Ichikawa, Y. *Tetrahedron Lett.* **1996**, *37*, 2549–2552.
- (350) Graf von Roedern, E.; Kessler, H. *Angew. Chem., Int. Ed. Engl.* **1994**, *33*, 687–689.
- (351) Graf von Roedern, E.; Lohof, E.; Hessler, G.; Hoffmann, M.; Kessler, H. *J. Am. Chem. Soc.* **1996**, *118*, 10156–10167.
- (352) Chakraborty, T. K.; Ghosh, S.; Jayaprakash, S.; Sharma, J. A. R. P.; Ravikanth, V.; Diwan, P. V.; Nagaraj, R.; Kunwar, A. C. *J. Org. Chem.* **2000**, *65*, 6441–6457.
- (353) Smith, M. D.; Long, D. D.; Marquess, D. G.; Claridge, T. D. W.; Fleet, G. W. J. *Chem. Commun.* **1998**, 2039–2040.
- (354) Gervay, J.; Flaherty, T. M.; Nguyen, C. *Tetrahedron Lett.* **1997**, *38*, 1493–1496.
- (355) Locardi, E.; Stöckle, M.; Gruner, S.; Kessler, H. *J. Am. Chem. Soc.* **2001**, *123*, 8189–8196.
- (356) Szabo, L.; Smith, B. L.; McReynolds, K. D.; Parrill, A. L.; Morris, E. R.; Gervay, J. *J. Org. Chem.* **1998**, *63*, 1074–1078.
- (357) McReynolds, K. D.; Gervay-Hague, J. *Tetrahedron Asymmetry* **2000**, *11*, 337–362.
- (358) Smith, M. D.; Claridge, T. D. W.; Tranter, G. E.; Sansom, M. S. P.; Fleet, G. W. J. *Chem. Commun.* **1998**, 2041–2042.
- (359) Brittain, D. E. A.; Watterson, M. P.; Claridge, T. D. W.; Smith, M. D.; Fleet, G. W. J. *J. Chem. Soc., Perkin Trans. 1* **2000**, 3655–3665.
- (360) Claridge, T. D. W.; Long, D. D.; Hungerford, N. L.; Aplin, R. T.; Smith, M. D.; Marquess, D. G.; Fleet, G. W. J. *Tetrahedron Lett.* **1999**, *40*, 2199–2202.

- (361) Hungerford, N. L.; Claridge, T. D. W.; Watterson, M. P.; Aplin, R. T.; Moreno, A.; Fleet, G. W. J. *J. Chem. Soc., Perkin Trans. 1* **2000**, 3666–3679.
- (362) Smith, M. D.; Long, D. D.; Martin, A.; Marquess, D. G.; Claridge, T. D. W.; Fleet, G. W. J. *Tetrahedron Lett.* **1999**, 40, 2191–2194.
- (363) Chakraborty, T. K.; Jayaprakash, S.; Srinivasu, P.; Chary, M. G.; Diwan, P. V.; Nagaraj, R.; Sankar, A. R.; Kunwar, A. C. *Tetrahedron Lett.* **2000**, 41, 8167–8171.
- (364) Schrey, A.; Vescovi, A.; Knoll, A.; Rickert, C.; Koert, U. *Angew. Chem., Int. Ed.* **2000**, 39, 900–902.
- (365) Koert, U.; Stein, M.; Harms, K. *Angew. Chem., Int. Ed. Engl.* **1994**, 33, 1180–1182.
- (366) Wagner, H.; Harms, K.; Koert, U.; Meder, S.; Boheim, G. *Angew. Chem., Int. Ed. Engl.* **1996**, 35, 2643–2646.
- (367) Kirshenbaum, K.; Zuckermann, R. N.; Dill, K. A. *Curr. Opin. Struct. Biol.* **1999**, 9, 530–535.
- (368) Magnus, P.; Danikiewicz, W.; Katoh, T.; Huffman, J. C.; Folting, K. *J. Am. Chem. Soc.* **1990**, 112, 2465–2468.
- (369) Takata, T.; Furusho, Y.; Murakawa, K.; Endo, T.; Matsuoka, H.; Hirasa, T.; Matsuo, J.; Sisido, M. *J. Am. Chem. Soc.* **1998**, 120, 4530–4531.
- (370) Grubbs, R. H.; Kratz, D. *Chem. Ber.* **1993**, 126, 149–157.
- (371) Blake, A. J.; Cooke, P. A.; Doyle, K. J.; Gair, S.; Simpkins, N. S. *Tetrahedron Lett.* **1998**, 39, 9093–9096.
- (372) Williams, D. J.; Colquhoun, H. M.; O'Mahoney, C. A. *J. Chem. Soc., Chem. Commun.* **1994**, 1643–1644.
- (373) Baxter, I.; Colquhoun, H. M.; Kohnke, F. H.; Lewis, D. F.; Williams, D. J. *Polymer* **1999**, 40, 607–612.
- (374) Li, C. J.; Slaven, W. T.; Chen, Y. P.; John, V. T.; Rachakonda, S. H. *Chem. Commun.* **1998**, 1351–1352.
- (375) Kilbinger, A. F. M.; Schenning, A.; Goldoni, F.; Feast, W. J.; Meijer, E. W. *J. Am. Chem. Soc.* **2000**, 122, 1820–1821.
- (376) Kilbinger, A. F. M.; Cooper, H. J.; McDonnell, L. A.; Feast, W. J.; Derrick, P. J.; Schenning, A.; Meijer, E. W. *Chem. Commun.* **2000**, 383–384.
- (377) Bassani, D. M.; Lehn, J.-M. *Bull. Chem. Soc. Fr.* **1997**, 134, 897–906.
- (378) Bassani, D. M.; Lehn, J.-M.; Baum, G.; Fenske, D. *Angew. Chem., Int. Ed.* **1997**, 1845–1847.
- (379) Ohkita, M.; Lehn, J.-M.; Baum, G.; Fenske, D. *Chem. Eur. J.* **1999**, 5, 3471–3481.
- (380) Ohkita, M.; Lehn, J.-M.; Baum, G.; Fenske, D. *Heterocycles* **2000**, 52, 103–109.
- (381) Gardinier, K. M.; Khoury, R. G.; Lehn, J.-M. *Chem. Eur. J.* **2000**, 6, 4124–4131.
- (382) Cuccia, L. A.; Lehn, J.-M.; Homo, J.-C.; Schmutz, M. *Angew. Chem., Int. Ed.* **2000**, 39, 233–237.
- (383) Tanatani, A.; Kagechika, H.; Azumaya, I.; Yamaguchi, K.; Shudo, K. *Chem. Pharm. Bull.* **1996**, 44, 1135–1137.
- (384) Tanatani, A.; Kagechika, H.; Azumaya, I.; Fukutomi, R.; Ito, Y.; Yamaguchi, K.; Shudo, K. *Tetrahedron Lett.* **1997**, 38, 4425–4428.
- (385) Tanatani, A.; Yamaguchi, K.; Azumaya, I.; Fukutomi, R.; Shudo, K.; Kagechika, H. *J. Am. Chem. Soc.* **1998**, 120, 6433–6442.
- (386) Fukutomi, R.; Tanatani, A.; Kakuta, H.; Tomioka, N.; Itai, A.; Hashimoto, Y.; Shudo, K.; Kagechika, H. *Tetrahedron Lett.* **1998**, 39, 6475–6478.
- (387) Kagechika, H.; Azumaya, I.; Tanatani, A.; Yamaguchi, K.; Shudo, K. *Tetrahedron Lett.* **1999**, 40, 3423–3426.
- (388) Lokey, R. S.; Iverson, B. L. *Nature* **1995**, 375, 303–305.
- (389) Zych, A. J.; Iverson, B. L. *J. Am. Chem. Soc.* **2000**, 122, 8898–8909.
- (390) Lokey, R. S.; Kwok, Y.; Guelev, V.; Pursell, C. J.; Hurley, L. H.; Iverson, B. L. *J. Am. Chem. Soc.* **1997**, 119, 7202–7210.
- (391) Nguyen, J. Q.; Iverson, B. L. *J. Am. Chem. Soc.* **1999**, 121, 2639–2640.
- (392) Martin, C. B.; Patrick, B. O.; Cammers-Goodwin, A. *J. Org. Chem.* **1999**, 64, 7807–7812.
- (393) Martin, C. B.; Mulla, H. R.; Willis, P. G.; Cammers-Goodwin, A. *J. Org. Chem.* **1999**, 64, 7802–7806.
- (394) Mulla, H. R.; Cammers-Goodwin, A. *J. Am. Chem. Soc.* **2000**, 122, 738–739.
- (395) Sindkhedkar, M. D.; Mulla, H. R.; Cammers-Goodwin, A. *J. Am. Chem. Soc.* **2000**, 122, 9271–9277.
- (396) Sindkhedkar, M. D.; Mulla, H. R.; Worth, M. A.; Cammers-Goodwin, A. *Tetrahedron* **2001**, 57, 2991–2996.
- (397) Josten, W.; Karbach, D.; Nieger, M.; Vögtle, F.; Hägele, K.; Svoboda, M.; Przybylski, M. *Chem. Ber.* **1994**, 127, 767–777.
- (398) Josten, W.; Neumann, S.; Vögtle, F.; Nieger, M.; Hägele, K.; Przybylski, M.; Beer, F.; Müllen, K. *Chem. Ber.* **1994**, 127, 2089–2096.
- (399) Breidenbach, S.; Ohren, S.; Nieger, M.; Vögtle, F. *J. Chem. Soc., Chem. Commun.* **1995**, 1237–1238.
- (400) Breidenbach, S.; Ohren, S.; Vögtle, F. *Chem. Eur. J.* **1996**, 2, 832–837.
- (401) Breidenbach, S.; Ohren, S.; Herbst-Irmer, R.; Kotila, S.; Nieger, M.; Vögtle, F. *Liebigs Ann.* **1996**, 2115–2121.
- (402) Boomgaarden, W.; Vögtle, F.; Nieger, M.; Hupfer, H. *Chem. Eur. J.* **1999**, 5, 345–355.
- (403) Schwierz, H.; Vögtle, F. *Synthesis* **1999**, 2, 295–305.
- (404) Sakurai, S.-i.; Goto, H.; Yashima, E. *Org. Lett.* **2001**, 3, 2379–2382.
- (405) Moore, J. S.; Nelson, J. C.; Prince, R. B. Fourth Francqui Symposium, Brussels, Belgium, 1999; p 263–290.
- (406) Nelson, J. C.; Saven, J. G.; Moore, J. S.; Wolynes, P. G. *Science* **1997**, 277, 1793–1796.
- (407) Defined according to classic polymer chemistry: see ref 31.
- (408) Monitored at 350 nm in the emission spectra.
- (409) Pace, C. N. In *Methods in Enzymology*; Hirs, C. H. W., Timasheff, S. N., Eds.; Academic Press: New York, 1986; Vol. 131.
- (410) See ref 62.
- (411) Prince, R. B.; Brunsveld, L.; Meijer, E. W.; Moore, J. S. *Angew. Chem., Int. Ed.* **2000**, 39, 228–230.
- (412) Gin, M. S.; Yokozawa, T.; Prince, R. B.; Moore, J. S. *J. Am. Chem. Soc.* **1999**, 121, 2643–2644.
- (413) Gin, M. S.; Moore, J. S. *Org. Lett.* **2000**, 2, 135–138.
- (414) Finkelstein, A. V.; Shakhnovich, E. I. *Biopolymers* **1989**, 28, 1681–1694.
- (415) Shakhnovich, E. I.; Finkelstein, A. V. *Biopolymers* **1989**, 28, 1667–1680.
- (416) Dill, K. A.; Stigter, D. *Adv. Protein Chem.* **1995**, 46, 59–104.
- (417) Prince, R. B.; Moore, J. S.; Brunsveld, L.; Meijer, E. W. *Chem. Eur. J.* **2001**, 7, 4150–4154.
- (418) Brunsveld, L.; Meijer, E. W.; Prince, R. B.; Moore, J. S. *J. Am. Chem. Soc.* **2001**, 123, 7978–7984.
- (419) Brunsveld, L.; Prince, R. B.; Meijer, E. W.; Moore, J. S. *Org. Lett.* **2000**, 2, 1525–1528.
- (420) Prince, R. B.; Barnes, S. A.; Moore, J. S. *J. Am. Chem. Soc.* **2000**, 122, 2758–2762.
- (421) Mecozzi, S.; Rebek, J., Jr. *Chem. Eur. J.* **1998**, 4, 1016–1022.
- (422) Tanatani, A.; Mio, M. J.; Moore, J. S. *J. Am. Chem. Soc.* **2001**, 123, 1792–1793.
- (423) Prest, P.-J.; Prince, R. B.; Moore, J. S. *J. Am. Chem. Soc.* **1999**, 121, 5933–5939.
- (424) Mio, M. J.; Moore, J. S. *MRS Bull.* **2000**, 25, 36–41.
- (425) Mio, M. J.; Prince, R. B.; Moore, J. S.; Kuebel, C.; Martin, D. C. *J. Am. Chem. Soc.* **2000**, 122, 6134–6135.
- (426) Mio, M. J. Ph.D. Thesis, University of Illinois, Urbana, IL, 2001.
- (427) Mindyuk, O. Y.; Stetzer, M. R.; Heiney, P. A.; Nelson, J. C.; Moore, J. S. *Adv. Mater.* **1998**, 10, 1363–1366.
- (428) Mindyuk, O. Y.; Stetzer, M. R.; Gidalevitz, D.; Heiney, P. A.; Nelson, J. C.; Moore, J. S. *Langmuir* **1999**, 15, 6897–6900.
- (429) Prince, R. B. Ph.D. Thesis, University of Illinois, Urbana, IL, June 2000.
- (430) Palmans, A. R. A.; Vekemans, J.; Meijer, E. W. *Rec. Trav. Chim. Pays-Bas* **1995**, 114, 277–284.
- (431) Delnoye, D. A. P.; Sijbesma, R. P.; Vekemans, J.; Meijer, E. W. *J. Am. Chem. Soc.* **1996**, 118, 8717–8718.
- (432) Pieterse, K.; Vekemans, J.; Kooijman, H.; Spek, A. L.; Meijer, E. W. *Chem. Eur. J.* **2000**, 6, 4597–4603.
- (433) Palmans, A. R. A.; Vekemans, J. A. J. M.; Fischer, H.; Hikmet, R. A.; Meijer, E. W. *Chem. Eur. J.* **1997**, 3, 300–307.
- (434) Palmans, A. R. A.; Vekemans, J. A. J. M.; Havinga, E. E.; Meijer, E. W. *Angew. Chem., Int. Ed. Engl.* **1997**, 36, 2648–2651.
- (435) Palmans, A. R. A.; Vekemans, J. A. J. M.; Hikmet, R. A.; Fischer, H.; Meijer, E. W. *Adv. Mater.* **1998**, 10, 873–876.
- (436) Brunsveld, L.; Zhang, H.; Glasbeek, M.; Vekemans, J. A. J. M.; Meijer, E. W. *J. Am. Chem. Soc.* **2000**, 122, 6175–6182.
- (437) Brunsveld, L.; Lohmeijer, B. G. G.; Vekemans, J. A. J. M.; Meijer, E. W. *Chem. Commun.* **2000**, 2305–2306.
- (438) van der Schoot, P.; Michels, M. A. J.; Brunsveld, L.; Sijbesma, R. P.; Ramzi, A. *Langmuir* **2000**, 16, 10076–10083.
- (439) Hamuro, Y.; Geib, S. J.; Hamilton, A. D. *Angew. Chem., Int. Ed. Engl.* **1994**, 446–448.
- (440) Hamuro, Y.; Geib, S. J.; Hamilton, A. D. *J. Am. Chem. Soc.* **1996**, 118, 7529–7541.
- (441) Hamuro, Y.; Geib, S. J.; Hamilton, A. D. *J. Am. Chem. Soc.* **1997**, 119, 10587–10593.
- (442) Recker, J.; Tomcik, D. J.; Parquette, J. R. *J. Am. Chem. Soc.* **2000**, 122, 10298–10307.
- (443) Huang, B.; Parquette, J. R. *Org. Lett.* **2000**, 2, 239–242.
- (444) Huang, B.; Parquette, J. R. *J. Am. Chem. Soc.* **2001**, 123, 2689–2690.
- (445) Gong, B.; Yan, Y. F.; Zeng, H. Q.; Skrzypczak-Jankun, E.; Kim, Y. W.; Zhu, J.; Ickes, H. *J. Am. Chem. Soc.* **1999**, 121, 5607–5608.
- (446) Zeng, H. Q.; Miller, R. S.; Flowers, R. A.; Gong, B. *J. Am. Chem. Soc.* **2000**, 122, 2635–2644.
- (447) Zhu, J.; Parra, R. D.; Zeng, H. Q.; Skrzypczak-Jankun, E.; Zeng, X. C.; Gong, B. *J. Am. Chem. Soc.* **2000**, 122, 4219–4220.
- (448) Berl, V.; Krische, M. J.; Huc, I.; Lehn, J. M.; Schmutz, R. *Chem. Eur. J.* **2000**, 6, 1938–1946.
- (449) Job, P. *Ann. Chim. (Paris)* **1928**, 9, 113.
- (450) Ingham, K. C. *Anal. Biochem.* **1975**, 68, 660–663.
- (451) Bielawski, C.; Chen, Y.-S.; Zhang, P.; Prest, P.-J.; Moore, J. S. *Chem. Commun.* **1998**, 1313–1314.
- (452) Archer, E. A.; Sochia, A. E.; Krische, M. J. *Tetrahedron* **2001**, 57, 1139–1159.

- (453) Lehn, J.-M.; Rigault, A.; Siegel, J.; Harrowfield, J.; Chevrier, B.; Moras, D. *Proc. Natl. Acad. Sci. U.S.A.* **1987**, *84*, 2565–2569.
- (454) Albrecht, M. *Chem. Soc. Rev.* **1998**, *27*, 281–287.
- (455) Caulder, D. L.; Raymond, K. N. *J. Chem. Soc., Dalton Trans.* **1999**, 1185–1200.
- (456) Constable, E. C. *Tetrahedron* **1992**, *48*, 10013–10059.
- (457) Piguet, C.; Bernardinelli, G.; Hopfgartner, G. *Chem. Rev.* **1997**, *97*, 2005–2062.
- (458) Mizutani, T.; Yagi, S.; Morinaga, T.; Nomura, T.; Takagishi, T.; Kitagawa, S.; Ogoshi, H. *J. Am. Chem. Soc.* **1999**, *121*, 754–759.
- (459) Yagi, S.; Morinaga, T.; Nomura, T.; Takagishi, T.; Mizutani, T.; Kitagawa, S.; Ogoshi, H. *J. Org. Chem.* **2001**, *66*, 3848–3853.
- (460) Yagi, S.; Sakai, N.; Yamada, R.; Takahashi, H.; Mizutani, T.; Takagishi, T.; Kitagawa, S.; Ogoshi, H. *Chem. Commun.* **1999**, 911–912.
- (461) Mizutani, T.; Yagi, S.; Honmaru, A.; Murakami, S.; Furusyo, M.; Takagishi, T.; Ogoshi, H. *J. Org. Chem.* **1998**, *63*, 8769–8784.
- (462) Mizutani, T.; Sakai, N.; Yagi, S.; Takagishi, T.; Kitagawa, S.; Ogoshi, H. *J. Am. Chem. Soc.* **2000**, *122*, 748–749.
- (463) Constable, E. C.; Elder, S. M.; Healey, J.; Tocher, D. A. *J. Chem. Soc., Dalton Trans.* **1990**, 1669–1674.
- (464) Von Henke, W.; Kremer, S.; Reinen, D. *Z. Anorg. Allg. Chem.* **1982**, *491*, 124–136.
- (465) Maslen, E. N.; Raston, C. L.; White, A. H. *J. Chem. Soc., Dalton Trans.* **1975**, 323–326.
- (466) Constable, E. C.; Elder, S. M.; Healy, J.; Ward, M. D.; Tocher, D. A. *J. Am. Chem. Soc.* **1990**, *112*, 4590–4592.
- (467) Constable, E. C.; Elder, S. M.; Tocher, D. A. *Polyhedron* **1992**, *11*, 1337–1342.
- (468) Constable, E. C.; Elder, S. M.; Tocher, D. A. *Polyhedron* **1992**, *11*, 2599–2604.
- (469) Constable, E. C.; Harverson, P.; Smith, D. R.; Whall, L. A. *Tetrahedron* **1994**, *50*, 7799–7806.
- (470) Potts, K. T.; Keshavarz-K, M.; Tham, F. S.; Gheysen, K. A.; Arana, C.; Abuña, H. D. *Inorg. Chem.* **1993**, *32*, 5477–5484.
- (471) Constable, E. C.; Drew, M. G. B.; Forsyth, G.; Ward, M. D. *J. Chem. Soc., Chem. Commun.* **1988**, 1450–1451.
- (472) Ho, P. K.-K.; Cheung, K.-K.; Peng, S.-M.; Che, C.-M. *J. Chem. Soc., Dalton Trans.* **1996**, 1411–1417.
- (473) Fu, Y.-J.; Sun, W.-Y.; Dai, W.-N.; Shu, M.-H.; Xue, F.; Wang, D.-F.; Mak, T. C. W.; Tang, W.-X.; Hu, H.-W. *Inorg. Chim. Acta* **1999**, *290*, 127–132.
- (474) Constable, E. C.; Chotalia, R.; Tocher, D. A. *J. Chem. Soc., Chem. Commun.* **1992**, 771–773.
- (475) Constable, E. C.; Ward, M. D.; Tocher, D. A. *J. Chem. Soc., Dalton Trans.* **1991**, 1675–1683.
- (476) See ref 110.
- (477) Sessler, J. L.; Weghorn, S. J.; Lynch, V.; Fransson, K. *J. Chem. Soc., Chem. Commun.* **1994**, 1289–1290.
- (478) Watson, J. D.; Crick, F. H. C. *Nature* **1953**, *171*, 737–738.
- (479) Eschenmoser, A.; Loewenthal, E. *Chem. Soc. Rev.* **1992**, *21*, 1–16.
- (480) Eschenmoser, A. *Origins Life Evol. Biosphere* **1994**, *24*, 389–423.
- (481) Eschenmoser, A.; Kisakürek, M. V. *Helv. Chim. Acta* **1996**, *79*, 1249–1259.
- (482) Uhlmann, E.; Peyman, A. *Chem. Rev.* **1990**, *90*, 543–584.
- (483) Milligan, J. F.; Matteucci, M. D.; Martin, J. C. *J. Med. Chem.* **1993**, *36*, 1923–1937.
- (484) De Mesmaeker, A.; Häner, R.; Martin, P.; Moser, H. E. *Acc. Chem. Res.* **1995**, *28*, 366–374.
- (485) Egli, M. *Angew. Chem., Int. Ed. Engl.* **1996**, *35*, 1894–1909.
- (486) Herdewijn, P. *Biochim. Biophys. Acta* **1999**, *1489*, 167–179.
- (487) Saenger, W. *Principles of Nucleic Acid Structure*; Springer-Verlag: New York, 1984.
- (488) Vesnaver, G.; Breslauer, K. J. *Proc. Natl. Acad. Sci. U.S.A.* **1991**, *88*, 3569–3573.
- (489) Levitt, M.; Warshel, A. *J. Am. Chem. Soc.* **1978**, *100*, 2607–2613.
- (490) Bush, C. A.; Brahm, J. In *Physico-Chemical Properties of Nucleic Acids*; Duchesne, J., Ed.; Academic Press: London and New York, 1973; Vol. 2.
- (491) Herdewijn, P. *Liebigs Ann.* **1996**, 1337–1348.
- (492) Kerr, I. M.; Brown, R. E. *Proc. Natl. Acad. Sci. U.S.A.* **1978**, *75*, 256–260.
- (493) Dougherty, J. P.; Rizzo, C. J.; Breslow, R. *J. Am. Chem. Soc.* **1992**, *114*, 6254–6255.
- (494) Hashimoto, H.; Switzer, C. *J. Am. Chem. Soc.* **1992**, *114*, 6255–6256.
- (495) Kierzek, R.; He, L.; Turner, D. H. *Nucleic Acids Res.* **1992**, *20*, 1685–1690.
- (496) Robinson, H.; Jung, K.-E.; Switzer, C.; Wang, A. H.-J. *J. Am. Chem. Soc.* **1995**, *117*, 837–838.
- (497) Jung, K.-E.; Switzer, C. *J. Am. Chem. Soc.* **1994**, *116*, 6059–6061.
- (498) Cheng, X.; Gao, Q.; Smith, R. D.; Jung, K.-E.; Switzer, C. *Chem. Commun.* **1996**, 747–748.
- (499) Giannaris, P. A.; Dahma, M. *Nucleic Acids Res.* **1993**, *21*, 4742–4749.
- (500) Sheppard, T. L.; Breslow, R. C. *J. Am. Chem. Soc.* **1996**, *118*, 9810–9811.
- (501) Prakash, T. P.; Jung, K.-E.; Switzer, C. *Chem. Commun.* **1996**, 1793–1794.
- (502) Kandimalla, E. R.; Manning, A.; Zhou, Q.; Shaw, D. R.; Byrn, R. A.; Sasisekharan, V.; Agrawal, S. *Nucleic Acids Res.* **1997**, *25*, 370–378.
- (503) Wasner, M.; Arion, D.; Borkow, G.; Noronha, A.; Uddin, A. H.; Parniak, M. A.; Damha, M. J. *Biochemistry* **1998**, *37*, 7478–7486.
- (504) Jin, R.; Chapman, W. H., Jr.; Srinivasa, A. R.; Olson, W. K.; Breslow, R.; Breslauer, K. J. *Proc. Natl. Acad. Sci. U.S.A.* **1993**, *90*, 10568–10572.
- (505) Sawai, H.; Seki, J.; Ozaki, H. *J. Biomol. Struct. Dyn.* **1996**, *13*, 1043–1051.
- (506) Joyce, G. F.; Visser, G. M.; van Boeckel, C. A. A.; van Boom, J. H.; Orgel, L. E.; van Westrenen, J. *Nature* **1984**, *310*, 602–604.
- (507) Prakash, T. P.; Roberts, C.; Switzer, C. *Angew. Chem., Int. Ed. Engl.* **1997**, *36*, 1522–1523.
- (508) Morvan, F.; Rayner, B.; Imbach, J.-L.; Chang, D.-K.; Lown, J. W. *Nucleic Acids Res.* **1986**, *14*, 5019–5035.
- (509) Morvan, F.; Rayner, B.; Imbach, J.-L.; Chang, D.-K.; Lown, J. W. *Nucleic Acids Res.* **1987**, *15*, 4241–4255.
- (510) Morvan, F.; Rayner, B.; Imbach, J.-L.; Lee, M.; Hartley, J. A.; Chang, D.-K.; Lown, J. W. *Nucleic Acids Res.* **1987**, *15*, 7027–7044.
- (511) Thuong, N.; Asseline, U.; Roig, V.; Takasugi, M.; Hélène, C. *Proc. Natl. Acad. Sci. U.S.A.* **1987**, *84*, 5129–5133.
- (512) Koga, M.; Moore, M. F.; Beaucage, S. L. *J. Org. Chem.* **1991**, *56*, 3757–3759.
- (513) Debart, F.; Tosquellas, G.; Rayner, B.; Imbach, J.-L. *Bioorg. Med. Chem. Lett.* **1994**, *4*, 1041–1046.
- (514) Koga, M.; Wilk, A.; Moore, M. F.; Scremin, C. L.; Zhou, L.; Beaucage, S. L. *J. Org. Chem.* **1995**, *60*, 1520–1530.
- (515) Gagnor, C.; Bertrand, J.-R.; Thenet, S.; Lemaître, M.; Morvan, F.; Rayner, B.; Malvy, C.; Lebleu, B.; Imbach, J.-L.; Paoletti, C. *Nucleic Acids Res.* **1987**, *15*, 10419–10436.
- (516) Paoletti, J.; Bazile, D.; Morvan, F.; Imbach, J.-L.; Paoletti, C. *Nucleic Acids Res.* **1989**, *17*, 2693–2704.
- (517) Fujimori, S.; Shudo, K.; Hashimoto, Y. *J. Am. Chem. Soc.* **1990**, *112*, 7436–7438.
- (518) Garbesi, A.; Capobianco, M. L.; Colonna, F. P.; Tondelli, L.; Arcamone, F.; Manzini, G.; Hilbers, C. W.; Aelen, J. M. E.; Blommers, M. J. *J. Nucleic Acids Res.* **1993**, *21*, 4159–4165.
- (519) Schöppe, A.; Hinz, H.-J.; Rosemeyer, H.; Seela, F. *Eur. J. Biochem.* **1996**, *239*, 33–41.
- (520) Giannaris, P. A.; Dahma, M. J. *Can. J. Chem.* **1994**, *72*, 909–918.
- (521) Eschenmoser, A. *Science* **1999**, *284*, 2118–2124.
- (522) Eschenmoser, A.; Krishnamurthy, R. *Pure Appl. Chem.* **2000**, *72*, 343–345.
- (523) Schöning, K.-U.; Scholz, P.; Guntha, S.; Wu, X.; Krishnamurthy, R.; Eschenmoser, A. *Science* **2000**, *290*, 1347–1351.
- (524) Herdewijn, P. *Angew. Chem., Int. Ed.* **2001**, *40*, 2249–2251.
- (525) Schlönvogt, I.; Pitsch, S.; Lesueur, C.; Eschenmoser, A.; Jaun, B.; Wolf, R. M. *Helv. Chim. Acta* **1996**, *79*, 2316–2345.
- (526) Böhringer, M.; Roth, H.-J.; Hunziker, J.; Göbel, M.; Krishnan, R.; Giger, A.; Schweizer, B.; Schreiber, J.; Leumann, C.; Eschenmoser, A. *Helv. Chim. Acta* **1992**, *75*, 1416–1477.
- (527) Pitsch, S.; Pombo-Villar, E.; Eschenmoser, A. *Helv. Chim. Acta* **1994**, *77*, 2251–2285.
- (528) Pitsch, S.; Wendeborn, S.; Jann, B.; Eschenmoser, A. *Helv. Chim. Acta* **1993**, *76*, 2161–2183.
- (529) Hunziker, J.; Roth, H.-J.; Böhringer, M.; Giger, A.; Diederichsen, U.; Göbel, M.; Krishnan, R.; Jaun, B.; Leumann, C.; Eschenmoser, A. *Helv. Chim. Acta* **1993**, *76*, 259–352.
- (530) Micura, R.; Kudick, R.; Pitsch, S.; Eschenmoser, A. *Angew. Chem., Int. Ed. Engl.* **1999**, *38*, 680–683.
- (531) Pitsch, S.; Krishnamurthy, R.; Bolli, M.; Wendeborn, S.; Holzner, A.; Minton, M.; Lesueur, C.; Schlönvogt, I.; Jaun, B.; Eschenmoser, A. *Helv. Chim. Acta* **1995**, *78*, 1621–1635.
- (532) Krishnamurthy, R.; Pitsch, S.; Minton, M.; Miculka, M.; Windhab, N.; Eschenmoser, A. *Angew. Chem., Int. Ed. Engl.* **1996**, *35*, 1537–1541.
- (533) Micura, R.; Bolli, M.; Windhab, N.; Eschenmoser, A. *Angew. Chem., Int. Ed. Engl.* **1997**, *36*, 870–873.
- (534) Beier, M.; Reck, F.; Wagner, T.; Krishnamurthy, R.; Eschenmoser, A. *Science* **1999**, *283*, 699–703.
- (535) Jungmann, O.; Wippo, H.; Stanek, M.; Huynh, H. K.; Krishnamurthy, R.; Eschenmoser, A. *Org. Lett.* **1999**, *1*, 1527–1530.
- (536) Reck, F.; Wippo, H.; Kudick, R.; Krishnamurthy, R.; Eschenmoser, A. *Helv. Chim. Acta* **2001**, *84*, 1778–1804.
- (537) Reck, F.; Wippo, H.; Kudick, R.; Bolli, M.; Ceulemans, G.; Krishnamurthy, R.; Eschenmoser, A. *Org. Lett.* **1999**, *1*, 1531–1534.
- (538) Eschenmoser, A.; Dobler, M. *Helv. Chim. Acta* **1992**, *75*, 218–259.
- (539) Augustyns, K.; Van Aerschot, A.; Urbanke, C.; Herdewijn, P. *Bull. Soc. Chim. Belg.* **1992**, *101*, 119–130.

- (540) Otting, G.; Billeter, M.; Wüthrich, K.; Roth, H.-J.; Leumann, C.; Eschenmoser, A. *Helv. Chim. Acta* **1993**, *76*, 2701–2756.
- (541) Groebke, K.; Hunziker, J.; Fraser, W.; Peng, L.; Diederichsen, U.; Zimmerman, K.; Holzner, A.; Leumann, C.; Eschenmoser, A. *Helv. Chim. Acta* **1998**, *81*, 375–474.
- (542) Augustyns, K.; Rozenski, J.; Van Aerschot, A.; Janssen, G.; Herdewijn, P. *J. Org. Chem.* **1993**, *58*, 2977–2982.
- (543) Augustyns, K.; Vandendriessche, F.; Van Aerschot, A.; Busson, R.; Urbanke, C.; Herdewijn, P. *Nucleic Acids Res.* **1992**, *20*, 4711–4716.
- (544) Yu, H.-W.; Zhang, L.-R.; Zhou, J.-C.; Ma, L.-T.; Zhang, L.-H. *Bioorg. Med. Chem.* **1996**, *4*, 609–614.
- (545) Yang, Z.-J.; Zhang, H.-Y.; Min, J.-M.; Ma, L.-T.; Zhang, L.-H. *Helv. Chim. Acta* **1999**, *82*, 2037–2043.
- (546) Lei, Z.; Zhang, L.; Zhang, L.-R.; Chen, J.; Min, J.-M.; Zhang, L.-H. *Nucleic Acids Res.* **2001**, *29*, 1470–1475.
- (547) Van Aerschot, A.; Verheggen, I.; Herdewijn, P. *Bioorg. Med. Chem. Lett.* **1993**, *3*, 1013–1018.
- (548) De Bouvere, B.; Kerremans, L.; Rozenski, J.; Janssen, G.; Van Aerschot, A.; Claes, P.; Busson, R.; Herdewijn, P. *Liebigs Ann.* **1997**, 1453–1461.
- (549) Hendrix, C.; Rosemeyer, H.; Verheggen, I.; Seela, F.; Van Aerschot, A.; Herdewijn, P. *Chem. Eur. J.* **1997**, *3*, 110–120.
- (550) Van Aerschot, A.; Verheggen, I.; Hendrix, C.; Herdewijn, P. *Angew. Chem., Int. Ed. Engl.* **1995**, *34*, 1338–1339.
- (551) Hendrix, C.; Rosemeyer, H.; De Bouvere, B.; Van Aerschot, A.; Seela, F.; Herdewijn, P. *Chem. Eur. J.* **1997**, *3*, 1513–1520.
- (552) Boudou, V.; Kerremans, L.; De Bouvere, B.; Lescrinier, E.; Schepers, G.; Busson, R.; Van Aerschot, A.; Herdewijn, P. *Nucleic Acids Res.* **1999**, *27*, 1450–1456.
- (553) Lescrinier, E.; Esnouf, R.; Schraml, J.; Busson, R.; Heus, H. A.; Hilbers, C. W.; Herdewijn, P. *Chem. Biol.* **2000**, *7*, 719–731.
- (554) De Winter, H.; Lescrinier, E.; Van Aerschot, A.; Herdewijn, P. *J. Am. Chem. Soc.* **1998**, *120*, 5381–5394.
- (555) Froeyen, M.; Wroblowski, B.; Esnouf, R.; De Winter, H.; Allart, B.; Lescrinier, E.; Herdewijn, P. *Helv. Chim. Acta* **2000**, *83*, 2153–2182.
- (556) Lescrinier, E.; Esnouf, R.; Schraml, J.; Busson, R.; Herdewijn, P. *Helv. Chim. Acta* **2000**, *83*, 1291–1310.
- (557) Allart, B.; Busson, R.; Rozenski, J.; Van Aerschot, A.; Herdewijn, P. *Tetrahedron* **1999**, *55*, 6527–6546.
- (558) Allart, B.; Khan, K.; Rosemeyer, H.; Schepers, G.; Hendrix, C.; Rothenbacher, K.; Seela, F.; Van Aerschot, A.; Herdewijn, P. *Chem. Eur. J.* **1999**, *5*, 2424–2431.
- (559) Hossain, N.; Wroblowski, B.; Van Aerschot, A.; Rozenski, J.; De Bruyn, A.; Herdewijn, P. *J. Org. Chem.* **1998**, *63*, 1574–1582.
- (560) Maurinsh, Y.; Schraml, J.; De Winter, H.; Blaton, N.; Peeters, O.; Lescrinier, E.; Rozenski, J.; Van Aerschot, A.; De Clercq, E.; Busson, R.; Herdewijn, P. *J. Org. Chem.* **1997**, *62*, 2861–2871.
- (561) Maurinsh, Y.; Rosemeyer, H.; Esnouf, R.; Medvedovici, A.; Wang, J.; Ceulemans, G.; Lescrinier, E.; Hendrix, C.; Busson, R.; Sandra, P.; Seela, F.; Van Aerschot, A.; Herdewijn, P. *Chem. Eur. J.* **1999**, *5*, 2139–2150.
- (562) Wang, J.; Busson, R.; Blaton, N.; Rozenski, J.; Herdewijn, P. *J. Org. Chem.* **1998**, *63*, 3051–3058.
- (563) Wang, J.; Verbeure, B.; Luyten, I.; Lescrinier, E.; Froeyen, M.; Hendrix, C.; Rosemeyer, H.; Seela, F.; Van Aerschot, A.; Herdewijn, P. *J. Am. Chem. Soc.* **2000**, *122*, 8595–8602.
- (564) Herdewijn, P.; De Clercq, E. *Bioorg. Med. Chem. Lett.* **2001**, *11*, 1591–1597.
- (565) Shimada, N.; Hasegawa, S.; Harada, T.; Tomisawa, T.; Fujii, A.; Takita, T. *J. Antibiot.* **1986**, *39*, 1623–1625.
- (566) Kakefuda, A.; Masuda, A.; Ueno, Y.; Ono, A.; Matsuda, A. *Tetrahedron* **1996**, *52*, 2863–2876.
- (567) Katagiri, N.; Morishita, Y.; Oosawa, I.; Yamaguchi, M. *Tetrahedron Lett.* **1999**, *40*, 6835–6840.
- (568) Honzawa, S.; Ohwada, S.; Morishita, Y.; Sato, K.; Katagiri, N.; Yamaguchi, M. *Tetrahedron* **2000**, *56*, 2615–2627.
- (569) Henlin, J.-M.; Rink, H.; Spieser, E.; Baschang, G. *Helv. Chim. Acta* **1992**, *75*, 589–603.
- (570) Henlin, J.-M.; Jaekel, K.; Moser, P.; Rink, H.; Spieser, E.; Baschang, G. *Angew. Chem., Int. Ed. Engl.* **1992**, *31*, 482–484.
- (571) Borthwick, A. D.; Biggadike, K. *Tetrahedron* **1992**, *48*, 571–623.
- (572) Agrofoglio, L.; Suhas, E.; Farese, A.; Condom, R.; Challand, S. R.; Earl, R. A.; Guedj, R. *Tetrahedron* **1994**, *50*, 10611–10670.
- (573) Meldgaard, M.; Wengel, J. *J. Chem. Soc., Perkin Trans. 1* **2000**, 3539–3554.
- (574) Tarköy, M.; Bolli, M.; Schweizer, B.; Leumann, C. *Helv. Chim. Acta* **1993**, *76*, 481–510.
- (575) Bolli, M.; Leumann, C. *Angew. Chem., Int. Ed. Engl.* **1995**, *34*, 694–696.
- (576) Tarköy, M.; Leumann, C. *Angew. Chem., Int. Ed. Engl.* **1993**, *32*, 1432–1434.
- (577) Tarköy, M.; Bolli, M.; Leumann, C. *Helv. Chim. Acta* **1994**, *77*, 716–744.
- (578) Bolli, M.; Litten, J. C.; Schütz, R.; Leumann, C. *J. Chem. Biol.* **1996**, *3*, 197–206.
- (579) Bolli, M.; Trafelet, H. U.; Leumann, C. *Chem. Biol.* **1996**, *24*, 4660–4667.
- (580) Litten, J. C.; Epple, C.; Leumann, C. *J. Bioorg. Med. Chem. Lett.* **1995**, *5*, 1231–1234.
- (581) Litten, J. C.; Leumann, C. *Helv. Chim. Acta* **1996**, *79*, 1129–1146.
- (582) Steffens, R.; Leumann, C. *J. Am. Chem. Soc.* **1997**, *119*, 11548–11549.
- (583) Steffens, R.; Leumann, C. *Helv. Chim. Acta* **1997**, *80*, 2426–2439.
- (584) Steffens, R.; Leumann, C. *J. Am. Chem. Soc.* **1999**, *121*, 3249–3255.
- (585) Epple, C.; Leumann, C. *Chem. Biol.* **1998**, *5*, 209–216.
- (586) Keller, B. M.; Leumann, C. *J. Angew. Chem., Int. Ed.* **2000**, *39*, 2278–2281.
- (587) Obika, S.; Nanbu, D.; Hari, Y.; Morio, K.; In, Y.; Ishida, T.; Imanishi, T. *Tetrahedron Lett.* **1997**, *38*, 8735–8738.
- (588) Singh, S. K.; Nielsen, P.; Koshkin, A. A.; Wengel, J. *Chem. Commun.* **1998**, 455–456.
- (589) Wengel, J. *Acc. Chem. Res.* **1999**, *32*, 301–310.
- (590) Koshkin, A. A.; Singh, S. K.; Nielsen, P.; Rajwanshi, V. K.; Kumar, R.; Meldgaard, M.; Olsen, C. E.; Wengel, J. *Tetrahedron* **1998**, *54*, 3607–3630.
- (591) Singh, S. K.; Wengel, J. *Chem. Commun.* **1998**, 1247–1248.
- (592) Nielsen, C. B.; Singh, S. K.; Wengel, J.; Jacobsen, J. P. *J. Biomol. Struct. Dyn.* **1999**, *17*, 175–191.
- (593) Christensen, U.; Jacobsen, N.; Rajwanshi, V. K.; Wengel, J.; Koch, T. *Biochem. J.* **2001**, *354*, 481–484.
- (594) Rajwanshi, V. K.; Håkansson, A. E.; Dahl, B. M.; Wengel, J. *Chem. Commun.* **1999**, 1395–1396.
- (595) Rajwanshi, V. K.; Håkansson, A. E.; Kumar, R.; Wengel, J. *Chem. Commun.* **1999**, 2073–2074.
- (596) Rajwanshi, V. K.; Håkansson, A. E.; Sørensen, D.; Pitsch, S.; Singh, S. K.; Kumar, R.; Nielsen, P.; Wengel, J. *Angew. Chem., Int. Ed.* **2000**, *39*, 1656–1659.
- (597) Håkansson, A. E.; Wengel, J. *Bioorg. Med. Chem. Lett.* **2001**, *11*, 935–938.
- (598) Petersen, M.; Nielsen, C. B.; Nielsen, K. E.; Jensen, G. A.; Bondensgaard, K.; Singh, S. K.; Rajwanshi, V. K.; Koshkin, A. A.; Dahl, B. M.; Wengel, J.; Jacobsen, J. P. *J. Mol. Recognit.* **2000**, *13*, 44–53.
- (599) Bondensgaard, K.; Petersen, M.; Singh, S. K.; Rajwanshi, V. K.; Kumar, R.; Wengel, J.; Jacobsen, J. P. *Chem. Eur. J.* **2000**, *6*, 2687–2695.
- (600) Egli, M.; Minasov, G.; Teplova, M.; Kumar, R.; Wengel, J. *Chem. Commun.* **2001**, 651–652.
- (601) Kværnø, L.; Wengel, J. *Chem. Commun.* **1999**, 657–658.
- (602) Kværnø, L.; Kumar, R.; Dahl, B. M.; Olsen, C. E.; Wengel, J. *J. Org. Chem.* **2000**, *65*, 5167–5176.
- (603) Wahlestedt, C.; Salmi, P.; Good, L.; Kela, J.; Johnsson, T.; Hökfelt, T.; Broberger, C.; Porreca, F.; Lai, J.; Ren, K.; Ossipov, M.; Koshkin, A.; Jakobsen, N.; Skouf, J.; Oerum, H.; Jacobsen, M. H.; Wengel, J. *Proc. Natl. Acad. Sci. U.S.A.* **2000**, *97*, 5633–5638.
- (604) Obika, S.; Nanbu, D.; Hari, Y.; Andoh, J.-i.; Morio, K.-i.; Doi, T.; Imanishi, T. *Tetrahedron Lett.* **1998**, *39*, 5401–5404.
- (605) Obika, S.; Hari, Y.; Sugimoto, T.; Sekiguchi, M.; Imanishi, T. *Tetrahedron Lett.* **2000**, *40*, 8923–8927.
- (606) Obika, S.; Uneda, T.; Sugimoto, T.; Nanbu, D.; Minami, T.; Doi, T.; Imanishi, T. *Bioorg. Med. Chem.* **2001**, *9*, 1001–1011.
- (607) Obika, S.; Hari, Y.; Morio, K.-i.; Imanishi, T. *Tetrahedron Lett.* **2000**, *40*, 221–224.
- (608) Obika, S.; Morio, K.-i.; Nanbu, D.; Imanishi, T. *Chem. Commun.* **1997**, 1643–1644.
- (609) Obika, S.; Morio, K.-i.; Hari, Y.; Imanishi, T. *Chem. Commun.* **1999**, 2423–2424.
- (610) Obika, S.; Morio, K.-i.; Hari, Y.; Imanishi, T. *Bioorg. Med. Chem. Lett.* **1999**, *9*, 515–518.
- (611) Scremin, C. L.; Boal, K. H.; Wilk, A.; Phillips, L. R.; Beaucage, S. L. *Bioorg. Med. Chem. Lett.* **1996**, *6*, 207–212.
- (612) Hossain, N.; Hendrix, C.; Lescrinier, E.; Van Aerschot, A.; Busson, R.; De Clercq, E.; Herdewijn, P. *Bioorg. Med. Chem. Lett.* **1996**, *6*, 1465–1468.
- (613) Scremin, C. L.; Boal, J. H.; Wilk, A.; Phillips, L. R.; Zhou, L.; Beaucage, S. L. *Tetrahedron Lett.* **1995**, *36*, 8953–8956.
- (614) Boal, J. H.; Wilk, A.; Scremin, C. L.; Gray, G. N.; Phillips, L. R.; Beaucage, S. L. *J. Org. Chem.* **1996**, *61*, 8617–8626.
- (615) Marangoni, M.; Van Aerschot, A.; Augustyns, P.; Rozenski, J.; Herdewijn, P. *Nucleic Acids Res.* **1997**, *25*, 3034–3041.
- (616) Ceulemans, G.; Van Aerschot, A.; Wroblowski, B.; Rozenski, J.; Hendrix, C.; Herdewijn, P. *Chem. Eur. J.* **1997**, *3*, 1997–2010.
- (617) Schneider, K. C.; Benner, S. A. *J. Am. Chem. Soc.* **1990**, *112*, 453–455.
- (618) Peng, L.; Roth, H.-J. *Helv. Chim. Acta* **1997**, *80*, 1494–1512.
- (619) Augustyns, K.; Van Aerschot, A.; Van Schepdael, A.; Urbanke, C.; Herdewijn, P. *Nucleic Acids Res.* **1991**, *19*, 2587–2593.
- (620) Vandendriessche, F.; Augustyns, K.; Van Aerschot, A.; Busson, R.; Hoogmartens, J.; Herdewijn, P. *Tetrahedron* **1993**, *49*, 7223–7238.
- (621) Nielsen, P.; Kirpekar, F.; Wengel, J. *Nucleic Acids Res.* **1994**, *22*, 703–710.

- (622) Nielsen, P.; Dreieø, L. H.; Wengel, J. *Bioorg. Med. Chem.* **1995**, *3*, 19–28.
- (623) Kim, S.-G.; Tsukahara, S.; Yokoyama, S.; Takaku, H. *FEBS Lett.* **1992**, *314*, 29–32.
- (624) Hacia, J. G.; Wold, B. J.; Dervan, P. B. *Biochemistry* **1994**, *33*, 5367–5369.
- (625) Torigoe, H.; Shimizume, R.; Sarai, A.; Shindo, H. *Biochemistry* **1999**, *38*, 14653–14659.
- (626) Stein, C. A.; Cheng, Y.-C. *Science* **1993**, *261*, 1004–1012.
- (627) Alunni-Fabroni, M.; Manioletti, G.; Manzini, G.; Xodo, L. E. *Eur. J. Biochem.* **1994**, *226*, 831–839.
- (628) Xodo, L.; Alunni-Fabroni, M.; Manzini, G.; Quadrifoglio, F. *Nucleic Acids Res.* **1994**, *22*, 3322–3330.
- (629) Lesnikowski, Z. J.; Jaworska, M.; Stec, W. J. *Nucleic Acids Res.* **1990**, *18*, 2112–2114.
- (630) Vinogradov, S.; Asseline, U.; Thuong, N. T. *Tetrahedron Lett.* **1993**, *34*, 5899–5902.
- (631) Chur, A.; Holst, B.; Dahl, O.; Valentinhanen, P.; Pedersen, E. B. *Nucleic Acids Res.* **1993**, *21*, 5179–5183.
- (632) Luo, P.; Leitzel, J. C.; Zhan, Z.-Y., J.; Lynn, D. G. *J. Am. Chem. Soc.* **1998**, *120*, 3019–3031.
- (633) Chan, M.-Y.; Fairhurst, R. A.; Collingwood, S. P.; Fisher, J.; Arnold, J. R. P.; Cosstick, R.; O'Neil, I. A. *J. Chem. Soc., Perkin Trans 1* **1999**, 315–320.
- (634) Musicki, B.; Widlanski, T. S. *Tetrahedron Lett.* **1991**, *32*, 1267–1270.
- (635) Perrin, K.; Huang, J.; McElroy, E. B.; Iams, K. P.; Widlanski, T. S. *J. Am. Chem. Soc.* **1994**, *116*, 7427–7428.
- (636) Baeschlin, D. K.; Hyrup, B.; Benner, S. A.; Richert, C. *J. Org. Chem.* **1996**, *61*, 7620–7626.
- (637) Okruszek, A.; Sierzchala, A.; Sochacki, M.; Stec, W. J. *Tetrahedron Lett.* **1992**, *33*, 7585–7588.
- (638) Pudio, J. S.; Cao, X.; Swaminathan, S.; Matteucci, M. D. *Tetrahedron Lett.* **1994**, *35*, 9315–9318.
- (639) Zou, R.; Matteucci, M. D. *Tetrahedron Lett.* **1996**, *37*, 941–944.
- (640) Rozners, E.; Strömberg, R. *J. Org. Chem.* **1997**, *62*, 1846–1850.
- (641) Jones, R. J.; Lin, K. Y.; Milligan, J. F.; Wadwani, S.; Matteucci, M. D. *J. Org. Chem.* **1993**, *58*, 2983–2991.
- (642) Cross, C. W.; Rice, S.; Gao, X. *Biochemistry* **1997**, *36*, 4096–4107.
- (643) Beauceage, S. L.; Iyer, R. P. *Tetrahedron* **1993**, *49*, 6123–6194.
- (644) Gryaznov, S.; Chen, J.-K. *J. Am. Chem. Soc.* **1994**, *116*, 3143–3144.
- (645) Chen, J.-K.; Schultz, R. G.; Lloyd, D. H.; Gryaznov, S. M. *Nucleic Acids Res.* **1995**, *23*, 2661–2668.
- (646) Gryaznov, S. M.; Lloyd, D. H.; Chen, J.-K.; Schultz, R. G.; DeDionisio, L. A.; Rattmeyer, L.; Wilson, W. D. *Proc. Natl. Acad. Sci. U.S.A.* **1995**, *92*, 5798–5802.
- (647) Ding, D.; Gryaznov, S. M.; Lloyd, D. H.; Chandrasekaran, S.; Yao, S.; Rattmeyer, L.; Pan, Y.; Wilson, W. D. *Nucleic Acids Res.* **1996**, *24*, 354–360.
- (648) Ding, D.; Gryaznov, S. M.; Wilson, W. D. *Biochemistry* **1998**, *37*, 12082–12093.
- (649) Tereshko, V.; Gryaznov, S.; Egli, M. *J. Am. Chem. Soc.* **1998**, *120*, 269–283.
- (650) Escudé, C.; Giovannangeli, C.; Sun, J.-S.; Lloyd, D. H.; Chen, J.-K.; Gryaznov, S. M.; Garestier, T.; Hélène, C. *Proc. Natl. Acad. Sci. U.S.A.* **1996**, *93*, 4365–4369.
- (651) Gryaznov, S. M.; Winter, H. *Nucleic Acids Res.* **1998**, *26*, 4160–4167.
- (652) Matray, T. J.; Gryaznov, S. M. *Nucleic Acids Res.* **1999**, *27*, 3976–3985.
- (653) Gryaznov, S.; Skorski, T.; Cucco, C.; Nieboroska-Skorska, M.; Chiu, C. Y.; Lloyd, D.; Chen, J.-K.; Koziolkiewicz, M.; Calabretta, B. *Nucleic Acids Res.* **1996**, *24*, 1508–1514.
- (654) Faria, M.; Wood, C. D.; Perrouault, L.; Nelson, J. S.; Winter, A.; White, M. R. H.; Hélène, C.; Giovannangeli, C. *Proc. Natl. Acad. Sci. U.S.A.* **2000**, *97*, 3862–3867.
- (655) Faria, M.; Spiller, D. G.; Dubertret, C.; Nelson, J. S.; White, M. R. H.; Scherman, D.; Hélène, C.; Giovannangeli, C. *Nat. Biotechnol.* **2001**, *19*, 40–44.
- (656) Rigl, C. T.; Lloyd, D. H.; Tsou, D. S.; Gryaznov, S. M.; Wilson, W. D. *Biochemistry* **1997**, *36*, 650–659.
- (657) Barsky, D.; Corvin, M. E.; Zon, G.; Gryaznov, S. M. *Nucleic Acids Res.* **1997**, *25*, 830–835.
- (658) Huang, Z.; Schneider, K. C.; Benner, S. A. *J. Org. Chem.* **1991**, *56*, 3869–3882.
- (659) Richert, C.; Roughton, A. L.; Benner, S. A. *J. Am. Chem. Soc.* **1996**, *118*, 4518–4531.
- (660) Roughton, A. L.; Portmann, S.; Benner, S. A.; Egli, M. *J. Am. Chem. Soc.* **1995**, *117*, 7249–7250.
- (661) Steinbeck, C.; Richert, C. *J. Am. Chem. Soc.* **1998**, *120*, 11576–11580.
- (662) Nielsen, P. E.; Haaima, G. *Chem. Soc. Rev.* **1997**, 73–78.
- (663) Dueholm, K. L.; Nielsen, P. E. *New J. Chem.* **1997**, *21*, 19–31.
- (664) Uhlmann, E.; Peyman, A.; Breipohl, G.; Will, D. W. *Angew. Chem., Int. Ed. Engl.* **1998**, *37*, 2796–2823.
- (665) Uhlmann, E. *Biol. Chem. Hoppe-Seyler* **1998**, *379*, 1045–1052.
- (666) Nielsen, P. E. *Acc. Chem. Res.* **1999**, *32*, 624–630.
- (667) Nielsen, P. E.; Egholm, M.; Berg, R. H.; Buchardt, O. *Science* **1991**, *254*, 1497–1500.
- (668) Egholm, M.; Buchardt, O.; Nielsen, P. E.; Berg, R. H. *J. Am. Chem. Soc.* **1992**, *114*, 1895–1897.
- (669) Egholm, M.; Behrens, C.; Christensen, L.; Berg, R. H.; Nielsen, P. E.; Buchardt, O. *J. Chem. Soc., Chem. Commun.* **1993**, 800–801.
- (670) Wittung, P.; Nielsen, P. E.; Buchardt, O.; Egholm, M.; Nordén, B. *Nature* **1994**, *368*, 561–563.
- (671) Tomac, S.; Sarkar, M.; Ratilainen, T.; Wittung, P.; Nielsen, P. E.; Nordén, B.; Gräslund, A. *J. Am. Chem. Soc.* **1996**, *118*, 5544–5552.
- (672) Egholm, M.; Buchardt, O.; Christensen, L.; Behrens, C.; Freier, S. M.; Driver, D. A.; Berg, R. H.; Kim, S. K.; Norden, B.; Nielsen, P. E. *Nature* **1993**, *365*, 566–568.
- (673) Ratilainen, T.; Holmén, A.; Tuite, E.; Nielsen, P. E.; Nordén, B. *Biochemistry* **2000**, *39*, 7781–7791.
- (674) Rasmussen, H.; Kastrop, J. S.; Nielsen, J. N.; Nielsen, J. M.; Nielsen, P. E. *Nat. Struct. Biol.* **1997**, *4*, 98–101.
- (675) Ratilainen, T.; Holmén, A.; Tuite, E.; Haaima, G.; Christensen, L.; Nielsen, P. E.; Nordén, B. *Biochemistry* **1998**, *37*, 12331–12342.
- (676) Brown, S. C.; Thomson, S. A.; Veal, J. M.; Davis, D. G. *Science* **1994**, *265*, 777–780.
- (677) Leijon, M.; Gräslund, A.; Nielsen, P. E.; Buchardt, O.; Nordén, B.; Kristensen, S. M.; Eriksson, M. *Biochemistry* **1994**, *33*, 9820–9825.
- (678) Eriksson, M.; Nielsen, P. E. *Nat. Struct. Biol.* **1996**, *3*, 410–413.
- (679) Almarsson, Ö.; Bruice, T. C. *Proc. Natl. Acad. Sci. U.S.A.* **1993**, *90*, 9542–9546.
- (680) Almarsson, Ö.; Bruice, T. C.; Kerr, J.; Zuckermann, R. N. *Proc. Natl. Acad. Sci. U.S.A.* **1993**, *90*, 7518–7522.
- (681) Chen, S.-M.; Mohan, V.; Kiely, J. S.; Griffith, M. C.; Griffey, R. H. *Tetrahedron Lett.* **1994**, *35*, 5105–5108.
- (682) Torres, R. A.; Bruice, T. C. *Proc. Natl. Acad. Sci. U.S.A.* **1996**, *93*, 649–653.
- (683) Armitage, B.; Ly, D.; Koch, T.; Frydenlund, H.; Ørum, H.; Schuster, G. B. *Biochemistry* **1998**, *37*, 9417–9425.
- (684) Soliva, R.; Sherer, E.; Luque, F. J.; Loughton, C. A.; Orozco, M. *J. Am. Chem. Soc.* **2000**, *122*, 5997–6008.
- (685) Uhlmann, E.; Will, D. W.; Breipohl, G.; Langner, D.; Ryte, A. *Angew. Chem., Int. Ed. Engl.* **1996**, *35*, 2632–2635.
- (686) Cherny, D. Y.; Belotserkovskii, B. P.; Frank-Kamenetskii, M. D.; Egholm, M.; Buchardt, O.; berg, R. H.; nielsen, P. E. *Proc. Natl. Acad. Sci. U.S.A.* **1993**, *90*, 1667–1670.
- (687) Peffer, N. J.; Hanvey, J. C.; Bisi, J. E.; Thomson, S. A.; Hassman, C. F.; Noble, S. A.; Babiss, L. E. *Proc. Natl. Acad. Sci. U.S.A.* **1993**, *90*, 10648–10652.
- (688) Bukanov, N. O.; Demidov, V. V.; Nielsen, P. E.; Frank-Kamenetskii, M. D. *Proc. Natl. Acad. Sci. U.S.A.* **1998**, *95*, 5516–5520.
- (689) Nielsen, P. E.; Egholm, M.; Buchardt, O. *J. Mol. Recognit.* **1994**, *7*, 165–170.
- (690) Wittung, P.; Nielsen, P.; Nordén, B. *J. Am. Chem. Soc.* **1997**, *119*, 3189–3190.
- (691) Nielsen, P. E.; Christensen, L. *J. Am. Chem. Soc.* **1996**, *118*, 2287–2288.
- (692) Lohse, J.; Dahl, O.; Nielsen, P. E. *Proc. Natl. Acad. Sci. U.S.A.* **1999**, *96*, 11804–11808.
- (693) Kim, S. K.; Nielsen, P. E.; Egholm, M.; Buchardt, O.; Berg, R. H.; Nordén, B. *J. Am. Chem. Soc.* **1993**, *115*, 6477–6481.
- (694) Demidov, V. V.; Yavnilovich, M. V.; Belotserkovskii, B. P.; Frank-Kamenetskii, M. D.; Nielsen, P. E. *Proc. Natl. Acad. Sci. U.S.A.* **1995**, *92*, 2637–2641.
- (695) Betts, L.; Josey, J. A.; Veal, J. M.; Jordan, S. R. *Science* **1995**, *270*, 1838–1841.
- (696) Kosaganov, Y. N.; Stetsenko, D. A.; Lubyako, E. N.; Kvitko, N. P.; Lazurkin, Y. S.; Nielsen, P. E. *Biochemistry* **2000**, *39*, 11742–11747.
- (697) Böhler, C.; Nielsen, P. E.; Orgel, L. E. *Nature* **1995**, *376*, 578–581.
- (698) Schmidt, J. G.; Nielsen, P. E.; Orgel, L. E. *Nucleic Acids Res.* **1997**, *25*, 4797–4802.
- (699) Lutz, M. J.; Benner, S. A.; Hein, S.; Breipohl, G.; Uhlmann, E. *J. Am. Chem. Soc.* **1997**, *119*, 3177–3178.
- (700) Hanvey, J. C.; Peffer, N. J.; Bisi, J. E.; Thomson, S. A.; Cadilla, R.; Josey, J. A.; Ricca, D. J.; Hassman, C. F.; Bonham, M. A.; Au, K. G.; Carter, S. G.; Bruckenstein, D. A.; Boyd, A. L.; Noble, S. A.; Babiss, L. E. *Science* **1992**, *258*, 1481–1485.
- (701) Ljungström, T.; Knudsen, H.; Nielsen, P. E. *Bioconjugate Chem.* **1999**, *10*, 965–972.
- (702) Lagriffoule, P.; Wittung, P.; Eriksson, M.; Jensen, K. K.; Nordén, B.; Buchardt, O.; Nielsen, P. E. *Chem. Eur. J.* **1997**, *3*, 912–919.
- (703) Egholm, M.; Christensen, L.; Dueholm, K. L.; Buchardt, O.; Coull, J.; Nielsen, P. E. *Nucleic Acids Res.* **1995**, *23*, 217–222.

- (704) Griffith, M. C.; Risen, L. M.; Greig, M. J.; Lesnik, E. A.; Sprankle, K. G.; Griffey, R. H.; Kiely, J. S.; Freier, S. M. *J. Am. Chem. Soc.* **1995**, *117*, 831–832.
- (705) Koch, T.; Naesby, M.; Wittung, P.; Jørgensen, M.; Larsson, C.; Buchardt, O.; Stanley, C. J.; Nordén, B.; Nielsen, P. E.; Ørum, H. *Tetrahedron Lett.* **1995**, *36*, 6933–6936.
- (706) Garner, P.; Dey, S.; Huang, Y. *J. Am. Chem. Soc.* **2000**, *122*, 2405–2406.
- (707) Karig, G.; Fuchs, A.; Büsing, A.; Brandstetter, T.; Scherer, S.; Bats, J. W.; Eschenmoser, A.; Quinkert, G. *Helv. Chim. Acta* **2000**, *83*, 1049–1078.
- (708) Schwalbe, H.; Wermuth, J.; Richter, C.; Szalma, S.; Eschenmoser, A.; Quinkert, G. *Helv. Chim. Acta* **2000**, *83*, 1079–1107.
- (709) Eppacher, S.; Solladie, N.; Bernet, B.; Vasella, A. *Helv. Chim. Acta* **2000**, *83*, 1311–1330.
- (710) Gunji, H.; Vasella, A. *Helv. Chim. Acta* **2000**, *83*, 1331–1345.
- (711) Gunji, H.; Vasella, A. *Helv. Chim. Acta* **2000**, *83*, 2975–2992.
- (712) Gunji, H.; Vasella, A. *Helv. Chim. Acta* **2000**, *83*, 3229–3245.
- (713) Czechtizky, W.; Vasella, A. *Helv. Chim. Acta* **2001**, *84*, 594–612.
- (714) Czechtizky, W.; Vasella, A. *Helv. Chim. Acta* **2001**, *84*, 1000–1016.
- (715) Vandendriessche, F.; Van Aerschot, A.; Voortmans, M.; Janssen, G.; Busson, R.; Van Overbeke, A.; Van den Bossche, W.; Hoogmartens, J.; Herdewijn, P. *J. Chem. Soc., Perkin Trans. 1* **1993**, 1567–1575.
- (716) Dempcy, R. O.; Almarsson, Ö.; Bruice, T. C. *Proc. Natl. Acad. Sci. U.S.A.* **1994**, *91*, 7864–7868.
- (717) Dempcy, R. O.; Browne, K. A.; Bruice, T. C. *J. Am. Chem. Soc.* **1995**, *117*, 6140–6141.
- (718) Dempcy, R. O.; Browne, K. A.; Bruice, T. C. *Proc. Natl. Acad. Sci. U.S.A.* **1995**, *92*, 6097–6101.
- (719) Linkletter, B. A.; Bruice, T. C. *Bioorg. Med. Chem. Lett.* **1998**, *8*, 1285–1290.
- (720) Barawkar, D. A.; Linkletter, B.; Bruice, T. C. *Bioorg. Med. Chem. Lett.* **1998**, *8*, 1517–1520.
- (721) Linkletter, B. A.; Szabo, I. E.; Bruice, T. C. *J. Am. Chem. Soc.* **1999**, *121*, 3888–3896.
- (722) Linkletter, B. A.; Szabo, I. E.; Bruice, T. C. *Nucleic Acids Res.* **2001**, *29*, 2370–2376.
- (723) Browne, K. A.; Dempcy, R. O.; Bruice, T. C. *Proc. Natl. Acad. Sci. U.S.A.* **1995**, *92*, 7051–7055.
- (724) Blaskó, A.; Dempcy, R. O.; Minyat, E. E.; Bruice, T. C. *J. Am. Chem. Soc.* **1996**, *118*, 7892–7899.
- (725) Blaskó, A.; Minyat, E. E.; Dempcy, R. O.; Bruice, T. C. *Biochemistry* **1997**, *36*, 7821–7831.
- (726) Luo, J.; Bruice, T. C. *J. Am. Chem. Soc.* **1998**, *120*, 1115–1123.
- (727) Dempcy, R. O.; Luo, J.; Bruice, T. C. *Proc. Natl. Acad. Sci. U.S.A.* **1996**, *93*, 4326–4330.
- (728) Luo, J.; Bruice, T. C. *J. Am. Chem. Soc.* **1997**, *119*, 6693–6701.
- (729) Kojima, N.; Bruice, T. C. *Org. Lett.* **2000**, *2*, 81–84.
- (730) Barawkar, D. A.; Bruice, T. C. *J. Am. Chem. Soc.* **1999**, *121*, 10418–10419.
- (731) Barawkar, D. A.; Kwok, Y.; Bruice, T. W.; Bruice, T. C. *J. Am. Chem. Soc.* **2000**, *122*, 5244–5250.
- (732) Linkletter, B. A.; Bruice, T. C. *Bioorg. Med. Chem.* **2000**, *8*, 1893–1901.
- (733) Arya, D. P.; Bruice, T. C. *J. Am. Chem. Soc.* **1998**, *120*, 6619–6620.
- (734) Arya, D. P.; Bruice, T. C. *J. Am. Chem. Soc.* **1998**, *120*, 12419–12427.
- (735) Arya, D. P.; Bruice, T. C. *Bioorg. Med. Chem. Lett.* **2000**, *10*, 691–693.
- (736) Arya, D. P.; Bruice, T. C. *Proc. Natl. Acad. Sci. U.S.A.* **1999**, *96*, 4384–4389.
- (737) Arya, D. P.; Bruice, T. C. *J. Am. Chem. Soc.* **1999**, *121*, 10680–10684.
- (738) Luo, J.; Bruice, T. C. *J. Biomol. Struct. Dyn.* **2000**, *17*, 629–643.
- (739) Kool, E. T.; Morales, J. C.; Guckian, K. M. *Angew. Chem., Int. Ed.* **2000**, *39*, 990–1009.
- (740) Ren, R. X.-F.; Chaudhuri, N. C.; Paris, P. L.; Rumney, S., IV; Kool, E. T. *J. Am. Chem. Soc.* **1996**, *118*, 7671–7678.
- (741) Guckian, K. M.; Schweitzer, B. A.; Ren, R. X.-F.; Sheils, C. J.; Paris, P. L.; Tahmassebi, D. C.; Kool, E. T. *J. Am. Chem. Soc.* **1996**, *118*, 8182–8183.
- (742) Guckian, K. M.; Schweitzer, B. A.; Ren, R. X.-F.; Sheils, C. J.; Tahmassebi, D. C.; Kool, E. T. *J. Am. Chem. Soc.* **2000**, *122*, 2213–2222.
- (743) Bain, J. D.; Switzer, C.; Chamberlain, A. R.; Benner, S. A. *Nature* **1992**, *356*, 537–539.
- (744) Switzer, C. Y.; Moroney, S. E.; Benner, S. A. *Biochemistry* **1993**, *32*, 10489–10496.
- (745) Roberts, C.; Bandaru, R.; Switzer, C. *J. Am. Chem. Soc.* **1997**, *119*, 4640–4649.
- (746) Lutz, M. J.; Horlacher, J.; Benner, S. A. *Bioorg. Med. Chem. Lett.* **1998**, *8*, 499–504.
- (747) Piccirilli, J. A.; Krauch, T.; Moroney, S. E.; Benner, S. A. *Nature* **1990**, *343*, 33–37.
- (748) Tor, Y.; Dervan, P. B. *J. Am. Chem. Soc.* **1993**, *115*, 4461–4467.
- (749) Horlacher, J.; Hottiger, M.; Podust, V. N.; Hübscher, U.; Benner, S. A. *Proc. Natl. Acad. Sci. U.S.A.* **1995**, *92*, 6329–6333.
- (750) Lutz, M. J.; Held, H. A.; Hottiger, M.; Hübscher, U.; Benner, S. A. *Nucleic Acids Res.* **1996**, *24*, 1308–1313.
- (751) McMinn, D. L.; Ogawa, A. K.; Wu, Y.; Liu, J.; Schultz, P. G.; Romesberg, F. E. *J. Am. Chem. Soc.* **1999**, *121*, 11585–11586.
- (752) Roberts, C.; Chaput, J. C.; Switzer, C. *Chem. Biol.* **1997**, *4*, 899–908.
- (753) Robinson, H.; Gao, Y.-G.; C., B.; Roberts, C.; Switzer, C.; Wang, A. H.-J. *Biochemistry* **1998**, *37*, 10897–10905.
- (754) Matray, T. J.; Kool, E. T. *J. Am. Chem. Soc.* **1998**, *120*, 6191–6192.
- (755) Guckian, K. M.; Morales, J. C.; Kool, E. T. *J. Org. Chem.* **1998**, *63*, 9652–9656.
- (756) Guckian, K. M.; Krugh, T. R.; Kool, E. T. *J. Am. Chem. Soc.* **2000**, *122*, 6841–6847.
- (757) Morales, J. C.; Kool, E. T. *Nat. Struct. Biol.* **1998**, *5*, 950–954.
- (758) Matray, T. J.; Kool, E. T. *Nature* **1999**, *399*, 704–708.
- (759) Morales, J. C.; Kool, E. T. *J. Am. Chem. Soc.* **2000**, *122*, 1001–1007.
- (760) Kool, E. T. *Curr. Opin. Chem. Biol.* **2000**, *4*, 602–608.
- (761) Ogawa, A. K.; Wu, Y.; McMinn, D. L.; Liu, J.; Schultz, P. G.; Romesberg, F. E. *J. Am. Chem. Soc.* **2000**, *122*, 3274–3287.
- (762) Wu, Y.; Ogawa, A. K.; Berger, M.; McMinn, D. L.; Schultz, P. G.; Romesberg, F. E. *J. Am. Chem. Soc.* **2000**, *122*, 7621–7632.
- (763) Berger, M.; Ogawa, A. K.; McMinn, D. L.; Wu, Y.; Schultz, P. G.; Romesberg, F. E. *Angew. Chem., Int. Ed.* **2000**, *39*, 2940–2942.
- (764) Ogawa, A. K.; Wu, Y.; Berger, M.; Schultz, P. G.; Romesberg, F. E. *J. Am. Chem. Soc.* **2000**, *122*, 8803–8804.
- (765) Tae, E. L.; Wu, Y.; Xia, G.; Schultz, P. G.; Romesberg, F. E. *J. Am. Chem. Soc.* **2001**, *123*, 7439–7440.
- (766) Meggers, E.; Holland, P. L.; Tolman, W. B.; Romesberg, F. E.; Schultz, P. G. *J. Am. Chem. Soc.* **2000**, *122*, 10714–10715.
- (767) Weizman, H.; Tor, Y. *J. Am. Chem. Soc.* **2001**, *123*, 3375–3376.
- (768) Weizman, H.; Tor, Y. *Chem. Commun.* **2001**, 453–454.
- (769) Brotschi, C.; Häberli, A.; Leumann, C. J. *Angew. Chem., Int. Ed.* **2001**, *40*, 3012–3014.
- (770) Tanaka, K.; Shionoya, M. *J. Org. Chem.* **1999**, *64*, 5002–5003.
- (771) Cao, H.; Tanaka, K.; Shionoya, M. *Chem. Pharm. Bull.* **2000**, *48*, 1745–1748.
- (772) Tanaka, K.; Tasaka, M.; Cao, H.; Shionoya, M. *Eur. J. Pharm. Sci.* **2001**, *13*, 77–83.
- (773) Nowick, J. S.; Tsai, J. H.; Bui, Q.-C. D.; Maitra, S. *J. Am. Chem. Soc.* **1999**, *121*, 8409–8410.
- (774) Jørgensen, W. L.; Pranata, J. *J. Am. Chem. Soc.* **1990**, *112*, 2008–2010.
- (775) Pranata, J.; Wierschke, S. G.; Jørgensen, W. L. *J. Am. Chem. Soc.* **1991**, *113*, 2810–2819.
- (776) Murray, T. J.; Zimmerman, S. C. *J. Am. Chem. Soc.* **1992**, *114*, 4010–4011.
- (777) Beijer, F. H.; Sijbesma, R. P.; Kooijman, H.; Spek, A. L.; Meijer, E. W. *J. Am. Chem. Soc.* **1998**, *120*, 6761–6769.
- (778) Söntjens, S. H.; Sijbesma, R. P.; van Genderen, M. H. P.; Meijer, E. W. *J. Am. Chem. Soc.* **2000**, *122*, 7487–7493.
- (779) Zeng, H.; Ickes, H.; Flowers, R. A.; Gong, B. *J. Org. Chem.* **2001**, *66*, 3574–3583.
- (780) Corbin, P. S.; Zimmerman, S. C. *J. Am. Chem. Soc.* **2000**, *122*, 3779–3780.
- (781) Folmer, B. J. B.; Sijbesma, R. P.; Kooijman, H.; Spek, A. L.; Meijer, E. W. *J. Am. Chem. Soc.* **1999**, *121*, 9001–9007.
- (782) Archer, E. A.; Goldberg, N. T.; Lynch, V.; Krische, M. J. *J. Am. Chem. Soc.* **2000**, *122*, 5006–5007.
- (783) Bisson, A. P.; Carver, F. J.; Hunter, C. A.; Waltho, J. P. *J. Am. Chem. Soc.* **1994**, *116*, 10292–10293.
- (784) Bisson, A. P.; Hunter, C. A. *Chem. Commun.* **1996**, 1723–1724.
- (785) Adams, H.; Carver, F. J.; Hunter, C. A.; Osborne, N. J. *Chem. Commun.* **1996**, 2529–2530.
- (786) Adams, H.; Harris, K. D. M.; Hembury, G. A.; Hunter, C. A.; Livingstone, D.; McCabe, J. F. *Chem. Commun.* **1996**, 2531–2532.
- (787) Bisson, A. P.; Hunter, C. A.; Morales, J. C.; Young, K. *Chem. Eur. J.* **1998**, *4*, 845–851.
- (788) Bisson, A. P.; Carver, F. J.; Eggleston, D. S.; Haltiwanger, R. C.; Hunter, C. A.; Livingstone, D. L.; McCabe, J. F.; Rotger, C.; Rowan, A. E. *J. Am. Chem. Soc.* **2000**, *122*, 8856–8868.
- (789) Berl, V.; Huc, I.; Khoury, R. G.; Lehn, J.-M. *Chem. Eur. J.* **2001**, *7*, 2798–2809.
- (790) Berl, V.; Huc, I.; Khoury, R. G.; Lehn, J.-M. *Chem. Eur. J.* **2001**, *7*, 2810–2820.
- (791) Constable, E. C. *Pure Appl. Chem.* **1996**, *68*, 253–260.
- (792) Kaes, C.; Katz, A.; Hosseini, M. W. *Chem. Rev.* **2000**, *100*, 3553–3590.
- (793) Constable, E. C.; Elder, S. M.; Hannon, M. J.; Martin, A.; Raithby, P. R.; Tocher, D. A. *J. Chem. Soc., Dalton Trans.* **1996**, 2423–2433.
- (794) Potts, K. T.; Keshavarz-K., M.; Tham, F. S.; Abruna, H. D.; Arana, C. *Inorg. Chem.* **1993**, *32*, 4450–4456.

- (795) Potts, K. T.; Keshavarz-K., M.; Tham, F. S.; Abruna, H. D.; Arana, C. *Inorg. Chem.* **1993**, *32*, 4422–4435.
- (796) Potts, K. T.; Keshavarz-K., M.; Tham, F. S.; Abruna, H. D.; Arana, C. *Inorg. Chem.* **1993**, *32*, 4436–4449.
- (797) Potts, K. T.; Raiford, K. A., G.; Keshavarz-K., M. *J. Am. Chem. Soc.* **1993**, *115*, 2793–2807.
- (798) Constable, E. C.; Hannon, M. J.; Tocher, D. A. *J. Chem. Trans., Dalton Trans.* **1993**, 1883–1890.
- (799) Constable, E. C.; Hannon, M. J.; Edwards, A. J.; Raithby, P. R. *J. Chem. Soc., Dalton Trans.* **1994**, 2669–2677.
- (800) Ho, P. K.-K.; Peng, S.-M.; Cheung, K.-K.; Wong, K.-Y.; Che, C.-M. *J. Chem. Soc., Dalton Trans.* **1996**, 1829–1834.
- (801) Potts, K. T.; Horwitz, C. P.; Fessak, A.; Keshavarz-K., M.; Nash, K. E.; Toscano, P. J. *J. Am. Chem. Soc.* **1993**, *115*, 10444–10445.
- (802) Chamchoumis, C. M.; Potvin, P. G. *J. Chem. Soc., Dalton Trans.* **1999**, 1373–1374.
- (803) Baum, G.; Constable, E. C.; Fenske, D.; Kulke, T. *Chem. Commun.* **1997**, 2043–2044.
- (804) Constable, E. C.; Kulke, T.; Neuburger, M.; Zehnder, M. *Chem. Commun.* **1997**, 489–490.
- (805) Baum, G.; Constable, E. C.; Fenske, D.; Housecroft, C. E.; Kulke, T. *Chem. Eur. J.* **1999**, *5*, 1862–1873.
- (806) Constable, E. C.; Heirtzler, F. R.; Neuburger, M.; Zehnder, M. *Supramol. Chem.* **1995**, *5*, 197–200.
- (807) Constable, E. C.; Heirtzler, F. R.; Neuburger, M.; Zehnder, M. *Chem. Commun.* **1996**, 933–934.
- (808) Constable, E. C.; Heirtzler, F.; Neuburger, M.; Zehnder, M. *J. Am. Chem. Soc.* **1997**, *119*, 5606–5617.
- (809) Constable, E. C.; Kulke, T.; Neuburger, M.; Zehnder, M. *Chem. Commun.* **1997**, 489–490.
- (810) Baum, G.; Constable, E. C.; Fenske, D.; Housecroft, C. E.; Kulke, T. *Chem. Commun.* **1998**, 2659–2660.
- (811) Baum, G.; Constable, E. C.; Fenske, D.; Housecroft, C. E.; Kulke, T.; Neuburger, M.; Zehnder, M. *J. Chem. Soc., Dalton Trans.* **2000**, 945–959.
- (812) Lehn, J.-M.; Rigault, A. *Angew. Chem., Int. Ed. Engl.* **1988**, *27*, 1095–1097.
- (813) Garrett, T. M.; Koert, U.; Lehn, J.-M.; Rigault, A.; Meyer, D.; Fischer, J. *J. Chem. Soc., Chem. Commun.* **1990**, 557–558.
- (814) Harding, M. M.; Koert, U.; Lehn, J.-M.; Marquis-Rigault, A.; Piguët, C.; Siegel, J. *Helv. Chim. Acta* **1991**, *74*, 594–610.
- (815) Krämer, R.; Lehn, J.-M.; Marquis-Rigault, A. *Proc. Natl. Acad. Sci. U.S.A.* **1993**, *90*, 5394–5398.
- (816) Garrett, T. M.; Koert, U.; Lehn, J.-M. *J. Phys. Org. Chem.* **1992**, *5*, 529–532.
- (817) Pfeil, A.; Lehn, J.-M. *J. Chem. Soc., Chem. Commun.* **1992**, 838–840.
- (818) Koert, U.; Harding, M. M.; Lehn, J.-M. *Nature* **1990**, *346*, 339–342.
- (819) Schoentjes, B.; Lehn, J.-M. *Helv. Chim. Acta* **1995**, *78*, 1–12.
- (820) Pauling, L.; Corey, R. B. *Nature* **1953**, *171*, 346.
- (821) Smith, V. C. M.; Lehn, J.-M. *Chem. Commun.* **1996**, 2733–2734.
- (822) Greenwald, M.; Wessely, D.; Goldberg, I.; Cohen, Y. *New J. Chem.* **1999**, 337–344.
- (823) Shaul, M.; Cohen, Y. *J. Org. Chem.* **1999**, *64*, 9358–9364.
- (824) Greenwald, M.; Wessely, D. K., E.; Willner, I.; Cohen, Y. *J. Org. Chem.* **2000**, *65*, 1050–1058.
- (825) Zarges, W.; Hall, J.; Lehn, J.-M.; Bolm, C. *Helv. Chim. Acta* **1991**, *74*, 1843–1852.
- (826) Woods, C. R.; Benaglia, M.; Cozzi, F.; Sigel, J. S. *Angew. Chem., Int. Ed. Engl.* **1996**, *35*, 1830–1833.
- (827) Annunziata, R.; Benaglia, M.; Cinquini, M.; Cozzi, F.; Woods, C. R.; Siegel, J. S. *Eur. J. Org. Chem.* **2001**, 173–180.
- (828) Funeriu, D.-P.; He, Y.-B.; Bister, H.-J.; Lehn, J.-M. *Bull. Soc. Chim. Fr.* **1996**, *133*, 673–678.
- (829) Stiller, R.; Lehn, J.-M. *Eur. J. Inorg. Chem.* **1998**, 977–982.
- (830) Krämer, R.; Lehn, J.-M.; De Cian, A.; Fisher, J. *Angew. Chem., Int. Ed. Engl.* **1993**, *32*, 703–706.
- (831) Hasenknopf, B.; Lehn, J.-M. *Helv. Chim. Acta* **1996**, *79*, 1643–1650.
- (832) Hasenknopf, B.; Lehn, J.-M.; Baum, G.; Fenske, D. *Proc. Natl. Acad. Sci. U.S.A.* **1996**, *93*, 1397–1400.
- (833) Hasenknopf, B.; Lehn, J.-M.; Kneisel, B. O.; Baum, G.; Fenske, D. *Angew. Chem., Int. Ed. Engl.* **1996**, *35*, 1838–1840.
- (834) Baxter, P. N. W.; Lehn, J.-M.; Rissanen, K. *Chem. Commun.* **1997**, 1323–1324.
- (835) Hasenknopf, B.; Lehn, J.-M.; Boumediene, N.; Dupont-Gervais, A.; van Dorsselaer, A.; Kneisel, B.; Fenske, D. *J. Am. Chem. Soc.* **1997**, *119*, 10956–10962.
- (836) Hasenknopf, B.; Lehn, J.-M.; Boumediene, N.; Leize, E.; van Dorsselaer, A. *Angew. Chem., Int. Ed. Engl.* **1998**, *37*, 3265–3268.
- (837) Williams, A. F.; Piguët, C.; Bernardinelli, G. *Angew. Chem., Int. Ed. Engl.* **1991**, *30*, 1490–1492.
- (838) Piguët, C.; Hopfgartner, G.; Bocquet, B.; Schaad, O.; Williams, A. F. *J. Am. Chem. Soc.* **1994**, *116*, 9092–9102.
- (839) Petoud, S.; Bunzli, J.-C. G.; Renaud, F.; Piguët, C.; Schenk, K. J.; Hopfgartner, G. *Inorg. Chem.* **1997**, *36*, 5750–5760.
- (840) Charbonniere, L. J.; Williams, A. F.; Piguët, C.; Bernardinelli, G.; Rivara-Minten, E. *Chem. Eur. J.* **1998**, *4*, 485–493.
- (841) Provent, C.; Hewage, S.; Brand, G.; Bernardinelli, G.; Charbonniere, L. J.; Williams, A. F. *Angew. Chem., Int. Ed. Engl.* **1997**, *36*, 1287–1289.
- (842) Provent, C.; Rivara-Minten, E.; Hewage, S.; Brunner, G.; Williams, A. F. *Chem. Eur. J.* **1999**, *5*, 3487–3494.
- (843) von Zelewsky, A.; Mamula, O. *J. Chem. Soc., Dalton Trans.* **2000**, 219–231.
- (844) Amendola, V.; Fabbrizzi, L.; Linati, L.; Mangano, C.; Pallavicini, P.; Pedrazzini, V.; Zema, M. *Chem. Eur. J.* **1999**, *5*, 3679–3688.
- (845) Amendola, V.; Fabbrizzi, L.; Mangano, C.; Pallavicini, P.; Roboli, E.; Zema, M. *Inorg. Chem.* **2000**, *39*, 5803–5806.
- (846) *Photomorphogenesis in Plants*, 2nd ed; Kluwer Academic: Dordrecht, 1994.
- (847) Zhang, Y.; Thompson, A.; Rettig, S. J.; Dolphin, D. *J. Am. Chem. Soc.* **1998**, *120*, 13537–13538.
- (848) Thompson, A.; Dolphin, D. *Org. Lett.* **2000**, *2*, 1315–1318.
- (849) Thompson, A.; Dolphin, D. *J. Org. Chem.* **2000**, *65*, 7870–7877.
- (850) Caulder, D. L.; Raymond, K. N. *Angew. Chem., Int. Ed. Engl.* **1997**, *36*, 1440–1442.
- (851) Kersting, B.; Meyer, M.; Power, R. E.; Raymond, K. N. *J. Am. Chem. Soc.* **1996**, *118*, 7221–7222.
- (852) Meyer, M.; Kersting, B.; Powers, R. E.; Raymond, K. N. *Inorg. Chem.* **1997**, *36*, 5179–5191.
- (853) Schere, M.; Caulder, D. L.; Johnson, D. W.; Raymond, K. N. *Angew. Chem., Int. Ed.* **1999**, *38*, 1588–1592.
- (854) Caulder, D. L.; Powers, R. E.; Parac, T. N.; Raymond, K. N. *Angew. Chem., Int. Ed. Engl.* **1998**, *37*, 1840–1843.
- (855) Albrecht, M.; Schneider, M.; Röttele, H. *Angew. Chem., Int. Ed.* **1999**, *38*, 557–559.
- (856) Albrecht, M. *Chem. Eur. J.* **1997**, *3*, 1466–1471.
- (857) Albrecht, M.; Kotaila, S. *Angew. Chem., Int. Ed. Engl.* **1996**, *35*, 1208–1210.
- (858) Albrecht, M.; Roettele, H.; Burger, P. *Chem. Eur. J.* **1996**, *2*, 1264–1268.
- (859) Airey, A. L.; Swiegers, G. F.; Willis, A. C.; Wild, S. B. *Inorg. Chem.* **1997**, *36*, 1588–1597.
- (860) Linton, B.; Hamilton, A. D. *Chem. Rev.* **1997**, *97*, 1669–1680.
- (861) Huc, I.; Krische, M. J.; Funeriu, D. P.; Lehn, J.-M. *Eur. J. Inorg. Chem.* **1999**, 1415–1420.
- (862) Haq, H.; Ladbury, J. *J. Mol. Recognit.* **2000**, *13*, 188–197.
- (863) Pelletier, H.; Sawaya, M. R.; Kumar, A.; Wilson, S. H.; Kraut, J. *Science* **1994**, *264*, 1891–1903.
- (864) Doublé, S.; Tabor, S.; Long, M. A.; Richardson, C. C.; Ellenberger, T. *Nature* **1998**, *391*, 251–258.
- (865) Kiefer, J. R.; Mao, C.; Braman, J. C.; Beese, L. S. *Nature* **1998**, *391*, 304–307.
- (866) Morales, J. C.; Kool, E. T. *J. Am. Chem. Soc.* **1999**, *121*, 2323–2324.
- (867) Morales, J. C.; Kool, E. T. *Biochemistry* **2000**, *39*, 12979–12988.
- (868) Dzantiev, L.; Alekseyev, Y. O.; Morales, J. C.; Kool, E. T.; Romano, L. J. *Biochemistry* **2001**, *40*, 3215–3221.
- (869) Finlay, A. C.; Hochstein, F. A.; Sobin, B. A.; Murphy, F. X. *J. Am. Chem. Soc.* **1951**, *73*, 341–343.
- (870) Pelton, J. G.; Wemmer, D. E. *Biochemistry* **1988**, *27*, 8088–8096.
- (871) Arcamone, F.; Penco, S.; Delle Monache, F. *Gazz. Chim. Ital.* **1969**, 620–631.
- (872) Arcamone, F.; Nicoletta, V.; Penco, S.; Redaelli, S. *Gazz. Chim. Ital.* **1969**, 632–640.
- (873) Kopka, M. L.; Yoon, C.; Goodsell, D.; Pjura, P.; Dickerson, R. E. *Proc. Natl. Acad. Sci. U.S.A.* **1985**, *82*, 1376–1380.
- (874) White, S.; Szweczyk, J. W.; Turner, J. M.; Baird, E. E.; Dervan, P. B. *Nature* **1998**, *391*, 468–471.
- (875) Dervan, P. B.; Bürli, R. W. *Curr. Opin. Chem. Biol.* **1999**, *3*, 688–693.
- (876) Turner, J. M.; Swalley, S. E.; Baird, E. E.; Dervan, P. B. *J. Am. Chem. Soc.* **1998**, *120*, 6219–6226.
- (877) Mrksich, M.; Parks, M. E.; Dervan, P. B. *J. Am. Chem. Soc.* **1994**, *116*, 7983–7988.
- (878) Traunger, J. W.; Baird, E. E.; Dervan, P. B. *Nature* **1996**, *382*, 559–561.
- (879) Baird, E. E.; Dervan, P. B. *J. Am. Chem. Soc.* **1996**, *118*, 6141–6146.
- (880) Lown, J. W. *J. Mol. Recognit.* **1994**, *7*, 79–88.
- (881) Walker, W. L.; Kopka, M. L.; Goodsell, D. S. *Biopolymers* **1997**, *44*, 323–334.
- (882) Bailly, C. B.; Chaires, J. B. *Bioconjugate Chem.* **1998**, *9*, 513–538.
- (883) Wemmer, D. E. *Annu. Rev. Biophys. Biomol. Struct.* **2000**, *29*, 439–461.
- (884) Hanka, L. J.; Dietz, A.; Gerpheide, S. A.; Kuentzel, S. L.; Martin, D. G. *J. Antibiot.* **1978**, *31*, 1211–1217.
- (885) Martin, D. G.; Biles, C.; Gerpheide, S. A.; Hanka, L. J.; Krueger, W. C.; McGovern, J. P.; Mizsak, S. A.; Neil, G. L.; Stewart, J. C.; Visser, J. *J. Antibiot.* **1981**, *34*, 1119–1125.
- (886) Boger, D. L.; Johnson, D. S. *Proc. Natl. Acad. Sci. U.S.A.* **1995**, *92*, 3642–3649.

- (887) Boger, D. L.; Johnson, D. S. *Angew. Chem., Int. Ed. Engl.* **1996**, *35*, 1438–1474.
- (888) Boger, D. L.; Boyce, C. W.; Garbaccio, R. M.; Goldberg, J. A. *Chem. Rev.* **1997**, *97*, 787–828.
- (889) Boger, D. L.; Garbaccio, R. M. *Acc. Chem. Res.* **1999**, *32*, 1043–1052.
- (890) Chidester, C. G.; Krueger, W. C.; Mizens, S. A.; Duchamp, D. J.; Martin, D. G. *J. Am. Chem. Soc.* **1981**, *103*, 7629–7236.
- (891) Scahill, T. A.; Jensen, R. M.; Swenson, D. H.; Natzenbuhler, N. T.; Petzold, G.; Wierenga, W.; Brahme, N. D. *Biochemistry* **1990**, *29*, 2852–2860.
- (892) Eis, P. S.; Smith, J. A.; Rydzewski, J. M.; A., C. D.; Boger, D. L.; Chazin, W. J. *J. Mol. Biol.* **1997**, *272*, 237–252.
- (893) Boger, D. L.; Coleman, R. S. *J. Am. Chem. Soc.* **1987**, *109*, 2717–2727.
- (894) Boger, D. L.; Invergo, B. J.; Coleman, R. S.; Zarrinmayer, H.; Kitos, P. A.; Thompson, S. C.; Leong, T.; McLaughlin, L. W. *Chem.-Biol. Interact.* **1990**, *73*, 29–52.
- (895) Boger, D. L.; Garbaccio, R. M. *Bioorg. Med. Chem.* **1997**, *5*, 263–276.
- (896) Pecuh, M. W.; Hamilton, A. D.; Sánchez-Quesada, J.; de Mendoza, J.; Haack, T.; Giralt, E. *J. Am. Chem. Soc.* **1997**, *119*, 9327–9328.
- (897) Haack, T.; Pecuh, M. W.; Salvatella, X.; Sánchez-Quesada, J.; de Mendoza, J.; Hamilton, A. D.; Giralt, E. *J. Am. Chem. Soc.* **1999**, *121*, 11813–11820.
- (898) Salvatella, X.; Pecuh, M. W.; Gairi, M.; Jain, R. K.; Sánchez-Quesada, J.; de Mendoza, J.; Hamilton, A. D.; Giralt, E. *Chem. Commun.* **2000**, 1399–1400.
- (899) IUPAC–IUB *Biochemistry* **1970**, *9*, 3471–3479.
- (900) See ref 241.
- (901) Eldrup, A. B.; Nielsen, B. B.; Haaima, G.; Rasmussen, H.; Kastrup, J. S.; Christensen, C.; Nielsen, P. E. In *The Protein Data Bank*, 2001.
- (902) Johnson, J., W. C. *Methods Biochem. Anal.* **1985**, *31*, 61–163 and references therein
- (903) Lakowicz, J. R. *Principles of Fluorescence*, 2nd ed; Kluwer Academic/Plenum Publishers: New York, 1999.
- (904) Nakanishi, K.; Solomon, P. H. *Infrared Absorption Spectroscopy*; Emerson-Adams Press: New York, 2000.
- (905) Gunther, H. *NMR Spectroscopy*; John Wiley & Sons: New York, 1995.
- (906) Thomas, M. J. K. *Ultraviolet and Visible Spectroscopy*; John Wiley & Sons: New York, 1996.
- (907) Watt, I. M. *The Principle and Practice of Electron Microscopy*; Cambridge University Press: New York, 1996.
- (908) Calvet, E.; Prat, H. *Recent Progress in Microcalorimetry*; Macmillan: New York, 1963.
- (909) Stout, G. H.; Jensen, L. H. *X-ray Structure Determination: A Practical Guide*; John Wiley & Sons: New York, 1989.

CR990120T

